MycoKeys 96: 1–23 (2023)
doi: 10.3897/mycokeys.96.98738
https://mycokeys.pensoft.net

RESEARCH ARTICLE

A peer-reviewed open-access journal
MycoKeys
Launched to accelerate biodiversity research

Taxonomy of *Thelidium auruntii* and *T. incavatum* complexes (lichenized Ascomycota, Verrucariales) in Finland

Juha Pykälä[1], Annina Kantelinen[2], Leena Myllys[2]

1 *Nature solutions, Finnish Environment Institute, Latokartanonkaari 11, 00790, Helsinki, Finland* **2** *Botany Unit, Finnish Museum of Natural History, P.O. Box 7, FI-00014, University of Helsinki, Helsinki, Finland*

Corresponding author: Juha Pykälä (juha.pykala@syke.fi)

Academic editor: T. Lumbsch | Received 12 December 2022 | Accepted 26 January 2023 | Published 8 March 2023

Citation: Pykälä J, Kantelinen A, Myllys L (2023) Taxonomy of *Thelidium auruntii* and *T. incavatum* complexes (lichenized Ascomycota, Verrucariales) in Finland. MycoKeys 96: 1–23. https://doi.org/10.3897/mycokeys.96.98738

Abstract

The taxonomy of lichen species morphologically similar to *Thelidium auruntii* and *T. incavatum* in Finland is being revised. Based on ITS and morphology, ten species occur in Finland. All species are restricted to calcareous rocks. The *Thelidium auruntii* morphocomplex includes six species: *T. auruntii*, *T. huuskonenii* **sp. nov.**, *T. pseudoauruntii* **sp. nov.**, *T. sallaense* sp. nov, *T. toskalharjiense* **sp. nov.** and *T.* sp. 1. In the ITS phylogeny, *T. auruntii*, *T. pseudoauruntii* and *T. sallaense* group together, but the remaining species are placed outside of this clade. All the species have northern distribution in Finland, occurring on fells in NW Finland and/or in gorges in the Oulanka area in NE Finland. The *Thelidium incavatum* morphocomplex includes four species: *T. declivum* **sp. nov.**, *T. incavatum*, *T. mendax* **sp. nov.** and *T.* sp. 2. This morphogroup is not resolved as monophyletic in the ITS phylogeny, with only *T. declivum* and *T. mendax* forming a strongly supported group. *Thelidium incavatum* is rather common in SW Finland, with one separate locality in eastern Finland. *Thelidium declivum* occurs only in the Oulanka area. *Thelidium mendax* occurs in the Oulanka area, but one locality is known from eastern central Finland. *Thelidium* sp. 2 is known from one locality in SW Lapland.

Keywords

Calcareous rocks, DNA barcoding, ITS, lichenized fungi, new species, phylogeny

Introduction

Recently, many new species of *Verrucaria*, *Polyblastia* and related genera have been described from calcareous rocks of Europe (Savíc and Tibell 2008, 2012; Breuss and Berger 2012; Orange 2014, 2020; Tibell and Tibell 2015; Pykälä and Myllys 2016; Pykälä et al. 2017a, b, 2018, 2019, 2020). However, during that time, only one new species of *Thelidium* has been described from Europe (Ceynowa-Giełdon 2007). Thüs and Nascimbene (2008) revised the taxonomy of the Central European freshwater species of *Thelidium*. No recent study exists on the taxonomy of any species complexes of *Thelidium* on calcareous rocks.

Thelidium A. Massal. is a polyphyletic genus widely dispersed within the Verrucariaceae (Gueidan et al. 2007, 2009). The core of the species belongs to the so-called *Thelium* group, which also includes several species included in *Polyblastia* and *Verrucaria*.

In a previous study, we investigated the taxonomy of species of *Verrucaria* belonging to the *Thelidium* group and producing perithecia that leave pits on rocks in Finland (Pykälä et al. 2020). Here, we continue the study on the taxonomy of the *Thelidium* group, focussing on the species morphologically similar to *Thelidium auruntii* (A. Massal.) Kremp. and *T. incavatum* Nyl. & Mudd. They are referred to here as *T. auruntii* and *T. incavatum* morphocomplexes. The *Thelidium auruntii* complex is characterised by 1-septate spores, an involucrellum (predominantly short), pale, thin or endolithic thallus and medium-sized perithecia. The *Thelidium incavatum* complex is characterised by 3-septate spores, perithecia leaving pits, medium-sized exciple (0.2–0.4 mm) and usually an endolithic pale thallus. Species belonging to the two complexes have similar habitat requirements and are restricted to calcareous rocks. Another species on calcareous rocks with 3-septate spores and perithecia leaving pits, *T. fontigenum* A. Massal., differs in its usually partly K+ violet thallus, smaller exciple (0.15–0.25 mm) and thin involucrellum.

Methods

This study is based on the material collected by the first author during the lichen inventory of calcareous rocks and lime quarries in Finland in 2003–2011, supplemented by one specimen collected in 2018. The sampling was most extensive in southern Finland (over 50% of all calcareous rocks and lime quarries studied) (Pykälä et al. 2017a, b). The type material of putatively morphologically similar *Thelidium* species from herbaria B, H, H-NYL, M, PRM, S, UPS, VER were studied for comparison.

Morphology

Perithecia and thalli were handsectioned with razor blades. The sections were examined and measured in tap water. Asci and ascospores were also studied in squash

preparations of perithecia mounted in water. Sections and squash preparations of old herbarium specimens were studied using potassium hydroxide (KOH). Additionally, involucrellum characters and exciple colour and diameter were examined by cutting perithecia into two pieces and studying the pieces using a binocular microscope.

The range of spore size is indicated as arithmetic mean and standard deviation. Minimum and maximum values are given in parentheses. The size of the perithecia (in diameter) is given in surface view. The colour of the wall of the exciple was assessed from the basal parts.

DNA extraction and sequencing

Total genomic DNA was extracted from perithecia (1–3) of two- to ten-year-old herbarium specimens. The samples were placed in 96-well microplates and sent to the Canadian Centre for DNA Barcoding (CCDB). CCDB's standard protocols (documentation available at https://ccdb.ca/resources) were used for extraction, PCR and sequencing. Primers ITS1 and ITS4 (White et al. 1990) were used both for PCR and sequencing of the nuclear ribosomal ITS regions. The barcode sequences, their trace files along with all relevant collection data and photographs of the voucher specimens were uploaded to the Barcode of Life Data Systems (BOLD, https://www.boldsystems.org) database. The sequences are available in GenBank (see Table 1 for accession numbers).

Phylogenetic analyses

We searched for the closest relatives of the new *Thelidium* species by using the BLAST search facility in Genbank (https://blast.ncbi.nlm.nih.gov/Blast.cgi). Based on BLAST, all species belong to the *Thelidium* group, but most of them do not have close relatives in GenBank. We used the following criteria for including GenBank sequences in our phylogeny: two sequences per species were selected if they have more than 95% similarity to any of our study species. Additionally, one sequence per species bearing more than 90% similarity to any study species was selected if they were among the 100 most similar sequences according to BLAST.

Based on this search, six ITS sequences of *Polyblastia*, six sequences of *Thelidium* and 17 sequences of *Verrucaria* in GenBank were selected to reconstruct a putative phylogeny of the species (Table 1). *Polyblastia albida* Arnold and *P. fuscoargillacea* Anzi were used as outgroups based on the studies of Gueidan et al. (2009) and Pykälä et al. (2020).

A total of 76 ITS sequences were aligned with MUSCLE v.3.8.31 (Edgar 2004) using EMBL-EBI's web service (https://www.ebi.ac.uk/Tools/msa/muscle/). The aligned data set was subjected to maximum likelihood analysis (ML). The analysis was performed with RAxML v.8.1.3 (Stamatakis 2014) located at CSC – IT Center for Science (https://www.csc.fi/english). The ITS region was partitioned into ITS1, 5.8S and ITS2. The GTRGAMMA model was used for all partitions. Node support was estimated with 1000 bootstrap replications using the rapid bootstrap algorithm.

Table 1. Specimens used in the phylogenetic analyses. New sequences are in bold.

Species	Country	Voucher	GenBank accession numbers
Polyblastia abscondita	Sweden	Tibell 23641 (UPS)	EU553507
P. albida	Sweden	Savíc 3021 (UPS)	EU553492
P. clandestina	Sweden	Nordin 5466 (UPS)	EU559740
P. lutosa	Sweden	Savíc 3163 (UPS)	EU559734
P. moravica	Sweden	Savíc 3154 (UPS)	EU553522
P. fuscoargillacea	Sweden	Palice 7666 (hb. Palice)	EU553498
P. sp.	Sweden	Tibell 23635 (UPS)	EU553503
	Sweden	Savíc 3164 (UPS)	EU553519
Thelidium auruntii	**Finland**	**Pykälä 36339 (H)**	**OP901843**
	Finland	**Pykälä 43414 (H)**	**OP901844**
	Finland	**Pykälä 43446 (H**	**OP901845**
	Finland	**Pykälä 43470 (H)**	**OP901846**
	Finland	**Pykälä 43829 (H)**	**OP901847**
	Finland	**Pykälä 43905 (H)**	**OP901848**
	Finland	**Pykälä 45171 (H)**	**OP901849**
T. declivum	**Finland**	**Pykälä 35996 (H)**	**OP901850**
	Finland	**Pykälä 36334 (H)**	**OP901851**
	Finland	**Pykälä 39640 (H)**	**OP901852**
	Finland	**Pykälä 39780b (H)**	**OP901853**
	Finland	**Pykälä 39997 (H)**	**OP901854**
	Finland	**Pykälä 40037 (H)**	**OP901855**
	Finland	**Pykälä 40047 (H)**	**OP901856**
	Finland	**Pykälä 44554 (H)**	**OP901857**
	Finland	**Pykälä 45123 (H)**	**OP901858**
T. huuskonenii	**Finland**	**Pykälä 31576 (H)**	**OP901859**
	Finland	**Pykälä 43243 (H)**	**OP901860**
	Finland	**Pykälä 43246 (H)**	**OP901861**
	Finland	**Pykälä 44167 (H)**	**OP901862**
T. incavatum	**Finland**	**Pykälä 34722 (H)**	**OP901863**
	Finland	**Pykälä 35282 (H)**	**OP901864**
	Finland	**Pykälä 36857 (H)**	**OP901865**
	Finland	**Pykälä 36867 (H)**	**OP901866**
	Finland	**Pykälä 37971 (H)**	**OP901867**
	Finland	**Pykälä 38227 (H)**	**OP901868**
	Finland	**Pykälä 38399 (H)**	**OP901869**
	Finland	**Pykälä 42871 (H)**	**OP901870**
	Finland	**Pykälä 46459 (H)**	**OP901871**
T. mendax	**Finland**	**Pykälä 39179 (H)**	**OP901872**
	Finland	**Pykälä 40152 (H)**	**OP901873**
	Finland	**Pykälä 42502 (H)**	**OP901874**
	Finland	**Pykälä 42503 (H)**	**OP901875**
T. methorium	Austria	Orange 21167 (NMW)	MT127220
	UK	Orange 16554 (NMW)	FJ645267
T. papulare	UK	Orange 16531 (NMW)	MT127197
T. pertusatii	Italy	Nascimbene JN1990	EU249471
T. pseudoauruntii	**Finland**	**Pykälä 45371 (H)**	**OP901876**
	Finland	**Pykälä 45374 (H)**	**OP901877**
T. pyrenophorum	Sweden	Tibell 23649 (UPS)	EU553500
T. sallaense	**Finland**	**Pykälä 44902 (H)**	**OP901878**

Species	Country	Voucher	GenBank accession numbers
T. toskalharjiense	**Finland**	**Pykälä 43090 (H)**	**OP901879**
	Finland	**Pykälä 43211 (H)**	**OP901880**
	Finland	**Pykälä 43364 (H)**	**OP901881**
	Finland	**Pykälä 43398 (H)**	**OP901882**
	Finland	**Pykälä 43848 (H)**	**OP901883**
	Finland	**Pykälä 43861 (H)**	**OP901884**
T. umbilicatum	Sweden	Tibell 23525 (UPS)	EU559737
***T.* sp. 1**	**Finland**	**Pykälä 43208 (H)**	**OP901885**
***T.* sp. 2**	**Finland**	**Pykälä 52038 (H)**	**OP901886**
Verrucaria aethiobola	Norway	Orange 18946 (NMW)	MT127203
V. anziana	Norway	Orange 17221 (NMW)	FJ664835
V. bifurcata	Finland	Pykälä 36722 (H)	MT229720
"V. calkinsiana"	Canada	McMullin (OAC)	KT695332
V. cavernarum	Finland	Pykälä 37975 (H)	MT229724
V. devergens	Finland	Pykälä 45367 (H)	MT229741
"V. deversa"	Sweden	Savíc 3063 (UPS)	EU553496
V. difficilis	Finland	Pykälä 39060 (H)	MT229743
V. karelica	Finland	Pykälä 40325 (H)	MT229762
V. kuusamoensis	Finland	Pykälä 44694 (H)	MT229774
V. latebrosa	UK	Orange 16309 (NMW)	FJ664864
V. pallidomurina	UK	Orange 22835 (NMW)	MT127221
V. subdevergens	Finland	Pykälä 44550 (H)	MT229782
V. subtilis	Finland	Pykälä 37329 (H)	MT229810
V. tephromela	UK	Orange 19135 (NMW)	MT127212
V. vacillans	Finland	Pykälä 43272 (H)	MT229831
V. **sp.**	Norway	Orange 18952 (NMW)	MT127205

Results

We generated 44 new ITS sequences for this study (Table 1). The alignment consisted of 526 sites of which sites 1-193 belonged to the ITS1 rDNA regions, sites 194–345 to the 5,8S rDNA gene and sites 346–526 to the ITS2 rDNA regions. The alignment is available in the Suppl. material 1. In the ITS phylogeny, eight new lineages are observed (Fig. 1). The lineages, when represented by multiple samples, received high support values (99–100%). We describe six of these as new species: 1) *T. huuskonenii* sp. nov., represented by four specimens, 2) *T. pseudoauruntii* sp. nov. with two specimens, 3) *T. sallaense* sp. nov., with one specimen 4) *T. toskalharjiense* sp. nov., including six specimens, 5) *T. declivum* sp. nov., with nine specimens and 6) *T. mendax* sp. nov., with four specimens. Based on morphological characters, the first four species belong to the *T. auruntii* complex, while *T. declivum* and *T. mendax* are members of the *T. incavatum* complex. The two remaining lineages, both represented by only one specimen, are named here as *Thelidium* sp. 1 and *Thelidium* sp. 2. *Thelidium* sp. 1 resembles *T. auruntii*, whereas *Thelidium* sp. 2 is morphologically similar to *T. incavatum*. Both lineages most likely represent new species, although more specimens with similar morphology are needed before their status can be discussed further.

Based on the ITS phylogeny, the study species belong to the *Thelidium* group in the sense of Gueidan et al. (2009). Neither of the two morphocomplexes is resolved monophyletic. Instead, the ingroup is divided into three main subclades. The first subclade is strongly supported (93%) and includes *T. methorium*, *T. pertusatii* and *T. pyrenophorum* in addition to the three species of the *T. auruntii* morphocomplex, i.e., T. *auruntii*, *T. pseudoauruntii* sp. nov. and *T. sallaense* sp. nov. An unnamed lineage *Thelidium* sp. 1 belongs to this clade as well. *Thelidium auruntii* and *T. pseudoauruntii* form a strongly supported group (89%) and *T. sallaense* is resolved as basal to them, although with low support (59%).

The second subclade remains unsupported and includes nine species in addition to one unnamed *Verrucaria* obtained from Genbank. *Thelidium declivum* sp. nov. and *T. mendax* sp. nov., both belonging to the *T. incavatum* morphocomplex, form a strongly supported clade within this group. The second group also includes two new species, *T. huuskonenii* and *T. toskalharjiense*, which morphologically resemble *T. auruntii* and its allies.

The remaining two lineages of the *T. incavatum* morphocomplex, i.e., *T. incavatum* and *Thelidium* sp. 2, are clustered in the third subclade. The subclade remains unsupported and includes also four *Polyblastia*, two unidentified *Polyblastia*, two *Thelidium* and nine *Verrucaria* species, all retrieved from GenBank.

The results show low infraspecific variation in the ITS sequences of the study species. All specimens of *T. declivum* (n = 9), *T. huuskonenii* (n = 4), *T. mendax* (n = 4) and *T. pseudoauruntii* (n = 2) have identical ITS sequences. Low variation (> 99% similarity) between all specimens is also found in other species with the exception of one specimen of *T. incavatum*, which has only 98.5% similarity with the other specimens belonging to the same species.

Most of the species are restricted to calcareous rocks of northern Finland. *Thelidium huuskonenii*, *T. toskalharjiense* and *T.* sp. 1 have been found only from the calcareous fells of Enontekiö in NE Finland; *T. declivum*, *T. pseudoauruntii* and *T. sallaense* only from the Oulanka area (parishes Kuusamo and/or Salla) in NE Finland. *Thelidium mendax* occurs in the Oulanka area with one locality in eastern central Finland. *Thelidium auruntii* occurs both in Enontekiö and the Kuusamo-Salla area. *Thelidium* sp. 2 has been found from one locality in SW Lapland. *Thelidium incavatum* is the only species with southern distribution in Finland, occurring widely in SW Finland. One separate locality is in central eastern Finland.

Discussion

The dominance of northern distribution within the study species may explain why most of them have remained undescribed. Only a few *Thelidium* species have been described from northern Europe and none from the calcareous fells. Particularly the crustose lichen flora of calcareous rocks in the fells of northern Finland is rather poorly known (Pykälä 2010a). Pyrenocarpous lichens in the calcareous fells of Sweden and

Norway are also poorly collected (Magnusson 1952). It remains to be studied whether our new species occur more widely in the Scandinavian Mountains and in other northern mountains.

Species restricted to calcareous fells and/or the Oulanka area may be particularly sensitive to climate change. Northern lichen species may not be directly limited by temperatures but may be poor competitors, sensitive to the increase of other species benefitting from increased temperatures, particularly vascular plants (Alatalo et al. 2017; Greiser et al. 2021). For such species, retarding the dispersal of more southern species to the north is needed as a conservation measure of northern species against climate change (Pykälä 2017).

A considerable number of new species in the study group are congruent with the previous studies of Verrucariales in Finland (Pykälä and Myllys 2016; Pykälä et al. 2019, 2020). This study and earlier studies suggest that the number of species in Verrucariales in northern Europe is much higher than is presently known. We could find previously published names for only two of the species. This suggests that Fennoscandian and Central European species composition of the group under study differs greatly from each other. Similar results have been obtained among other previously studied groups of Verrucariales (e.g., Savić and Tibell 2012; Pykälä et al. 2017a, b, 2019, 2020).

Taxonomy

The species descriptions are based on the sequenced specimens collected in Finland.

Thelidium auruntii (A. Massal.) Kremp., Denkschr. Kgl. Bayer. Bot. Ges. 2(4): 248 (1861).

Verrucaria auruntii A. Massal., Symmict. Lich. 77. (1855). Basionym.

Type. [Italy] ad saxa dolomitica in opp. Auronzo (Col della Favola) (VER!).

Description. Prothallus not visible. Thallus pale brownish grey to pale greyish brown, rarely medium brown, continuous to rimose, rarely areolate, up to 0.2 mm thick, in one specimen surrounded by one dark line, algal cells c. 6–11 µm. Perithecia 0.21–0.38 mm in diam., 1/2–3/4-immersed, not leaving pits to leaving shallow pits; c. 60–160 perithecia / cm^2. Ostiole dark, plane to depressed, c. 20–50 µm wide, ostiolar depression up to 120 µm wide. Involucrellum apical, exceeding half of the exciple to rarely to the exciple base level, 30–80 µm thick, appressed to the exciple or to clearly diverging from it. Exciple 0.16–0.29 mm, wall pale to dark brown (usually brown), c. 17–20 µm thick. Periphysoids c. 20–40(–50) × 1.5–2 µm. Asci c. 62–72 × 26–32 µm, 8-spored. Ascospores 0–1-septate, (20.3–)24.5–26.9–29.2(–32.1) × (9.2–)10.6–11.5–12.4(–13.3) µm (n = 86).

Habitat and distribution. The species occurs in northern Finland in Enontekiö, Kuusamo and Salla parishes on dolomite rock outcrops, boulders, stones and pebbles. Several collections come from the calcareous fells of Saana and Toskalharji in Enontekiö. In the biogeographical province Koillismaa, the species is very rare, and it has been confirmed only from two localities (one in Kuusamo and one in Salla). The species grows mostly on dry sun-exposed calcareous rocks. However, some localities on river and brook shores are probably periodically submerged.

Notes. The Finnish specimens are included in *T. auruntii*, because no clear morphological differences between the type of *T. auruntii* and the Finnish specimens were found. However, the type has slightly shorter spores: 20–26 × 10–14 μm. The type of *T. auruntii* is from the Dolomites in northern Italy. It is possible that *T. auruntii* is an arctic-alpine species. Sequences from the Dolomites are needed to confirm whether the Finnish specimens are conspecific with *T. auruntii*.

Pykälä (2007) reported the species as *T. pyrenophorum* (Ach.) Körb. from Finland, but the specimens differ morphologically from *T. pyrenophorum* (type: Helvetia, H-ACH-685!). The type of *T. pyrenophorum* differs in larger perithecia: 0.35–0.7 mm. According to our ITS phylogeny, the two species are rather closely related (Fig. 1) if the GenBank specimen of *T. pyrenophorum* from Sweden is correctly identified. *Thelidium methorium* (Nyl.) Hellb. is characterised by large perithecia, thick involucrellum, larger spores (mean 34 × 14 μm) and occurrence on siliceous rocks (Thüs and Nascimbene 2008; Orange 2013). *Thelidium pertusatii* (Garov.) Jatta resembles *T. methorium* but has a very thick involucrellum (110–170 μm thick) (Thüs and Nascimbene 2008). The differences between closely related *T. pseudoauruntii* and *T. sallaense* are discussed below.

Several other *Thelidium* species are morphologically rather similar to *T. auruntii*. *Thelidium incinctum* (Vain.) Vain. (Finland, Kuusamo, Porontimajärvi, 12.8.1867, F.Sileń (H!, H-NYL6941, syntypes)) differs in thicker involucrellum (70–80 μm thick), larger spores (25–38 × 12–15 μm) and occurrence on siliceous rock. It is only known from the type collection. *Thelidium bubulcae* (A.Massal.) Arnold described from Italy (ad saxa ipocretacea (Preapura) M. Bolca (M. Colle), 1854, A.Massalongo (VER!); Veneto; ad saxa arenacea oppidi Bolca (M. Colle) in prov. Veronensi Massalongo, Anzi: Lich. Rar. Veneti 136 (UPS-L-686416!, syntypes?) is rather similar to *T. auruntii* but may possibly differ by shorter, apical involucrellum and areolate thallus. *Thelidium lacromense* Zschacke ([Croatia] ins. Lacroma: An frei liegenden Gestein, c. 10 m, Kalk, 11.9.1907, A.Latzel (PRM-858048!, syntype)) is morphologically similar to *T. auruntii*, but the type locality is close to sea level in Croatia and thus not likely to belong to the same species as the Finnish material of *T. auruntii*. *Thelidium athallinum* Servít (Slovakia, Vysoké Tatry, monte Tokárna, supra saxa conglom., 1100–1200 m, 1925, Suza (PRM-858571!, syntype)) differs in thicker involucrellum (c. 80–100 μm thick).

Other specimens examined. Finland, Koillismaa, Salla, Oulanka National Park, 400 m N of Savilampi, shore of river Savinajoki, dolomite rock outcrop, on NE-slope, 177 m a.s.l, 66°25'N, 29°10'E, 13 August 2009, J.Pykälä 36339 (H); Kuusamo, Oulanka National Park, Mataraniemi, shore of Oulankajoki river, treeless stony river shore, on dolomite stones, 145 m a.s.l, 66°22'N, 29°20'E, 26 August 2011, J.Pykälä

Figure 1. Phylogenetic relationships of the studied species. Strict consensus based on ITS data set with bootstrap values (>50%) at nodes. New species described in this study are indicated in bold.

45171 (H); Enontekiön Lappi, Enontekiö, Porojärvet, Toskalharji, Toskaljärvi N, fell, dried old brook bottom, stony bottom, on dolomite pebbles, 707 m a.s.l., 69°11'N, 21°26'E, 3 August 2011, J.Pykälä 43414 (H); Enontekiö, Porojärvet, Toskalharji, Toskaljärvi N, fell, brook, W-shore, dolomite rock, outcrop, on N-slope, 710 m a.s.l, 69°11'N, 21°26'E, 3 August 2011, J.Pykälä 43446 (H); Enontekiö, Porojärvet, Toskalharji, Toskaljärvi N, fell, brook, W-shore, dolomite rock outcrop, on dolomite stones,

710 m a.s.l, 69°11'N, 21°26'E, 3 August 2011, J.Pykälä 43470 (H); Enontekiö, Porojärvet, Toskalharji, Toskaljärvi N, gentle SE-slope, alpine grassland, on dolomite boulder, 705 m a.s.l, 69°11'N, 21°26'E, 3 August 2011, J.Pykälä 43829 (H); Enontekiö, Kilpisjärvi, Saana, nature reserve, W-part, fell, dolomite rock outcrop, on SW-facing wall, 695 m a.s.l, 69°03'N, 20°48'E, 9 August 2011, J.Pykälä 43905 (H).

Thelidium declivum **Pykälä & Myllys, sp. nov.**
MycoBank No: 846775
Figs 2A, 3H, I

Diagnosis. Differing from *T. incavatum* by the perithecia often less immersed in rock, the involucrellum present in most perithecia and the exciple wall is thicker, most difficult to separate from *T. mendax* but the involucrellum on average is shorter.

Type. Finland, Koillismaa, Salla, Oulanka National Park, 400 m N of Savilampi, shore of river Savinajoki, dolomite rock outcrop, on NE-slope, scarce, 178 m a.s.l, 66°25'N, 29°10'E, 13 August 2009, J.Pykälä 36334 (H-9204893, holotype, UPS, isotype, GenBank accession number: OP901851).

Description. Prothallus not visible. Thallus white, grey or pale brown, endolithic to rarely thinly epilithic, algal cells c. 5–8 µm, in one specimen (type) surrounded by dark lines. Perithecia 0.12–0.44 mm in diam., 1/2–1-immersed, often surrounded by thalline collar, leaving shallow to usually deep pits; c. 20–80 perithecia / cm^2. Ostiole pale to dark, plane to depressed, c. 20–50 µm wide. Involucrellum absent, apical or covering half of the exciple, 0–70 µm thick, appressed to the exciple or clearly diverging from it. Exciple 0.22–0.38 mm, wall dark brown to black, c. 25–40 µm thick, apex may be thickened to 50–70 µm thick. Periphysoids c. 30–50 × 1.5–2.5 µm. Asci c. 91–132 × 31–48 µm, 8-spored. Ascospores (1–2–)3-septate, few spores submuriform with 5–6(–8) cells, (32.3–)35.3–37.8–40.4(–44.4) × (12.6–)14.0–15.0–16.1(–17.3) µm (n = 69).

Habitat and distribution. The species occurs in NE Finland, in the parishes of Kuusamo and Salla, on dolomite rock outcrops and boulders. The species may prefer rather shady habitats. Most localities are close to river shores.

Etymology. The species prefers steep rock outcrops.

Notes. This species was previously reported from Finland as *T. larianum* A. Massal. (Pykälä 2010b). The type specimen of *T. larianum* A. Massal. (in calcaris ubique, Garovaglio, VER!) is in poor condition, and thus, the identity of the species cannot be solved. According to Zschacke (1934), the spore size of *T. larianum* is smaller: 25–36 × 11–15 µm than the size in the Finnish specimens. The protologue (Massalongo 1855): "in circa Larium Lacum ad saxa calcareo-bituminosa Clar. Prof. Garov.", i.e., the locality is close to Lake Como, and the collector is S. Garovaglio. Thus, the climatic conditions of the type locality are likely to strongly differ from those in NE Finland, and it is likely that the Finnish specimens do not belong to *T. larianum*. Based on the Finnish distribution, it could be assumed that *T. declivum* may be an eastern species, which has its main distribution in Russia and/or in North America.

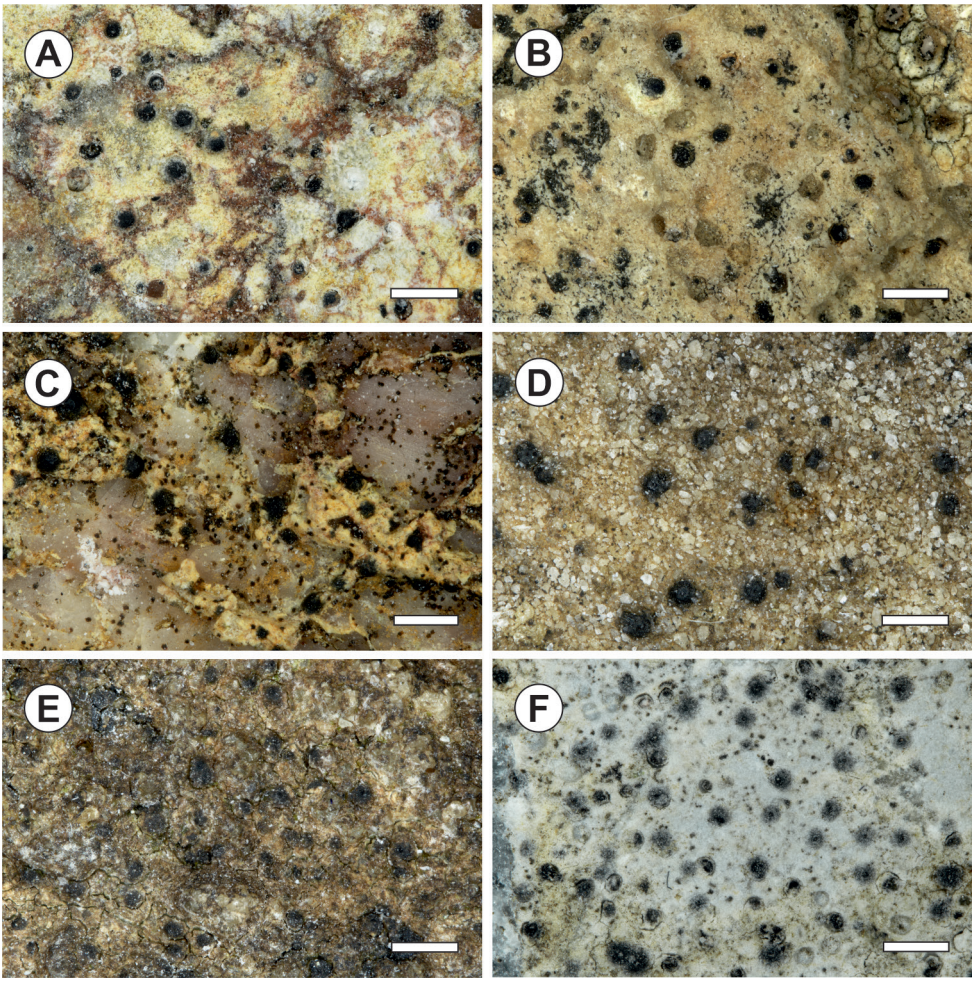

Figure 2. A *Thelidium declivum* (holotype) **B** *T. huuskonenii* (holotype) **C** *T. mendax* (holotype) **D** *T. pseudoauruntii* (holotype) **E** *T. sallaense* (holotype) **F** *T. toskalharjiense* (holotype). Scale bars: 1 mm (**A–C, E, F**); 0.5 mm (**D**).

Polyblastia torrentis Servít (Sweden. Torne Lappmark: Jukkasjärvi par., Abisko, Regio subalpina by the torrent, alt. 400 m, 29.7.1921, A.H.Magnusson; UPS!, syntype) differs in less immersed perithecia (1/4–1/2-immersed) leaving shallow pits. Exciple may also be smaller (in studied perithecia c. 0.2–0.22 mm), but according to Servít (1953) the size of the exciple is c. 0.3 mm.

Thelidium declivum is difficult to separate from *T. incavatum* and the closely related *T. mendax*. *Thelidium incavatum* has predominantly fully immersed perithecia, and 3/4-immersed perithecia are usually overmature, whereas *T. declivum* has predominantly 3/4–immersed perithecia. Furthermore, the involucrellum is absent from most specimens of *T. incavatum*, whereas the involucrellum occurs in most perithecia, and in all studied specimens of *T. declivum*. *Thelidium incavatum* also has a thinner exciple

wall: c. 15–25 µm thick. *Thelidium mendax* may differ in longer involucrellum, but more material is needed to determine whether this character can be used to separate the species from *T. declivum*.

Other specimens examined. Finland, Koillismaa, Kuusamo, Oulanka, Putaanoja, 500 m W-NW of Hautala, dolomite rock outcrop, beneath N-facing wall, on boulder, 228 m a.s. l., 66°22'N, 29°25'E, 9 August 2009, J.Pykälä 35996 (H); Salla, Oulanka National Park, Savikoski 300 m N, shore of lake Savilampi, calciferous (dolomite) schistose rock outcrop, on N-facing wall, 175 m a.s.l, 66°25'N, 29°10'E, 10 August 2010, J.Pykälä 39640 (H); Salla, Oulanka National Park, Savilamminniemi, shore of lake Savilampi, cliff, calciferous (dolomite) schistose rock outcrop, on S-facing wall, 172 m a.s.l, 66°25'N, 29°10'E, 12 August 2010, J.Pykälä 39780b (H); Kuusamo, Oulanka, Putaanoja, 500 m W-NW of Hautala, dolomite rock outcrop, on NE-facing wall, 230 m a.s.l., 66°22'N, 29°25'E, 15 August 2010, J.Pykälä 39997 (H), 40037 (H), 40047 (H); Kuusamo, Oulanka National Park, Taivalköngäs, shore of Oulankajoki river, *Picea abies*-dominated herb-rich forest, dolomite rock outcrop, NE-slope, on dolomite boulder, 174 m a.s.l, 66°24'N, 29°11'E, 20 August 2011, J.Pykälä 44554 (H); Kuusamo, Oulanka National Park, Taivalköngäs, shore of Oulankajoki river, dolomite rock outcrop, on NW-facing wall, 165 m a.s.l, 66°24'N, 29°11'E, 25 August 2011, J.Pykälä 45123 (H).

Thelidium huuskonenii Pykälä & Myllys, sp. nov.

MycoBank No: 846776
Figs 2B, 3A, B

Diagnosis. Species morphologically rather similar to *T. auruntii*, but the spores smaller, perithecia often leaving deep pits, and the thallus predominantly endolithic.

Type material. ***Holotype.*** Finland, Enontekiön Lappi, Enontekiö, Kilpisjärvi, Saana, fell, steep NE-slope, dolomite rock outcrop, on NE-facing wall, abundant, 820 m a.s.l, 69°02'N, 20°51'E, 11 August 2011, J.Pykälä 44167 (H9204900, GenBank accession number: OP901862).

Description. Prothallus not visible. Thallus white to grey, endolithic to thinly epilithic, only surrounding perithecia, algal cells, c. 4–7 µm, in one specimen surrounded by one dark line. Perithecia 0.18–0.32 mm in diam., (1/2–)3/4–1-immersed, leaving shallow to deep pits; c. 80–120 perithecia / cm^2. Ostiole pale to dark, plane to depressed, c. 20–40 µm wide. Involucrellum absent, apical or covering half of the exciple, 0–60 µm thick, appressed to the exciple or clearly diverging from it. Exciple 0.20–0.28 mm, wall dark brown to black, c. 15–20 µm thick, apex may be thickened to 50–80 µm thick. Periphysoids c. 20–45 × 1.5–2 µm, branching. Asci c. 58–74 × 22–25 µm, 8-spored. Ascospores (0–)1-septate, (16.4–)18.2–20.7–23.2(–27.6) × (8.0–)8.6–9.9–11.2(–14.4) µm (n = 69).

Habitat and distribution. Four specimens have been confirmed by sequencing, but more than twenty morphologically similar specimens have been collected from the calcareous fells of Saana and Toskalharji. The species seems to occur only in northern

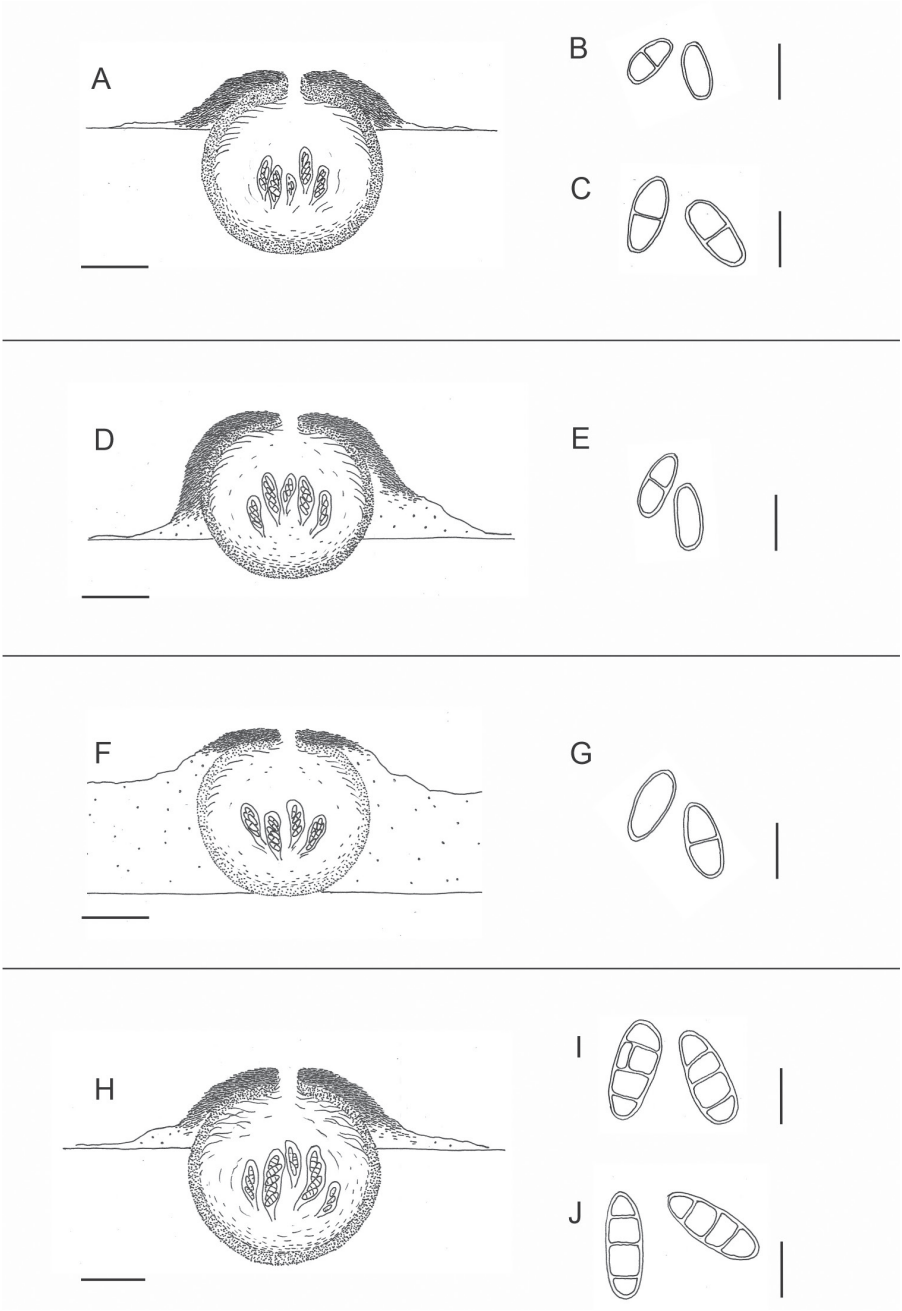

Figure 3. Drawn anatomical features of the newly described *Thelidium* species. Represented perithecial features are similar between *T. huuskonenii* and *T. toskalharjiense*, as well as between *T. declivum* and *T. mendax*; therefore, they are shown combined. Spores are represented as intermediate size for all species **A** perithecia of *T. huuskonenii* and *T. toskalharjiense* combined **B** spores of *T. huuskonenii* **C** spores of *T. toskalharjiense* **D** perithecium of *T. pseudoauruntii* **E** spores of *T. pseudoauruntii* **F** perithecium of *T. sallaense* **G** spores of *T. sallaense* **H** perithecia of *T. declivum* and *T. mendax* combined **I** spores of *T. declivum* **J** spores of *T. mendax*. Scale bars for perithecia are 100 µm, and for spores 20 µm. Illustration: A. Kantelinen

Finland, in Enontekiö on fells on dolomite rock outcrops, boulders, stones and pebbles. It grows on southern and northern slopes and on rather flat surfaces. The altitudinal range is 705–890 m a.s.l.

Etymology. The species is named after A.J.Huuskonen, the Finnish amateur lichenologist, who most intensively collected lichens from the Enontekiö area.

Notes. The species differs from *T. auruntii* in smaller spores, perithecia often leaving deep pits and thinner, predominantly endolithic, thallus. The species has been previously reported from Finland as *T. decussatum* (Pykälä 2010a). The Finnish specimens have similar perithecia and involucrellum as *T. decussatum*. However, *T. decussatum* ([Germany] Trier, 1862, Mezler, Rabenhorst Lichenes Europaei 646 (UPS!, syntype)) has a rimose thallus and the spores may be slightly larger (20–25 × 10–11 µm). Furthermore, the type locality is in a temperate zone in lowland Germany. Phytogeographically, it is unlikely that such species would occur only in fells in the northwestern most part of Finland. *Thelidium stenosporum* Servít (Slovakia: Bielské Tatry: in rup. calc. in convalle Dominův důl, … m. Havran … norg, 1700 m, 1937, Suza (PRM-858497!, syntype)) has smaller perithecia and narrower spores. *Thelidium bubulcae* (A.Massal.) Arnold (syntypes: VER, UPS-L-686416!)) has larger rimose to areolate thallus, larger perithecia (0.2–0.37 mm) and larger spores: 20–27 × 9–13 µm. *Thelidium polycarpum* Servít (Montenegro, Lovčen, Ljubin potok, 1230 m, 1929, Servít (PRM-858491!, holotype)) has smaller perithecia (0.13–0.23 mm) and spores (15–23 × 8–9 µm). *Thelidium klementii* Servít has rather thick rimose to areolate thallus and slightly larger spores and is only known from a temporarily inundated calcareous rock (Thüs and Nascimbene 2008).

Other specimens examined. Finland. Enontekiön Lappi, Enontekiö, Kilpisjärvi, Saana fell, Saana nature reserve, low arctic zone, on SW-facing wall of dolomite rock outcrop, 880 m a.s.l., 69°02'N, 20°51'E, 27 July 2007, J.Pykälä 31576 (H); Enontekiö, Porojärvet, Toskalharji, Toskaljärvi N, fell, dolomite rock outcrop, on S-slope, 730 m a.s.l, 69°12'N, 21°26'E, 2 August 2011, J.Pykälä 43243 (H); Enontekiö, Porojärvet, Toskalharji, Toskaljärvi N, fell, dolomite rock outcrop, on dolomite pebbles, 735 m a.s.l, 69°12'N, 21°26'E, 2 August 2011, J.Pykälä 43246 (H).

Thelidium incavatum Nyl. & Mudd, Man. Brit. Lich. 295 (1861)

= *Thelidium anisomerum* Hellb., Kgl. Svensk. Vet. Akad. Handl. 9(11):34 (1871). Type. Sweden, Gotland, Linde klint, C.Stenhammar (S-L-347!); Gotland in colle calcareo ad Linde, Stenhammar 34 (S-L-250!), syntypes.

= *Thelidium decipiescens* Vain., Acta Soc. Fauna Flora Fenn. 49(2): 129 (1921). Type. Finland, Ab, Finby [= Varsinais-Suomi, Salo, Särkisalo], Förby, in rupe calcaria, 20 August 1920, E.Vainio (TUR-V!).

= ?*Polyblastia sepulta* A.Massal., Lotos 6: 81 (1856). Type: [Italy,] Circa Veronam ad saxa eocenica, A.Massalongo (VER!, syntype).

Type. [England] 282. Bilsdale, Yorkshire, W.Mudd (M-0207325!, syntype?).

Description. Prothallus not visible. Thallus white to grey, endolithic, in two specimens partly epilithic, slightly rimose, up to 0.1–0.15 mm thick, algal cells c. 4–6 µm. Perithecia 0.06–0.36 mm in diam., (1/2–)3/4–1-immersed, often thalline covered except apex, leaving deep pits; c. 20–160 perithecia / cm^2. Ostiole pale to dark, plane, c. 20–40 µm wide. Involucrellum absent or apical, c. 30–60(–90) µm thick. Exciple 0.16–0.39 mm, wall dark brown to black, c. 15–25 µm thick, often with ostiolar neck, often pear-shaped. Periphysoids c. 40–50 × 1.5–2 µm. Asci c. 93–122 × 33–52 µm, 8-spored. Ascospores 3-septate, few spores submuriform with 5–7 cells, (32.3–)37.5–40.9–44.3(–49.4) × (12.2–)13.7–14.9–16.2(–18.1) µm (n = 78), rarely with a perispore c. 1 µm thick.

Habitat and distribution. The species occurs in many localities in SW Finland on calcareous rocks and in lime quarries. It occurs on south- as well as on north-facing walls and on gentle slopes. More rarely, it grows on boulders, stones and pebbles. At present, more than 50 localities are known. Most localities are in the hemiboreal vegetation zone, a few in the southern boreal vegetation zone, only some tens of kilometres north of the limit of the hemiboreal zone. However, one separate locality occurs in Kuopio (former Juankoski) in eastern central Finland. *Thelidium incavatum* may be the most common species of *Thelidium* in SW Finland, together with *T. minutulum* Körb.

Notes. The observed syntype of *Polyblastia sepulta* is somewhat similar to *T. incavatum*, and *P. sepulta* may be the oldest name available for the species. However, better material of *P. sepulta* is needed to confirm it. Furthermore, it is uncertain whether *T. incavatum* is the correct name for the Finnish specimens. The syntype in M differs in rimose thallus. However, several localities have been included in the protologue, and the specimen in M may be untypical for *T. incavatum*. The Finnish specimens fit well with the description of *T. incavatum* by Orange (2013).

If the Finnish specimens do not belong to *T. incavatum*, there are two other putative younger names available for them. *Thelidium decipiescens* was described from SW Finland (Vainio 1921) and is morphologically similar to the sequenced Finnish specimens of *T. incavatum*. Already Vainio (1921) considered *T. decipiescens* to be similar to some material of *T. incavatum*. *Thelidium anisomerum* Hellb., described from Sweden, is also similar to *T. incavatum*.

Thelidium bavaricum Dalla Torre & Sarnth. has broader spores (Germany, Bavaria, an den aus den begrasten Boden hervorstehenden Dolomitblöcken oberhalb des Tiefenthales bei Eichstätt, April 1859, Arnold, in Arnold: Lich.. Exs. 87 (UPS-L-165297!, syntype): 30–48 × 15–20 µm, and submuriform spores may be more frequent.

The ITS sequence of the *T. incavatum* specimen, collected in the separate locality in eastern Finland, differs from the other sequenced specimens (98.5% similarity). The specimen also differs morphologically from the other specimens by less immersed perithecia (1/4–1/2-immersed) and thicker involucrellum (c. 70–90 µm thick). The spores may also be slightly shorter: 28.1–35.7 x 12.8–15.4 µm (n=15). It may represent a separate species but is now included in *T. incavatum*, awaiting more material.

Other specimens examined. Finland, Varsinais-Suomi, Parainen (Korppoo), Åfvensår, Kälklot island, calcareous rock outcrop on shore of the Baltic Sea, E-slope,

on pebbles, 5 m a.s.l., 60°18'N, 21°31'E, 27 July 2009, J.Pykälä 35282 (H); Salo (Särkisalo), Förby, 200 m S of lime factory, calcareous rock outcrop, on SW-slope, 60°05'N, 22°52'E, 8 September 2009, J.Pykälä 36857 (H); Salo (Särkisalo), Förby, 200 m S of lime factory, abandoned lime quarry, on 40 cm high NW-facing wall, 18 m a.s.l, 60°05'N, 22°52'E, 8 September 2009, J.Pykälä 36867 (H); Parainen (Iniö), Söderby, Biskopsö island, calcareous rock outcrop on shore of the Baltic Sea, on N-slope, 8 m a.s.l, 60°20'N, 21°28'E, 9 June 2010, J.Pykälä 37971 (H); Parainen (Korppoo), Elfsjö, Stora Limskär island, shallow abandoned lime quarry, on N-facing wall, 6 m a.s.l., 60°09'N, 21°26'E, 21 June 2010, J.Pykälä 38227 (H); Parainen (Houtskari), Björkö, Östra Långholm, Norrnäs, siliceous rock outcrop on shore of the Baltic Sea, NW-slope, on narrow calcareous vein, scarce, 9 m a.s.l., 60°15'N, 21°26'E, 29 June 2010, J.Pykälä 38399 (H); Parainen, Petteby, Kalkudden, abandoned lime quarry, on W-facing wall, 18 m a.s.l., 60°17'N, 22°10'E, 5 October 2011, J. Pykälä 46459 (H); Uusimaa, Hyvinkää, Myllykylä, Kalkkikallio, abandoned lime quarry, on N-facing wall, 100 m a.s.l, 60°36'N, 25°03'E, 7 July 2009, J.Pykälä 34722 & H. Rämä (H); Pohjois-Karjala, Kuopio (Juankoski), Siikajärvi, Huosiaisniemi, nature reserve, dolomite rock outcrop on shore of lake Ala-Siikajärvi, on gentle NE-slope, scarce, 97 m a.s.l., 63°12'N, 28°21'E, 26 July 2011, J.Pykälä 42871(H).

Thelidium mendax **Pykälä & Myllys, sp. nov.**
MycoBank No: 846777
Figs 2C, 3H, J

Diagnosis. Species morphologically rather similar to *T. declivum* and *T. incavatum*, but the involucrellum is on average longer.

Type material. ***Holotype.*** Finland, Koillismaa, Salla, Oulanka National Park, Pikkuköngäs, shore of river Oulankajoki, high cliff, calciferous (dolomite) schistose rock outcrop, W-facing wall, on dolomite patch, 180 m a.s.l, 66°25'N, 29°08'E, 4 August 2010, J.Pykälä 39179 (H-9206536, GenBank accession number: OP901872).

Description. Prothallus not visible. Thallus white to pale brown, endolithic to weakly rimose, algal cells, c. 4–7 µm. Perithecia 0.18–0.38 mm in diam., 1/2–1-immersed, often surrounded by thalline collar, leaving shallow to deep pits; c. 20–60 perithecia / cm^2. Ostiole pale to dark, plane, c. 20–60 µm wide. Involucrellum apical to exceeding half of the exciple, c. 40–80 µm thick, appressed to the exciple or clearly diverging from it. Exciple 0.18–0.36 mm, wall dark brown to black, rarely pale, c. 20–30 µm thick. Periphysoids c. 40–60 × 1.5–2.5 µm. Asci c. 90–128 × 31–43 µm, 8-spored. Ascospores 3-septate, (34.8–)36.1–40.1–44.1(–51.0) × (11.8–)12.8–13.4–14.0(–14.9) µm (n = 48), perispore 1–1.5 µm thick in few spores.

Habitat and distribution. The species is known from three localities, two in NE Finland, in the parishes Kuusamo and Salla, and one in Juuka in central eastern Finland. *Thelidium mendax* grows on calcareous rocks and calciferous (dolomite) schistose rocks. Two collection sites are affected by spring flooding and may periodically be submerged.

Etymology. The species is easily misidentified.

Notes. Based on the ITS phylogeny, this species is closely related to *T. declivum*. It is also morphologically difficult to separate from that species. *Thelidium mendax* has, on average, longer involucrellum than in *T. declivum*. *Thelidium mendax* is here kept separated from *T. declivum* because this solution received high support value in the ITS phylogeny (99%). Within the species *T. declivum* and *T. mendax* have identical ITS sequences and the species have a clear barcoding gap (3% difference).

Polyblastia torrentis (Sweden. Torne Lappmark: Jukkasjärvi par., Abisko, Regio subalpina by the torrent, alt. 400 m, 29 July 1921, A.H.Magnusson (UPS!, syntype)) differs in less immersed perithecia (1/4–1/2-immersed) and thinner involucrellum (c. 30–40 µm thick).

Other specimens examined. Finland, Koillismaa, Kuusamo, Juuma, Oulanka National Park, Jäkälävuoma, gorge, calciferous (dolomite) schistose rock outcrop, on bottom, shore of a pond, on dolomite coated stone, 200 m a.s.l., 66°15'N, 29°26'E, 16 August 2010, J.Pykälä 40152 (H); Pohjois-Karjala, Juuka, Petrovaara, Riihilahti S, calcareous rock outcrop, on W-facing wall, 190 m a.s.l, 63°09'N, 28°58'E, 13 July 2011, J.Pykälä 42502 (H), 42503 (H).

***Thelidium pseudoauruntii* Pykälä & Myllys, sp. nov.**
MycoBank No: 846779
Figs 2D, 3D, E

Diagnosis. Species morphologically rather similar to *T. auruntii*, but the spores are smaller and the perithecia tend to be less immersed.

Type material. ***Holotype*.** Finland, Kollismaa, Kuusamo, Oulanka National Park, Mataraniemi W, shore of Oulankajoki river, small dolomite rock outcrop, on SE-slope, 147 m a.s.l, 66°22'N, 29°20'E, 28 August 2011, J.Pykälä 45374 (H9220350, GenBank accession number: OP901877).

Description. Prothallus not visible. Thallus pale greyish brown to medium brown, endolithic to rimose, algal cells c. 5–7 µm, with one dark brown thalline line. Perithecia 0.18–0.36 mm in diam., 1/4–1/2-immersed, not leaving pits to leaving shallow pits; c. 50–140 perithecia / cm^2. Ostiole dark, depressed, c. 20–50 µm wide. Involucrellum covering half of the exciple, c. 40–70 µm thick, appressed to clearly diverging from the exciple. Exciple c. 0.17–0.24 mm, wall pale brown to usually dark brown, c. 15–20 µm thick. Periphysoids c. 20–25 × 2 µm. Asci c. 64–83 × 22–32 µm, 8-spored. Ascospores 0–1-septate, (21.3–)23.9–25.1–26.2(–26.6) × (8.6–)9.2–10.1–11.0(–12.2) µm (n = 23), perispore 1 µm thick present in some spores.

Habitat and distribution. The species is only known from the type locality on small dolomite rock outcrop on the rivershore. The locality is likely to be under water during spring floods. Potentially suitable habitats for the species may be very rare in Finland.

Etymology. The species resembles morphologically *T. auruntii* and is also closely related to the species based on the ITS sequences.

Notes. The species is closely related to *T. auruntii* and *T. sallaense*. Only two specimens are known and from the same locality. We prefer to treat *T. pseudoauruntii* as a species separate from *T. auruntii* because of high support value (100%) in the ITS phylogeny. Furthermore, there is a clear barcoding gap (3%) between the species. The species have also different distribution areas. *Thelidium pseudoauruntii* seems to be absent from the calcareous fells of NW Finland, i.e., from the main distribution area of *T. auruntii* in Finland. *Thelidium pseudoauruntii* may be an eastern species with the main distribution area in North America and/or Russia. The specimens of *T. pseudoauruntii* have smaller spores than in *T. auruntii* and *T. sallaense*. Furthermore, the perithecia are less immersed. However, more material is needed to determine whether the species differs unambiguously morphologically from the related species.

Other specimens examined. Finland, Koillismaa, Kuusamo, Oulanka National Park, Mataraniemi W, shore of Oulankajoki river, small dolomite rock outcrop, on dolomite stones, 145 m a.s.l., 66°22'N, 29°20'E, 28 August 2011, J.Pykälä 45371 (H).

***Thelidium sallaense* Pykälä & Myllys, sp. nov.**
MycoBank No: 846780
Figs 2E, 3F, G

Diagnosis. Species morphologically rather similar to *T. auruntii*, but the thalli may be more brown-pigmented.

Type material. ***Holotype*.** Finland, Koillismaa, Salla, Oulanka National Park, Savilampi 1,4 km NE, shore of Savinajoki river, river shore, on dolomite stone, 185 m a.s.l., 66°26'N, 29°11'E, 23 August 2011, J.Pykälä 44902 (H9220340, GenBank accession number: OP901878).

Description. Prothallus not visible. Thallus pale brown to medium brown, rimose, algal cells c. 5–8 µm. Perithecia 0.21–0.28 mm in diam., 3/4(–1)-immersed in thallus, not leaving pits; c. 60–80 perithecia / cm^2. Ostiole brown, plane to depressed, c. 20–60 µm wide. Involucrellum apical, c. 40–50 µm thick, slightly diverging from the exciple. Exciple c. 0.16–0.27 mm, wall pale to brown, K+ olive. Periphysoids c. 20–30 × 2 µm. Asci c. 67–83 × 25–32 µm, 8-spored. Ascospores (0–)1-septate, (26.3–)27.3–28.8–30.2(–31.1) × (12.0–)12.2–12.6–12.9(–13.4) µm (n = 12), perispore 1 µm thick present in some spores.

Habitat and distribution. The species is only known from the type locality growing on dolomite stone on a rivershore. The species is likely to be very rare and threatened in Finland.

Etymology. The name is according to the parish Salla from where the only known specimen has been collected.

Notes. More material is needed to solve whether the species can be morphologically separated from *T. auruntii*. It may differ from *T. auruntii* by a more clearly brown pigmented thallus.

Thelidium toskalharjiense **Pykälä & Myllys, sp. nov.**
MycoBank No: 846781
Figs 2F, 3A, C

Diagnosis. Species morphologically rather similar to *T. auruntii*, but the spores are larger, and the involucrellum is, on average, shorter and thinner.

Type material. ***Holotype.*** Finland, Enontekiön Lappi, Enontekiö, Porojärvet, Toskalharji, Toskaljärvi N, fell, stony lake shore, on dolomite stones, 705 m a.s.l., 69°11'N, 21°26'E, 3 August 2011, J.Pykälä 43398 (H9206484, GenBank accession number: OP901882).

Description. Prothallus not visible. Thallus grey to pale brownish grey, endolithic to thinly epilithic, rarely rimose, algal cells c. 5–8 µm, sometimes surrounded by dark lines. Perithecia 0.17–0.36 mm in diam., 1/2–3/4(–1)-immersed, leaving shallow to deep pits; c. 60–160 perithecia / cm^2. Ostiole pale to dark, plane, c. 20–30(–60) µm wide. Involucrellum apical to covering half of the exciple, 20–50 µm thick, appressed to the exciple or strongly diverging from it. Exciple c. 0.15–0.24 mm, wall dark brown to black, c. 20–30 µm thick. Periphysoids c. 20–30 × 2–2.5 µm. Asci c. 73–83 × 23–29 µm, 8-spored. Ascospores 1-septate, (22.4–)26.8–29.1–31.3(–35.5) × (11.8–)12.5–13.4–14.2(–16.1) µm (n = 91).

Habitat and distribution. The species occurs in the fell Toskalharji in northern Finland in Enontekiö within an area of three square kilometres and is divided into three subpopulations. It grows on dolomite boulders, stones and pebbles. Most specimens are from dolomite pebbles. It mostly grows on gentle slopes. The altitudinal range is 705–875 m a.s.l.

Etymology. The species has been found only in the Toskalharji area.

Notes. The species differs from *T. auruntii* by larger spores, but there is a considerable overlap in the spore size. The involucrellum is, on average, shorter and thinner, but few specimens of *T. auruntii* may have similar involucrellum to *T. toskalharjiense*. Nevertheless, based on ITS phylogeny, the species is not closely related to *T. auruntii*.

Other specimens examined. Finland, Enontekiön Lappi, Enontekiö, Porojärvet, Toskalharji, Toskalpahta fell, SW-slope, scree, on dolomite pebbles, 790 m a.s.l, 69°11'N, 21°29'E, 1 August 2011, J.Pykälä 43090 (H); Enontekiö, Porojärvet, Toskalharji, Toskaljärvi N, fell, gentle SE-slope, on dolomite boulder, 715 m a.s.l, 69°11'N, 21°26'E, 2 August 2011, J.Pykälä 43211 (H); Enontekiö, Porojärvet, Toskalharji, Toskaljärvi N, fell, gentle SW-slope, dolomite rock outcrop, on dolomite pebbles, 715 m a.s.l, 69°11'N, 21°26'E, 3 August 2011, J.Pykälä 43364 (H); Enontekiö, Porojärvet, Toskalharji, Toskaljärvi N, close by lake shore, gentle NE-slope, alpine grassland on dolomite stone, 706 m a.s.l, 69°11'N, 21°26'E, 7 August 2011, J.Pykälä 43848 (H); Enontekiö, Porojärvet, Toskalharji, Toskaljärvi N, close by lake shore, alpine grassland, gentle SE-slope, dolomite rock outcrop, on dolomite pebbles, 706 m a.s.l, 69°11'N, 21°26'E, 7 August 2011, J.Pykälä 43861 (H).

Thelidium sp. 1

Description. Prothallus not visible. Thallus whitish grey, endolithic. Perithecia 0.25–0.33 mm in diam., 1/4–1/2-immersed, leaving shallow pits; c. 50 perithecia / cm^2. Ostiole, tiny, dark, plane. Involucrellum almost to the exciple base, 30–50 µm thick, may thicken to the base to c. 50–60 µm thick, slightly diverging from the exciple. Exciple c. 0.17–0.25 mm, wall dark brown. Periphysoids c. 25–30 × 2 µm. Asci 8-spored. Ascospores 0–1-septate, 23–28 × 10–12 µm.

Habitat and distribution. The specimen has been collected from a dolomite rock outcrop on a fell in northern Finland in Enontekiö.

Notes. The specimen probably represents an undescribed species belonging to the *T. auruntii* complex. However, the specimen is quite small, and thus, better material is needed.

Specimen examined. Finland, Enontekiön Lappi, Enontekiö, Porojärvet, Toskalharji, Toskaljärvi N, fell, dolomite rock outcrop, on SW-slope, 715 m a.s.l., 69°11'N, 21°26'E, 2 August 2011, J.Pykälä 43208 (H).

Thelidium sp. 2

Description. Prothallus not seen. Thallus whitish grey, endolithic. Perithecia 0.17–0.26 mm, 3/4–immersed, leaving deep pits; c. 40–60 perithecia /cm^2. Ostiole dark, plane to depressed, c. 20–40 µm wide. Involucrellum absent. Exciple c. 0.26–0.32 mm, wall black, apex thickened.

Spores 3-septate, 30–37 x 16–18 µm.

Habitat and distribution. The only specimen has been collected from calcareous pebbles in a lime quarry spoil in SW Lapland.

Notes. The specimen is small. It is morphologically similar to *T. incavatum* and probably closely related to that species, although the relationship remains unsupported. The species may be undescribed but a better specimen is needed for type material.

Specimen examined. Finland, Kittilän Lappi, Kolari, Äkäsjokisuu, Mannajoki, former cement factory 200 m N-NW, lime quarry spoil, on calcareous pebbles, 165 m a.s.l, 67°27'N, 23°38'E, 16 August 2018, J.Pykälä 52038 (H).

Acknowledgements

The field work was done in the research project "Threatened lichens of calcareous rocks" (Grant number YTB059). The manuscript preparation was supported by the research project "Key habitats for red-listed lichens" (Grant number 700T-MTX003). Both projects belonged to the research programme of deficiently known and threatened forest species (PUTTE), financed by the Finnish Ministry of the Environment. DNA barcoding was supported by the Kone Foundation, the Finnish Cultural Foundation and the Academy of Finland through their grants to the Finnish Barcode of Life (FinBOL) and

the Finnish Biodiversity Information Facility (FinBIF). We would like to thank Diana Weckman for help in the laboratory work, and Pekka Malinen, from the Zoology Unit of the Finnish Museum of Natural History, for his help with the photos. The curators of the herbaria B, G, S, UPS and W are thanked for the specimen loans. We would also like to thank Andreas Beck, František Bouda, Francesco Di Carlo and Martin Westberg for their hospitality during the visits to M, PRM, VER and UPS, respectively. Herbarium visits were supported by a grant from Societas pro Fauna et Flora Fennica. Finally, thank you to Teuvo Ahti and Starri Heiðmarsson for their helpful comments on the manuscript.

References

Alatalo JM, Jägerbrand AK, Chen S, Molau U (2017) Responses of lichen communities to 18 years of natural and experimental warming. Annals of Botany 120(1): 159–170. https://doi.org/10.1093/aob/mcx053

Breuss O, Berger F (2012) Die Validierung von *Verrucaria finitima* und Bemerkungen über den Formenkreis von *Verrucaria tristis* (lichenisierte Ascomyceten, Verrucariaceae). Österreichische Zeitschrift für Pilzkunde 21: 117–126.

Ceynowa-Giełdon M (2007) *Thelidium rimosulum* (Verrucariaceae, lichenized Ascomycota), a new lichen species from Poland. Lichenologist (London, England) 39(3): 217–220. https://doi.org/10.1017/S0024282907006287

Edgar RC (2004) MUSCLE: Multiple sequence alignment with high accuracy and high throughput. Nucleic Acids Research 32(5): 1792–1797. https://doi.org/10.1093/nar/gkh340

Greiser C, Ehrlén J, Luoto M, Meineri E, Merinero S, Willman B, Hylander K (2021) Warm range margin of boreal bryophytes and lichens not directly limited by temperatures. Journal of Ecology 109(10): 3724–3736. https://doi.org/10.1111/1365-2745.13750

Gueidan C, Roux C, Lutzoni F (2007) Using a multigene phylogenetic analysis to assess generic delineation and character evolution in Verrucariaceae (Verrucariales, Ascomycota). Mycological Research 111(10): 1147–1168. https://doi.org/10.1016/j.mycres.2007.08.010

Gueidan C, Savić S, Thüs H, Roux C, Keller C, Tibell L, Prieto M, Heiðmarsson S, Breuss O, Orange A, Fröberg L, Amtoft Wynns A, Navarro-Rosinés P, Krzewicka B, Pykälä J, Grube M, Lutzoni F (2009) Generic classification of the Verrucariaceae (Ascomycota) based on molecular and morphological evidence: Recent progress and remaining challenges. Taxon 58(1): 184–08. https://doi.org/10.1002/tax.581019

Magnusson AH (1952) Lichens from Torne Lappmark. Arkiv för Botanik, serie 2 2(2): 45–249.

Massalongo A (1855) Symmicta lichenum novorum vel minus cognitorum. Typis Antonellanis, Veronae.

Orange A (2013) British and Other Pyrenocarpous Lichens. Department of Biodiversity and Systematic Biology, National Museum of Wales, 250 pp. https://www.museum.wales/media/13849/Orange-A-2013-British-and-other-pyrenocarpous-lichens.pdf

Orange A (2014) Two new or misunderstood species related to *Verrucaria praetermissa* (Verrucariaceae, lichenized Ascomycota). Lichenologist (London, England) 46(5): 605–615. https://doi.org/10.1017/S0024282914000176

Orange A (2020) The *Verrucaria aethiobola* group (lichenised Ascomycota, Verrucariaceae) in North-west Europe. Phytotaxa 459(1): 1–15. https://doi.org/10.11646/phytotaxa.459.1.1

Pykälä J (2007) Additions to the lichen flora of Finland. II. Calcareous rocks and associated soils in Lohja. Graphis Scripta 19: 17–32.

Pykälä J (2010a) Notes on the lichen flora of Saana and Malla fells in northern Finland. Memoranda Societatis Pro Fauna et Flora Fennica 86: 34–42.

Pykälä J (2010b) Additions to the lichen flora of Finland. V. Graphis Scripta 22: 54–62.

Pykälä J (2017) Relation between extinction and assisted colonization of plants in the arctic-alpine and boreal regions. Conservation Biology 31(3): 524–530. https://doi.org/10.1111/cobi.12847

Pykälä J, Myllys L (2016) Three new species of *Atla* from calcareous rocks (Verrucariaceae, lichenized Ascomycota). Lichenologist (London, England) 48(2): 111–120. https://doi.org/10.1017/S0024282915000523

Pykälä J, Launis A, Myllys L (2017a) Four new species of *Verrucaria* from calcareous rocks in Finland Lichenologist 49(1): 27–37. https://doi.org/10.1017/S0024282916000542

Pykälä J, Launis A, Myllys L (2017b) *Verrucaria ahtii*, *V. oulankaensis* and *V. vitikainenii*, three new species from the *Endocarpon* group (Verrucariaceae, lichenized Ascomycota). Lichenologist (London, England) 49(2): 107–116. https://doi.org/10.1017/S0024282916000694

Pykälä J, Launis A, Myllys L (2018) *Verrucaria tenebrosa* (Verrucariaceae), a new lichen species from Finland and Norway, and notes on the taxonomy of epiphytic taxa belonging to the *V. hydrophila* complex. Phytotaxa 361(2): 211–221. https://doi.org/10.11646/phytotaxa.361.2.6

Pykälä J, Launis A, Myllys L (2019) Taxonomy of the *Verrucaria kalenskyi* – *V. xyloxena* species complex in Finland. Nova Hedwigia 109(3–4): 489–511. https://doi.org/10.1127/nova_hedwigia/2019/0553

Pykälä J, Kantelinen A, Myllys L (2020) Taxonomy of *Verrucaria* species characterised by large spores, perithecia leaving pits in the rock and a pale thin thallus in Finland. MycoKeys 72: 43–92. https://doi.org/10.3897/mycokeys.72.56223

Savíc S, Tibell L (2008) *Atla*, a new genus in the Verrucariaceae. Lichenologist 40(4): 269–282. https://doi.org/10.1017/S0024282908007512

Savíc S, Tibell L (2012) *Polyblastia* in Northern Europe and the adjacent Arctic. Symbolae Botanicae Upsalienses 36(1): 1–69.

Servít M (1953) Nové druhy Verrucarií a příbuzných rodu. Species novae Verrucariarum et gene-rum affinium. Rozpravy Československé Akademie Věd 63(7): 1–33.

Stamatakis A (2014) RAxML version 8: A tool for phylogenetic analysis and post-analysis of large phylogenies. Bioinformatics 30(9): 1312–1313. https://doi.org/10.1093/bioinformatics/btu033

Thüs H, Nascimbene J (2008) Contributions toward a new taxonomy of Central European freshwater species of the lichen genus *Thelidium* (Verrucariales, Ascomycota). Lichenologist 40(6): 499–521. https://doi.org/10.1017/S0024282908007603

Tibell S, Tibell L (2015) Two new species of *Atla* (Verrucariaceae). Lichenologist 47(2): 93–98. https://doi.org/10.1017/S0024282915000018

Vainio EA (1921) Lichenographica Fennica. I. Pyrenolichenes. Acta Societatis pro Fauna et Flora Fennica 49(2): 1–274.

White TJ, Bruns T, Lee S, Taylor J (1990) Amplification and direct sequencing of fungal ribosomal DNA genes for phylogenetics. In: Innis MA, Gelfand DH, Sninsky JJ, White TJ (Eds) PCR Protocols: a Guide to Methods and Applications. Academic Press, San Diego, 315–322. https://doi.org/10.1016/B978-0-12-372180-8.50042-1

Zschacke H (1934) Epigloeaceae, Verrucariaceae und Dermatocarpaceae. Dr. L. Rabenhorst's Kryptogamen-Flora von Deutschland, Österreich und der Schweiz 9 1(1): 44–695.

Supplementary material 1

The alignment

Authors: Juha Pykälä, Annina Kantelinen, Leena Myllys

Data type: PDF file

Link: https://doi.org/10.3897/mycokeys.96.98738.suppl1

MycoKeys 96: 25–56 (2023)
doi: 10.3897/mycokeys.96.99327
https://mycokeys.pensoft.net

RESEARCH ARTICLE

A peer-reviewed open-access journal
MycoKeys
Launched to accelerate biodiversity research

Five new species of Schizoporaceae (Basidiomycota, Hymenochaetales) from East Asia

Qian-Xin Guan[1], Jing Huang[1], Jian Huang[2], Chang-Lin Zhao[1,3,4]

1 *College of Biodiversity Conservation, Southwest Forestry University, Kunming 650224, China* **2** *Yunnan General Administration of Forestry Seeds and Seedlings, Kunming, 650215, China* **3** *Yunnan Academy of Biodiversity, Southwest Forestry University, Kunming 650224, China* **4** *Yunnan Key Laboratory for Fungal Diversity and Green Development, Kunming Institute of Botany, Chinese Academy of Science, Kunming 650201, China*

Corresponding author: Chang-Lin Zhao (fungi@swfu.edu.cn)

Academic editor: Jennifer Luangsa-ard | Received 27 December 2022 | Accepted 6 March 2023 | Published 14 March 2023

Citation: Guan Q-X, Huang J, Huang J, Zhao C-L (2023) Five new species of Schizoporaceae (Basidiomycota, Hymenochaetales) from East Asia. MycoKeys 96: 25–56. https://doi.org/10.3897/mycokeys.96.99327

Abstract

Five new wood-inhabiting fungi, *Lyomyces albopulverulentus*, *L. yunnanensis*, *Xylodon daweishanensis*, *X. fissuratus*, and *X. puerensis* **spp. nov.**, are proposed based on a combination of morphological features and molecular evidence. *Lyomyces albopulverulentus* is characterized by brittle basidiomata, pruinose hymenophore with a white hymenial surface, a monomitic hyphal system with clamped generative hyphae, and ellipsoid basidiospores. *Lyomyces yunnanensis* is characterized by a grandinioid hymenial surface, the presence of capitate cystidia, and ellipsoid basidiospores. *Xylodon daweishanensis* is characterized by an odontioid hymenial surface, a monomitic hyphal system with clamped generative hyphae, and broad ellipsoid-to-subglobose basidiospores. *Xylodon fissuratus* is characterized by a cracking basidiomata with a grandinioid hymenial surface, and ellipsoid basidiospores. *Xylodon puerensis* is characterized by a poroid hymenophore with an angular or slightly daedaleoid configuration, and ellipsoid-to-broad-ellipsoid basidiospores. Sequences of ITS and nLSU rRNA markers of the studied samples were generated and phylogenetic analyses were performed with the maximum likelihood, maximum parsimony, and Bayesian inference methods. The phylogram based on the ITS+nLSU rDNA gene regions (Fig. 1) included six genera within the families Chaetoporellaceae, Hyphodontiaceae, Hymenochaetaceae, and Schizoporaceae (Hymenochaetales)—*Fasciodontia*, *Hastodontia*, *Hyphodontia*, *Kneiffiella*, *Lyomyces*, and *Xylodon*—in which the five new species were grouped into genera *Lyomyces* and *Xylodon*. The phylogenetic tree inferred from the ITS sequences highlighted that *Lyomyces albopulverulentus* formed a monophyletic lineage and was then grouped closely with *L. bambusinus*, *L. orientalis*, and *L. sambuci*; additionally, *L. yunnanensis* was sister to *L. niveus* with strong supports. The topology, based on the ITS sequences, revealed that *Xylodon daweishanensis* was retrieved as a sister to *X. hyphodontinus*; *X. fissuratus* was grouped with the four taxa *X. montanus*, *X. subclavatus*, *X. wenshanensis*, and *X. xinpingensis*; and *X. puerensis* was clustered with *X. flaviporus*, *X. ovisporus*, *X. subflaviporus*, *X. subtropicus*, and *X. taiwanianus*.

Keywords
Biodiversity, China, molecular systematics, taxonomy, wood-inhabiting fungi, Yunnan Province

Introduction

Fungi represent one of the most diverse groups of organisms on the earth, with an indispensable role in the processes and functioning of ecosystems (Hyde 2022). The family Schizoporaceae Jülich includes many variations of the fruiting body types among the order Hymenochaetales Oberw. (Larsson et al. 2006; Wu et al. 2022a), in which it comprises many representative wood-inhabiting fungal taxa, including hydnoid, corticioid, and polyporoid basidiomes with diverse hymenophoral and cystidial morphology (Yurchenko and Wu 2016; Riebesehl and Langer 2017; Yurchenko et al. 2017; Cui et al. 2019; Riebesehl et al. 2019; Jiang et al. 2021; Wu et al. 2022a, b). In addition, the species of Schizoporaceae have been described from different countries, and they cause a white rot (Langer 1994).

The genus *Lyomyces* P. Karst. is a small corticioid group, typified by *L. sambuci* (Pers.) P. Karst. It is characterized by the resupinate-to-effused basidiomata with a smooth-to-odontioid hymenophore, a monomitic hyphal system with generative hyphae bearing clamp connections, the presence of several types of cystidia, and with smooth, thin- to slightly thick-walled basidiospores (Karsten 1881; Bernicchia and Gorjón 2010). The species of *Lyomyces* are found on fallen angiosperm branches, dead woody or herbaceous stems, or, occasionally, on gymnosperm wood (Yurchenko et al. 2017). Approximately 40 species of *Lyomyces* are currently known (Rabenhorst 1851; Karsten 1881, 1882; Cunningham 1959, 1963; Wu 1990; Hjortstam and Ryvarden 2009; Xiong et al. 2009; Dai 2010, 2011; Yurchenko et al. 2013, 2017, 2020; Gafforov et al. 2017; Riebesehl and Langer 2017; Chen and Zhao 2020; Luo et al. 2021b, c; Viner et al. 2022). The genus *Xylodon* (Pers.) Gray is typified by *X. quercinus* (Pers.) Gray (Bernicchia and Gorjón 2010). The taxa of this genus grow on rotten gymnosperm or angiosperm trunks and stumps, bamboo and ferns (Girometta et al. 2020; Greslebin and Rajchenberg 2000; Kotiranta and Saarenoksa 2000). They are characterized by resupinate or effuse basidiomata with a smooth, tuberculate, grandinioid, odontioid, coralloid, irpicoid, or poroid hymenophore; a monomitic or dimitic hyphal system with clamped generative hyphae; the presence of different types of cystidia, i.e., utriform or suburniform basidia; and cylindrical-to-ellipsoid-to-globose basidiospores, which can cause a white rot (Gray 1821; Bernicchia and Gorjón 2010). Based on the MycoBank database (http://www.mycobank.org, accessed on 24 December 2022) and the Index Fungorum (http://www.indexfungorum.org, accessed on 24 December 2022), *Xylodon* has registered 221 specific and infraspecific names, and the actual number of the species has reached 100 species (Chevallier 1826; Kuntze 1898; Wu 1990, 2000, 2001, 2006; Hjortstam and Ryvarden 2007, 2009; Xiong et al. 2009, 2010; Bernicchia and Gorjón 2010; Tura et al. 2011; Dai 2012; Lee and Langer 2012;

Yurchenko et al. 2013; Yurchenko and Wu 2014; Zhao et al. 2014; Chen et al. 2016; Kan et al. 2017a, b; Riehl and Langer 2017; Wang and Chen 2017; Viner et al. 2018, 2022; Riebesehl et al. 2019; Shi et al. 2019; Dai et al. 2021; Luo et al. 2021a, 2022; Qu and Zhao 2022; Qu et al. 2022).

Classification of the kingdom of fungi has been updated continuously, based on the frequent inclusion of data from DNA sequences in many phylogenetic studies (Wijayawardene et al. 2020). Based on the early embrace of molecular systematics by mycologists, both the discovery and classification of fungi, among the more basal branches of the tree, are now coming to light from genomic analyses and environmental DNA surveys that have been conducted (James et al. 2020). *Hyphodontia* s.l. was indicated to be a polyphyletic group, and *Xylodon* and *Kneiffiella* P. Karst. included the most species (Yurchenko and Wu 2016; Riebesehl and Langer 2017; Riebesehl et al. 2019). Given the lack of sequences for a part of the fungal taxa, it is difficult to clearly separate the many genera in this group using molecular data; therefore, a broad concept of *Hyphodontia* s.l. was accepted (Yurchenko and Wu 2016; Riebesehl and Langer 2017; Wang and Chen 2017; Riebesehl et al. 2019). On the basis of the nuclear DNA sequence data, six well-distinguished clades—*Lagarobasidium* clade, *Kneiffiella-Alutaceodontia* clade, *Hyphodontia* clade, *Hastodontia* clade, *Xylodon-Lyomyces*, *Rogersella* clade, and *Xylodon-Schizopora-Palifer* clade—were included based on the phylogenetical studies for *Hyphodontia* s.l., in which the genera *Xylodon* and *Lyomyces* were nested within the *Xylodon-Lyomyces-Rogersella* clade and *Xylodon-Schizopora-Palifer* clade, respectively (Yurchenko and Wu 2013). Riebesehl and Langer (2017) revealed that *Hyphodontia* s.l. was divided into six genera, viz., *Hastodontia* (Parmasto) Hjortstam & Ryvarden, *Hyphodontia* J. Erikss, *Kneiffiella*, *Lagarobasidium* Jülich, *Lyomyces*, and *Xylodon*, in which 35 new combinations were proposed, including fourteen *Lyomyces* species. Yurchenko et al. (2017) clarified the *Lyomyces sambuci* complex on the basis of the sequences of the internal transcribed spacer (ITS) and the nuclear large subunit (nLSU) ribosomal DNA gene, in which four new species were described. To confirm the taxonomic relationship of *Xylodon* species, Viner et al. (2018) proposed two genera, *Lagarobasidium* and *Xylodon*, which should be synonymous based on molecular data from the ITS and nLSU regions, and in which the three species were combined into *Xylodon*. Riebesehl et al. (2019) clarified the generic concept and their phylogenetic reconstruction of *Lyomyces*, in which *L. sambuci* was sister to *L. crustosus* (Pers.) P. Karst. Based on a combination of morphological and molecular evidence, the wood-inhabiting fungal diversity within the family Schizoporaceae of the order Hymenochaetales were analyzed, including *Lyomyces fissuratus* C.L. Zhao, *L. fumosus* C.L. Zhao, *L. niveus* C.L. Zhao and *L. ochraceoalbus* C.L. Zhao. (Luo et al. 2021b, 2021c). Viner et al. (2022) described three new species from Africa as *Xylodon angustisporus* Viner & Ryvarden, *X. dissiliens* Viner & Ryvarden, and *X. laxiusculus* Viner & Ryvarden, based on the morphological descriptions and molecular analyses that they conducted. A phylogenetic and taxonomic study on *Xylodon* showed that three new species of *Xylodon* were from southern China; in addition, it was also found that it enriched the fungal diversity of these areas (Qu et al. 2022).

During investigations on the wood-inhabiting fungi in the Yunnan–Guizhou Plateau of China, samples representing five additional species belonging to genera *Lyomyces* and *Xylodon* were collected. To clarify the placement and relationships of the five species, we carried out a phylogenetic and taxonomic study on *Lyomyces* and *Xylodon*, based on the ITS and nLSU sequences.

Materials and methods

Morphology

The studied specimens were deposited at the Herbarium of Southwest Forestry University (SWFC), Kunming, Yunnan Province, P.R. China. Macromorphological descriptions are based on field notes and photos captured in the field and lab. Color terminology follows Petersen (Petersen 1996). Micromorphological data were obtained from the dried specimens when observed under a light microscope following Dai (2012). The following abbreviations are used: KOH = 5% potassium hydroxide water solution, CB = Cotton Blue, CB– = acyanophilous, IKI = Melzer's Reagent, IKI– = both inamyloid and indextrinoid, L = mean spore length (arithmetic average for all spores), W = mean spore width (arithmetic average for all spores), Q = variation in the L/W ratios between the specimens studied and n = a/b (number of spores (a) measured from given number (b) of specimens).

Molecular phylogeny

The CTAB rapid plant genome extraction kit-DN14 (Aidlab Biotechnologies Co., Ltd, Beijing) was used to obtain genomic DNA from the dried specimens following the manufacturer's instructions (Zhao and Wu 2017). The nuclear ribosomal ITS region was amplified with the primers ITS5 and ITS4 (White et al. 1990). The nuclear ribosomal LSU gene was amplified with the primers LR0R and LR7 (Vilgalys and Hester 1990; Rehner and Samuels 1994). The PCR procedure for ITS and nLSU followed previous study (Zhao and Wu 2017). All newly-generated sequences were deposited in NCBI GenBank (Table 1).

The sequences were aligned in MAFFT version 7 (Katoh et al. 2019) using the G-INS-i strategy. The alignment was adjusted manually using AliView version 1.27 (Larsson 2014). Each dataset was aligned separately at first and then the ITS and nLSU regions were combined with Mesquite version 3.51. The combined dataset was deposited in TreeBASE (submission ID 29868). Sequences of *Hymenochaete ochromarginata* P.H.B. Talbot and *H. rubiginosa* (Dicks.) Lév. retrieved from GenBank were used as an outgroup in the ITS+nLSU analysis (Fig. 1); Sequences of *Xylodon quercinus* and *X. ramicida* Spirin & Miettinen retrieved from GenBank were used as an outgroup in the ITS analysis (Fig. 2); *Lyomyces bambusinus* C.L. Zhao and *L. sambuci* were selected as outgroup (Fig. 3) as inspired by a previous study (Luo et al. 2021c).

Table 1. List of species, specimens and GenBank accession numbers of sequences used in this study.

Species name	Specimen No.	GenBank accession No.		Country	References
		ITS	*nLSU*		
Fasciodontia brasiliensis	MSK-F 7245a	MK575201	MK598734	Brazil	Yurchenko et al. 2020
F. bugellensis	KAS-FD 10705a	MK575203	MK598735	France	Yurchenko et al. 2020
	MSK-F 7353	MK575205	MK598736	Belarus	Yurchenko et al. 2020
F. yunnanensis	CLZhao 6280	MK811275	MZ146327	China	Luo and Zhao 2021
	CLZhao 6385	MK811277	–	China	Luo and Zhao 2021
Hastodontia halonata	HHB-17058	MK575207	MK598738	Mexico	Yurchenko et al. 2020
Hymenochaete ochromarginata	He 47	KU978861	JQ279666	China	Unpublished
H. rubiginosa	He 458	JQ279580	–	China	He and Li 2013
Hyphodontia arguta	KHL 11938 (GB)	EU118632	EU118633	Sweden	Larsson 2007
H. pallidula	GEL 2097	DQ340317	DQ340372	Germany	Unpublished
H. zhixiangii	LWZ 20160909-4	KY440396	–	Uzbekistan	Kan et al. 2017
	LWZ 20160909-9	KY440398	–	Uzbekistan	Kan et al. 2017
Kneiffiella eucalypticola	LWZ20180515-9	MT319411	MT319143	Australia	Wang et al. 2021
K. palmae	GEL3456	DQ340333	DQ340369	China	Yurchenko et al. 2020
K. subalutacea	GEL2196	DQ340341	DQ340362	Norway	Yurchenko et al. 2020
Lyomyces albopulverulentus	**CLZhao 21478***	**OP730712**	**OP730724**	**China**	**Present study**
L. allantosporus	KAS-GEL4933	KY800401	–	France	Yurchenko et al. 2017
	FR-0249548	KY800397	–	La Réunion	Yurchenko et al. 2017
L. bambusinus	CLZhao 4831	MN945968	–	China	Chen and Zhao 2020
	CLZhao 4808	MN945970	–	China	Chen and Zhao 2020
	CLZhao 4831	MN945968	–	China	Chen and Zhao 2020
L. cremeus	CLZhao 4138	MN945974	–	China	Chen and Zhao 2020
	CLZhao 8295	MN945972	–	China	Chen and Zhao 2020
L. crustosus	TASM:YG G39	MF382993	–	Uzbekistan	Gafforov et al. 2017
	UC2022841	KP814310	–	USA	Unpublished
L. densiusculus	Ryvarden 44818	OK273853	–	Uganda	Viner et al. 2022
L. elaeidicola	LWZ20180411-20	MT319458	–	Malaysia	Wang et al. 2021
	LWZ20180411-19	MT319457	–	Malaysia	Wang et al. 2021
L. erastii	TASM:YG 022	MF382992	–	Uzbekistan	Gafforov et al. 2017
	23cSAMHYP	JX857800	–	Spain	Unpublished
L. fimbriatus	Wu910620-7	MK575209	–	China	Yurchenko et al. 2020
	Wu911204-4	MK575210	–	China	Yurchenko et al. 2020
L. fissuratus	CLZhao 4352	MW713742	–	China	Luo et al. 2021a
	CLZhao 4291	MW713738	–	China	Luo et al. 2021a
L. fumosus	CLZhao 8188	MW713744	–	China	Luo et al. 2021a
L. gatesiae	LWZ20180515-3	MT319447	–	Australia	Wang et al. 2021
	LWZ20180515-32	MT319448	–	Australia	Wang et al. 2021
L. griseliniae	KHL 12971 (GB)	DQ873651	–	Costa Rica	Larsson et al. 2006
L. juniperi	FR-0261086	KY081799	–	La Réunion	Riebesehl and Langer 2017
L. leptocystidiatus	LWZ20170818-1	MT326514	–	China	Wang et al. 2021
	LWZ20170818-2	MT326513	–	China	Wang et al. 2021
L. macrosporus	CLZhao 4516	MN945977	–	China	Chen and Zhao 2020
L. mascarensis	KAS-GEL4833	KY800399	–	La Réunion	Yurchenko et al. 2020
	KAS-GEL4908	KY800400	–	La Réunion	Yurchenko et al. 2020
L. microfasciculatus	CLZhao 5109	MN954311	–	China	Chen and Zhao 2020
L. niveus	CLZhao 6431	MZ262541	MZ262526	China	Luo et al. 2021b
	CLZhao 6442	MZ262542	MZ262527	China	Luo et al. 2021b
L. ochraceoalbus	CLZhao 4385	MZ262535	MZ262521	China	Luo et al. 2021b
	CLZhao 4725	MZ262536	MZ262522	China	Luo et al. 2021b
L. organensis	MSK7247	KY800403	–	Brazil	Yurchenko et al. 2017
L. orientalis	GEL3376	DQ340325	–	China	Yurchenko et al. 2017

Species name	Specimen No.	GenBank accession No.		Country	References
		ITS	*nLSU*		
L. pruni	GEL2327	DQ340312	–	Germany	Larsson et al. 2006
	Ryberg 021018 (GB)	DQ873624	–	Sweden	Larsson et al. 2006
L. sambuci	KAS-JR7	KY800402	KY795966	Germany	Yurchenko et al. 2017
	83SAMHYP	JX857721	–	USA	Yurchenko et al. 2017
L. vietnamensis	TNM F9073	JX175044	–	Vietnam	Yurchenko et al. 2013
L. wuliangshanensis	CLZhao 4108	MN945980	–	China	Chen and Zhao 2020
	CLZhao 4167	MN945979	–	China	Chen and Zhao 2020
L. yunnanensis	**CLZhao 2463**	**OP730711**	**OP730723**	**China**	**Present study**
	CLZhao 9375	**OP730710**	**–**	**China**	**Present study**
	CLZhao 10041*	**OP730709**	**–**	**China**	**Present study**
Xylodon acystidiatus	LWZ20180514-9	MT319474	–	Australia	Wang et al. 2021
X. apacheriensis	Wu 0910-58	KX857797	–	China	Chen et al. 2017
X. aspera	KHL 8530	AY463427	–	Sweden	Larsson et al. 2004
X. astrocystidiata	Wu 9211-71	JN129972	–	China	Yurchenko and Wu 2014
X. attenuatus	Spirin 8775	MH324476	–	America	Viner et al. 2018
X. australis	LWZ20180509-8	MT319503	–	China	Wang et al. 2021
X. bambusinus	CLZhao 9174	MW394657	–	China	Ma and Zhao 2021
X. borealis	JS26064	AY463429	–	Norway	Larsson et al. 2004
X. brevisetus	JS17863	AY463428	–	Norway	Larsson et al. 2004
X. crystalliger	LWZ20170816-33	MT319521	–	China	Wang et al. 2021
X. cystidiatus	FR-0249200	MH880195	MH884896	Réunion	Riebesehl et al. 2019
X. damansaraensis	LWZ20180417-23	MT319499	–	Malaysia	Wang et al. 2021
X. daweishanensis	**CLZhao 18357***	**OP730715**	**–**	**China**	**Present study**
	CLZhao 18425	**OP730716**	**–**	**China**	**Present study**
	CLZhao 18446	**OP730717**	**OP730725**	**China**	**Present study**
	CLZhao 18458	**OP730718**	**OP730726**	**China**	**Present study**
	CLZhao 18492	**OP730719**	**OP730727**	**China**	**Present study**
X. detriticus	Zíbarová 30.10.17	MH320793	–	Czech Republic	Viner et al. 2018
X. filicinus	MSK-F 12869	MH880199	NG067836	China	Riebesehl et al. 2019
X. fissuratus	**CLZhao 9407***	**OP730714**	**–**	**China**	**Present study**
	CLZhao 7007	**OP730713**	**–**	**China**	**Present study**
X. flaviporus	FR-0249797	MH880201	–	Réunion	Riebesehl et al. 2019
X. flocculosus	CLZhao 18342	MW980776	–	China	Qu and Zhao 2022
X. follis	FR-0249814	MH880204	–	Réunion	Riebesehl et al. 2019
X. gossypinus	CLZhao 8375	MZ663804	MZ663813	China	Luo et al. 2021
X. grandineus	CLZhao 16075	OM338091	–	China	Luo et al. 2022
	CLZhao 6425	OM338090	–	China	Luo et al. 2022
X. hastifer	K(M) 172400	NR166558	–	USA	Riebesehl and Langer 2017
X. heterocystidiatus	Wei 17-314	MT731753	–	China	Unpublished
X. hyphodontinus	KAS-GEL9222	MH880205	MH884903	Kenya	Riebesehl et al. 2019
X. kunmingensis	TUB-FO 42565	MH880198	–	China	Riebesehl et al. 2019
X. lacerates	CLZhao 9892	OL619258	–	China	Qu et al. 2022
X. lagenicystidiatus	LWZ20180513-16	MT319634	–	Australia	Wang et al. 2021
X. lenis	Wu890714-3	KY081802	–	China	Riebesehl and Langer 2017
X. macrosporus	CLZhao 10226	MZ663809	MZ663817	China	Luo et al. 2021
X. mollissimus	LWZ 20160318-3	KY007517	–	China	Wang et al. 2021
X. montanus	CLZhao 8179	OL619260	–	China	Qu et al. 2022
X. nespori	LWZ20180921-35	MT319655	MT319238	China	Wang et al. 2021
X. niemelaei	LWZ20150707-13	MT319630	–	China	Wang et al. 2021
X. nongravis	GC 1412-22	KX857801	–	China	Chen et al. 2017
X. nothofagi	ICMP 13842	AF145583	–	China	Paulus et al. 2000
X. ovisporus	LWZ20170815-31	MT319666	–	China	Wang et al. 2021
X. papillosa	CBS:114.71	MH860026	–	Netherlands	Vu et al. 2019

Species name	Specimen No.	GenBank accession No.		Country	References
		ITS	*nLSU*		
X. paradoxus	Dai14983	MT319519	–	China	Wang et al. 2021
X. pruinosus	Spirin 2877	MH332700	–	Estonia	Viner et al. 2018
X. pseudolanatus	CFMR FP-150922	MH880220	–	Belize	Riebesehl et al. 2019
X. pseudotropicus	Dai16167	MT319509	–	China	Wang et al. 2021
X. puerensis	**CLZhao 8142***	**OP730720**	**OP730728**	**China**	**Present study**
	CLZhao 8639	**OP730721**	**OP730729**	**China**	**Present study**
X. punctus	CLZhao 17691	OM338092	–	China	Luo et al. 2022
X. quercinus	Larsson 11076 (GB)	KT361633	–	Sweden	Larsson et al. 2004
X. ramicida	Spirin 7664	NR138013	–	usa	Unpublished
X. rhododendricola	LWZ20180513-9	MT319621	–	Australia	Wang et al. 2021
X. rimosissima	Ryberg 021031 (GB)	DQ873627	–	Sweden	Larsson et al. 2006
X. serpentiformis	LWZ20170816-15	MT319673	–	China	Wang et al. 2021
X. sinensis	CLZhao 11120	MZ663811	–	China	Luo et al. 2021
X. spathulatus	LWZ20180804-10	MT319646	–	China	Wang et al. 2021
X. subclavatus	TUB-FO 42167	MH880232	–	China	Riebesehl et al. 2019
X. subflaviporus	Wu 0809-76	KX857803	–	China	Chen et al. 2017
X. subserpentiformis	LWZ20180512-16	MT319486	–	Australia	Wang et al. 2021
X. subtropicus	LWZ20180510-24	MT319541	–	China	Wang et al. 2021
X. taiwanianus	CBS:125875	MH864080	–	Netherlands	Vu et al. 2019
X. tropicus	CLZhao 3351	OL619261	OL619269	China	Qu et al. 2022
X. ussuriensis	KUN 1989	NR166241	–	USA	Unpublished
X. verecundus	KHL 12261 (GB)	DQ873642	–	Sweden	Larsson et al. 2006
X. victoriensis	LWZ20180510-29	MT319487	–	Australia	Wang et al. 2021
X. wenshanensis	CLZhao 10790	OM338095	–	China	Luo et al. 2022
	CLZhao 15729	OM338097	OM338104	China	Luo et al. 2022
X. xinpingensis	CLZhao 11224	MW394662	MW394654	China	Luo et al. 2022
X. yarraensis	LWZ20180510-5	MT319639	–	Australia	Wang et al. 2021
X. yunnanensis	LWZ20180922-47	MT319660	–	China	Wang et al. 2021

* Indicates type materials.

Maximum parsimony analysis in PAUP* version 4.0a169 (http://phylosolutions.com/paup-test/) was applied to ITS and the combined ITS+nLSU datasets following a previous study (Zhao and Wu 2017). All characters were equally weighted and gaps were treated as missing data. Trees were inferred using the heuristic search option with TBR branch swapping and 1,000 random sequence additions. Max-trees were set to 5,000, branches of zero length were collapsed and all parsimonious trees were saved. Clade robustness was assessed using bootstrap (BT) analysis with 1,000 pseudo replicates (Felsenstein 1985). Descriptive tree statistics – tree length (TL), composite consistency index (CI), composite retention index (RI), composite rescaled consistency index (RC) and composite homoplasy index (HI) – were calculated for each maximum parsimonious tree generated. The combined dataset was also analysed using Maximum Likelihood (ML) in RAxML-HPC2 through the CIPRES Science Gateway (Miller et al. 2012). Branch support (BS) for the ML analysis was determined by 1000 bootstrap pseudoreplicates.

MrModeltest 2.3 (Nylander 2004) was used to determine the best-fit evolution model for each dataset for the purposes of Bayesian inference (BI). which was performed using MrBayes 3.2.7a with a GTR+I+G model of DNA substitution and a

gamma distribution rate variation across sites (Ronquist et al. 2012). A total of four Markov chains were run for two runs from random starting trees for 8 million generations for ITS+nLSU (Fig. 1); 0.5 million generations for ITS (Fig. 2) and 9.5 million generations for ITS (Fig. 3) with trees and parameters sampled every 1,000 generations. The first quarter of all of the generations were discarded as burn-ins. A majority rule consensus tree was computed from the remaining trees. Branches were considered as significantly supported if they received a maximum likelihood bootstrap support value (BS) of > 70%, a maximum parsimony bootstrap support value (BT) of > 70% or a Bayesian posterior probability (BPP) of > 0.95.

Results

Molecular phylogeny

The ITS+nLSU dataset (Fig. 1) comprised sequences from 43 fungal specimens representing 31 taxa. The dataset had an aligned length of 2,100 characters, of which 1,323 characters were constant, 156 were variable and parsimony-uninformative and 621 (35%) were parsimony-informative. Maximum parsimony analysis yielded 1 equally parsimonious tree (TL = 2,867, CI = 0.4423, HI = 0.5577, RI = 0.6488 and RC = 0.2869). The best model of nucleotide evolution for the ITS+nLSU dataset estimated and applied in the Bayesian analysis was found to be GTR+I+G. Bayesian analysis and ML analysis resulted in a similar topology as in the MP analysis. The Bayesian analysis had an average standard deviation of split frequencies = 0.008603 (BI) and the effective sample size (ESS) across the two runs is double the average ESS (avg. ESS) = 1,623. The phylogram based on the ITS+nLSU rDNA gene regions (Fig. 1) include six genera within Schizoporaceae (Hymenochaetales), which are *Fasciodontia*, *Hastodontia*, *Hyphodontia*, *Kneiffiella*, *Lyomyces*, and *Xylodon*—in which five new species were grouped into the genera *Lyomyces* and *Xylodon*.

The ITS dataset (Fig. 2) comprised sequences from 47 fungal specimens representing 29 taxa. The dataset had an aligned length of 661 characters, of which 316 characters were constant, 53 were variable and parsimony-uninformative and 292 (35%) were parsimony-informative. Maximum parsimony analysis yielded 1 equally parsimonious tree (TL = 1,371, CI = 0.4136, HI = 0.5864, RI = 0.6984 and RC = 0.2888). The best model of nucleotide evolution for the ITS dataset estimated and applied in the Bayesian analysis was found to be GTR+I+G. Bayesian analysis and ML analysis resulted in a similar topology as in the MP analysis. The Bayesian analysis had an average standard deviation of split frequencies = 0.006564 (BI) and the effective sample size (ESS) across the two runs is double the average ESS (avg. ESS) = 359. The phylogenetic tree (Fig. 2), inferred from the ITS sequences, highlighted that *L. albopulverulentus* formed a monophyletic lineage. It was then grouped closely with *L. bambusinus*, *L. orientalis* Riebesehl, Yurch. & Langer, and *L. sambuci*. In addition, *L. yunnanensis* was found to be the sister to *L. niveus* with strong supports.

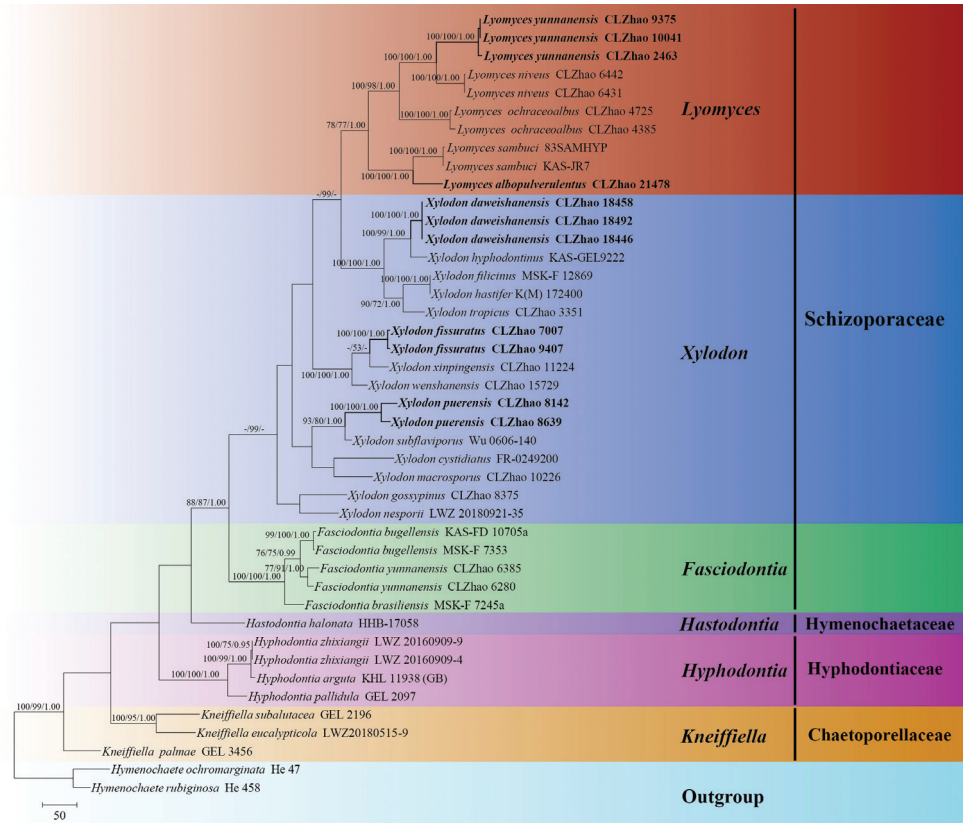

Figure 1. Maximum parsimony strict consensus tree illustrating the phylogeny of *Xylodon*, *Lyomyces* and related genera in the order Hymenochaetales based on ITS+nLSU sequences. Branches are labelled with maximum likelihood bootstrap values > 70%, parsimony bootstrap values > 50% and Bayesian posterior probabilities > 0.95, respectively.

The ITS dataset (Fig. 3) comprised sequences from 72 fungal specimens representing 65 taxa. The dataset had an aligned length of 702 characters, of which 283 characters were constant, 96 were variable and parsimony-uninformative and 323 (35%) were parsimony-informative. Maximum parsimony analysis yielded 5,000 equally parsimonious trees (TL = 2,726, CI = 0.2748, HI = 0.7252, RI = 0.4280 and RC = 0.1176). The best model of nucleotide evolution for the ITS dataset estimated and applied in the Bayesian analysis was found to be GTR+I+G. Bayesian analysis and ML analysis resulted in a similar topology as in the MP analysis. The Bayesian analysis had an average standard deviation of split frequencies = 0.02518 (BI) and the effective sample size (ESS) across the two runs is double the average ESS (avg. ESS) = 1,440. The topology (Fig. 3), based on ITS sequences, revealed that *X. daweishanensis* was retrieved as a sister to *X. hyphodontinus* (Hjortstam & Ryvarden) Riebesehl, Yurchenko & G. Gruhn. Furthermore, *X. fissuratus* was grouped with four taxa: *X. montanus* C.L. Zhao; *X. subclavatus* (Yurchenko, H.X. Xiong & Sheng H. Wu) Riebesehl, Yurch. &

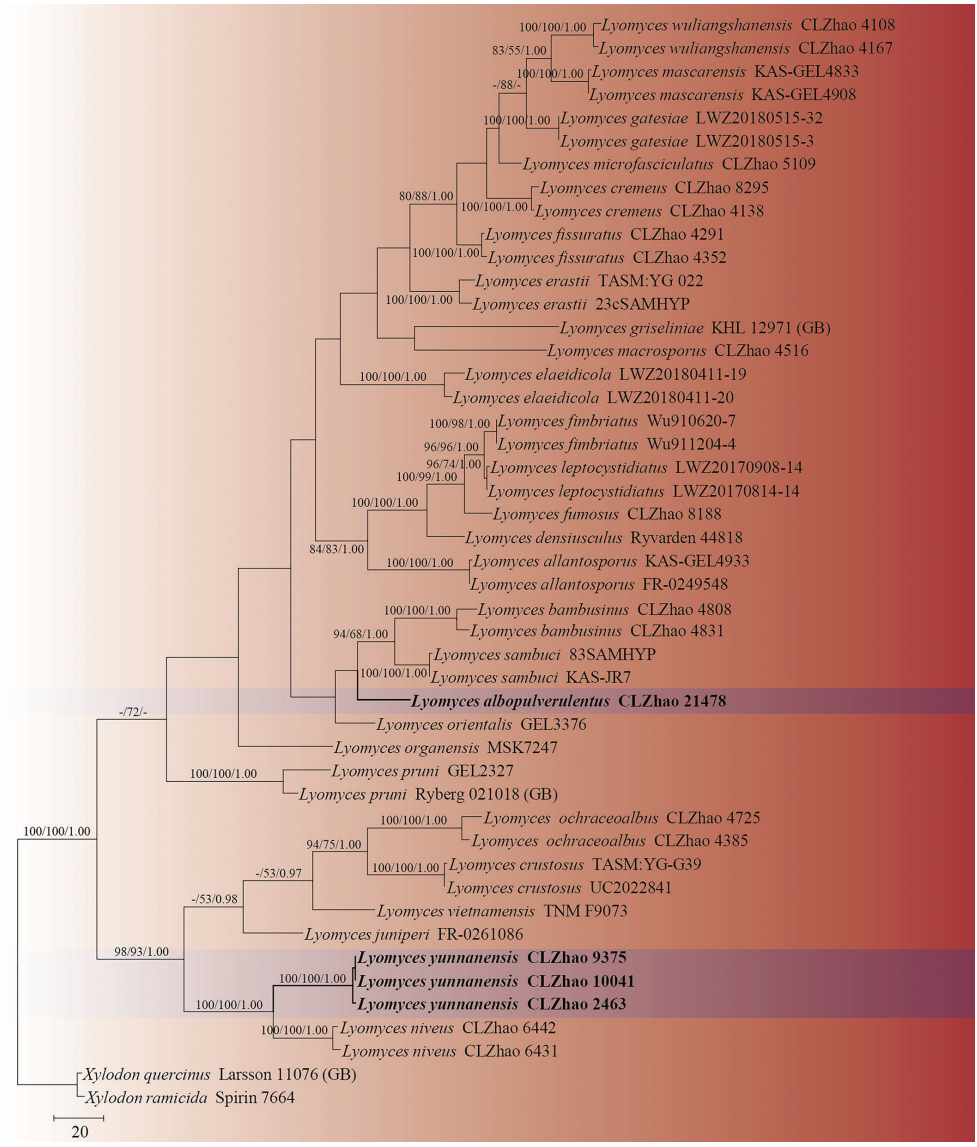

Figure 2. Maximum parsimony strict consensus tree illustrating the phylogeny of the two new species and related species in *Lyomyces*, based on ITS sequences. Branches are labelled with maximum likelihood bootstrap values > 70%, parsimony bootstrap values > 50% and Bayesian posterior probabilities > 0.95, respectively.

Langer; *X. wenshanensis* K.Y. Luo & C.L. Zhao; and *X. xinpingensis* C.L. Zhao & X. Ma. Moreover, *X. puerensis* was clustered with *X. flaviporus* (Berk. & M.A. Curtis ex Cooke) Riebesehl & Langer, *X. ovisporus* (Corner) Riebesehl & Langer, *X. subflaviporus* C.C. Chen & Sheng H. Wu, *X. subtropicus* (C.C. Chen & Sheng H. Wu) C.C. Chen & Sheng H. Wu, and *X. taiwanianus* (Sheng H. Wu) Hjortstam & Ryvarden.

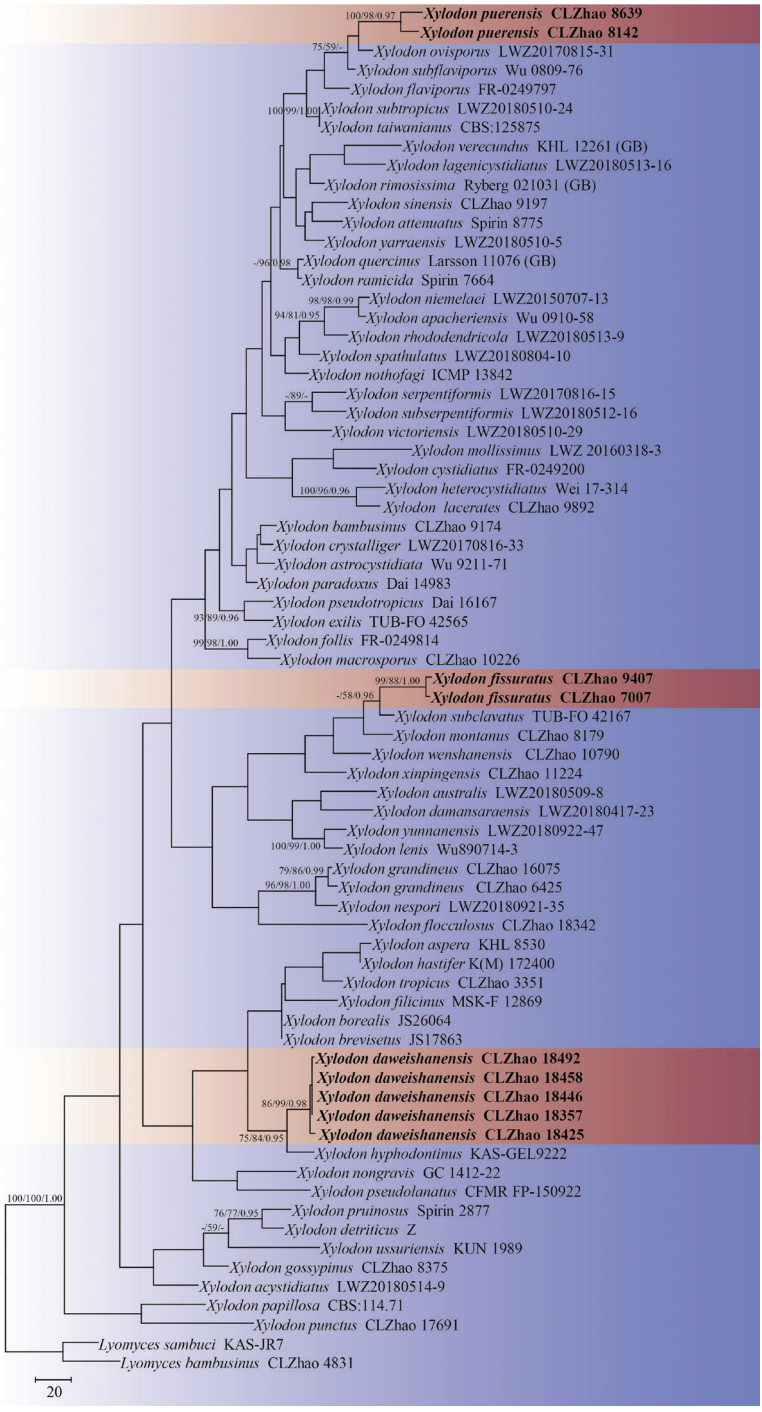

Figure 3. Maximum parsimony strict consensus tree illustrating the phylogeny of the three new species and related species in *Xylodon*, based on ITS sequences. Branches are labelled with maximum likelihood bootstrap values > 70%, parsimony bootstrap values > 50% and Bayesian posterior probabilities > 0.95, respectively.

Taxonomy

***Lyomyces albopulverulentus* C.L. Zhao, sp. nov.**
MycoBank No: 846525
Figs 4, 5

Type material. *Holotype*. China. Yunnan Province, Lijiang, Lashihai Nature Reserve, 26°51'37"N, 100°8'14"E, altitude 2450 m a.s.l., on fallen angiosperm branch, leg. C.L. Zhao, 19 July 2021, CLZhao 21478 (SWFC).

Etymology. *Albopulverulentus* (Lat.): referring to the white and pruinose hymenial surface.

Description. Basidiomata annual, resupinate, adnate, brittle, without odor or taste when fresh, up to 12 cm long, 1.5 cm wide, and 150 μm thick. Hymenial surface pruinose, white when fresh and drying. Sterile margin indistinct, white, and up to 2 mm wide.

Hyphal system monomitic, generative hyphae with clamp connections, colorless, thick-walled, frequently branched, interwoven, 3.5–5.5 μm in diameter; IKI–, CB–, tissues unchanged in KOH; subhymenial hyphae densely covered by crystals.

Cystidia capitate, colorless, thin-walled, smooth, slightly constricted at the neck, with a globose tip, 37–54 × 5–9 μm; basidia clavate, slightly sinuous, with four sterigmata and a basal clamp connection, 24.5–28.5 × 7–9 μm.

Basidiospores ellipsoid, colorless, thin-walled, smooth, IKI–, CB–, (7.5–)8–10.5(–11) × (5–)5.5–7 μm, L =9.12 μm, W = 6 μm, Q = 1.52 (n = 30/1).

Additional specimen examined (paratype). China. Yunnan Province, Yuxi, Xinping County, the Ancient Tea Horse Road, 23°57'10"N, 101°30'41"E, altitude 2,600 m a.s.l., on fallen angiosperm branch, leg. C.L. Zhao, 13 January 2018, CLZhao 5234 (SWFC).

***Lyomyces yunnanensis* C.L. Zhao, sp. nov.**
MycoBank No: 846527
Figs 6, 7

Type material. *Holotype*. China. Yunnan Province, Dali, Nanjian County, Lingbaoshan, 24°46'2"N, 100°30'26"E, altitude 2350 m a.s.l., on fallen angiosperm branch, leg. C.L. Zhao, 9 January 2019, CLZhao 10041 (SWFC).

Etymology. *Yunnanensis* (Lat.): referring to the locality (Yunnan Province) of the type specimen.

Description. Basidiomata annual, resupinate, adnate, coriaceous when fresh, becoming farinaceous upon drying, without odor or taste when fresh, up to 15 cm long, 2.5 cm wide, and 150 μm thick. Hymenial surface grandinioid, cream to buff when fresh, and buff upon drying. Sterile margin indistinct, buff, and up to 1 mm wide.

Figure 4. Basidiomata of *Lyomyces albopulverulentus* (holotype). Scale bars: 2 cm (**A**); 1 mm (**B**).

Hyphal system monomitic, generative hyphae with clamp connections, colorless, thick-walled, frequently branched, interwoven, 2.5–3 μm in diameter; IKI–, CB–, tissues unchanged in KOH. Numerous crystals present among hyphae.

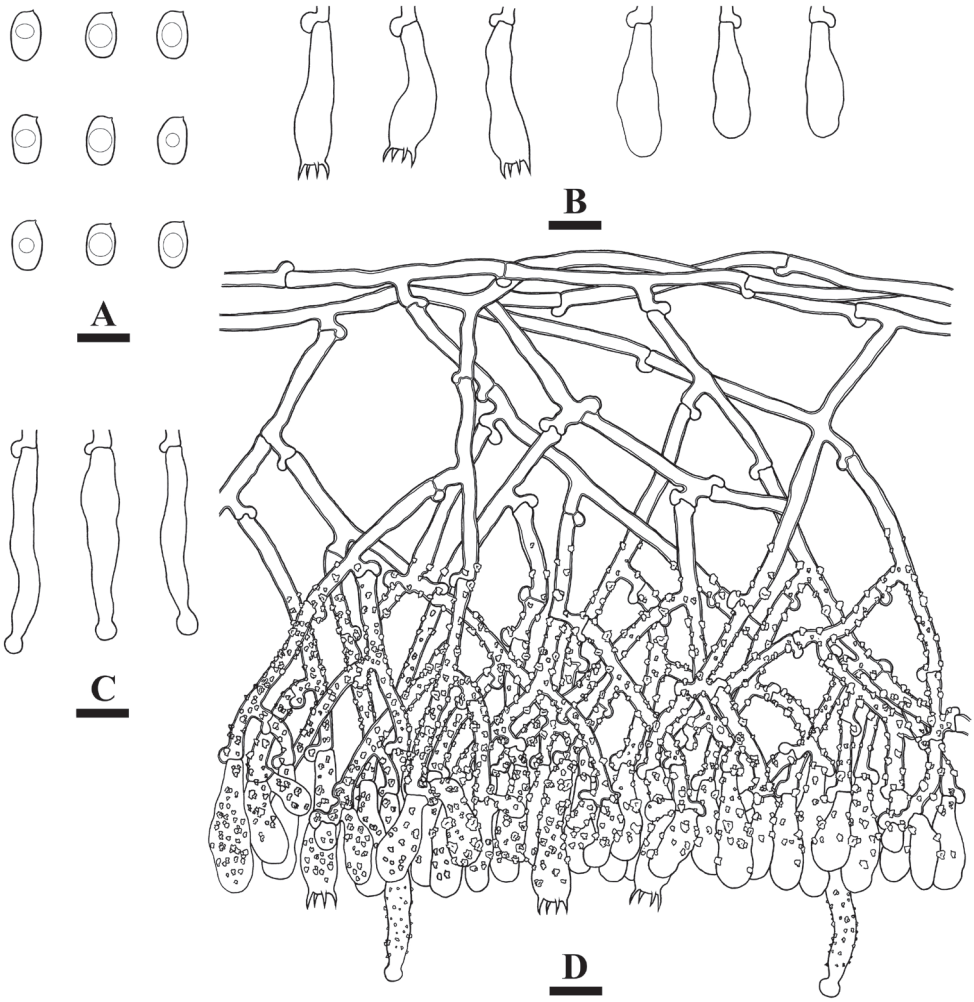

Figure 5. Microscopic structures of *Lyomyces albopulverulentus* (holotype) **A** basidiospores **B** basidia and basidioles **C** capitate cystidia **D** a section of hymenium. Scale bars: 10 μm (**A–D**).

Cystidia of two types: (1) fusiform, tapering, colorless, thin-walled, 18–39 × 4–6 μm; (2) capitate cystidia, colorless, thin-walled, 16–23.5 × 3–5 μm; fusoid cystidioles present, colorless, thin-walled, 18–25 × 3–6 μm; basidia clavate, slightly sinuous, with four sterigmata and a basal clamp connection, 16.5–27 × 4–5.5 μm.

Basidiospores ellipsoid, colorless, thin-walled, smooth, IKI–, CB–, (4.5–)5–7 × 3–4.5 μm, L = 5.72 μm, W = 3.6 μm, Q = 1.54–1.65 (n = 90/3).

Additional specimens examined (paratypes). China. Yunnan Province, Yuxi, Xinping County, Mopanshan National Forestry Park, 23°55'48"N, 101°59'22"E, altitude 2150 m a.s.l., on fallen angiosperm branch, leg. C.L. Zhao, 19 August 2017,

Figure 6. Basidiomata of *Lyomyces yunnanensis* (holotype). Scale bars: 2 cm (**A**); 1 mm (**B**).

CLZhao 2463 (SWFC); Puer, Jingdong County, the Forest of Pineapple, 24°21'32"N, 100°48'12"E, altitude 2110 m a.s.l., on fallen angiosperm branch, leg. C.L. Zhao, 4 January 2019, CLZhao 9375 (SWFC).

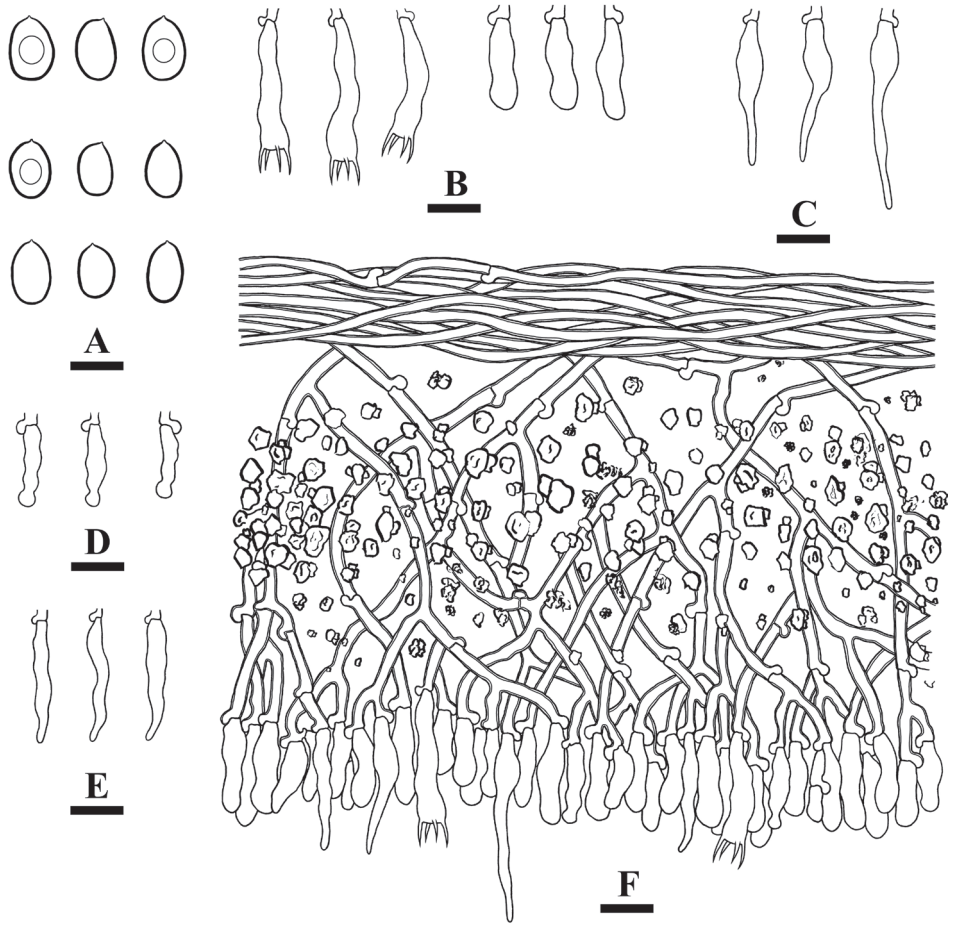

Figure 7. Microscopic structures of *Lyomyces yunnanensis* (holotype) **A** basidiospores **B** basidia and basidioles **C** tapering cystidia **D** capitate cystidia **E** fusoid cystidioles **F** a section of hymenium. Scale bars: 5 μm (**A**); 10 μm (**B–F**).

Xylodon daweishanensis **C.L. Zhao, sp. nov.**
MycoBank No: 846530
Figs 8, 9

Type material. ***Holotype.*** China. Yunnan Province, Honghe, Pingbian County, Daweishan National Nature Reserve, 22°53'26"N, 103°35'37"E, altitude 1990 m a.s.l., on angiosperm trunk, leg. C.L. Zhao, 3 August 2019, CLZhao 18357 (SWFC).

Etymology. *Daweishanensis* (Lat.): referring to the locality (Daweishan) of the type specimen.

Description. Basidiomata annual, resupinate, adnate, without odor or taste when fresh, coriaceous, up to 10 cm long, 5 cm wide, and 150 μm thick. Hymenial surface odontioid, slightly buff when fresh, and buff upon drying. Margin sterile, slightly buff, and 1 mm wide.

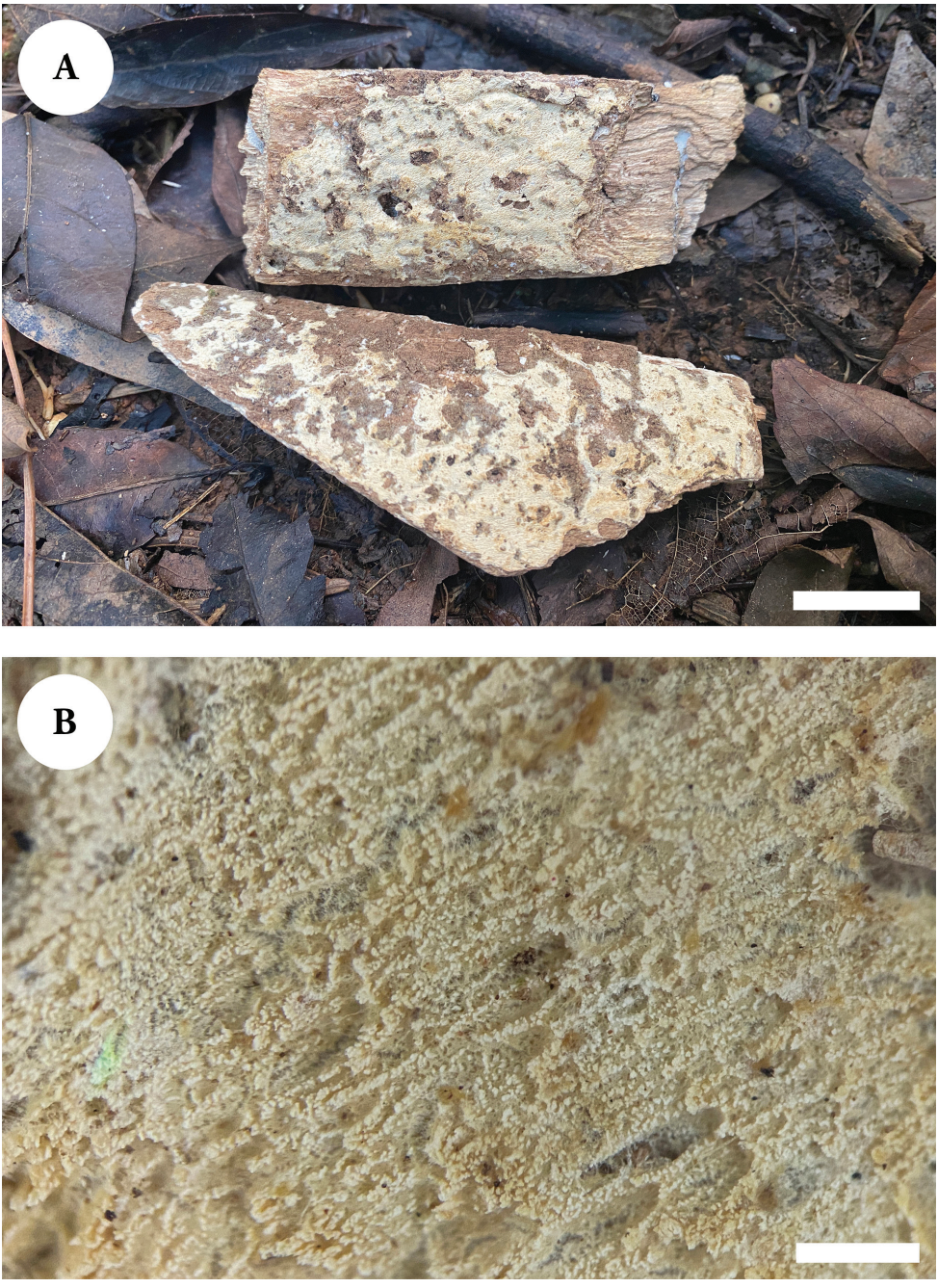

Figure 8. Basidiomata of *Xylodon daweishanensis* (holotype). Scale bars: 2 cm (**A**); 1 mm (**B**).

Hyphal system monomitic, generative hyphae with clamp connections, colorless, thin to thick-walled, frequently branched, interwoven, 1.5–4 μm in diameter, IKI–, CB–, tissues unchanged in KOH.

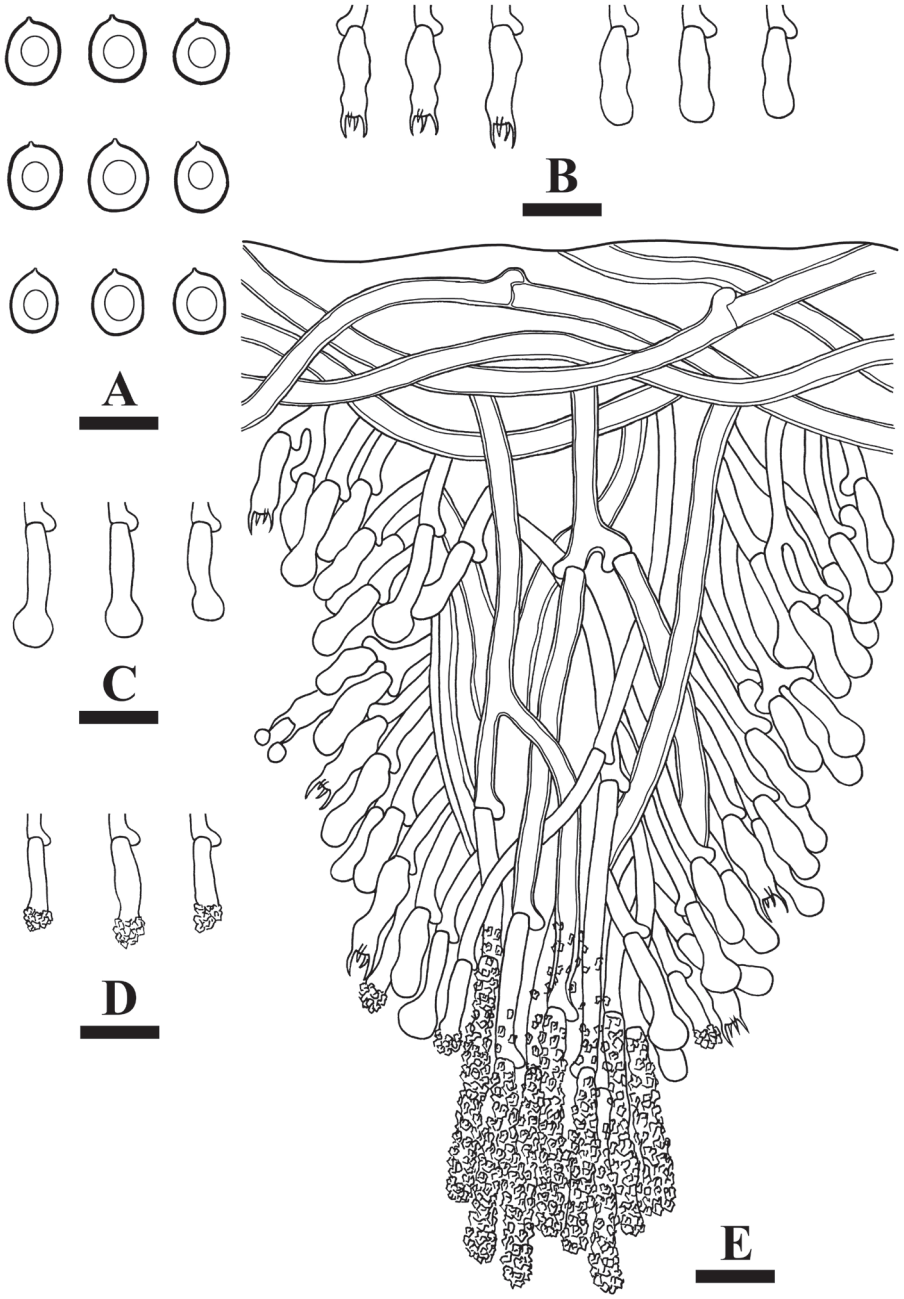

Figure 9. Microscopic structures of *Xylodon daweishanensis* (holotype) **A** basidiospores **B** basidia and basidioles **C** capitate cystidia **D** asterocystidia **E** a section of hymenium. Scale bars: 5 μm (**A**); 10 μm (**B–E**).

Cystidia of two types: (1) capitate cystidia thin-walled, smooth, slightly constricted at the neck, with a globose tip, 11–23.5 × 2.5–5 μm; (2) asterocystidia thin-walled, with the apical part encrusted, 11–26.5 × 2.5–4.5 μm; basidia clavate to subcylindrical,

constricted, somewhat sinuous, with four sterigmata and a basal clamp connection, 11–15.5 × 2.5–4 μm.

Basidiospores broad ellipsoid to subglobose, colorless, thin-walled, smooth, with oil drops, IKI–, CB–, 3–4 × 2.5–3.5(–4) μm, L = 3.51 μm, W = 3.14 μm, Q = 1.09–1.15 (n = 150/5).

Additional specimens examined (paratypes). China. Yunnan Province, Honghe, Pingbian County, Daweishan National Nature Reserve, 22°53'26"N, 103°35'37"E, altitude 1990 m a.s.l., on angiosperm trunk, leg. C.L. Zhao, 3 August 2019, CLZhao 18425, CLZhao 18446, CLZhao 18458, and CLZhao 18492 (SWFC).

Xylodon fissuratus **C.L. Zhao, sp. nov.**
MycoBank No: 846532
Figs 10, 11

Type material. ***Holotype.*** China. Yunnan Province, Puer, Jingdong County, the Forest of Pineapple, 24°21'32"N, 100°48'12"E, altitude 2110 m a.s.l., on fallen angiosperm branch, leg. C.L. Zhao, 4 January 2019, CLZhao 9407 (SWFC).

Etymology. *Fissuratus* (Lat.): referring to the cracking hymenial surface.

Description. Basidiomata annual, resupinate, adnate, coriaceous, without odor or taste when fresh, up to 12 cm long, 2.5 cm wide, and 150 μm thick. Hymenial surface grandinioid, and white when fresh, white to slightly cream on drying, cracking. Sterile margin indistinct, white, and up to 1 mm wide.

Hyphal system monomitic, generative hyphae with clamp connections, colorless, thin-walled, frequently branched, interwoven, 2–3 μm in diameter; IKI–, CB–, tissues unchanged in KOH.

Cystidia capitate, thin-walled, smooth, slightly constricted at the neck, with a globose tip, 11.5–16.5 × 3–4.5 μm; basidia clavate to subcylindrical, slightly constricted in the middle to somewhat sinuous, with four sterigmata and a basal clamp connection, 10.5–16.5 × 2–4 μm.

Basidiospores ellipsoid, colorless, thin-walled, smooth, IKI–, CB–, 4–5 × 3–4 μm, L = 4.44 μm, W = 3.4 μm, Q = 1.3 (n = 30/1).

Additional specimen examined (paratype). China. Yunnan Province, Chuxiong, Zixishan Forestry Park, 25°01'26"N, 101°24'37"E, altitude 2313 m a.s.l., on fallen angiosperm branch, leg. C.L. Zhao, 1 July 2018, CLZhao 7007 (SWFC).

Xylodon puerensis **C.L. Zhao, sp. nov.**
MycoBank No: 846533
Figs 12, 13

Type material. ***Holotype.*** China. Yunnan Province, Puer, Zhenyuan County, Heping Town, Jinshan Virgin Forest Park, 23°56'21"N, 101°25'32"E, altitude 2240 m a.s.l., on fallen angiosperm branch, leg. C.L. Zhao, 21 August 2018, CLZhao 8142 (SWFC).

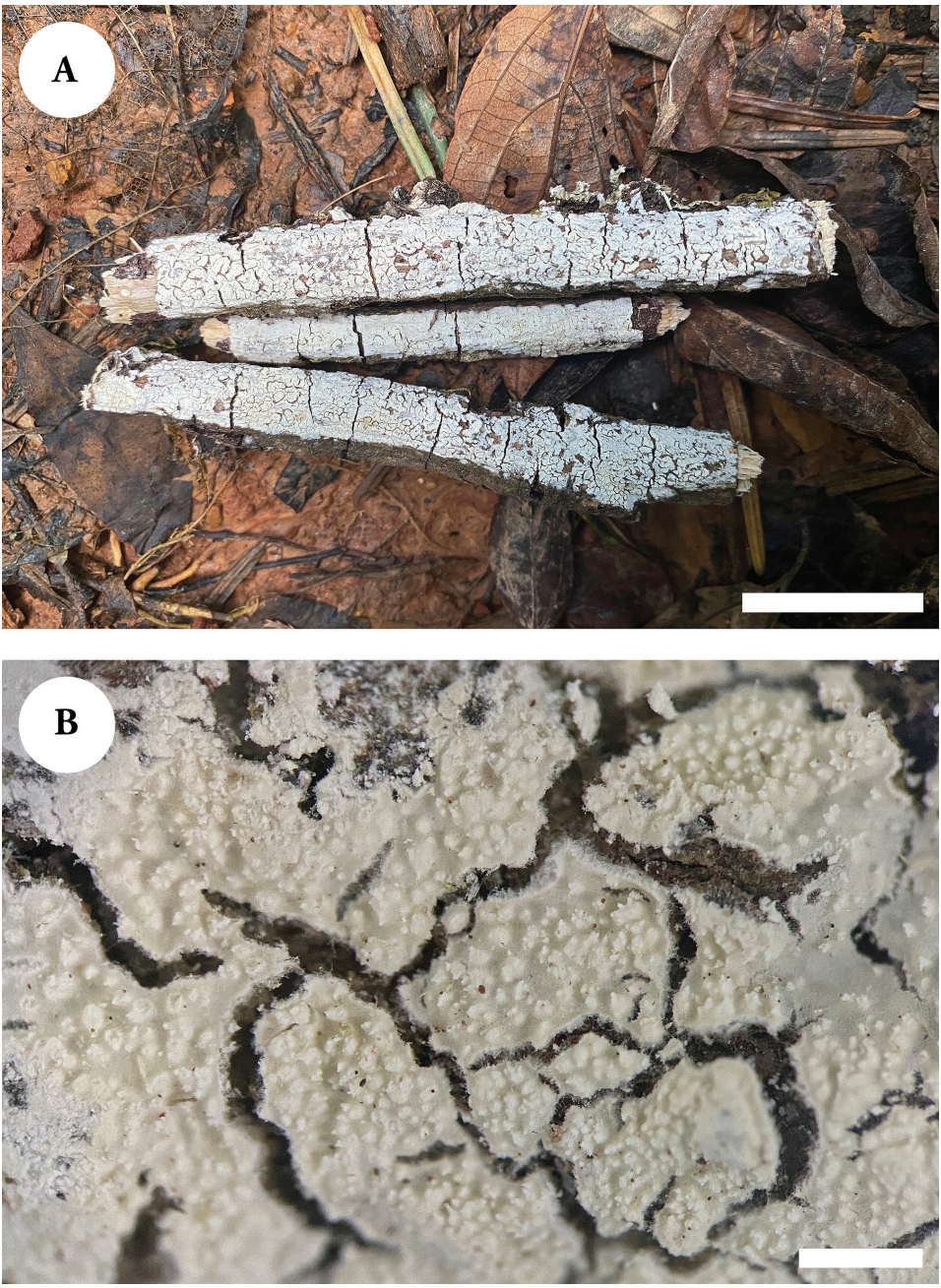

Figure 10. Basidiomata of *Xylodon fissuratus* (holotype). Scale bars: 2 cm (**A**); 1 mm (**B**).

Etymology. *Puerensis* (Lat.): referring to the locality (Yunnan Province) of the type specimen.

Description. Basidiomata annual, resupinate, adnate, coriaceous, without odor or taste when fresh, up to 12 cm long, 5 cm wide, and 200 μm thick. Hymenial surface

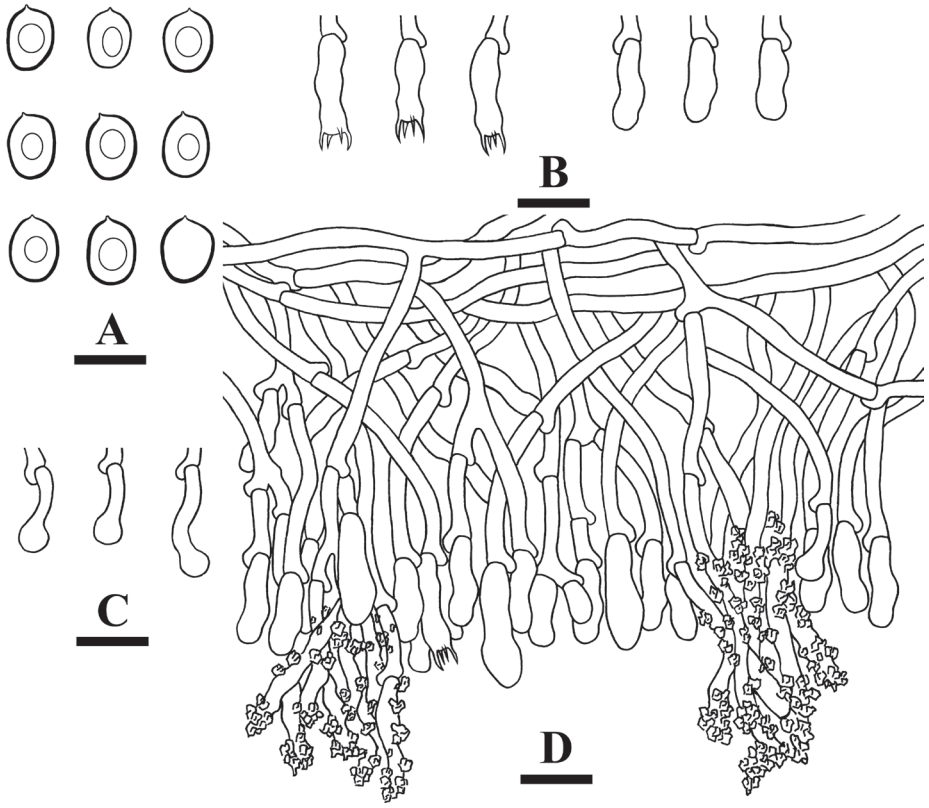

Figure 11. Microscopic structures of *Xylodon fissuratus* (holotype) **A** basidiospores **B** basidia and basidioles **C** capitate cystidia **D** a section of hymenium. Scale bars: 5 μm (**A**); 10 μm (**B–D**).

poroid, pores angular or slightly daedaleoid, 3–6 per mm, and cream when fresh, buff on drying. Sterile margin slightly buff, and up to 1 mm wide.

Hyphal system monomitic, generative hyphae with clamps, colorless, thick-walled, frequently branched, interwoven, 2.5–4.5 μm in diameter; IKI–, CB–, tissues unchanged in KOH.

Cystidia of four types: (1) paraphysoid cystidia colorless, smooth, 12–20.5 × 3–5 μm; (2) astrocystidia colorless, thin-walled, smooth, 9–11 × 3.5–5.5 μm; (3) capitate cystidia, colorless, thin-walled, smooth, embedded, 22–29.5 × 6.5–12 μm; (4) septocystidia, thin-walled, smooth, with the apical part encrusted, 32–51 × 3.5–6 μm; basidia clavate to subcylindrical, slightly sinuous or distinctly sinuous, with four sterigmata and a basal clamp connection, 14.5–20 × 5–7 μm.

Basidiospores ellipsoid to broad ellipsoid, colorless, thin-walled, smooth, with oil drops, IKI–, CB–, (5.5–)6–7 × 4.5–5.5 μm, L = 6.41 μm, W = 5.01 μm, Q = 1.28 (n = 30/1).

Additional specimen examined (paratype). China. Yunnan Province, Puer, Jingdong County, Taizhong Town, Ailaoshan Ecological Station, 24°29'41"N, 100°56'32"E, altitude 1930 m a.s.l., on angiosperm trunk, leg. C.L. Zhao, 24 August 2018, CLZhao 8639 (SWFC).

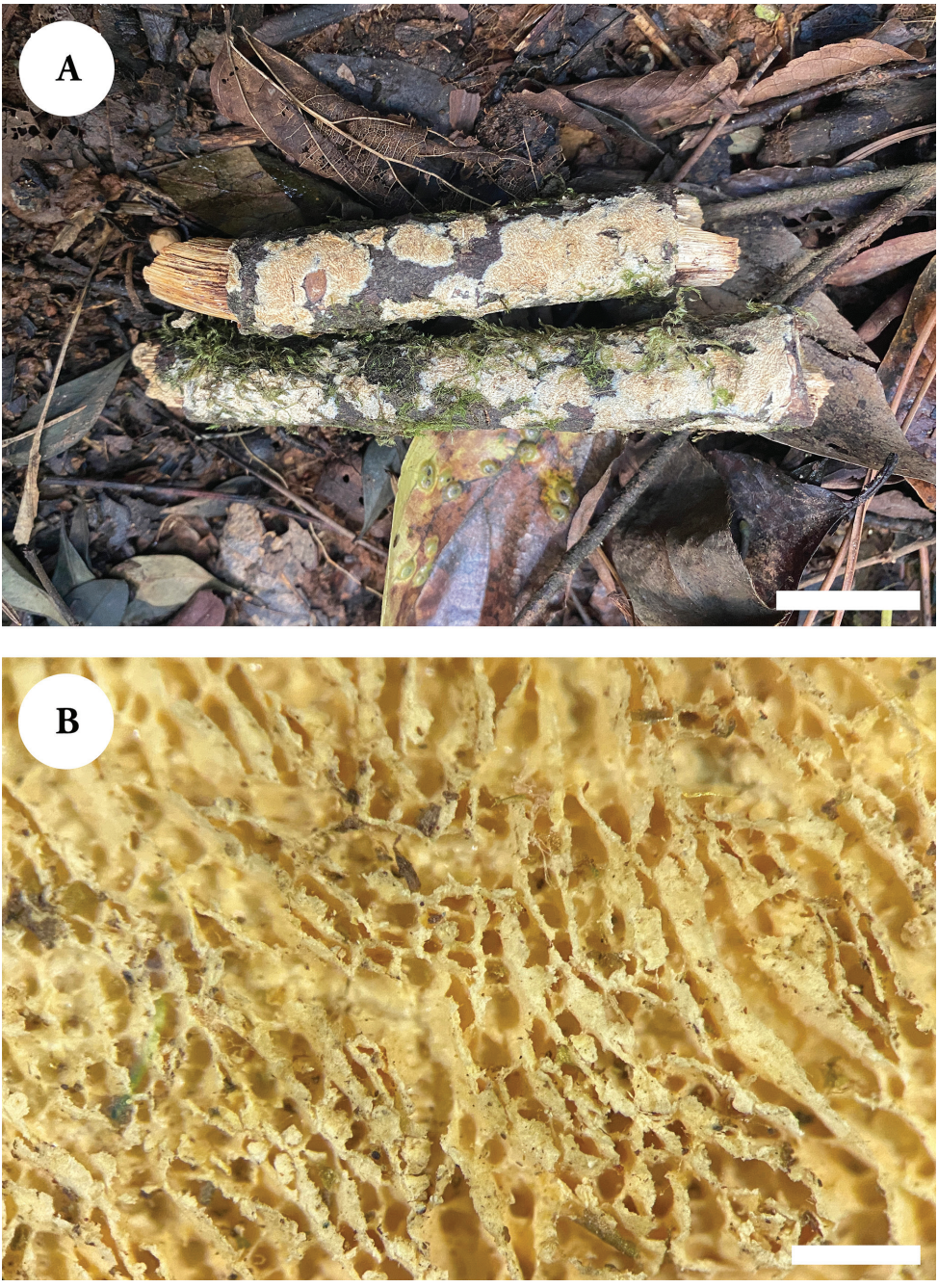

Figure 12. Basidiomata of *Xylodon puerensis* (holotype). Scale bars: 2 cm (**A**); 1 mm (**B**).

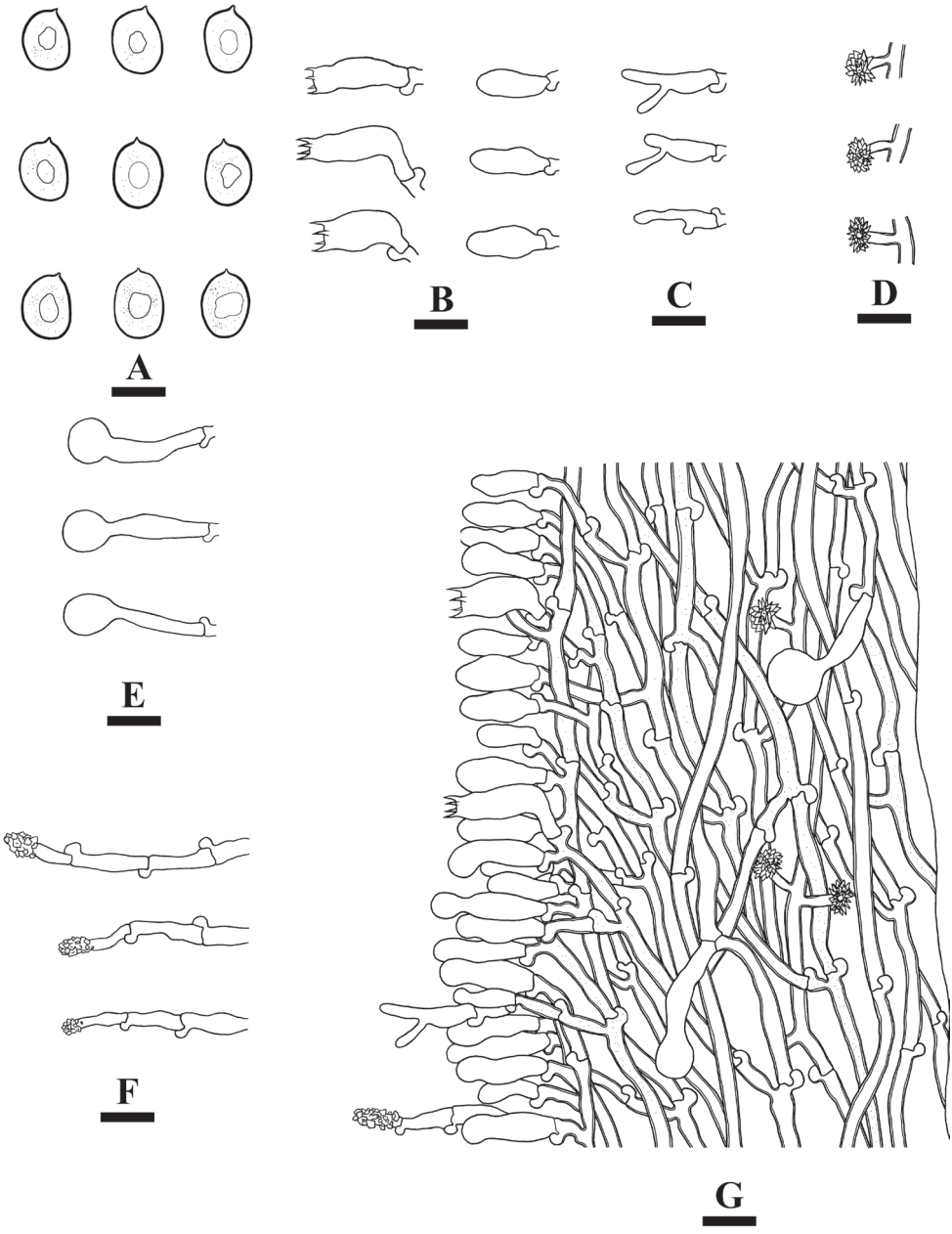

Figure 13. Microscopic structures of *Xylodon puerensis* (holotype) **A** basidiospores **B** basidia and basidioles **C** paraphysoid cystidia **D** astrocystidium **E** capitate cystidia **F** septocystidium cystidia **G** a section of hymenium. Scale bars: 5 μm (**A**); 10 μm (**B–G**).

Discussion

Many recently described wood-inhabiting fungal taxa have been reported in the subtropics and tropics, including in the genera *Lyomyces* and *Xylodon* (Xiong et al. 2009; Chen et al. 2017; Kan et al. 2017a, b; Riebesehl and Langer 2017; Viner et al. 2018; Chen and Zhao 2020; Luo et al. 2021a, b, c; Luo et al. 2022; Qu and Zhao 2022; Qu et al. 2022; Viner et al. 2022). Prior to this study, the following fourteen *Lyomyces* species were reported from China: *L. albus* (Sheng H. Wu) Riebesehl & Langer, *L. bambusinus*, *L. capitatocystidiatus* (H.X. Xiong, Y.C. Dai & Sheng H. Wu) Riebesehl & Langer, *L. cremeus* C.L. Zhao, *L. fissuratus*, *L. fumosus*, *L. leptocystidiatus* Xue W. Wang & L.W. Zhou, *L. macrosporus* C.L. Zhao & K.Y. Luo, *L. microfasciculatus* (Yurchenko & Sheng H. Wu) Riebesehl & Langer, *L. niveus*, *L. ochraceoalbus*, *L. sambuci*, *L. tenuissimus* (Yurchenko & Sheng H. Wu) Riebesehl & Langer and *L. wuliangshanensis* C.L. Zhao. (Xiong et al. 2009; Yurchenko et al. 2013; Riebesehl and Langer 2017; Chen and Zhao 2020; Luo et al. 2021b, c; Wang et al. 2021). The present study reports five new species in *Lyomyces* and *Xylodon*, based on a combination of morphological features and molecular evidence.

Phylogenetically, based on the multiple loci in *Hyphodontia* s.l., six genera, *Fasciodontia*, *Hastodontia*, *Hyphodontia*, *Lyomyces*, *Kneiffiella*, and *Xylodon*, were divided into four clades in the order Hymenochaetales (Wang et al. 2021). In the present study, based on the ITS+nLSU data (Fig. 1), *Lyomyces* and *Xylodon* were grouped with *Fasciodontia*, *Hastodontia*, *Hyphodontia* and *Kneiffielle*, in which five new species were grouped into the genera *Lyomyces* and *Xylodon*. Based on ITS topology (Figs 2, 3), *L. albopulverulentus* formed a monophyletic lineage, and was then grouped closely with *L. bambusinus*, *L. orientalis*, and *L. sambuci*. In addition, *L. yunnanensis* was found to be a sister to *L. niveus* with strong supports. The topology, based on ITS sequences, revealed that *X. daweishanensis* was retrieved as a sister to *X. hyphodontinus*. Moreover, *X. fissuratus* was grouped with the four taxa *X. montanus*, *X. subclavatus*, *X. wenshanensis*, and *X. xinpingensis*. *X. puerensis* was clustered with *X. flaviporus*, *X. ovisporus*, *X. subflaviporus*, *X. subtropicus*, and *X. taiwanianus*. However, morphologically, *L. bambusinus* can be delimited from *L. albopulverulentus* by its colliculose-to-tuberculate hymenial surface, its narrower basidia (16.5–35 × 3.5–7 μm), and its smaller and more broadly ellipsoid basidiospores (4.7–5.9 × 3.7–4.6 μm; Chen and Zhao 2020); Further, *L. orientalis* can be delimited from *L. albopulverulentus* by its smooth or slightly tuberculate hymenial surface, and by both its smaller basidia (13–20 × 3.5–4.5 μm) and basidiospores (5–6 × 4–4.5 μm; Yurchenko et al. 2017); *L. sambuci* can be delimited from *L. albopulverulentus* by its smooth-to-tuberculate hymenial surface and its smaller basidiospores (4.5–6 × 3.5–4 μm; Bernicchia and Gorjón 2010); *L. niveus* can be delimited from *L. yunnanensis* by a smaller basidia (9.5–15.0 × 3.5–5.5 μm) and broadly ellipsoid basidiospores (3.5–5 × 3–4 μm; Luo et al. 2021c). *Xylodon hyphodontinus* differs from *X. daweishanensis* by its larger basidiospores (4–5 × 4.5 μm; Hjortstam and Ryvarden 1980). *X. montanus* could be delimited from *X. fissuratus* by its smooth hymenial surface and moniliform cystidia (19.5–47.6 × 3.6–7.1 μm; Qu et al. 2022);

X. subclavatus differs from *X. fissuratus* by its larger capitate cystidia (20–25 × 3–4 μm) and wider basidiospores (4–5.5 × 3.5–4; Yurchenko et al. 2013); *X. wenshanensis* can be delimited from *X. fissuratus* by its smaller capitate cystidia (6–11 × 3–6.5 μm; Luo et al. 2022); *X. xinpingensis* can be delimited from *X. fissuratus* by its reticulate hymenial surface and larger basidia (18.5–33 × 3–6.5 μm; Ma and Zhao 2021). *Xylodon flaviporus* differs from *X. puerensis* by its wider basidia (14.5–20 × 5–7 μm) and smaller basidiospores (4.5–5.5 × 3–3.5 μm; Ryvarden 1985); *X. ovisporus* differs from *X. puerensis* by its smaller basidiospores (3.5–4.3 × 2.8–3.3 μm; Riebesehl and Langer 2017); *X. subflaviporus* is distinguishable from *X. puerensis* by its narrower basidia (8–18 × 4–5 μm) and smaller basidiospores (3.9–4.8 × 2.7–3.5 μm; Chen et al. 2017); *X. subtropicus* differs from *X. puerensis* by its smaller basidiospores (5–5.8 × 3.5–4 μm; Chen et al. 2017); *X. taiwanianus* differs from *X. puerensis* by its smaller basidiospores (4.5–5.5 × 2.6–3 μm; Wu 2001).

Morphologically, *Lyomyces albopulverulentus* resembles *L. bambusinus*, *L. cremeus*, *L. mascarensis* Riebesehl, Yurch. & Langer, *L. orientalis*, and *L. wuliangshanensis*, by sharing capitate cystidia and ellipsoid basidiospores. However, *L. bambusinus* differs from *L. albopulverulentus* by possessing a tapering cystidia (40–65 × 4–5.5 μm) and smaller basidiospores (4.7–5.9 × 3.7–4.6 μm; Chen and Zhao 2020); *L. cremeus* differs from *L. albopulverulentus* by its narrower capitate cystidia (20–40 × 3–5 μm), both smaller basidia (9–18.5 × 3–6 μm) and basidiospores (4.5–5.6 × 3.3–4.3 μm; Chen and Zhao 2020); *L. mascarensis* can be delimited from *L. albopulverulentus* by smaller capitate cystidia (17–38 × 3.5–6 μm), basidia (16–17.5 × 3.5–4.5 μm) and basidiospores (4.5–6 × 3.3–4 μm; Yurchenko et al. 2017); *L. orientalis* can be delimited from *L. albopulverulentus* due to its smaller capitate cystidia (17–38 × 3.5–6 μm), basidia (16–17.5 × 3.5–4.5 μm) and basidiospores (4.5–6 × 3.3–4 μm; Yurchenko et al. 2017); *L. wuliangshanensis* is different from *L. albopulverulentus* by smaller capitate cystidia (22–37 × 3–6 μm), basidia (12–20 × 3–4.3 μm) and basidiospores (3.5–5.3 × 2.8–4 μm; Chen and Zhao 2020).

Morphologically, *Lyomyces yunnanensis* resembles *L. bambusinus*, *L. cremeus*, *L. fumosus*, *L. fissuratus* and *L. wuliangshanensis* in both its capitate and tapering cystidia. However, *L. bambusinus* differs from *L. yunnanensis* by possessing a larger capitate cystidia (35–55 × 4–7 μm; Chen and Zhao 2020); *L. cremeus* differs from *L. yunnanensis* due to its smooth hymenial surface and smaller basidia (9–18.5 × 3–6 μm; Chen and Zhao 2020); *L. fissuratus* can be delimited from *L. yunnanensis* by its white-to-cream hymenial surface, and the presence of submoniliform cystidia (15.5–22 × 2.7–4 μm; Luo et al. 2021b); *L. fumosus* differs from *L. yunnanensis* due to its smooth hymenial surface, the presence of moniliform cystidia (8.5–22.7 × 2.5–3.7 μm), and its smaller basidia (11.5–17.5 × 3–5 μm; Luo et al. 2021b); *L. wuliangshanensis* is distinguishable from *L. yunnanensis* by its larger capitate cystidia (22–37 × 3–6 μm) and its smaller basidiospores (3.5–5.3 × 2.8–4 μm; Chen and Zhao 2020).

Morphologically, *Xylodon daweishanensis* is similar to *X. follis* Riebesehl et al., *X. grandineus* K.Y. Luo & C.L. Zhao, *X. laceratus* C.L. Zhao, *X. macrosporus*, *X. sinensis* C.L. Zhao & K.Y. Luo and *X. tropicus* C.L. Zhao due to its grandinioid,

or odontioid, hymenial surface. However, *X. follis* differs from *X. daweishanensis* due to its cream hymenial surface, wider capitate cystidia (17–30 × 4.5–9 μm), and larger, globose to subglobose basidiospores (8–9.5 × 7–8.5 μm; Riebesehl et al. 2019); *X. grandineus* differs from *X. daweishanensis* by its subulate cystidia (11–19 × 3–5 μm; Luo et al. 2022); *X. laceratus* can be delimited from *X. daweishanensis* by its fusiform cystidia (20.3–26.8 × 5.3–6.4 μm) and its larger basidiospores (3.9–5.3 × 2.6–4.1 μm; Qu et al. 2022); *X. macrosporus* differs from *X. daweishanensis* by its cylindrical cystidia (44–79.5 × 3–6 μm), larger basidia (11.5–36 × 5–11 μm) and thick-walled basidiospores (8–10.5 × 7.5–9 μm; Luo et al. 2021a); *X. sinensis* differs from *X. daweishanensis* by its fusiform cystidia (10–21 × 3–6 μm), and its buff-to-brown hymenial surface (Luo et al. 2021a); *X. tropicus* can be delimited from *X. daweishanensis* by its subglobose, slightly thick-walled basidiospores (Qu et al. 2022).

Xylodon fissuratus resembles *X. attenuatus* Spirin & Viner, *X. borealis* (Kotir. & Saaren.) Hjortstam & Ryvarden, *X. bresinskyi* (Langer) Hjortstam & Ryvarden, *X. dimiticus* (Jia J. Chen & L.W. Zhou) Riebesehl & E. Langer, *X. grandineus* and *X. vesiculosus* Yurchenko et al. by it sharing similar ellipsoid basidiospores. However, *X. attenuatus* differs from *X. fissuratus* due to its odontoid hymenial surface, the presence of hyphoid cystidia (17.6–39 × 2.7–4.6 μm) and its larger capitate cystidia (14.2–27.2 × 3.3–4.5 μm; Viner et al. 2018); *X. borealis* differs from *X. fissuratus* by its slender hypha-like cystidia (40–70 × 3–5 μm), larger capitate cystidia (20–50 × 4–6 μm) and basidia (15–20 × 4–5 μm; Bernicchia and Gorjón 2010); *X. bresinskyi* differs from *X. fissuratus* by its poroid hymenial surface with rudimentary console shaping (Langer 2000); *X. dimiticus* is distinguishable from *X. fissuratus* by poroid hymenial surface with angular pores (2–4 per mm; Chen et al. 2016); *X. grandineus* differs from *X. fissuratus* due to its subulate cystidia (11–19 × 3–5 μm) and its smaller basidiospores (3–4.5 × 2–3 μm; Luo et al. 2022); *X. vesiculosus* can be delimited from *X. fissuratus* by its odontioid hymenial surface and larger basidiospores (5.3–6.3 × 3–4 μm; Riebesehl et al. 2019).

Xylodon puerensis is similar to *X. bresinskyi*, *X. dimiticus*, *X. hallenbergii* (Sheng H. Wu) Hjortstam & Ryvarden, *X. poroideoefibulatus* (Sheng H. Wu) Hjortstam & Ryvarden, *X. reticulatus* (C.C. Chen & Sheng H. Wu) C.C. Chen & Sheng H. Wu, *X. subtropicus* and *X. syringae* (Langer) Hjortstam & Ryvarden by sharing a similar poroid hymenophore. However, *X. bresinskyi* can be delimited from *X. puerensis* by possessing smaller basidiospores (4.5–5.5 × 3–3.5 μm; Langer 2000); *X. dimiticus* differs from *X. puerensis* by possessing smaller basidia (9–13 × 4.5–6 μm) and basidiospores (3.8–4.6 × 2.8–3.5 μm; Chen et al. 2016); *X. hallenbergii* can be delimited from *X. fissuratus* by its both smaller capitate cystidia (15–23 × 4–5.3 μm) and basidiospores (4.2–5 × 4–4.3 μm; Wu 2001); *X. poroideoefibulatus* differs from *X. puerensis* by possessing smaller capitate cystidia (12–23 × 5.5–6.5 μm) and basidiospores (5–5.7 × 4–4.5 μm; Wu 2001); *X. reticulatus* can be delimited from *X. puerensis* by possessing smaller basidiospores (5–5.5 × 3.5–4 μm; Wu 1990); *X. syringae* differs from *X. puerensis* by its larger basidia (20–32 × 4–5 μm) and suballantoid basidiospores (8–9 × 3–3.5 μm; Hjortstam and Ryvarden 2009).

Acknowledgements

The research was supported by the National Natural Science Foundation of China (Project No. 32170004); the Yunnan Fundamental Research Project (Grant No. 202001AS070043); the High-level Talents Program of Yunnan Province (YNQR-QNRC-2018-111).

References

Bernicchia A, Gorjón SP (2010) Fungi Europaei 12: Corticiaceae s.l. Edizioni Candusso, Alassio, Italy, 1008 pp.

Chen JZ, Zhao CL (2020) Morphological and molecular identification of four new resupinate species of *Lyomyces* (Hymenochaetales) from southern China. MycoKeys 65: 101–118. https://doi.org/10.3897/mycokeys.65.48660

Chen JJ, Zhou LW, Ji XH, Zhao CL (2016) *Hyphodontia dimitica* and *H. subefibulata* spp. nov. (Schizoporaceae, Hymenochaetales) from southern China based on morphological and molecular characters. Phytotaxa 269: 001–013. https://doi.org/10.11646/phytotaxa.269.1.1

Chen CC, Wu SH, Chen CY (2017) Three new species of *Hyphodontia* s.l. (Basidiomycota) with poroid or raduloid hymenophore. Mycological Progress 16(5): 553–564. https://doi.org/10.1007/s11557-017-1286-0

Chevallier FF (1826) Flore Générale des Environs de Paris. Ferra Jeune, Paris, 674 pp.

Cui BK, Li HJ, Ji X, Zhou JL, Song J, Si J, Yang ZL, Dai YC (2019) Species diversity, taxonomy and phylogeny of Polyporaceae (Basidiomycota) in China. Fungal Diversity 97(1): 137–392. https://doi.org/10.1007/s13225-019-00427-4

Cunningham GH (1959) Hydnaceae of New Zealand. Part II. The genus *Odontia*. Transactions of the Royal Society of New Zealand 86: 65–103.

Cunningham GH (1963) The Thelephoraceae of Australia and New Zealand. Bulletin of the New Zealand Department of Scientific and Industrial Research 145: 1–359.

Dai YC (2010) Hymenochaetaceae (Basidiomycota) in China. Fungal Diversity 45(1): 131–343. https://doi.org/10.1007/s13225-010-0066-9

Dai YC (2011) A revised checklist of corticioid and hydnoid fungi in China for 2010. Mycoscience 52(1): 69–79. https://doi.org/10.1007/S10267-010-0068-1

Dai YC (2012) Polypore diversity in China with an annotated checklist of Chinese polypores. Mycoscience 53(1): 49–80. https://doi.org/10.1007/s10267-011-0134-3

Dai YC, Yang ZL, Cui BK, Wu G, Yuan HS, Zhou LW, He SH, Ge ZW, Wu F, Wei YL, Yuan Y, Si J (2021) Diversity and systematics of the important macrofungi in Chinese forests. Junwu Xuebao 40: 770–805.

Felsenstein J (1985) Confidence intervals on phylogenetics: An approach using bootstrap. Evolution. International Journal of Organic Evolution 39(4): 783–791. https://doi.org/10.2307/2408678

Gafforov Y, Riebesehl J, Ordynets A, Langer E, Yarasheva M, Ghobad-Nejhad M, Zhou L-W, Wang X-W, Gugliotta AM (2017) *Hyphodontia* (Hymenochaetales, Basidiomycota) and similar taxa from Central Asia. Botany 95(11): 1041–1056. https://doi.org/10.1139/cjb-2017-0115

Girometta CE, Bernicchia A, Baiguera RM, Bracco F, Buratti S, Cartabia M, Picco AM, Savino E (2020) An italian researchculture collection of wood decay fungi. Diversity (Basel) 12(2): 58. https://doi.org/10.3390/d12020058

Gray SF (1821) A Natural Arrangement of British Plants. Nabu Press, London, UK, 649 pp.

Greslebin AG, Rajchenberg M (2000) The genus *Hyphodontia* in the Patagonian Andes Forest of Argentina. Mycologia 92(6): 1155–1165. https://doi.org/10.1080/00275514.2000.12061263

He SH, Li HJ (2013) *Pseudochaete latesetosa* and *P. subrigidula* spp. nov. (Hymenochaetales, Basidiomycota) from China based on morphological and molecular characters. Mycological Progress 12(2): 331–339. https://doi.org/10.1007/s11557-012-0838-6

Hjortstam K, Ryvarden L (1980) Studies in tropical Corticiaceae (Basidiomycetes). II. Mycotaxon 12: 168–184.

Hjortstam K, Ryvarden L (2007) Studies in corticioid fungi from Venezuela III (Basidiomycotina, Aphyllophorales). Synopsis Fungorum 23: 56–107.

Hjortstam K, Ryvarden L (2009) A checklist of names in *Hyphodontia* sensu stricto-sensu lato and *Schizopora* with new combinations in *Lagarobasidium*, *Lyomyces*, *Kneiffiella*, *Schizopora*, and *Xylodon*. Synopsis Fungorum 26: 33–55.

Hyde KD (2022) The numbers of fungi. Fungal Diversity 114(1): 1. https://doi.org/10.1007/s13225-022-00507-y

James TY, Stajich JE, Hittinger CT, Rokas A (2020) Toward a fully resolved fungal tree of life. Annual Review of Microbiology 74(1): 291–313. https://doi.org/10.1146/annurev-micro-022020-051835

Jiang N, Voglmayr H, Bian DR, Piao CG, Wnag SK, Li Y (2021) Morphology and phylogeny of *Gnomoniopsis* (Gnomoniaceae, Diaporthales) from fagaceae leaves in China. Journal of Fungi (Basel, Switzerland) 7(10): 792. https://doi.org/10.3390/jof7100792

Kan YH, Gafforov Y, Li T, Zhou LW (2017a) *Hyphodontia zhixiangii* sp. nov. (Schizoporaceae, Basidiomycota) from Uzbekistan. Phytotaxa 299(2): 273–279. https://doi.org/10.11646/phytotaxa.299.2.12

Kan YH, Qin WM, Zhou LW (2017b) *Hyphodontia mollissima* sp. nov. (Schizoporaceae, Hymenochaetales) from Hainan, southern China. Mycoscience 58(4): 297–301. https://doi.org/10.1016/j.myc.2017.04.003

Karsten PA (1881) Enumeratio Thelephorearum Fr. et Clavariearum Fr. Fennicarum, systemate novo dispositarum. Revue Mycologique Toulouse 3: 21–23.

Karsten PA (1882) Rysslands, Finlands och den Skandinaviska halföns Hattsvampar. Sednare Delen: Pip-, Tagg-, Hud-, Klubboch Gelésvampar. Bidrag till Kännedom av Finlands Natur och. Folk (Kobenhavn) 37: 1–257.

Katoh K, Rozewicki J, Yamada KD (2019) MAFFT online service: Multiple sequence alignment, interactive sequence choice and visualization. Briefings in Bioinformatics 20(4): 1160–1166. https://doi.org/10.1093/bib/bbx108

Kotiranta H, Saarenoksa R (2000) Three new species of *Hyphodontia* (Coritciaceae). Annales Botanici Fennici 37(4): 255–278.

Kuntze OI (1898) Revisio Generum Plantarum. A. Felix, Leipzig, Germany, 576 pp.

Langer E (1994) Die Gattung *Hyphodontia* John Eriksson. Bibliotheca Mycologica, Schweizerbart Science Publishers, Stuttgart, Germany, Volume 154, 298 pp.

Langer E (2000) Bemerkenswerte pilze aus dem Nationalpark Bayerischer Wald: *Schizopora bresinskyi* sp. nov. Hoppea 61: 229–235.

Larsson KH (2007) Re-thinking the classification of corticioid fungi. Mycological Research 111(9): 1040–1063. https://doi.org/10.1016/j.mycres.2007.08.001

Larsson A (2014) AliView: A fast and lightweight alignment viewer and editor for large data sets. Bioinformatics 30(22): 3276–3278. https://doi.org/10.1093/bioinformatics/btu531

Larsson KH, Larsson E, Kõljalg U (2004) High phylogenetic diversity among corticioid homobasidiomycetes. Mycological Research 108(9): 983–1002. https://doi.org/10.1017/S0953756204000851

Larsson KH, Parmasto E, Fischer M, Langer E, Nakasone KK, Redhead SA (2006) Hymenochaetales: A molecular phylogeny for the hymenochaetoid clade. Mycologia 98(6): 926–936. https://doi.org/10.1080/15572536.2006.11832622

Lee IS, Langer E (2012) New records of *Hyphodontia* species from Taiwan. Nova Hedwigia 94(1–2): 239–244. https://doi.org/10.1127/0029-5035/2012/0094-0239

Luo KY, Zhao CL (2021) *Fasciodontia yunnanensis* (Schizoporaceae, Hymenochaetales), a new species from southern China. Annales Botanici Fennici 58(4–6): 259–266. https://doi.org/10.5735/085.058.0411

Luo KY, Qu MH, Zhao CL (2021a) Additions to the knowledge of Corticioid *Xylodon* (Schizoporaceae, Hymenochaetales): Introducing three new *Xylodon* species from southern China. Diversity (Basel) 13(11): 581. https://doi.org/10.3390/d13110581

Luo X, Chen YH, Zhao CL (2021b) *Lyomyces fissuratus* and *L. fumosus* (Schizoporaceae, Hymenochaetales), new species from southern China. Annales Botanici Fennici 4(4–6): 58. https://doi.org/10.5735/085.058.0404

Luo X, Chen YH, Zhao CL (2021c) Morphological and phylogenetic characterization of fungi within Hymenochaetales: Introducing two new species from southern China. Nordic Journal of Botany 12(12): 39. https://doi.org/10.1111/njb.03414

Luo KY, Chen ZY, Zhao CL (2022) Phylogenetic and taxonomic analyses of three new wood-inhabiting Fungi of *Xylodon* (Basidiomycota) in a Forest Ecological System. Journal of Fungi (Basel, Switzerland) 8(4): 405. https://doi.org/10.3390/jof8040405

Ma X, Zhao CL (2021) *Xylodon bambusinus* and *X. xinpingensis* spp. nov. (Hymenochaetales) from southern China. Phytotaxa 511(3): 231–247. https://doi.org/10.11646/phytotaxa.511.3.3

Miller MA, Pfeiffer W, Schwartz T (2012) The CIPRES Science Gateway: Enabling high-impact science for phylogenetics researchers with limited resources. Association for Computing Machinery 39: 1–8. https://doi.org/10.1145/2335755.2335836

Nylander JAA (2004) MrModeltest v.2. Program Distributed by the Author; Evolutionary Biology Centre, Uppsala University, Uppsala, Sweden.

Paulus B, Hallenberg N, Buchanan PK, Chambers GK (2000) A phylogenetic study of the genus *Schizopora* (Basidiomycota) based on ITS DNA sequences. Mycological Research 104(10): 1155–1163. https://doi.org/10.1017/S0953756200002720

Petersen JH (1996) The Danish Mycological Society's colour-chart. Foreningen til Svampekundskabens Fremme, Greve.

Qu MH, Zhao CL (2022) *Xylodon flocculosus* sp. nov. from Yunnan, China. Mycotaxon 137(2): 189–201. https://doi.org/10.5248/137.189

Qu MH, Wang DQ, Zhao CL (2022) A phylogenetic and taxonomic study on *Xylodon* (Hymenochaetales): Focusing on three new *Xylodon* species from southern China. Journal of Fungi (Basel, Switzerland) 8(1): 35. https://doi.org/10.3390/jof8010035

Rabenhorst GL (1851) Klotzschii herbarium vivum mycologicum sistens fungorum per totam Germaniam crescentium collectionem perfectam. Editio prima. Centuria 8: 1501–1600.

Rehner SA, Samuels GJ (1994) Taxonomy and phylogeny of *Gliocladium* analysed from nuclear large subunit ribosomal DNA sequences. Mycological Research 98(6): 625–634. https://doi.org/10.1016/S0953-7562(09)80409-7

Riebesehl J, Langer E (2017) *Hyphodontia* s.l. (Hymenochaetales, Basidiomycota): 35 new combinations and new keys to currently all 120 species. Mycological Progress 16(6): 637–666. https://doi.org/10.1007/s11557-017-1299-8

Riebesehl J, Yurchenko E, Nakasone KK, Langer E (2019) Phylogenetic and morphological studies in *Xylodon* (Hymenochaetales, Basidiomycota) with the addition of four new species. MycoKeys 47: 97–137. https://doi.org/10.3897/mycokeys.47.31130

Ronquist F, Teslenko M, van der Mark P, Ayres DL, Darling A, Hohna S, Larget B, Liu L, Suchard MA, Huelsenbeck JP (2012) MrBayes 3.2: Efficient Bayesian phylogenetic inference and model choice across a large model space. Systematic Biology 61(3): 539–542. https://doi.org/10.1093/sysbio/sys029

Ryvarden L (1985) Type studies in the Polyporaceae 17. Species described by W.A. Murrill. Mycotaxon 23: 169–198.

Shi ZW, Wang XW, Zhou LW, Zhao CL (2019) *Xylodon kunmingensis* sp. nov. (Hymenochaetales, Basidiomycota) from southern China. Mycoscience 60(3): 184–188. https://doi.org/10.1016/j.myc.2019.02.002

Tura DA, Zmitrovich IV, Wasser SP, Spirin WA, Nevo E (2011) Biodiversity of the Heterobasidiomycetes and Non-Gilled Hymenomycetes (Former Aphyllophorales) of Israel. ARA Gantner Verlag K-G, Ruggell, Liechtenstein, 566 pp.

Vilgalys R, Hester M (1990) Rapid genetic identification and mapping of enzymatically amplified ribosomal DNA from several *Cryptococcus* species. Journal of Bacteriology 172(8): 4238–4246. https://doi.org/10.1128/jb.172.8.4238-4246.1990

Viner I, Spirin V, Zíbarová L, Larsson KH (2018) Additions to the taxonomy of *Lagarobasidium* and *Xylodon* (Hymenochaetales, Basidiomycota). MycoKeys 41: 65–90. https://doi.org/10.3897/mycokeys.41.28987

Viner I, Bortnikov F, Miettinen O (2022) On six African species of *Lyomyces* and *Xylodon*. Fungal Systematics and Evolution 8: 163–178. https://doi.org/10.3114/fuse.2021.08.13

Vu D, Groenewald M, Vries M, Gehrmann T, Stielow B, Eberhardt U (2019) Large-scale generation and analysis of filamentous fungal DNA barcodes boosts coverage for kingdom Fungi and reveals thresholds for fungal species and higher taxon delimitation. Studies in Mycology 92(1): 135–154. https://doi.org/10.1016/j.simyco.2018.05.001

Wang M, Chen YY (2017) Phylogeny and taxonomy of the genus *Hyphodontia* (Hymenochaetales, Basidiomycota) in China. Phytotaxa 309(1): 45–54. https://doi.org/10.11646/phytotaxa.309.1.4

Wang XW, May TW, Liu SL, Zhou LW (2021) Towards a natural classification of *Hyphodontia* sensu lato and the trait evolution of basidiocarps within Hymenochaetales (Basidiomycota). Journal of Fungi (Basel, Switzerland) 7(6): 478. https://doi.org/10.3390/jof7060478

White TJ, Bruns T, Lee S, Taylor J (1990) Amplification and direct sequencing of fungal ribosomal RNA genes for phylogenetics. In: Innis MA, Gelfand DH, Sninsky JJ, White TJ (Eds) PCR protocols: A Guide to Methods And Applications. Academic Press, San Diego, CA, 315–322. https://doi.org/10.1016/B978-0-12-372180-8.50042-1

Wijayawardene NN, Hyde KD, Al-Ani LKT, Tedersoo L, Haelewaters D, Rajeshkumar KC, et al. (2020) Outline of Fungi and fungus-like taxa. Mycosphere 11(1): 1060–1456. https://doi.org/10.5943/mycosphere/11/1/8

Wu SH (1990) The Corticiaceae (Basidiomycetes) subfamilies Phlebioideae, Phanerochaetoideae and Hyphodermoideae in Taiwan. Acta Botanica Fennica 142: 1–123.

Wu SH (2000) Studies on *Schizopora flavipora* s.l., with special emphasis on specimens from Taiwan. Mycotaxon 76: 51–66.

Wu SH (2001) Three new species of *Hyphodontia* with poroid hymenial surface. Mycologia 93(5): 1019–1025. https://doi.org/10.1080/00275514.2001.12063235

Wu SH (2006) *Hyphodontia tubuliformis*, a new species from Taiwan. Mycotaxon 95: 185–188.

Wu F, Zhou LW, Vlasák J, Dai YC (2022a) Global diversity and systematics of Hymenochaetaceae with poroid hymenophore. Fungal Diversity 113(1): 1–192. https://doi.org/10.1007/s13225-021-00496-4

Wu F, Man XW, Tohtirjap A, Dai YC (2022b) A comparison of polypore fungal and species composition in forest ecosystems of China, North America, and Europe. Forest Ecosystems 9: 100051. https://doi.org/10.1016/j.fecs.2022.100051

Xiong HX, Dai YC, Wu SH (2009) Three new species of *Hyphodontia* from Taiwan. Mycological Progress 8(3): 165–169. https://doi.org/10.1007/s11557-009-0587-3

Xiong HX, Dai YC, Wu SH (2010) Two new species of *Hyphodontia* from China. Mycologia 102(4): 918–922. https://doi.org/10.3852/09-139

Yurchenko E, Wu SH (2013) Three new species of *Hyphodontia* with peg-like hyphal aggregations. Mycological Progress 13(3): 533–545. https://doi.org/10.1007/s11557-013-0935-1

Yurchenko E, Wu SH (2014) *Hyphoderma formosanum* sp. nov. (Meruliaceae, Basidiomycota) from Taiwan. Sydowia 66: 19–23.

Yurchenko E, Wu SH (2016) A key to the species of *Hyphodontia* sensu lato. MycoKeys 12: 1–27. https://doi.org/10.3897/mycokeys.12.7568

Yurchenko E, Xiong HX, Wu SH (2013) Four new species of *Hyphodontia* (*Xylodon* ss. Hjortstam & Ryvarden, Basidiomycota) from Taiwan. Nova Hedwigia 96(3–4): 545–558. https://doi.org/10.1127/0029-5035/2013/0092

Yurchenko E, Riebesehl J, Langer E (2017) Clarification of *Lyomyces sambuci* complex with the descriptions of four new species. Mycological Progress 16(9): 865–876. https://doi.org/10.1007/s11557-017-1321-1

Yurchenko E, Riebesehl J, Langer E (2020) *Fasciodontia* gen. nov. (Hymenochaetales, Basidiomycota) and the taxonomic status of *Deviodontia*. Mycological Progress 19(2): 171–184. https://doi.org/10.1007/s11557-019-01554-7

Zhao CL, Wu ZQ (2017) *Ceriporiopsis kunmingensis* sp. nov. (Polyporales, Basidiomycota) evidenced by morphological characters and phylogenetic analysis. Mycological Progress 16(1): 93–100. https://doi.org/10.1007/s11557-016-1259-8

Zhao CL, Cui BK, Dai YC (2014) Morphological and molecular identification of two new species of *Hyphodontia* (Schizoporaceae, Hymenochaetales) from southern China. Cryptogamie. Mycologie 35(1): 87–97. https://doi.org/10.7872/crym.v35.iss1.2014.87

MycoKeys 96: 57–75 (2023)
doi: 10.3897/mycokeys.96.100037
https://mycokeys.pensoft.net

RESEARCH ARTICLE

A peer-reviewed open-access journal
MycoKeys
Launched to accelerate biodiversity research

Mycobiont-specific primers facilitate the amplification of mitochondrial small subunit ribosomal DNA: a focus on the lichenized fungal genus *Melanelia* (Ascomycota, Parmeliaceae) in Iceland

Maonian Xu[1], Yingkui Liu[2], Erik Möller[3], Scott LaGreca[4], Patricia Moya[5], Xinyu Wang[6], Einar Timdal[3], Hugo de Boer[3], Eva Barreno[5], Lisong Wang[6], Holger Thüs[7], Ólafur Andrésson[8], Kristinn Pétur Magnússon[9,10], Elín Soffia Ólafsdóttir[1], Starri Heiðmarsson[11]

1 *Faculty of Pharmaceutical Sciences, University of Iceland, Hofsvallagata 53, IS-107 Reykjavik, Iceland* **2** *Jiangsu Key Laboratory of Brain Disease Bioinformation, Research Center for Biochemistry & Molecular Biology, College of Life Sciences, Xuzhou Medical University, 209 Tongshan Road, Xuzhou, 221004, China* **3** *Natural History Museum, University of Oslo, NO-0318 Oslo, Norway* **4** *Department of Biology, Duke University, NC 27708-0338 Durham, USA* **5** *Instituto Cavanilles de Biodiversidad y Biologia Evolutiva (ICBIBE), Dpto. Botánica, Facultat de Ciències Biològiques, Universitat de València, C/ Dr. Moliner 50, 46100-Burjassot, València, Spain* **6** *Laboratory for Plant Diversity and Biogeography of East Asia, Kunming Institute of Botany, Chinese Academy of Sciences, 650204 Kunming, China* **7** *Botany Department, State Museum of Natural History Stuttgart, D-70191 Stuttgart, Germany* **8** *Faculty of Life and Environmental Sciences, University of Iceland, IS-102 Reykjavik, Iceland* **9** *Faculty of Natural Resource Sciences, University of Akureyri, IS-600 Akureyri, Iceland* **10** *Icelandic Institute of Natural History, IS-600 Akureyri, Iceland* **11** *Northwest Iceland Nature Research Centre, IS-550 Sauðárkrókur, Iceland*

Corresponding author: Starri Heiðmarsson (starri@nnv.is)

Academic editor: F. Dal Grande | Received 8 January 2023 | Accepted 7 March 2023 | Published 21 March 2023

Citation: Xu M, Liu Y, Möller E, LaGreca S, Moya P, Wang X, Timdal E, de Boer H, Barreno E, Wang L, Thüs H, Andrésson Ó, Magnússon KP, Ólafsdóttir ES, Heiðmarsson S (2023) Mycobiont-specific primers facilitate the amplification of mitochondrial small subunit ribosomal DNA: a focus on the lichenized fungal genus *Melanelia* (Ascomycota, Parmeliaceae) in Iceland. MycoKeys 96: 57–75. https://doi.org/10.3897/mycokeys.96.100037

Abstract

The fungal mitochondrial small subunit (mtSSU) ribosomal DNA is one of the most commonly used loci for phylogenetic analysis of lichen-forming fungi, but their primer specificity to mycobionts has not been evaluated. The current study aimed to design mycobiont-specific mtSSU primers and highlights their utility with an example from the saxicolous lichen-forming fungal genus *Melanelia* Essl. in Iceland. The study found a 12.5% success rate (3 out of 24 specimens with good-quality mycobiont mtSSU sequences)

using universal primers (i.e. mrSSU1 and mrSSU3R), not including off-target amplification of environmental fungi, e.g. *Cladophialophora carrionii* and *Lichenothelia convexa*. New mycobiont-specific primers (mt-SSU-581-5' and mt-SSU-1345-3') were designed by targeting mycobiont-specific nucleotide sites in comparison with environmental fungal sequences, and assessed for mycobiont primer specificity using *in silico* PCR. The new mycobiont-specific mtSSU primers had a success rate of 91.7% (22 out of 24 specimens with good-quality mycobiont mtSSU sequences) on the studied *Melanelia* specimens. Additional testing confirmed the specificity and yielded amplicons from 79 specimens of other Parmeliaceae mycobiont lineages. This study highlights the effectiveness of designing mycobiont-specific primers for studies on lichen identification, barcoding and phylogenetics.

Keywords
Melanelia, mtSSU, Parmeliaceae, PCR, primer design

Introduction

In addition to the accepted fungal barcode of nuclear ribosomal internal transcribed spacer (nrITS) locus (Schoch et al. 2012), the fungal mitochondrial small subunit (mtSSU) ribosomal DNA region is one of the most frequently used molecular markers, for two reasons: 1) it has higher mutation rate than its nuclear small subunit counterparts; and 2) it contains both conservative regions that allow for higher taxonomic level analysis, as well as highly variable regions that are suitable for lower taxonomic level analysis. The mtSSU is commonly incorporated into multi-locus phylogenetic analyses of various lichen-forming fungal lineages (Crespo et al. 2007; Nelsen et al. 2011; Divakar et al. 2017; Xu et al. 2020). Due to the utility and popularity of this marker, the paper publishing the universal mtSSU primer pair (i.e. mrSSU1 and mrSSU3R) (Zoller et al. 1999) is well cited (543 times by Feb 15, 2023).

In total, eight universal and conserved regions (i.e. U1 to U8) are recognized in the fungal mtSSU locus (Cummings et al. 1989), and published primer pairs, such as MS1&MS2, NMS1&NMS2, MSU1&MSU7 and mrSSU1&mrSSU3R, were all designed from those universal regions to enable the amplification of a large variety of fungal taxa (Cummings et al. 1989; Zoller et al. 1999; Zhou and Stanosz 2001). They work well for fungal isolates, and even microbial communities like lichens. The most used primer pair in lichen systematics, mrSSU1 and mrSSU3R, is fungus-specific and yields no PCR products from isolated photobionts (Zoller et al. 1999). However, primer specificity to the lichen-forming fungi (mycobionts) has not been evaluated, and the utility of universal mtSSU primers (e.g. mrSSU1 and mrSSU3R) in challenging lichen herbarium specimens, as opposed to freshly collected specimens that are more favorable for PCR, is not well-known. Taking the advantage of the vast number of reference sequences deposited in publicly available databases (e.g. GenBank), *in silico* PCR can be an efficient tool to evaluate primer specificity or potential bias during simulated PCR conditions (Bellemain et al. 2010).

In our recent phylogenetic diversity analyses of Icelandic cetrarioid lichens (Xu et al. 2020), we reported a remarkably low PCR success rate when using the primer pair

mrSSU1 and mrSSU3R to amplify herbarium specimens of the saxicolous genus *Melanelia* Essl. (12.5%, 3 out of 24 specimens). For some specimens, instead of the targeted mycobionts, we ended up with good Sanger sequencing results of environmental fungi (unpublished), such as *Cladophialophora carrionii* (Trejos) de Hoog, Kwon-Chung & McGinnis (Herpotrichiellaceae, Ascomycota) and *Lichenothelia convexa* Henssen (Lichenotheliaceae, Ascomycota). This raised questions about primer specificity to the genus *Melanelia*, and mycobionts in general. In the current study, our goal was to design mycobiont-specific mtSSU primers for the genus *Melanelia*, and assess the specificity of these primers to mycobionts. Additionally, we intended to investigate universality of these primers in the Parmeliaceae family using both *in silico* PCR and *in vitro* PCR screening of taxa sampled broadly from specimens across the family.

Methods

Primer design

Using a multiple sequence alignment, shared primer binding sites were identified in the conserved mtSSU regions among mycobiont genera, that are absent from other ascomycetous fungal genera. Special focus was given to 3' end unique amplification. The multiple sequence alignment was compiled (Suppl. material 1) from 48 mycobiont mtSSU sequences (10 in-house curated and 38 downloaded from GenBank) and six non-mycobiont/non-lichen-forming fungal sequences of different fungal classes, including *Mycocalicium subtile* (Pers.) Szatala (Class: Eurotiomycetes), *Taphrina flavorubra* W.W. Ray (Class: Taphrinomycetes) and *Botryotinia fuckeliana* (de Bary) Whetzel (Class: Leotiomycetes). Non-mycobiont fungal sequences also include one reference sequence of the ascomycete *Triangularia anserina* (Rabenh.) X. Wei Wang & Houbraken (Basionym: *Podospora anserina* (Rabenh.) Niessl; Class: Sordariomycetes; GenBank accession No. X14734), as well as two environmental fungal sequences from *Cladophialophora carrionii* (Trejos) de Hoog, Kwon-Chung & McGinnis (Class: Eurotiomycetes) and *Lichenothelia convexa* Henssen (Class: Dothideomycetes), both of which were found to co-inhibit with *Melanelia* mycobionts. Melting temperature and primer dimer formation were estimated using Multiple Primer Analyzer (ThermoFisher, MA, USA).

In silico PCR

EcoPCR (Ficetola et al. 2010) was used for simulated *in silico* amplification of the mtSSU locus and also to verify amplicon possibilities against an in-house reference ecoPCR database containing overall 2,233,856 fungal sequences. We followed the published procedure (Bellemain et al. 2010) to construct the in-house reference database: all fungal sequences were downloaded from the EMBL fungal database of standard targeted annotated assembled sequences (STD), and sequences were annotated using

NCBI taxonomy. Data containing the vast number of annotated fungal sequences were transformed into ecoPCR format before *in silico* simulation. Two pairs of primers were tested: the commonly used pair mrSSU1 and mrSSU3R, and our newly designed mycobiont-specific primer pair mt-SSU-581-5' and mt-SSU-1345-3'. In the setting of simulations, amplicon sizes were accepted between 200 bp to 2500 bp, and only up to three nucleotide mismatches between primers and templates were allowed (except for the last two positions at the 3' end), according to described parameters (Bellemain et al. 2010; Riaz et al. 2011; Liu and Erséus 2017).

Taxon sampling and DNA extraction

The current study included 24 *Melanelia* herbarium specimens collected from 1997 to 2014, consisting of *M. agnata* (n=8), *M. hepatizon* (n=12) and *M. stygia* (n=4), all of which were morphologically identified and verified with fungal nrITS DNA barcoding and chemotaxonomic analyses in a previous study (Xu et al. 2017). In addition to the *Melanelia* specimens, 79 specimens of other genera in the same family were also included to test primer universality in the family. The specimen list is provided in Appendix 1. Visible substrates attached to thalli were removed with sterile tweezers or brushes before DNA extraction. Whole genomic DNA was extracted from lichen thalli (ca. 15–20 mg per specimen) using the CTAB method (Cubero et al. 1999).

In vitro PCR and sequence analysis

The PCR master mix and thermal cycler conditions were followed from our published protocol (Xu et al. 2020). Two touchdown programmes were used, where the annealing temperature ramp 61–57 °C (decreasing 1 °C per cycle) was used for mrSSU1 and mrSSU3R, and 54–50 °C for the newly designed primer pair, mt-SSU-581-5' and mt-SSU-1345-3', according to predicted melting temperatures (Table 1). Presence and sizes of amplicons were determined by performing 2% agarose gel electrophoresis, using SYBR safe stain (Invitrogen, CA, USA). Amplicons showing single bands were purified with ExoSAP (Fermentas Inc., Hanover, MD, USA) and sequenced in both directions using Sanger sequencing (Macrogen Europe BV, the Netherlands). The same primers were used for both PCRs and Sanger sequencing.

Ambiguous sequences at both ends of the raw sequencing data were trimmed with the software PhyDE v0.9971. Sequence contigs were assembled from both directions and ambiguous base calling was checked. Sequences were identified by BLAST searches. Successful PCR amplification was defined as on-target/mycobiont-specific amplification and clean mycobiont mtSSU sequences without ambiguous base calling. Success rates in percentages were calculated as the number of specimens with successful PCR amplification divided by the total number of specimens. Multiple sequence alignment was performed using MAFFT (Katoh and Standley 2013) and then manually adjusted.

Table 1. Primers used for the amplification of the mtSSU locus.

Primer[a]	Location[b]	Sequence 5' – 3'	T_m[c]	Reference
Major primers				
mrSSU1(F)	533-552	AGCAGTGAGGAATATTGGTC	58.7	Zoller et al. 1999
mt-SSU-581-5'(F)	581-600	GGAGGAATGTATAGCAATAG	53.5	This study
mt-SSU-862-5'(F)[d]	862-880	GAAAGCATCYCCTTATGTG	56.7	This study
mt-SSU-1345-3'(R)	1345-1324	CGCTTGTAAATATATCTTATTG	53.4	This study
mrSSU3R(R)	1524-1505	ATGTGGCACGTCTATAGCCC	64.2	Zoller et al. 1999
Alternative primers				
mt-SSU-574-5'(F)	574-594	GCAACTTGRARGAATGTATAG	56.0	This study
mt-SSU-897-3'(R)	897-880	CCCTCAACGTCAGTTATC	56.0	This study
mt-SSU-1093-3'(R)	1093-1073	TCTAATGATTTCARTTCCAA	55.3	This study
mt-SSU-1372-3'(R)	1372-1353	CGACATTAACTGAAGACAGC	58.1	This study
mt-SSU-1492-3'(R)	1492-1472	CCATGATGACTTGTCTTAGTC	56.8	This study
mt-SSU-1548-3'(R)	1548-1529	ATTTCACACCCTTTTGTAAG	56.3	This study

[a]: primer nomenclature follows the recommendation (Gargas and DePriest 1996). Forward or reverse primers are indicated by (F) or (R);
[b]: location is relative to the reference fungal mtSSU sequence with GenBank accession No. X14734;
[c]: melting temperature (T_m) is estimated using the multiple primer analyzer online tool;
[d]: the primer mt-SSU-862-5' is recommended for herbarium specimens, focusing on the amplification of the highly variable region between U5 and U6 (numbers of variable sites refer to Table 3).

Results

Primer design

Multiple sequence alignments at the primer binding sites are shown in Fig. 1. The universal primers mrSSU1 and mrSSU3R were designed at the conserved region U2 and U6, respectively, with an expected amplicon size of around 900 base pairs (bp). From the alignments, this primer pair shows little discriminating power between lichen-forming and environmental ascomycetes. Therefore, searching for mycobiont-specific priming sites in the universal regions was not possible, and more variable regions were checked. New primers were designed at the genetic regions where high discriminations were found, particularly at the 3' end. The new forward primer is located at the variable sites between U2 and U3, showing ca. nine nucleotide differences between Parmeliaceae and environmental fungi. Similarly, the reverse primer was designed at the connecting zone between U5 and U6 with potential discriminating power including roughly nine nucleotide differences.

The newly designed primers, mt-SSU-581-5' with mt-SSU-1345-3', were named according to the primer nomenclature recommendation (Gargas and DePriest 1996): "mt-SSU" indicates the mitochondrial small subunit ribosomal DNA, and -5' or -3' defines the primer annealing to the coding strand (-5' for forward primers) or the non-coding one (-3' for reverse primers). The number before -5' or -3' is the nucleotide position relative to the reference sequence of the fungus *Triangularia anserina* at the 5' end, so these numbers help the estimation of amplicon sizes. For instance, mt-SSU-581-5' with mt-SSU-1345-3' will result in amplicons estimated around 700 bp. The numbering of primers, i.e. 581 and 1345, is based on the reference fungus

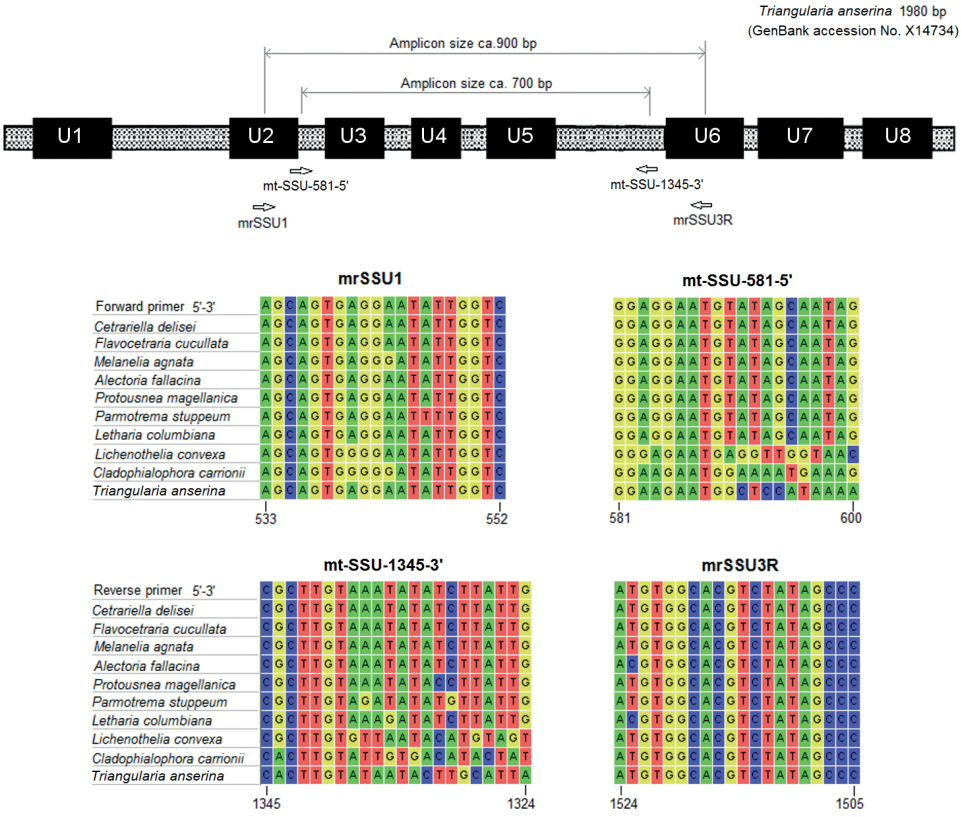

Figure 1. Primer design and sequence alignments at the priming locations. Conservative regions (i.e. U1 to U8) are marked as previously designated (Cummings et al. 1989) with adjustments from the reference. Nucleotide sites are relative to the 1980 bp-long sequence of the fungus *Triangularia anserina* (GenBank accession No. X14734).

Triangularia anserina, which gives rise to an amplicon size of 764 bp. However, amplicons of Parmeliaceae mtSSU are usually shorter the reference fungus, as seen from Suppl. material 1.

In silico primer specificity

The amplification success was significantly affected by the allowed number of mismatches and positions between archived fungal sequences and primers (Fig. 2). As more mismatches between primers and templates are allowed, the numbers of amplicons increase. The amplicon profiles between the new and universal primer pairs are considerably different. Universal primers give rise to an overwhelming proportion (ca. 98%) of sequences from non-Parmeliaceae fungi, regardless of the number of nucleotide mismatches. Our *in silico* results show that the amplicons are mainly from three fungal families in the example of three mismatches: Nectriaceae (n=589),

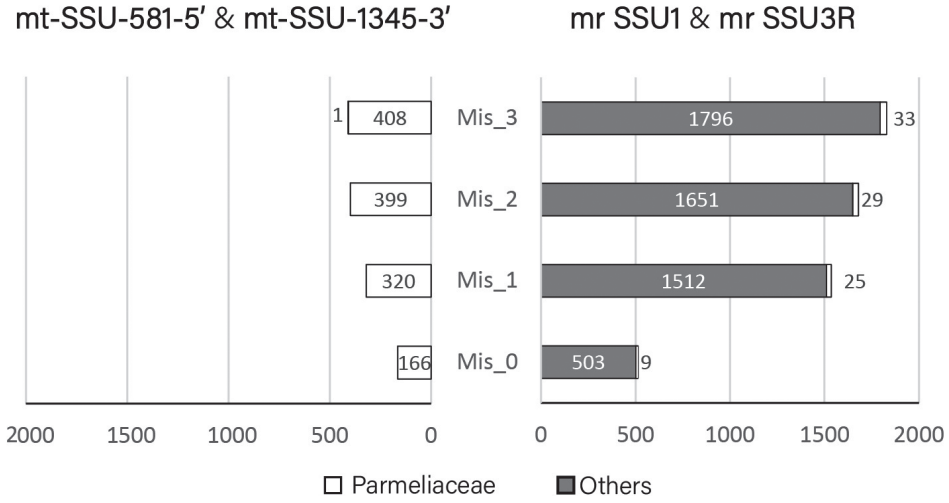

Figure 2. Comparison of primer specificity between the new and the universal primer pairs using *in silico* PCR. The number of off-target amplifications is classified as others in grey, while desired amplifications of lichen-forming fungi in Parmeliaceae are marked in white. The number of nucleotide mismatches in the priming sites is shown as Mis_0 to Mis_3, indicating 0 to 3 nucleotide mismatches.

Aspergillaceae (n=201) and Trichocomaceae (n=156). A full list of in silico amplicons is provided in Suppl. material 2. In contrast, the new primer pair only produced sequences of Parmeliaceae fungi when less than two mismatches were allowed, and only a single non-Parmeliaceae fungal sequence was amplified with three mismatches.

PCR screening and *in vitro* validation

Amplicons resulting from the universal primer pair mrSSU1 and mrSSU3R are around 1000 bp in length (lanes 1–3 in Fig. 3A). However, after sequencing, only the amplicons in lane 1 are identified as the lichen-forming fungus *M. agnata* after BLAST search, while lanes 2 and 3 are off-target amplification of non-lichen-forming fungi, *Lichenothelia convexa* (GenBank accession No. OQ450499) and *Cladophialophora carrionii* (GenBank accession No. OQ450500), respectively. The amplicon of *C. carrionii* is slightly shorter than the other two. Among 24 *Melanelia* specimens, we only obtained three sequences from the mycobionts (3/24, 12.5% success), while the others showed messy and ambiguous base calling or even no PCR products in gel electrophoresis. Fig. 3B shows Sanger electropherograms resulting from the same DNA extract of one *M. agnata* specimen but different primers during PCR and sequencing, and the importance of mycobiont-specific primer is highlighted in generating good-quality sequences. Amplicons from the newly designed primers were around 700 bp long. The resulting Sanger electropherograms show unambiguous nucleotides with good quality (Fig. 3B, lower electropherogram), and we obtained 22 mycobiont sequences out of 24 specimens (22/24, 91.7% success). The remaining two specimens yielded no bands after PCR.

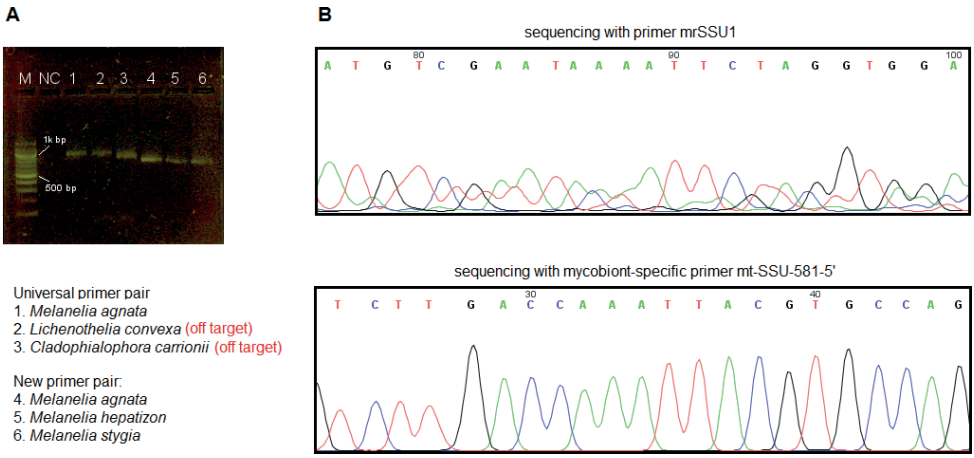

Figure 3. PCR amplification and sequencing results of the mtSSU locus in the genus *Melanelia* **A** 2% agarose gel electrophoresis of PCR products, where lanes 1-3 contain amplicons from the universal primer pair mrSSU1 and mrSSU3R, and lanes 4-6 are from the mycobiont-specific primer pair mt-SSU-598-5'and mt-SSU-1324-3'. Abbreviations: M-molecular ladder 100 bp; NC-negative control **B** illustration of sequencing results (*M. agnata*, voucher number LA29683) using the forward primers: the universal primer mrSSU1 (upper) and the mycobiont-specific primer mt-SSU-581-5' (lower), respectively.

Using the new primers, the mtSSU region was also successfully amplified from DNA extracts of other genera in Parmeliaceae (Table 2), e.g. *Alectoria*, *Evernia*, *Flavoparmelia*, *Xanthoparmelia*, etc. The exception is the genus *Usnea*, from which we did not succeed with the newly designed primers (mt-SSU-581-5' and mt-SSU-1345-3') or universal primers (mrSSU1 and mrSSU3R). To solve the amplification problem in *Usnea*, a multiple sequence alignment (Suppl. material 3) was specially made for this genus, which contained 13 reference sequences: six partial mtSSU sequences from PCR, and seven mitochodrial genomes containing the whole mtSSU region. The alignment in (Suppl. material 3) shows that: 1) there are unique and long introns inserted in U4 (e.g. 907 bp for *U. trachycarpa* (Stirt.) Müll.Arg. and *U. antarctica* Du Rietz), U5 (e.g. 757-1110 bp for *U. halei* P.Clerc, *U. subgracilis* Vain. and *U. ceratina* Ach.) and U6 (e.g. 535–848 bp for *U. subfusca* Stirt., *U. subscabrosa* Nyl. ex Motyka, *U. ceratina*, *U. pennsylvanica* Motyka and *U. subgracilis*) regions, and thus when the primers mrSSU1 and mrSSU3R are used, the estimated size of PCR amplicons may reach ca. 3000 bp; 2) there is a high nucleotide variation in the primer binding sites for the newly designed mycobiont-specific primers mt-SSU-581-5' and mt-SSU-1345-3', which prohibit primer binding, especially at the 3' end (Suppl. material 2: fig. S1).

Therefore, we designed alternative primers (the pair mt-SSU-574-5' and mt-SSU-897-3') for the amplification of shorter mtSSU sequences (ca. 400 bp) in *Usnea*, to avoid amplifying the introns in U4 or U5 region. For *Usnea* species lacking the intron in the U4 region, we recommend the the primer pair mt-SSU-574-5' and mt-SSU-1093-3', which produces amplicons as long as ca. 500 bp. These primers are also

Table 2. PCR amplification summary in different lichen groups using newly designed primers.

Lichens	Number of amplified/sampled specimens
Cetrarioid	
Cetraria clade[a]	18/18
Nephromopsis clade[a]	6/6
Melanelia	22/24
Parmelioid	
Flavoparmelia	5/5
Melanelixia	4/5
Melanohalea	9/11
Parmotrema	2/2
Xanthoparmelia	4/4
Others	
Alectoria	9/9
Evernia	11/11
Protousnea	1/1
Usnea	6/7[b]

[a]: *Cetraria* and *Nephromopsis* clades follow the circumscription of Divakar et al. (2017);
[b]: Amplification for the *Usnea* genus used alternative primers in Table 1.

useful for old herbarium specimens, for which longer amplicons can not be obtained. The same PCR condition was used for the genus *Usnea*, except for the adjustment of annealing temperatures: 56–52 °C for touchdown cycles (decrease 1 °C per cycle), and 52 °C for the last 30 to 32 cycles. The primers (mt-SSU-574-5' and mt-SSU-897-3'/ mt-SSU-1093-3') have been tested with *in vitro* PCR screening and we got six mycobiont mtSSU sequences out of seven *Usnea* specimens. The improved success rate is at the cost of variable sites after the U5 zone. The reverse primers, mt-SSU-897-3' or mt-SSU-1093-3', can also be used with the mycobiont-specific forward primer mt-SSU-581-5' for other genera in Parmeliaceae.

We also provide two universal reverse primers (i.e. mt-SSU-1372-3' and mt-SSU-1492-3') to replace mt-SSU-1345-3' when the latter is not working. In this case, we recommend combining a mycobiont-specific forward primer, either mt-SSU-574-5' or mt-SSU-581-5', to enhance the specificity for PCR. Two reverse primer mt-SSU-1492-3' and mt-SSU-1548-3' were designed to replace the published primer mrSSU3R, for two reasons: 1) the primer mrSSU3R has a much higher melting temperature (T_m 64.2 °C) than the newly designed primers, which have their T_m around 55 °C; 2) mrSSU3R has four consecutive G/C at the 3' end with a higher risk of non-specific binding.

Notably, the region between U5 and U6 has the highest number of variable sites (Table 3). For the genus *Melanelia*, nearly all variable sites (18 out of 22 variable nucleotide sites) come from this region, which is the most informative for specimen discrimination. Therefore, we designed an alternative forward primer, mt-SSU-862-5' in combined use with the reverse primer mt-SSU-1345-3', which focuses on the amplification of the region between U5 and U6. Although a fairly short amplicon size around 450 bp is obtained from this primer pair (mt-SSU-862-5' and mt-SSU-1345-3'), it actually contains the majority of the total variable sites (Table 3), which is the most informative

Table 3. Numbers of variable sites between mtSSU universal regions in selected genera. Numbers are shown as variable nucleotide sites/total nucleotide sites.

Lichens	Number of variable sites (bp)			
	U2-U3[a]	U3-U4[a]	U4-U5[a]	U5-U6[a]
Cetrarioid				
Cetraria clade[b]	11/107	17/166	1/39	26/247
Nephromopsis clade[b]	6/107	9/166	4/39	19/249
Melanelia	1/107	3/166	0/39	18/233
Others				
Alectoria	2/107	14/167	1/39	37/258
Evernia	4/107	9/171	0/39	21/224
Flavoparmelia	4/107	34/166	1/39	45/241

[a]: Universal regions (U2-U6) refer to designations in Fig. 1;
[b]: *Cetraria* and *Nephromopsis* clades follow the circumscription of Divakar et al. (2017).

region of the mtSSU locus. We have obtained successful PCR products and good sequencing results (i.e. clean mycobiont mtSSU sequence without ambiguous base calling) with this primer pair from specimens which failed in obtaining longer amplicons.

Discussion

Of all PCR optimization approaches, primer design is a critical but usually neglected factor, since one tends to pick up the primers from existing literature (Ekman 1999). Universal primers may show good performance in some lichen taxa, presumably with freshly collected specimens. However, with regards to Icelandic saxicolous *Melanelia* lichens, we demonstrated low success rate using universal primers (Xu et al. 2020), since off-target amplification is prone to happen in microbial communities like lichens. Primer design should be incorporated as an essential part of Sanger sequencing-based molecular systematics studies. This is facilitated by the deposition of large amounts of sequence data in publicly available databases that can be used for designing mycobiont-specific primers.

Selecting primer binding sites in variable (e.g. the region between U2 and U3 for forward primer, the region between U5 and U6 for reverse primer) instead of conserved regions (e.g. U2, U6) will favour the design of mycobiont-specific primers, while still keeping most variable sites, in comparison with the often used primer pair mrSSU1 (designed at U2) and mrSSU3R (designed at U6). In the latter primer pair, the universal regions (i.e. U2 and U6) are highly conserved, and few nucleotide variations are present at the species level. Amplification of universal sites at U2 and U6 may help sequence alignment, but it will not add a significant number of variable sites. Instead, targeting a shorter amplicon with enhanced primer binding to mycobiont DNA templates will conceivably increase the PCR success, particularly for herbarium specimens which contain degraded DNA templates (Kistenich et al. 2019).

Regions between universal sites (e.g. the region between U5 and U6 in Fig. 1) have been shown to have high variations in sequence lengths (Zoller et al. 1999). These noticeable differences in sequence length could explain the observed off-target PCR amplification with universal primers, in which the fungal templates with shorter amplicons are preferentially targeted. Our alignment shows that the amplified environmental fungi have shorter mtSSU amplicons (by ca. 50–100 bp) than the lichen-forming fungi, and the largest sequence length differences reside in the region between U5 and U6 (see Suppl. material 1).

Our *in vitro* PCR tests only compared the effectiveness of new primers with the most commonly used primer pair – mrSSU1 and mrSSU3R, instead of other known mtSSU primers, such as MS1&MS2 (White et al. 1990), NMS1&NMS2 (Li et al. 1994) and MSU1&MSU7 (Zhou and Stanosz 2001). The reason why we did not include MS1&MS2, NMS1&NMS2 are twofold: 1) these primers were designed as universal primers for different fungal lineages (see alignment in Suppl. material 1), not specifically designed for lichenized ascomycetes (Suppl. material 2: fig. S2), and 2) these two primer pairs were designed to amplify the conserved region between U2 and U5, neglecting the most informative region between U5 and U6 for specimen identification (Table 3). The reason why we excluded MSU1&MSU7 is also twofold: 1) they are not mycobiont-specific (Suppl. material 2: fig. S2), and 2) they will lead to impractically long amplicons for Sanger sequencing, which are close to 2000 bp for most Parmeliaceae and over 3000 bp for intron-rich *Usnea* species.

Co-amplification of non-lichen-forming fungi revealed the intrinsic complexity and habitat ecology of lichen symbiosis (Banchi et al. 2018; Gueidan et al. 2019; Smith et al. 2020). For instance, the amplified fungus *Lichenothelia convexa* is a known saxicolous and lichenicolous fungus, often co-inhabiting with lichen-forming fungi (Kocourková and Knudsen 2011). The other amplified fungus, *Cladophialophora carrionii*, is mostly found on decaying plants, but it has also been reported in association with lichens (Diederich et al. 2013).

In addition to our success in the genus *Melanelia*, the new primers also gave good results on other genera in the family Parmeliaceae, indicating good primer universality in Parmeliaceae. The only exception is the genus *Usnea*, which is intron-rich and more variable at primer binding sites. This explains why the mtSSU locus was not included in recent phylogenetic studies of the genus *Usnea* (Mark et al. 2016; Gerlach et al. 2019; Ohmura 2020). To this end, we designed alternative mtSSU primers (Table 1), to target shorter amplicons and to avoid amplification of introns (Suppl. material 3). For unsampled Parmeliaceae taxa, we expect that the mycobiont-specific primers as well as alternative primers will also work out.

The Parmeliaceae sequences amplified with the universal primer pair may be underestimated in the simulation of *in silico* PCR. Theoretically, the shorter amplicons using newly designed primers are more likely to be amplified than longer amplicons with the universal primers. Some submitted mtSSU sequences may contain neither the forward nor reverse primer binding sites, and thus are not sufficiently long to be served as *in*

silico PCR templates. Therefore, amplification would fail with the universal primers using *in silico* PCR for these samples. Relying on the number and position of primer-template mismatches alone may be insufficient for *in silico* PCR; however, the *in silico* results coincide with the *in vitro* PCR results. Here, we have validated the higher specificity of the newly designed primers compared to universal primers during *in vitro* PCR. Therefore, *in silico* specificity check of primers followed by *in vitro* analysis is recommended to confirm the appropriate choice of primers, thus preventing the amplification of unspecific sequences and ensuring appropriate amplification of target sequences.

Our mtSSU sequence data can be incorporated into multi-locus phylogenetic analyses to assess species relationship in the genus *Melanelia*, for which a phylogeny has yet to be reconstructed. Using the nuclear ribosomal internal transcribed spacer (nrITS) marker, previous fungal barcoding studies have detected multiple haplotypes within *Melanelia* species, and hypervariability of the nrITS regions suggest the presence of hidden species diversity (Leavitt et al. 2014; Xu et al. 2017; Szczepańska et al. 2021), which must be tested using multi-locus phylogenetic analyses. Before PCR amplification of additional mycobiont loci, however, precautions must be taken to make sure that the mycobiont DNA templates are targeted, as we have shown in the current study. It is expected that more mycobiont-specific primers will be designed for other loci (e.g. RPB2 and MCM7), after which species relationship can be assessed by reconstructing multi-locus phylogenies. Chemotaxonomic tools can also be applied to aid in species delimitation (Xu et al. 2016, 2017).

Conclusion

Here we demonstrate an efficient and effective approach for successful PCR amplification. We designed mycobiont-specific mtSSU primers, which significantly enhanced the successful PCR rate from 12.5% to 91.7% for Icelandic *Melanelia* lichens. Moreover, the primers show strong specificity within the family Parmeliaceae. This study emphasizes the importance of thoughtful primer design in molecular systematics studies of lichen-forming fungi.

Acknowledgements

The authors have no support to report.

The research was funded by the European Union's Seventh Framework Programme for research, technological development and demonstration to FP7-MCA-ITN MedPlant (grant number 606895), the Icelandic Research Fund (grant number 185442051), University of Iceland Research Fund (grant number 92257) and the Landsvirkjun Fund (NÝR-31-2021). We thank the Second Tibetan Plateau Scientific Expedition and Research (STEP) program (2019QZKK0503) for financial support in field work and sampling.

References

Banchi E, Stankovic D, Fernández-Mendoza F, Gionechetti F, Pallavicini A, Muggia L (2018) ITS2 metabarcoding analysis complements lichen mycobiome diversity data. Mycological Progress 17(9): 1049–1066. https://doi.org/10.1007/s11557-018-1415-4

Bellemain E, Carlsen T, Brochmann C, Coissac E, Taberlet P, Kauserud H (2010) ITS as an environmental DNA barcode for fungi: An *in silico* approach reveals potential PCR biases. BMC Microbiology 10(1): e189. https://doi.org/10.1186/1471-2180-10-189

Crespo A, Lumbsch HT, Mattsson JE, Blanco O, Divakar PK, Articus K, Wiklund E, Bawingan PA, Wedin M (2007) Testing morphology-based hypotheses of phylogenetic relationships in Parmeliaceae (Ascomycota) using three ribosomal markers and the nuclear RPB1 gene. Molecular Phylogenetics and Evolution 44(2): 812–824. https://doi.org/10.1016/j.ympev.2006.11.029

Cubero OF, Crespo A, Fatehi J, Bridge PD (1999) DNA extraction and PCR amplification method suitable for fresh, herbarium-stored, lichenized, and other fungi. Plant Systematics and Evolution 216(3–4): 243–249. https://doi.org/10.1007/BF01084401

Cummings DJ, Domenico JM, Nelson J, Sogin ML (1989) DNA sequence, structure, and phylogenetic relationship of the small subunit rRNA coding region of mitochondrial DNA from *Podospora anserina*. Journal of Molecular Evolution 28(3): 232–241. https://doi.org/10.1007/BF02102481

Diederich P, Ertz D, Lawrey JD, Sikaroodi M, Untereiner WA (2013) Molecular data place the hyphomycetous lichenicolous genus *Sclerococcum* close to *Dactylospora* (Eurotiomycetes) and *S. parmeliae* in *Cladophialophora* (Chaetothyriales). Fungal Diversity 58(1): 61–72. https://doi.org/10.1007/s13225-012-0179-4

Divakar PK, Crespo A, Kraichak E, Leavitt SD, Singh G, Schmitt I, Lumbsch HT (2017) Using a temporal phylogenetic method to harmonize family- and genus-level classification in the largest clade of lichen-forming fungi. Fungal Diversity 84(1): 101–117. https://doi.org/10.1007/s13225-017-0379-z

Ekman S (1999) PCR optimization and troubleshooting with special reference to the amplification of ribosomal DNA in lichenized fungi. Lichenologist 31(5): 517–531. https://doi.org/10.1006/lich.1999.0226

Ficetola GF, Coissac E, Zundel S, Riaz T, Shehzad W, Bessière J, Taberlet P, Pompanon F (2010) An *in silico* approach for the evaluation of DNA barcodes. BMC Genomics 11(1): 434. https://doi.org/10.1186/1471-2164-11-434

Gargas A, DePriest PT (1996) A Nomenclature for Fungal PCR Primers with Examples from Intron-Containing SSU rDNA. Mycologia 88(5): 745–748. https://doi.org/10.1080/00275514.1996.12026712

Gerlach A da CL, Toprak Z, Naciri Y, Caviró EA, da Silveira RMB, Clerc P (2019) New insights into the *Usnea cornuta* aggregate (Parmeliaceae, lichenized Ascomycota): Molecular analysis reveals high genetic diversity correlated with chemistry. Molecular Phylogenetics and Evolution 131: 125–137. https://doi.org/10.1016/j.ympev.2018.10.035

Gueidan C, Elix JA, McCarthy PM, Roux C, Mallen-Cooper M, Kantvilas G (2019) PacBio amplicon sequencing for metabarcoding of mixed DNA samples from lichen herbarium specimens. MycoKeys 53: 73–91. https://doi.org/10.3897/mycokeys.53.34761

Katoh K, Standley DM (2013) MAFFT multiple sequence alignment software version 7: Improvements in performance and usability. Molecular Biology and Evolution 30(4): 772–780. https://doi.org/10.1093/molbev/mst010

Kistenich S, Halvorsen R, Schrøder-Nielsen A, Thorbek L, Timdal E, Bendiksby M (2019) DNA sequencing historical lichen specimens. Frontiers in Ecology and Evolution 7: 1–20. https://doi.org/10.3389/fevo.2019.00005

Kocourková J, Knudsen K (2011) Lichenological notes 2: *Lichenothelia convexa*, a poorly known rock-inhabiting and lichenicolous fungus. Mycotaxon 115(1): 345–351. https://doi.org/10.5248/115.345

Leavitt SD, Esslinger TL, Hansen ES, Divakar PK, Crespo A, Loomis BF, Lumbsch HT (2014) DNA barcoding of brown Parmeliae (Parmeliaceae) species: A molecular approach for accurate specimen identification, emphasizing species in Greenland. Organisms, Diversity & Evolution 14(1): 11–20. https://doi.org/10.1007/s13127-013-0147-1

Li KN, Rouse DI, German TL (1994) PCR primers that allow intergeneric differentiation of ascomycetes and their application to *Verticillium* spp. Applied and Environmental Microbiology 60(12): 4324–4331. https://doi.org/10.1128/aem.60.12.4324-4331.1994

Liu Y, Erséus C (2017) New specific primers for amplification of the internal transcribed spacer region in Clitellata (Annelida). Ecology and Evolution 7(23): 10421–10439. https://doi.org/10.1002/ece3.3212

Mark K, Saag L, Leavitt SD, Will-Wolf S, Nelsen MP, Tõrra T, Saag A, Randlane T, Lumbsch HT (2016) Evaluation of traditionally circumscribed species in the lichen-forming genus *Usnea*, section *Usnea* (Parmeliaceae, Ascomycota) using a six-locus dataset. Organisms, Diversity & Evolution 16(3): 497–524. https://doi.org/10.1007/s13127-016-0273-7

Nelsen MP, Chavez N, Sackett-Hermann E, Thell A, Randlane T, Divakar PK, Rico VJ, Lumbsch HT (2011) The cetrarioid core group revisited (Lecanorales: Parmeliaceae). Lichenologist 43(6): 537–551. https://doi.org/10.1017/S0024282911000508

Ohmura Y (2020) *Usnea nipparensis* and *U. sinensis* form a "species pair" presuming morphological, chemical and molecular phylogenetic data. Plant and Fungal Systematics 65(2): 265–271. https://doi.org/10.35535/pfsyst-2020-0023

Riaz T, Shehzad W, Viari A, Pompanon F, Taberlet P, Coissac E (2011) ecoPrimers: Inference of new DNA barcode markers from whole genome sequence analysis. Nucleic Acids Research 39(21): e145. https://doi.org/10.1093/nar/gkr732

Schoch CL, Seifert KA, Huhndorf S, Robert V, Spouge JL, Levesque C, Chen W, Bolchacova E, Voigt K, Crous PW, Miller AN, Wingfield MJ, Aime MC, An K-D, Bai F-Y, Barreto RW, Begerow D, Bergeron M-J, Blackwell M, Boekhout T, Bogale M, Boonyuen N, Burgaz AR, Buyck B, Cai L, Cai Q, Cardinali G, Chaverri P, Coppins BJ, Crespo A, Cubas P, Cummings C, Damm U, de Beer ZW, de Hoog GS, Del-Prado R, Dentinger B, Diéguez-Uribeondo J, Divakar PK, Douglas B, Dueñas M, Duong TA, Eberhardt U, Edwards JE, Elshahed MS, Fliegerova K, Furtado M, García MA, Ge Z-W, Griffith GW, Griffiths K, Groenewald JZ, Groenewald M, Grube M, Gryzenhout M, Guo L-D, Hagen F, Hambleton S, Hamelin RC, Hansen K, Harrold P, Heller G, Herrera C, Hirayama K, Hirooka Y, Ho H-M, Hoffmann K, Hofstetter V, Högnabba F, Hollingsworth PM, Hong S-B, Hosaka K, Houbraken J, Hughes K, Huhtinen S, Hyde KD, James T, Johnson EM, Johnson JE, Johnston PR, Jones EBG, Kelly LJ, Kirk PM, Knapp DG, Kõljalg U, Kovács

GM, Kurtzman CP, Landvik S, Leavitt SD, Liggenstoffer AS, Liimatainen K, Lombard L, Luangsa-ard JJ, Lumbsch HT, Maganti H, Maharachchikumbura SSN, Martin MP, May TW, McTaggart AR, Methven AS, Meyer W, Moncalvo J-M, Mongkolsamrit S, Nagy LG, Nilsson RH, Niskanen T, Nyilasi I, Okada G, Okane I, Olariaga I, Otte J, Papp T, Park D, Petkovits T, Pino-Bodas R, Quaedvlieg W, Raja HA, Redecker D, Rintoul TL, Ruibal C, Sarmiento-Ramírez JM, Schmitt I, Schüßler A, Shearer C, Sotome K, Stefani FOP, Stenroos S, Stielow B, Stockinger H, Suetrong S, Suh S-O, Sung G-H, Suzuki M, Tanaka K, Tedersoo L, Telleria MT, Tretter E, Untereiner WA, Urbina H, Vágvölgyi C, Vialle A, Vu TD, Walther G, Wang Q-M, Wang Y, Weir BS, Weiß M, White MM, Xu J, Yahr R, Yang ZL, Yurkov A, Zamora J-C, Zhang N, Zhuang W-Y, Schindel D, Fungal Barcoding Consortium (2012) Nuclear ribosomal internal transcribed spacer (ITS) region as a universal DNA barcode marker for Fungi. Proceedings of the National Academy of Sciences of the United States of America 109(16): 6241–6246. https://doi.org/10.1073/pnas.1117018109

Smith HB, Dal Grande F, Muggia L, Keuler R, Divakar PK, Grewe F, Schmitt I, Lumbsch HT, Leavitt SD (2020) Metagenomic data reveal diverse fungal and algal communities associated with the lichen symbiosis. Symbiosis 82(1–2): 133–147. https://doi.org/10.1007/s13199-020-00699-4

Szczepańska K, Guzow-Krzemińska B, Urbaniak J (2021) Infraspecific variation of some brown Parmeliae (in Poland) – a comparison of ITS rDNA and non-molecular characters. MycoKeys 85: 127–160. https://doi.org/10.3897/mycokeys.85.70552

White TJ, Bruns T, Lee S, Taylor JW (1990) Amplification and direct sequencing of fungal ribosomal RNA genes for phylogenetics. In: Innis MA, Gelfand DH, Sninsky JJ, White TJ (Eds) PCR Protocols: a Guide to Methods and Applications. Academic Press INC, San Diego, 315–322. https://doi.org/10.1016/B978-0-12-372180-8.50042-1

Xu M, Heidmarsson S, Olafsdottir ES, Buonfiglio R, Kogej T, Omarsdottir S (2016) Secondary metabolites from cetrarioid lichens: Chemotaxonomy, biological activities and pharmaceutical potential. Phytomedicine 23(5): 441–459. https://doi.org/10.1016/j.phymed.2016.02.012

Xu M, Heidmarsson S, Thorsteinsdottir M, Eiriksson FF, Omarsdottir S, Olafsdottir ES (2017) DNA barcoding and LC-MS metabolite profiling of the lichen-forming genus *Melanelia*: Specimen identification and discrimination focusing on Icelandic taxa. PLoS ONE 12(5): e0178012. https://doi.org/10.1371/journal.pone.0178012

Xu M, De Boer H, Olafsdottir ES, Omarsdottir S, Heidmarsson S (2020) Phylogenetic diversity of the lichenized algal genus *Trebouxia* (Trebouxiophyceae, Chlorophyta): A new lineage and novel insights from fungal-algal association patterns of Icelandic cetrarioid lichens (Parmeliaceae, Ascomycota). Botanical Journal of the Linnean Society 194(4): 460–468. https://doi.org/10.1093/botlinnean/boaa050

Zhou S, Stanosz GR (2001) Primers for amplification of mt SSU rDNA, and a phylogenetic study of *Botryosphaeria* and associated anamorphic fungi. Mycological Research 105(9): 1033–1044. https://doi.org/10.1016/S0953-7562(08)61965-6

Zoller S, Scheidegger C, Sperisen C (1999) PCR primers for the amplification of mitochondrial small subunit ribosomal DNA of lichen-forming ascomycetes. Lichenologist 31(5): 511–516. https://doi.org/10.1006/lich.1999.0220

Appendix 1

Table A1. Voucher information and GenBank accession numbers of the amplified mtSSU loci by newly designed primers. [a]: *Usnea* specimens were amplified with alternative primers.

Species	Location	Collection date	Herbarium number	GenBank accession number
Alectoria mexicana	Mexico: Jalisco	2009-Jan-14	0197880 (DUKE)	OP901526
Alectoria ochroleuca	Iceland: INo	2012-Jul-26	LA32005 (AMNH)	OP901527
Alectoria ochroleuca	Iceland: IVe	2020-Oct-9	LA32013 (AMNH)	OP901528
Alectoria ochroleuca	Iceland: INo	1997-May-18	LA28088 (AMNH)	OP901529
Alectoria ochroleuca	China: Yunnan	2012-Sep-10	L35822 (KUN)	OP901530
Alectoria sarmentosa	Norway: Trondelag	2018-Aug-6	LF00037 (AMNH)	OP901531
Alectoria sarmentosa	Iceland: IVe	2013-Jul-23	LA32003 (AMNH)	OP901532
Alectoria sarmentosa	Iceland: INo	2012-Aug-21	LA32002 (AMNH)	OP901533
Alectoria sarmentosa	Iceland: INo	2006-Jul-3	LA30049 (AMNH)	OP901534
Allocetraria flavonigrescens	China: Yunnan	2015-Nov-1	L52601 (KUN)	OP901604
Cetrariella fastigiata	Norway: Malselv	2011-Sep-12	L177156 (O)	OP901535
Cetrariella fastigiata	Norway: Finnmark	2014-Jul-4	L195985 (O)	OP901536
Cetrariella fastigiata	Norway: Finnmark	2011-Jun-23	L170481 (O)	OP901537
Cetrariella fastigiata	Norway: Hedmark	2018-Aug-16	L208163 (O)	OP901538
Cetraria ericetorum	Iceland: INo	2016-Aug-29	LA31901 (AMNH)	OP901539
Cetraria ericetorum	Iceland: INo	2010-Sep-10	LA31538 (AMNH)	OP901540
Cetraria islandica	Poland: Jelenia Gora	2017-Aug-26	SMNS-STU-F 0005174 (STU)	OP901541
Cetraria islandica	Germany: Feldberg	2017-Aug-15	SMNS-STU-F 0000549 (STU)	OP901542
Evernia divaricata	USA: Utah	2006-Aug-10	0188304 (DUKE)	OP901543
Evernia divaricata	Austria: Salzburg	2019-Sep-2	SMNS-STU-F 0004925 (STU)	OP901544
Evernia mesomorpha	Norway: Innlandet	2009-Sep-17	L158139 (O)	OP901545
Evernia mesomorpha	Norway: Viken	2014-Oct-25	L200008 (O)	OP901546
Evernia mesomorpha	Canada: Ontario	2015-July-13	0405706 (DUKE)	OP901547
Evernia mesomorpha	China: Yunnan	2018-Sep-27	L64081 (KUN)	OP901548
Evernia mesomorpha	China: Inner Mongolia	2011-Jun-1	L24002 (KUN)	OP901549
Evernia mesomorpha	China: Yunnan	2017-Jul-8	L58746 (KUN)	OP901550
Evernia prunastri	Norway: Hordaland	2011-Jul-27	L194342 (O)	OP901551
Evernia prunastri	USA: Idaho	2009-Oct-4	0154766 (DUKE)	OP901552
Evernia prunastri	Spain: Castellon	2007	LF00002 (AMNH)	OP901553
Flavocetraria cucullata	Iceland: INo	2002-Jul-29	LA28953 (AMNH)	OP901554
Flavocetraria cucullata	Iceland: INo	2000-Aug-1	LA28174 (AMNH)	OP901555
Flavocetraria cucullata	Norway: Buskerud	2015-Jun-16	L200903 (O)	OP901556
Flavocetraria cucullata	Norway: Buskerud	2013-Sep-29	L184721 (O)	OP901557
Flavoparmelia caperata	Spain: Galicia	-	LF00008 (AMNH)	OP901558
Flavoparmelia caperata	Spain: Vigo	-	LF00013 (AMNH)	OP901559
Flavoparmelia soredians	Spain: Pontevedra	2015-Aug-10	LF00004 (AMNH)	OP901560
Flavoparmelia soredians	Spain: Pontevedra	2015-Aug-10	LF00005 (AMNH)	OP901561
Flavoparmelia soredians	Spain: Castellon	2017	LF00007 (AMNH)	OP901562
Melanelia agnata	Iceland: IMi	1999	LA29195 (AMNH)	OP901563
Melanelia agnata	Iceland: IMi	2002-Aug-7	LA29683 (AMNH)	OP901564
Melanelia agnata	Iceland: INo	2005-Jun-28	LA27562 (AMNH)	OP901565
Melanelia agnata	Iceland: IAu	2008-Oct-1	LA30974 (AMNH)	OP901566
Melanelia agnata	Iceland: INo	2012-Jun-27	LA31859 (AMNH)	OP901567
Melanelia agnata	Iceland: IMi	1999-Aug-11	LA27454 (AMNH)	OP901568
Melanelia agnata	Iceland: IMi	2000-Aug-11	LA26648 (AMNH)	OP901569
Melanelia agnata	Iceland: IMi	1998-Aug-1	LA33428 (AMNH)	OP901570

Species	Location	Collection date	Herbarium number	GenBank accession number
Melanelia hepatizon	Iceland: IAu	2003-Jul-24	LA30501 (AMNH)	OP901571
Melanelia hepatizon	Iceland: IAu	1997-Jul-19	LA27296 (AMNH)	OP901572
Melanelia hepatizon	Iceland: IVe	2007-Aug-23	LA30676 (AMNH)	OP901573
Melanelia hepatizon	Iceland: INv	2007-Aug-24	LA30674 (AMNH)	OP901574
Melanelia hepatizon	Iceland: IVe	2007-Aug-23	LA30675 (AMNH)	OP901575
Melanelia hepatizon	Iceland: INv	2007-Aug-24	LA30673 (AMNH)	OP901576
Melanelia hepatizon	Iceland: INo	2014-Jun-26	LA20781 (AMNH)	OP901577
Melanelia hepatizon	Iceland: IAu	1998-Aug-25	LA30117 (AMNH)	OP901578
Melanelia hepatizon	Iceland: INv	2012-Jul-25	LA31861 (AMNH)	OP901579
Melanelia hepatizon	Iceland: INo	2012-Jun-25	LF00036 (AMNH)	OP901580
Melanelia stygia	Iceland: IAu	1998-Aug-25	LA19972 (AMNH)	OP901581
Melanelia stygia	Iceland: IAu	2000-Jul-20	LA28243 (AMNH)	OP901582
Melanelia stygia	Iceland: IAu	2014-Jun-10	LA20775 (AMNH)	OP901583
Melanelia stygia	Iceland: IAu	2013-Jul-19	LA16894 (AMNH)	OP901584
Melanelixia fuliginosa	Iceland: IVe	2005-Jul-21	LA27514 (AMNH)	OP901585
Melanelixia fuliginosa	Iceland: INv	2005-Jul-6	LA27518 (AMNH)	OP901586
Melanelixia fuliginosa	Iceland: INv	2013-Jul-8	LA16895 (AMNH)	OP901587
Melanelixia fuliginosa	Iceland: INo	2014-Jun-25	LA20777 (AMNH)	OP901588
Melanelixia subaurifera	Iceland: IAu	2001-May-26	LA27950 (AMNH)	OP901597
Melanohalea exasperata	Iceland: IAu	1997-Aug-6	LA27384 (AMNH)	OP901589
Melanohalea exasperata	Iceland: IAu	2001-May-25	LA27958 (AMNH)	OP901590
Melanohalea exasperatula	Iceland: INo	2012-Sep-5	LA31766 (AMNH)	OP901591
Melanohalea infumata	Iceland: INo	2007-Jun-8	LA30618 (AMNH)	OP901592
Melanohalea infumata	Iceland: INo	2007-Apr-29	LA30623 (AMNH)	OP901593
Melanohalea olivacea	Iceland: INo	2010-Jun-29	LA31446 (AMNH)	OP901594
Melanohalea septentrionalis	Iceland: IAu	1997-Aug-6	LA27382 (AMNH)	OP901595
Melanohalea septentrionalis	Iceland: IAu	2001-May-25	LA27954 (AMNH)	OP901596
Nephromopsis pseudocomplicata	China: Yunnan	2017-Aug-20	L60353 (KUN)	OP901598
Parmotrema perlatum	Spain: Asturias	-	LF00024 (AMNH)	OP901599
Parmotrema pseudotinctorum	Spain: Lanzarote	2013	LF00020 (AMNH)	OP901600
Protousnea magellanica	Chile: Araucania	2017-Dec-3	0402940 (DUKE)	OP901601
Tuckermannopsis chlorophylla	Iceland: IAu	1996-Jul-12	LA18869 (AMNH)	OP901602
Usnea flammea[a]	Portugal: Alentejo	2015	LF00029 (AMNH)	OP901603
Usnea longissimi[a]	Russia: Khabarovsk Krai	2013-Jul-30	0339139 (DUKE)	OP901605
Usnea pangiana[a]	Japan: Kyushu	2014-Nov-12	0346943 (DUKE)	OP901606
Usnea cavernosa[a]	USA: Michigan	2013-Jun-28	0338717 (DUKE)	OP901607
Usnea himalayana[a]	Taiwan: Taichung	2009-Oct-4	0311007 (DUKE)	OP901608
Usnea trichodeoides[a]	Russia: Khabarovsk Krai	2013-Jul-30	0339133 (DUKE)	OP901609
Usnocetraria oakesiana	Norway: Buskerud	2016-Jun-21	L222316 (O)	OP901610
Usnocetraria oakesiana	Norway: Buskerud	2016-Jun-21	L222312 (O)	OP901611
Vulpicida canadensis	USA: California	2013-Jul-28	0332704 (DUKE)	OP901612
Vulpicida juniperinus	Norway: Hedmark	2019-Jul-11	L19277 (O)	OP901613
Vulpicida juniperinus	Norway: Hordaland	2019-Jul-27	L19175 (O)	OP901614
Vulpicida juniperinus	Norway: Sogn og Fjordane	2019-Apr-27	L19052 (O)	OP901615
Vulpicida pinastri	Canada: Ontario	2015-Jul-13	015998 (DUKE)	OP901616
Vulpicida pinastri	Norway: Sor-Trondelag	2019-Aug-24	L19217 (O)	OP901617
Vulpicida pinastri	Norway: Nordland	2019-Aug-6	L19202 (O)	OP901618
Xanthoparmelia camtschadalis	Spain: Castellon	2007	LF00025 (AMNH)	OP901619
Xanthoparmelia protomatrae	Spain: Castellon	2011	LF00027 (AMNH)	OP901620
Xanthoparmelia subdiffluens	Spain: Castellon	2007	LF00026 (AMNH)	OP901621
Xanthoparmelia tinctina	Spain: Castellon	2011	LF00028 (AMNH)	OP901622

[a]: *Usnea* specimens were amplified with alternative primers.

Supplementary material 1

Multiple sequence alignment for fungal mtSSU primer design in the family Parmeliaceae (except for *Usnea*)

Authors: Maonian Xu, Yingkui Liu, Erik Möller, Scott LaGreca, Patricia Moya, Xinyu Wang, Einar Timdal, Hugo de Boer, Eva Barreno, Lisong Wang, Holger Thüs, Ólafur Andrésson, Kristinn Pétur Magnússon, Elín Soffia Ólafsdóttir, Starri Heiðmarsson

Data type: alignment

Link: https://doi.org/10.3897/mycokeys.96.100037.suppl1

Supplementary material 2

Priming sites for alternative mtSSU primers, Nanodrop results and *in silico* PCR amplicons

Authors: Maonian Xu, Yingkui Liu, Erik Möller, Scott LaGreca, Patricia Moya, Xinyu Wang, Einar Timdal, Hugo de Boer, Eva Barreno, Lisong Wang, Holger Thüs, Ólafur Andrésson, Kristinn Pétur Magnússon, Elín Soffia Ólafsdóttir, Starri Heiðmarsson

Data type: figures, table (word document)

Link: https://doi.org/10.3897/mycokeys.96.100037.suppl2

Supplementary material 3

Multiple sequence alignment for fungal mtSSU primer design of the genus *Usnea*

Authors: Maonian Xu, Yingkui Liu, Erik Möller, Scott LaGreca, Patricia Moya, Xinyu Wang, Einar Timdal, Hugo de Boer, Eva Barreno, Lisong Wang, Holger Thüs, Ólafur Andrésson, Kristinn Pétur Magnússon, Elín Soffia Ólafsdóttir, Starri Heiðmarsson

Data type: alignment

Link: https://doi.org/10.3897/mycokeys.96.100037.suppl3

MycoKeys 96: 77–95 (2023)
doi: 10.3897/mycokeys.96.101033
https://mycokeys.pensoft.net

SHORT COMMUNICATION

A peer-reviewed open-access journal
MycoKeys
Launched to accelerate biodiversity research

MycoPins: a metabarcoding-based method to monitor fungal colonization of fine woody debris

Maria Shumskaya[1], Nicholas Lorusso[1,2], Urvi Patel[1], Madison Leigh[1], Panu Somervuo[3], Dmitry Schigel[3]

1 *Department of Biology, Kean University, Union, USA* **2** *University of North Texas at Dallas, Dallas, USA* **3** *Biological and Environmental Sciences, University of Helsinki, Helsinki, Finland*

Corresponding author: Maria Shumskaya (mshumska@kean.edu)

Academic editor: Imke Schmitt | Received 26 January 2023 | Accepted 2 March 2023 | Published 21 March 2023

Citation: Shumskaya M, Lorusso N, Patel U, Leigh M, Somervuo P, Schigel D (2023) MycoPins: a metabarcoding-based method to monitor fungal colonization of fine woody debris. MycoKeys 96: 77–95. https://doi.org/10.3897/mycokeys.96.101033

Abstract

The MycoPins method described here is a rapid and affordable protocol to monitor early colonization events in communities of wood-inhabiting fungi in fine woody debris. It includes easy to implement field sampling techniques and sample processing, followed by data processing, and analysis of the development of early dead wood fungal communities. The method is based on fieldwork from a time series experiment on standard sterilized colonization targets followed by the metabarcoding analysis and automated molecular identification of species. This new monitoring method through its simplicity, moderate costs, and scalability paves a way for a broader and scalable project pipeline. MycoPins establishes a standard routine for research stations or regularly visited field sites for monitoring of fungal colonization of woody substrates. The routine uses widely available consumables and therefore presents a unifying method for monitoring of fungi of this type.

Keywords

Dead wood, metabarcoding, mycobiome, saproxylic fungi

Introduction

Biological communities are formed at intersections of species niches and local environment, with assembly history strongly influencing overall community structure (Fukami et al. 2010). Early colonization events play a key role in establishment of

pioneer communities, with species at these seminal stages competing for habitats and resources which are limited both spatially and temporally. An example of a habitat limited in both space and metabolic resources, and, at the same time, relatively slow in community turnover rates, is dead wood (Stokland et al. 2012). Saproxylic fungi are the major wood decaying organisms able to digest lignin and cellulose that would undergo community assembly as woody tissues undergo decomposition (Baldrian 2017). These fungal taxa form competitive meta-communities and coexist both in space and for the time of decaying (Abrego et al. 2014). Wood-decaying fungi have been shown to be latently present in angiosperms (Boddy et al. 2007; Parfitt et al. 2010), but for conifers the necessary information on structure and functioning of Basidiomycete and Ascomycete communities is limited (Boddy 2001; Küffer and Senn-Irlet 2005). The information on ecology of saproxylic fungi is essential for evaluating environmental threats to key fungal species, conservation, and management policies (Hawksworth 1991; Mueller and Schmit 2007; Allen and Lendemer 2015; Seibold et al. 2015; Moose et al. 2019). For example, the loss of dead wood has posed a threat to a quarter of all forest species in Finland (Siitonen 2001; Rassi et al. 2010).

While lignicolous Basidiomycota are taxonomically well-known (Niemelä 2005; Kotiranta et al. 2009) most ecological studies of this group have been based on fruit body survey data (Rayner and Boddy 1988; Boddy et al. 2007; Halme 2010). Recent advances in DNA sequencing and metabarcoding allow the analysis of cryptic fungi via extracting DNA from substrates such as soil or wood where the fungi are found but not identifiable using fruiting body morphology. Fungal metabarcoding is widely used in mycorrhiza mycology (Bruns and Kennedy 2009; Öpik et al. 2009; Tedersoo et al. 2009), but most molecular studies on fungi in dead wood focus on coarse woody debris (Kubartova et al. 2009; Gherbawy and Voigt 2010; Arnstadt et al. 2016; Moll et al. 2021). Fungal ecology of fine woody debris remains largely neglected with a few exceptions (Norden et al. 2004; Bassler et al. 2010; Juutilainen et al. 2011; Juutilainen et al. 2014; Krah et al. 2018; Brabcova et al. 2022) and this gap presents an opportunity to leverage metabarcoding to identify cryptic taxa.

The niche boundaries and ecological processes governing community assembly of saproxylic species are important for shaping trajectories for dead wood decomposition (Fukasawa 2018), but a standard workflow for sampling these species is still lacking. Here, we describe a straightforward method for studying and monitoring dead wood colonization by fungi to fill this gap in knowledge and allow for consistency regardless of sampling location or other aspects of study design. The method combines standardized fieldwork protocol that includes experimental exposure of wooden furniture pins to lignicolous fungi in the environment, followed by subsequent metabarcoding analysis of fungal DNA from the colonized pins (Fig. 1). This standardized pipeline utilizes previously established metabarcoding methods, and we suggest that together with the sampling protocol the clear baseline will reduce difficulty in comparing studies that employ widely different designs.

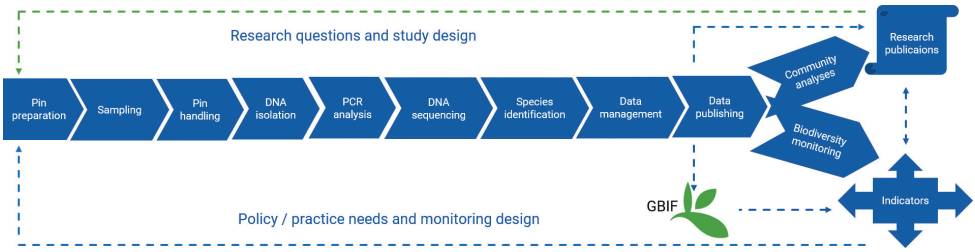

Figure 1. Scheme of the MycoPins method pipeline.

Furniture pins are widely available and can be ordered from wood suppliers to match desired local timber species. The selection of pins appropriate for the local forest community through coordination of timber with local wood suppliers allows for tailoring of the method to account for issues such as the interrelationship between host and fungal community composition, e.g. (Balint et al. 2013). Transporting dry construction wood pins acquired prior to fieldwork should also be likely not problematic in terms of travelling to study locations that may involve crossing state or governmental borders. In the work presented here, we evaluate this method to explore its research potential and reliability in a hope to trigger higher resolution worldwide monitoring of fungal wood colonization. Using autoclaved (industry clean) pins, we also compared the effect of preservation method (dry *vs.* frozen) on the pins exposed to the fungal colonization in the environment.

We hypothesized that the pins placed in the soil would be colonized by decaying fungi (hypothesis 1). The null hypothesis states that the pins would not be colonized by fungi. Within the hypothesis 1, there are three options available: 1a – the pins would be colonized by saproxylic fungi with the communities undergoing succession during the decomposition, 1b – the pins would be colonized by soil mycorrhizal fungi, 1c – the fungi would be colonized by both groups of fungi. Our hypothesis 2 is that storage and handling methods would not affect the results of the experiment. The null hypothesis states that drying and freezing methods would preserve a different number of species.

Materials and methods

Field experiment

A poplar pin 1 cm in diameter was purchased at a local hardware store in New Jersey, USA, and segmented into 3 cm long pins. The pins were then placed in a sterilizing jar and autoclaved (121 °C, 50 min). After sterilization, the pins were positioned in sets of three next to each other (Fig. 2), on November 23rd, 2020 in soil 2 cm from the surface, covered with debris and allowed to decay while being monitored for a set number

Figure 2. Preparation of pins for further analysis **A** sterilized pins **B** pin placement in soil **C** the interior of the colonized pins was extracted via drilling. Saw dust then was used to extract DNA.

of days (Table 1). Triplicates were placed 1 m from each other along one transect. Pins were placed in an urbanized wooded area in central New Jersey, USA. Upon extraction from soil, two pins for each triplicate were wrapped in brown paper and dried for 5 hours at 45 °C in a conventional food dehydrator, and one pin was frozen at -80 °C. Two sterile negative control pins were exposed to air in the field for 30 min and then one was dried and one frozen using the same methods used to store sample pins.

DNA extraction

The interior of each pin was drilled by a 2 mm fire-sterilized drill bit and the sawdust was collected into sterile plastic centrifuge tubes. DNA was isolated using PowerSoil DNA isolation kit (Qiagen, MD, USA) according to manufacturer's instructions. For the homogenization of the cell lysis solution with the saw dust, BeadBug (Benchmark Scientific, NJ, USA) homogenizer was utilized. Concentrations of extracted DNA for each sample were measured using NanoDrop spectrophotometer (ThermoFisher Scientific, USA) (absorbance at 260 nm). Extracted DNA was stored in 10 mM Tris buffer pH 8.0 at -80 °C.

Table 1. Sample list for each pin (=sample), time from placement, and storage methods used.

Sample number	Date of extraction	Days decaying	Storage
0	–	0. Sterilized pins.	1: dried, 1: frozen at -80 °C
1	December 07, 2020	14	2: dried, 1: frozen at -80 °C
2	December 21, 2020	28	2: dried, 1: frozen at -80 °C
3	January 04, 2021	42	2: dried, 1: frozen at -80 °C
4	February 08, 2021	77	2: dried, 1: frozen at -80 °C
5	May 02, 2021	160	2: dried, 1: frozen at -80 °C

PCR

PCR for the ITS2 gene region from the extracted DNA was carried out as in (Clemmensen et al. 2016). The primers used were tagged versions of fITS7 forward (F), 5'-GTGARTCATCGAATCTTTG, and ITS4 as reverse (R), 5'-TCCTCCGCTTATTGATATGC (White et al. 1990; Ihrmark et al. 2012). To each primer, an individual 10-nucleotide sequence (tag) was added. Altogether, 10 pairs of primers were used which allowed to perform ITS2 amplification for 10 different samples and then mix them in one multiplex to be analyzed later by high-throughput sequencing. The list of resultant primers is presented in Suppl. material 1: table S1. 100 ng of extracted DNA from each individual pin was amplified with PCR using a primer pair with an individual tag (such as pair #1, #2 etc) for each DNA sample. PCR amplification was performed using Phusion High-Fidelity Master Mix (Thermo Fisher Scientific, MA, USA). The mix is supplied as X2 concentrate, and a typical PCR reaction of 50 µl consisted of 25 µl of the PCR mix, 1 µl of each 5 µM primer, DNA to make a final amount of 100 ng in a PCR reaction tube, and DNAse-free water to make up the volume to 50 µl. The PCR conditions were 5 min at 94 °C, 30 cycles of: 30 s at 94 °C, 30 s at 52 °C and 30 s 72 °C, and the final step of 5 min at 72 °C. While we provided our PCR conditions, they can be modified depending on the PCR mix or Taq-polymerase available at the research laboratory.

For a negative control of PCR and subsequent sequencing and data analysis, DNAse-free water was used in place of the DNA. The reaction was set with a pair of primers with an individual tag, and the reaction was processed the same way as all other samples. Since no PCR product was detected in this control, all volume of the negative control reaction was used for the subsequent purification and sequencing steps. For a positive control, a SynMock plasmid collection provided by Drs. J. Palmer and D. Lindner, USDA Forest services (Palmer et al. 2018) was used. SynMock collection consists of a mix of 11 pUC57 bacterial plasmids each containing an insert of an individual artificially synthesized fungal ITS region. The ITS sequences were generated by Lindner laboratory and are available in the OSF repository (https://osf.io/4xd9r/, (Palmer et al. 2018). Amplification of this artificial "fungal community" was processed as a separate sample with its own tag. The resultant amplicon was added to the mix of the amplicons of investigated communities, which serves as a control to both PCR amplification, high-throughput sequencing and data analysis. This SynMock plasmid mix was prepared with a concentration of 0.1ng/ul of each plasmid in a mix, and then amplified with a pair of primers with an individual tag, mixed with the rest of the

samples and processed the same way as all other samples. After the high-throughput sequencing analysis and bioinformatics analysis, the SynMock "species" were detected in amounts correlating with the added plasmid concentration and were detected only in the amplicons with the tagged primers used for its preparation. This way, we were able to confirm the validity of the method.

The PCR products were then visualized for successful PCR confirmation by gel electrophoresis (see an example in Suppl. material 1: fig. S1). Mag-Bind RXN Pure Plus Quick kits (Omega Biotek, GA, USA) were used to purify the PCR products according to the manufacturer's standard protocol. Concentrations of the purified tagged amplicons were measured using Qubit 3.0 fluorimeter using dsDNA HS Assay kit (ThermoFisher Scientific, MA, USA).

High-throughput sequencing

Purified tagged PCR amplicons were pooled in a multiplex in equal 100 ng amounts, then the pooled sample was concentrated using Amicon Ultra-0.5 30K centrifugal filters (Millipore Sigma) to the volume and concentration required by the sequencing facility (at least 20 μl, 20 ng/μl). DNA library preparations, sequencing reactions, and adapter sequences trimming were conducted by Genewiz (now Azenta, South Plainfield, NJ, USA), using their Amplicon EZ service (provides approximately 50 000 reads per sample). DNA library preparation was performed using NEBNext Ultra DNA Library Prep kit following the manufacturer's recommended procedure (Illumina, San Diego, CA, USA). In short, end repaired adapters were ligated after adenylation of the 3'ends followed by enrichment by limited cycle PCR. DNA libraries were validated on the Agilent TapeStation (Agilent Technologies, Palo Alto, CA, USA), and quantified using Qubit 2.0 fluorimeter (Invitrogen, Carlsbad, CA) before loading, then multiplexed in equal molar mass. The pooled DNA libraries were loaded on the Illumina MiSeq instrument according to manufacturer's instructions. The samples were sequenced using a 2× 250 paired-end (PE) configuration. Image analysis and base calling were conducted by the Illumina Control Software on the Illumina instrument by Genewiz.

Data analysis

During pre-processing, raw pair-end sequences were merged using PEAR (Zhang et al. 2014), and cutadapt (Martin 2011) was used for trimming and removing adapter sequences (and later tag sequences). Tags were used to de-multiplex the sequences. In order to reduce the number of sequences, they were clustered within their tag-group using VSEARCH (Rognes et al. 2016) with 99% sequence similarity threshold. Taxonomic classification of sequences was performed using PROTAX (Abarenkov et al. 2018) based on the resulting centroid sequences from VSEARCH. When calculating abundances of different taxa, the cluster sizes were taken into account. Identification of species was performed using UNITE database (https://unite.ut.ee/) version 7.1. We would like to note that the UNITE database, used in our metabarcoding-based species identification, is updated periodically and its potential to resolve species ID is expected to improve each year.

PROTAX-fungi is a tool for taxonomic placement of ITS sequences implemented into the PlutoF platform of the UNITE database for molecular identification of fungi. This tool is able to perform statistically reliable identifications of fungi in spite of the incompleteness of extant reference sequence databases and unresolved taxonomic relationships (Abarenkov et al. 2018). In our study, sample-taxon tables were produced for both the species and genus level of taxonomy. Abundances were counted as the number of sequences whose taxon membership probability exceeded a given threshold of 0.9 to serve as a strict determination of which taxa were included. The choice of 0.9 in generating these tables was selected to serve as a conservative way of determining taxonomic resolution across samples in terms of species and genus identity. This threshold, generally speaking, could be lowered depending on future study designs and available data quality. Here, the estimates of abundance for each taxa generated with this 0.9 threshold were used for subsequent statistical analyses.

The resultant list of species was published at GBIF.org https://doi.org/10.15468/r7rxf6 (Shumskaya et al. 2022).

For the statistical analysis, the "species" identified as SynMock taxa were removed from the total list of identified species. Also, several species were identified in sterilized pins sample 0 (Table 1): *Candida albicans*, *Candida zeylanoides*, *Wallemia tropicalis*, which could be explained by contamination; these species were removed from all samples before statistical analysis.

Statistical analysis of the occurrence dataset was performed in R (R Core Team 2020) on a filtered version of the dataset without the species found in the negative control or that were not found in more than ten percent of samples. The dataset was then checked for multivariate normality using Mardia's test in the MVN package (Korkmaz et al. 2014) prior to omnibus analyses. A non-parametric multivariate analysis of variance (PERMANOVA) was then used to determine if fungal community composition varied either based on pin preservation method (dry vs. frozen) or time in days (14, 28, 42, 77, 160). Following omnibus testing, non-metric multidimensional scaling (NMDS) was used to evaluate differences between treatments and time points. We also used a Mann-Whitney (non-parametric t-test) and Kruskal-Wallis (non-parametric ANOVA) to evaluate potential differences between calculated diversity measures for preservation methods and over time. Both the PERMANOVA and NMDS were performed using vegan package for R (Dixon 2003; Oksanen et al. 2020) with all other significance tests for diversity measures being performed in base R. To determine any relevant change to indicator taxa across time an indicator taxa analysis was performed at the genus level following previous multivariate comparisons using the labdsv package (Roberts 2019). To compare annotations for fungal species ecology we retrieved available ecological roles and guild data for each species and its corresponding genus from the FUNguild database (Nguyen et al. 2016) using the fungarium package (Simpson and Schilling 2021). Species and genera with annotations in FUNguild were used for a comparison of both trophic mode and guild annotations using PERMANOVA with reciprocal Kruskal-Wallis tests to evaluate significant differences in fungal roles observed across time.

Results

DNA isolated from all collected pins (Table 1) was amplified using PCR with tagged primers (Suppl. material 1: table S1). All PCR amplification results were verified using gel electrophoresis (see Suppl. material 1: fig. S1 for an example). SynMock served as a positive control for both successful PCR reaction settings (Suppl. material 1: fig. S1, lane 5) and high-throughput sequencing runs. Negative control, amplified with the assigned tagged primers, never showed on a gel electrophoresis, or in sequencing or data analysis, confirming no contamination was introduced at the PCR step.

After processing of the high-throughput sequencing results of the PCR amplicons, the subsequent dataset was presented by 67 species for statistical analysis in R. For the statistical analysis, the "species" identified as SynMock taxa were removed from the total list of identified species.

In evaluating the effectiveness of the MycoPins method we used a series of multivariate analyses to determine if 1) a significant effect exists between pin preservation method (dry vs. frozen) and if 2) the method is capable of distinguishing differences that emerge in the fungal community over time (days since placement). We observed in our PERMANOVA results that there was no significant difference in community composition between our two preservation methods ($p > 0.05$) while there were significant differences in communities over time ($F_{(4,14)} = 1.7337$, $p = 0.036$) with no detectable interaction between time and preservation type ($p > 0.05$).

The results from the PERMANOVA can be visualized in the NMDS plots (Fig. 3) which show the fungal community clustered both by preservation type (Fig. 3A) and time in days elapsed from pin placement (Fig. 3B). The results of the NMDS support the PERMANOVA showing strong clustering overlap for the two preservation methods (Fig. 3A) and segregation between clusters for the time points sampled (Fig. 3B) which aligns with the findings from the omnibus test.

Through the lens of time elapsed from placement, the NMDS support that the MycoPins method resolved differences in the fungal community over the 160 days in the sampling period despite them being in the same environment. The confidence interval orientation for the time points sampled also shows more similarity for sampling times which are closer together with early fungal communities resembling each other with a slight gradient moving from early time points (upper right) to later time points (bottom left) emerging in the NMDS results.

We have also evaluated trends in measures of species richness (Fig. 4A), evenness (if the sample had a good representation of one species or was dominated by a few, Fig. 4B), and Shannon's diversity (index usually reported for comparing # of taxa, Fig. 4C). We also compared these diversity measures using significance tests and observed no significant differences between any of our diversity measures based on preservation method ($p > 0.05$, Fig. 5). Our Kruskal-Wallis test also did not return detectable significant differences between the time points for any of our diversity measures ($p > 0.05$), though there is a notable visual trend downward in species richness over time (Fig. 6).

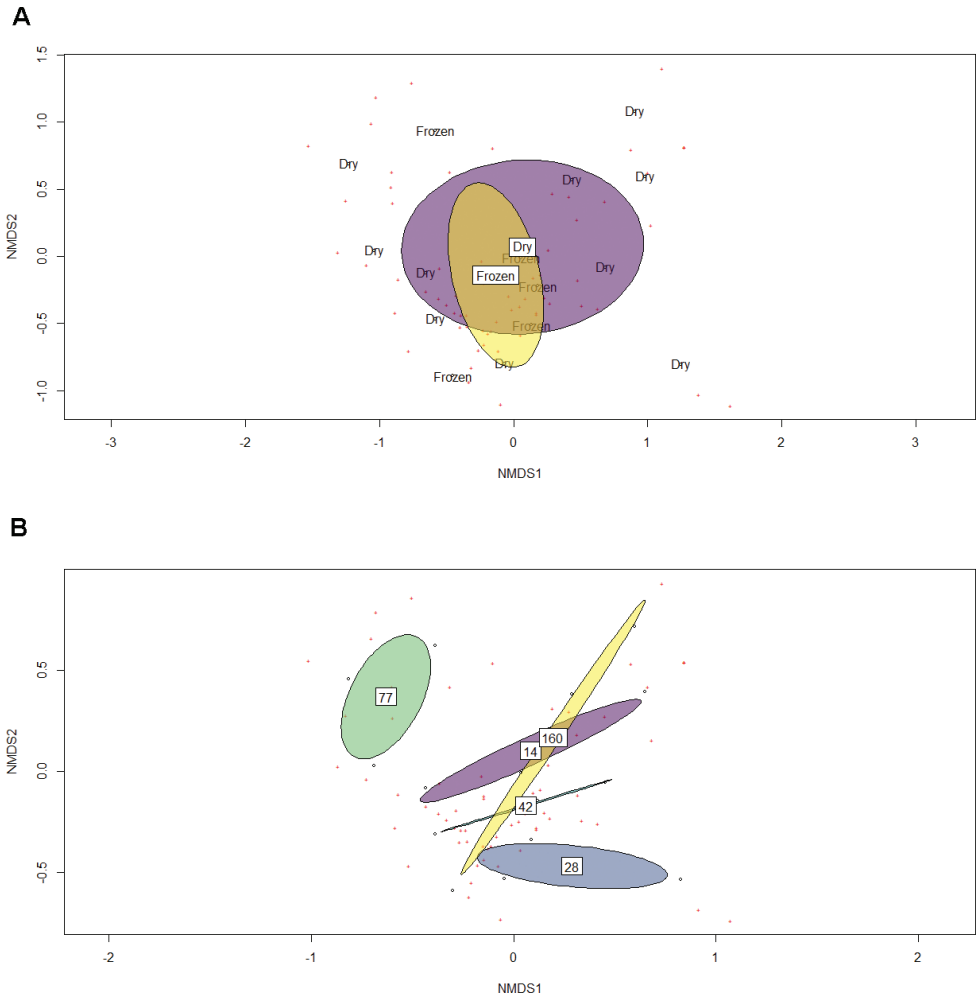

Figure 3. Non-metric multidimensional scaling plots for fungal communities sampled using MycoPins. Ellipses represent 95% confidence intervals with labels for pin preservation method or time elapsed from placement in the center **A** NMDS of the fungal communities observed in pins across 160 days clustered by pin storage method **B** NMDS of fungal communities observed in pins clustered according to date DNA was extracted from placement, numbers: days after inoculation.

To evaluate our hypothesis that the MycoPins method can be effectively used to sample saproxylic fungal taxa we retrieved annotations for ecological roles and guilds at the species and genus level. Summaries of available ecological role data at the species level (32% assigned), genus level (54% assigned) and total taxa are presented on Fig. 7. Most represented groups were discovered to be saprotrophic and pathotrophic fungal taxa. Functional guild data for taxa annotated on FUNguild used to evaluate common guilds detected with the MycoPins method highlight the ability of the MycoPins method to detect many plant pathogens, saproxylic, and litter associated taxa. We

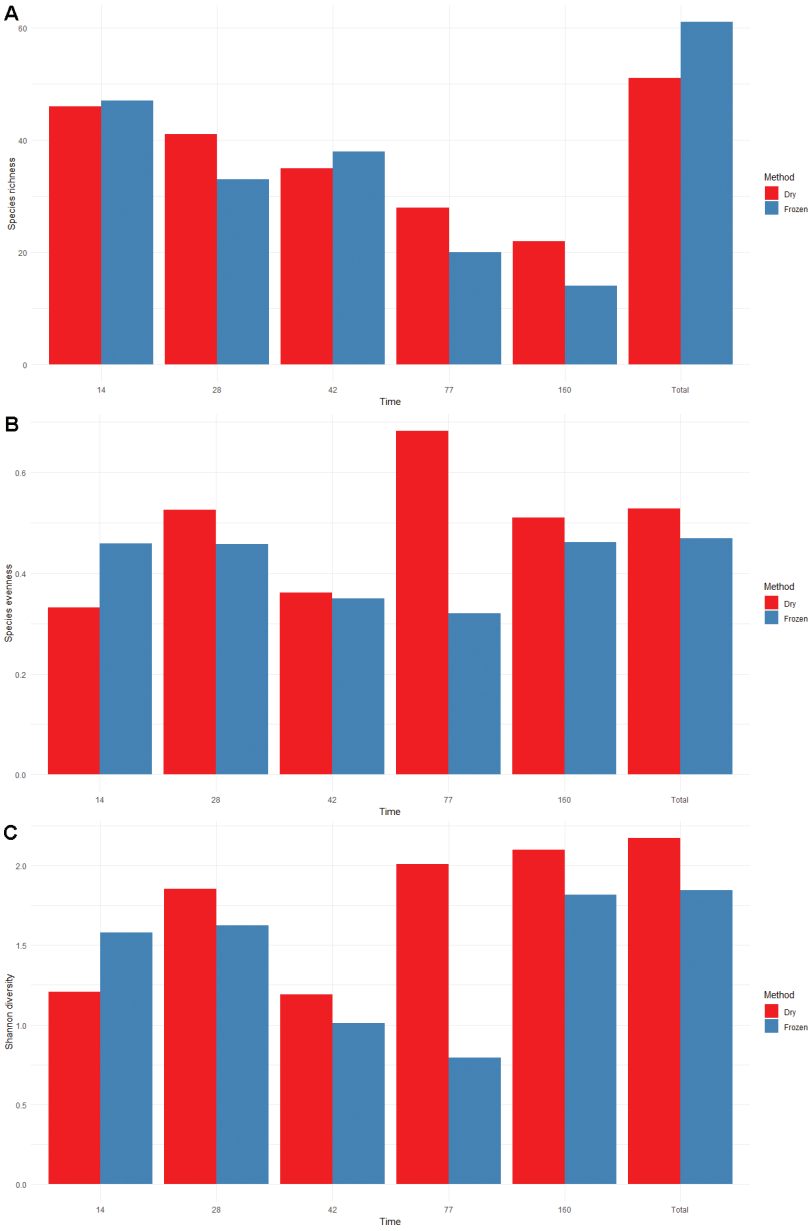

Figure 4. Species richness (**A**), species evenness (**B**), and Shannon diversity (**C**) for both dry (red) and frozen (blue) pins for each time point as well as total values. Time: days from the pin placement.

failed to observe significant differences in our PERMANOVA evaluating trophic mode overall or in guild type ($p > 0.05$) when considering the data collected by stage overall and reciprocal follow-up tests also were non-significant for trophic groups and guilds when considered in isolation.

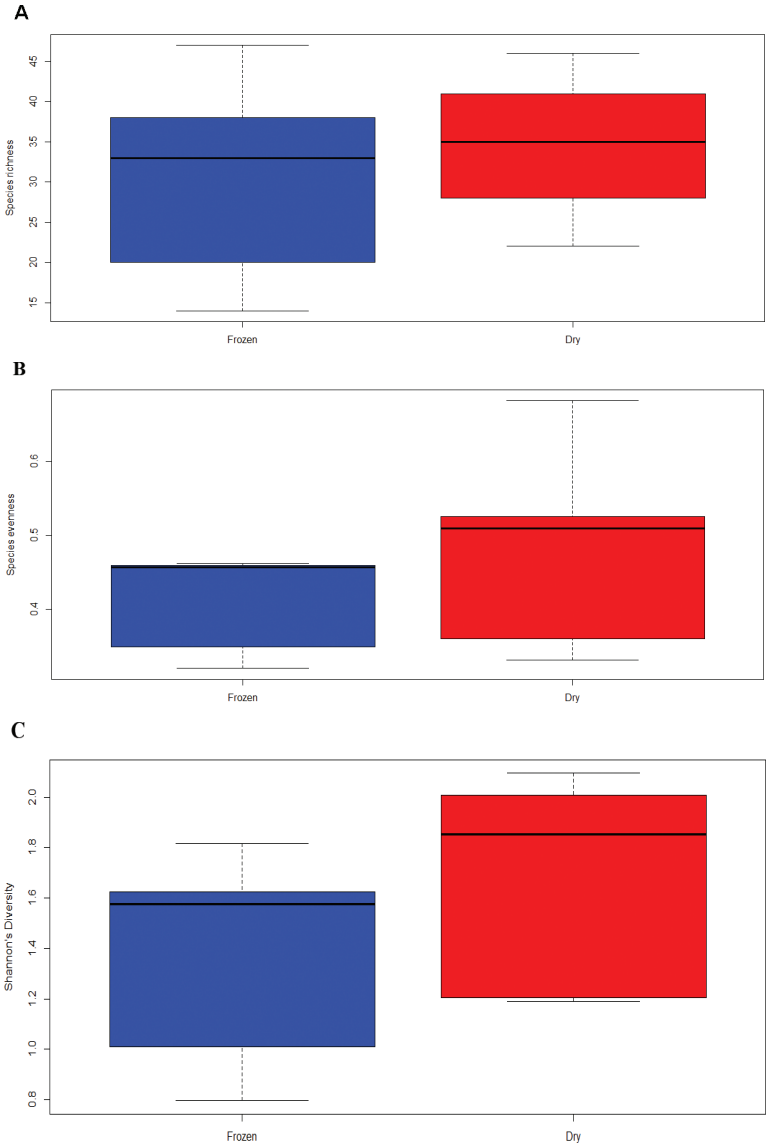

Figure 5. Box plots for values of species richness (**A**), species evenness (**B**), and Shannon's diversity index (**C**) between our two preservation methods. Box plots: middle line, median; box, interquartile range; whiskers, 5th and 95th percentiles.

To characterize genera that may have indicated changes in the fungal community over time we determined significant indicator genera at each time step and reviewed if they have been previously found to be saproxylic. Table 2 highlights that all of the taxa observed to indicate progression (changes over time) in the fungal community have been observed to be active in wood decomposition or activity in litter layer cellulosic matter decomposition.

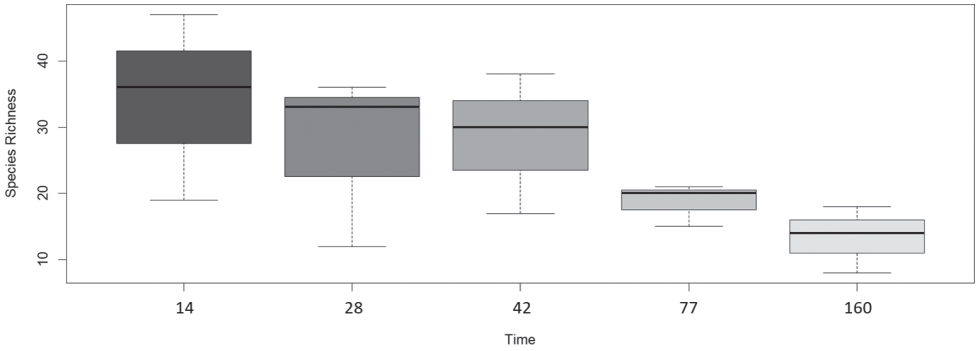

Figure 6. Box plot for values of species richness over time. Box plots: middle line, median; box, interquartile range; whiskers, 5th and 95th percentiles. Time: days after the pin placement.

Table 2. Indicator genera for time points evaluated in the present study. Indicator values were calculated with subsequent significance tests.

Genus	Saproxylic	Litter Saprotroph	Time Step indicated	Indicator Value	p-value
Taphrina	X		1	0.748503	0.034
Sporobolomyces		X	1	0.936306	0.014
Myrmecridium		X	3	0.75	0.037
Doratomyces	X		4	0.899293	0.014
Trichosporon	X		4	0.92941	0.009
Diplodia		X	5	0.962963	0.018
Valsa	X		5	1	0.008
Puccinia	X		5	0.867925	0.012

Discussion

Here we suggest a pin-based monitoring method of fungal colonization as a new protocol of biodiversity exploration that is not yet widely utilized. The method allows monitoring of fungal colonization in various biotopes. In effect, pins act as standardized traps and colonizable targets mimicking with some limitations natural inputs of fine woody debris: despite the convenience of their use, pins are still a semi-artificial, processed, autoclaved, no-bark artifacts, dried before placement. Sterile (autoclaved) wood, obviously, does not occur in nature, but to study colonization process we believe it is more important and more cost efficient to use autoclaved wood rather than account for resident fungi (which would dramatically increase processing time and cost). At the same time, wood is natural material, which can only be standardized to a certain limit – while choice of tree species and wood treatment improve comparability, differences in wood density (fast vs. slow wood) across pins remain beyond our full control; however, pins in the same batch are typically very uniform. We can recommend for the future studies to document or to unify ranges of tree rings per pin. We emphasize that the suggested method is not designed to attempt an exhaustive sampling of fungal communities *in situ*, hence, there is no need to replace an alternative direct sampling of soil or fine

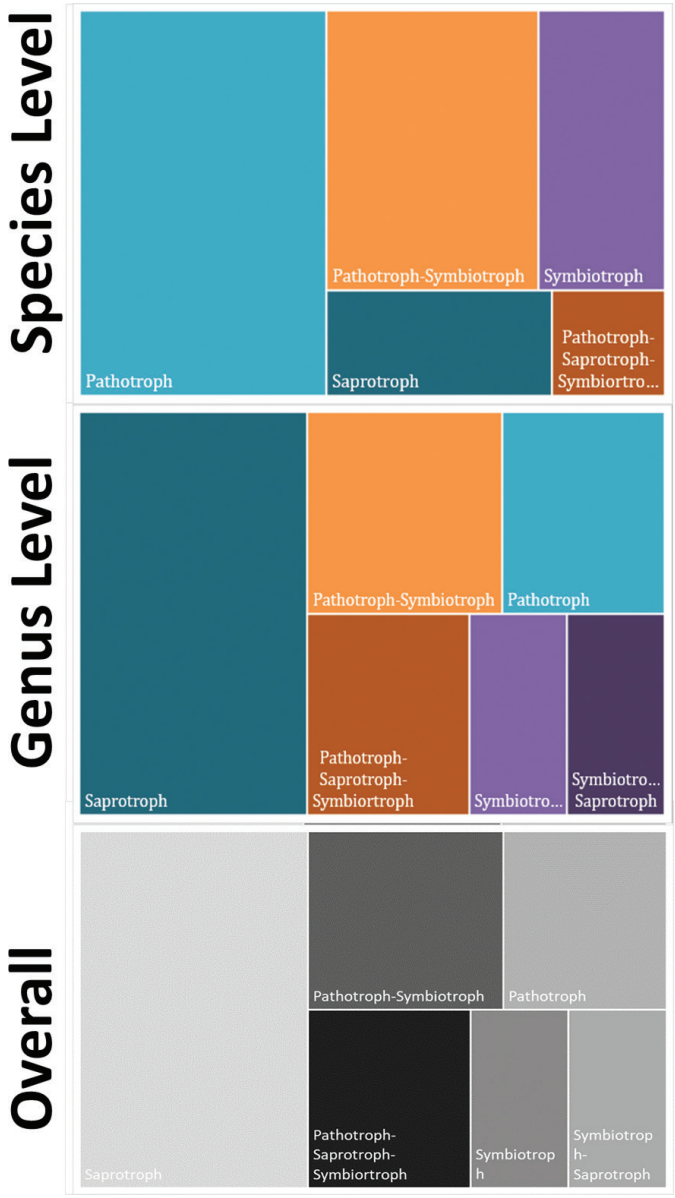

Figure 7. Relative proportion of fungal species, genera and overall fungal taxa (genus or species) identified in the experiment using MycoPins method, with ecological function annotations in FUNguild. Larger segments of the treemap indicate higher numbers of species within an ecological group. Included annotations for species and genus level show feeding modalities, while the overall panel shows observed proportions of ecological guilds.

woody debris for the metabarcoding based surveys. Instead, using the sterile wood pins, we offer an opportunity to uncover still mysterious processes of fungal colonization of wood. There is a great deal of flexibility for study designs with the pins placement pat-

terns and with removal frequencies for the field experiments resulting in the time series data; direct sampling of the environment can be combined with pin-based studies.

The outlined protocol used in our test dataset demonstrate that the pipeline suggested is capable of resolving differences in community assembly over time for fungal species monitoring.

Our study was inspired by the Global Teabag index study (Keuskamp et al. 2013), but shifted the focus of the approach from loss of biomass to colonization processes. The method was capable of resolving fungal community differences effectively using either dried or frozen pins. When comparing dried and frozen pins, pins collected at the same time point are more similar in fungal community composition than pins of the same preservation type at other time points. This likely means that, while freezing or drying may capture different rare taxa, researchers do not need to have access to a freezer to store samples if in the field to generate an imprint of the common taxa. The significant difference in the overall fungal community composition observed in our omnibus test between pins collected at different times, on the other hand, indicates that this method is likely well suited to evaluating how fungal communities change over time and are distributed based on community assembly. Trends observed in the diversity measures presented above highlight a gradual reduction in species richness over time (Fig. 6), though a relatively consistent evenness and diversity, potentially suggesting succession favoring a set of species being recruited in the progression of decay.

Beyond the ability of the MycoPins method to detect changes in the fungal community over time, we were also able to use it to detect changes in relevant ecological functional groups and guilds. While there are a wide range of fungal types within our sampled pins (e.g. endophytes, pathogens), suggesting that this method could be broadly used for fungal community sampling, we found support for our hypothesis that wood saprobes/saproxylic taxa colonize sterile furniture pins (Hypothesis 1a). Our approach allows for flexibility depending on observed taxa when considering functional roles by reviewing widely available annotations in databases such as FUNguild. As mentioned above, however, annotations for many taxa in our sample data were missing and manual research for annotations for individual taxa may not be tenable as an option for many researchers wishing to employ our method. We explored an alternate approach for monitoring specific taxa that contribute to wood decay that we suggest for researchers who also face annotation issues when considering functional roles in the form of our presented use of indicator values. As seen in Table 2, our method was able to detect significantly active indicator genera at four out of five of our time stages (with time stage two not having significantly high indicator values and therefore no indicator species). Subsequent manual annotation and research demonstrated that many of the taxa which have significant indicator values also have been shown to be saproxylic or contribute to the overall process of wood decay with the later time points having increasing numbers of taxa involved in wood decay compared to earlier stages. This shows that, despite cases like ours where existing database annotation may be a limitation, this method can still be employed to monitor potential changes in saproxylic species without placing unreasonable time burdens on researchers.

A tradeoff of the proposed method to study colonization processes is that pins are exposed to natural communities but the method is blind to priority effects, which is known to determine further colonization of the wood (Hiscox et al. 2015). A more elaborate study setup, still in natural habitats, may include use of pins precolonized by target species, (e.g. those common at the study site at the early colonization stages); such a workflow would start from i) the morphological or DNA survey of the pioneer species, ii) precolonization of pins with these species, see method developed by Schigel and Oivanen for species reintroduction (Abrego et al. 2016), and iii) colonization studies as presented here. To maximize designs that allow for comparison with natural forest communities, we recommend researchers order pins from sawmills that use locally and sustainably harvested timber in their study area, and that pins be made from the same tree species as at the sampling sites. As timber trade and timber certification is not always transparent and trustworthy, partnering with a local sawmill, even if more costly than using mass market pins, is preferred.

We were also able to support the hypothesis that the preservation method used by researchers will not significantly change the observations made by researchers using the MycoPins method (Hypothesis 2). Overall trends for species composition in our omnibus test and NMDS (Fig. 3B) find a high degree of similarity for fungal community composition observed using the two methods. In addition, trends observed for our diversity measures show that similar trends are captured using either dried or frozen pins such as the overall decline over time for species richness observed using both preservation methods (Fig. 4A) and all three diversity measures lack detectably significant differences. We conclude, overall, that the two preservation methods can be used depending on researcher preference and available equipment, though slightly higher (though non-significant) overall community richness in frozen pins, as well as better DNA preservation over time, lead us to suggest freezing when possible if DNA extraction and handling is considerably delayed after the pins collection. Many fungal taxa are also known to be active in plant decomposition or to be plant pathogens with the potential that they may be opportunistically contributing to wood decomposition. Given that our knowledge of fungal functional group and guild are still developing (many taxa we identified lack any annotation) coupled with the fact that many taxa known to be endophytic were found within the pins, it seems likely that our method can expand our knowledge of previously unknown saproxylic species as well as increasing resolution on global distribution for those already known.

Acknowledgements

We are grateful to Jonathan M. Palmer and Daniel L. Lindner from USDA Forest Service for providing the collection of plasmids carrying mock ITS sequences (SynMock ITS collection). DS and MS thank EU-INTERACT for supporting the further development of the MycoPins method. We also thank Elisabet Ottosson, Otso Ovaskainen, Ilya Viner, Heini Ali-Kovero and Pekka Oivanen for inspirational discussions and collaborations leading to this study. The work was supported by RTR2020-2021 grant from Kean University to MS.

References

Abarenkov K, Somervuo P, Nilsson RH, Kirk PM, Huotari T, Abrego N, Ovaskainen O (2018) Protax-fungi: A web-based tool for probabilistic taxonomic placement of fungal internal transcribed spacer sequences. The New Phytologist 220(2): 517–525. https://doi.org/10.1111/nph.15301

Abrego N, Garcia-Baquero G, Halme P, Ovaskainen O, Salcedo I (2014) Community turnover of wood-inhabiting fungi across hierarchical spatial scales. PLoS ONE 9(7): e103416. https://doi.org/10.1371/journal.pone.0103416

Abrego N, Oivanen P, Viner I, Norden J, Penttila R, Dahlberg A, Heilmann-Clausen J, Somervuo P, Ovaskainen O, Schigel D (2016) Reintroduction of threatened fungal species via inoculation. Biological Conservation 203: 120–124. https://doi.org/10.1016/j.biocon.2016.09.014

Allen JL, Lendemer JC (2015) Fungal conservation in the USA. Endangered Species Research 28(1): 33–42. https://doi.org/10.3354/esr00678

Arnstadt T, Hoppe B, Kahl T, Kellner H, Kruger D, Bauhus J, Hofrichter M (2016) Dynamics of fungal community composition, decomposition and resulting deadwood properties in logs of *Fagus sylvatica*, *Picea abies* and *Pinus sylvestris*. Forest Ecology and Management 382: 129–142. https://doi.org/10.1016/j.foreco.2016.10.004

Baldrian P (2017) Forest microbiome: Diversity, complexity and dynamics. FEMS Microbiology Reviews 41: 109–130. https://doi.org/10.1093/femsre/fuw040

Balint M, Tiffin P, Hallstrom B, O'Hara RB, Olson MS, Fankhauser JD, Piepenbring M, Schmitt I (2013) Host genotype shapes the foliar fungal microbiome of balsam poplar (*Populus balsamifera*). PLoS ONE 8(1): e53987. https://doi.org/10.1371/journal.pone.0053987

Bassler C, Muller J, Dziock F, Brandl R (2010) Effects of resource availability and climate on the diversity of wood-decaying fungi. Journal of Ecology 98(4): 822–832. https://doi.org/10.1111/j.1365-2745.2010.01669.x

Boddy L (2001) Fungal community ecology and wood decomposition processes in angiosperms: From standing tree to complete decay of coarse woody debris. Ecological Bulletins 49: 43–56.

Boddy L, Frankland J, van West P (2007) Ecology of Saprotrophic Basidiomycetes. Academic Press, 386 pp.

Brabcova V, Tlaskal V, Lepinay C, Zrustova P, Eichlerova I, Stursova M, Mueller J, Brandl R, Baessler C, Baldrian P (2022) Fungal community development in decomposing fine deadwood is largely affected by microclimate. Frontiers in Microbiology 13: 835274. https://doi.org/10.3389/fmicb.2022.835274

Bruns TD, Kennedy PG (2009) Individuals, populations, communities and function: The growing field of ectomycorrhizal ecology. The New Phytologist 182(1): 12–14. https://doi.org/10.1111/j.1469-8137.2009.02788.x

Clemmensen KE, Ihrmark K, Durling MB, Lindahl BD (2016) Sample preparation for fungal community analysis by high-throughput sequencing of barcode amplicons. Methods in Molecular Biology (Clifton, N.J.) 1399: 61–88. https://doi.org/10.1007/978-1-4939-3369-3_4

Dixon P (2003) VEGAN, a package of R functions for community ecology. Journal of Vegetation Science 14(6): 927–930. https://doi.org/10.1111/j.1654-1103.2003.tb02228.x

Fukami T, Dickie IA, Wilkie JP, Paulus BC, Park D, Roberts A, Buchanan PK, Allen RB (2010) Assembly history dictates ecosystem functioning: Evidence from wood decomposer communities. Ecology Letters 13(6): 675–684. https://doi.org/10.1111/j.1461-0248.2010.01465.x

Fukasawa Y (2018) Fungal succession and decomposition of *Pinus densiflora* snags. Ecological Research 33(2): 435–444. https://doi.org/10.1007/s11284-017-1557-x

Gherbawy Y, Voigt K (2010) Molecular identification of fungi. Springer, Berlin, Heidelberg, 501 pp. https://doi.org/10.1007/978-3-642-05042-8

Halme P (2010) Developing tools for biodiversity surveys – studies with wood-inhabiting fungi. Jyväskylä Studies in Biological and Environmental Science 212: 1–51.

Hawksworth DL (1991) The fungal dimension of biodiversity – magnitude, significance, and conservation. Mycological Research 95(6): 641–655. https://doi.org/10.1016/S0953-7562(09)80810-1

Hiscox J, Savoury M, Mueller CT, Lindahl BD, Rogers HJ, Boddy L (2015) Priority effects during fungal community establishment in beech wood. The ISME Journal 9(10): 2246–2260. https://doi.org/10.1038/ismej.2015.38

Ihrmark K, Bodeker ITM, Cruz-Martinez K, Friberg H, Kubartova A, Schenck J, Strid Y, Stenlid J, Brandstrom-Durling M, Clemmensen KE, Lindahl BD (2012) New primers to amplify the fungal ITS2 region – evaluation by 454-sequencing of artificial and natural communities. FEMS Microbiology Ecology 82(3): 666–677. https://doi.org/10.1111/j.1574-6941.2012.01437.x

Juutilainen K, Halme P, Kotiranta H, Mönkkönen M (2011) Size matters in studies of dead wood and wood-inhabiting fungi. Fungal Ecology 4(5): 342–349. https://doi.org/10.1016/j.funeco.2011.05.004

Juutilainen K, Mönkkönen M, Kotiranta H, Halme P (2014) The effects of forest management on wood-inhabiting fungi occupying dead wood of different diameter fractions. Forest Ecology and Management 313: 283–291. https://doi.org/10.1016/j.foreco.2013.11.019

Keuskamp JA, Dingemans BJJ, Lehtinen T, Sarneel JM, Hefting MM (2013) Tea Bag Index: A novel approach to collect uniform decomposition data across ecosystems. Methods in Ecology and Evolution 4(11): 1070–1075. https://doi.org/10.1111/2041-210X.12097

Korkmaz S, Goksuluk D, Zararsiz G (2014) MVN: An R package for assessing multivariate normality. The R Journal 6(2): 151–162. https://doi.org/10.32614/RJ-2014-031

Kotiranta H, Saarenoksa R, Kytövuori I (2009) Aphyllophoroid fungi of Finland. A check-list with ecology, distribution, and threat categories. Norrlinia 19: 1–224.

Krah FS, Seibold S, Brandl R, Baldrian P, Muller J, Bassler C (2018) Independent effects of host and environment on the diversity of wood-inhabiting fungi. Journal of Ecology 106(4): 1428–1442. https://doi.org/10.1111/1365-2745.12939

Kubartova A, Ranger J, Berthelin J, Beguiristain T (2009) Diversity and decomposing ability of saprophytic fungi from temperate forest litter. Microbial Ecology 58(1): 98–107. https://doi.org/10.1007/s00248-008-9458-8

Küffer N, Senn-Irlet B (2005) Influence of forest management on the species richness and composition of wood-inhabiting basidiomycetes in Swiss forests. Biodiversity and Conservation 14(10): 2419–2435. https://doi.org/10.1007/s10531-004-0151-z

Martin M (2011) Cutadapt removes adapter sequences from high-throughput sequencing reads. EMBnet. Journal 17(1): 10–12. https://doi.org/10.14806/ej.17.1.200

Moll J, Heintz-Buschart A, Bassler C, Hofrichter M, Kellner H, Buscot F, Hoppe B (2021) Amplicon Sequencing-Based Bipartite Network Analysis Confirms a High Degree of Specialization and Modularity for Fungi and Prokaryotes in Deadwood. MSphere 6(1): e00856-20. https://doi.org/10.1128/mSphere.00856-20

Moose RA, Schigel D, Kirby LJ, Shumskaya M (2019) Dead wood fungi in North America: An insight into research and conservation potential. Nature Conservation 32: 1–17. https://doi.org/10.3897/natureconservation.32.30875

Mueller GM, Schmit JP (2007) Fungal biodiversity: What do we know? What can we predict? Biodiversity and Conservation 16(1): 1–5. https://doi.org/10.1007/s10531-006-9117-7

Nguyen NH, Song Z, Bates ST, Branco S, Tedersoo L, Menke J, Schilling JS, Kennedy PG (2016) FUNGuild: An open annotation tool for parsing fungal community datasets by ecological guild. Fungal Ecology 20: 241–248. https://doi.org/10.1016/j.funeco.2015.06.006

Niemelä T (2005) Polypores, lignicolous fungi. Norrlinia 13: 1–320.

Norden B, Ryberg M, Gotmark F, Olausson B (2004) Relative importance of coarse and fine woody debris for the diversity of wood-inhabiting fungi in temperate broadleaf forests. Biological Conservation 117(1): 1–10. https://doi.org/10.1016/S0006-3207(03)00235-0

Oksanen J, Blanchet GF, Friendly M, Kindt R, Legendre P, McGlinn D, Minchin PR, O'Hara RB, Simpson GL, Solymos P, Stevens MHH, Szoecs E, Wagner H (2020) vegan: Community Ecology Package. R package version 2.5-7. https://CRAN.R-project.org/package=vegan

Öpik M, Metsis M, Daniell TJ, Zobel M, Moora M (2009) Large-scale parallel 454 sequencing reveals host ecological group specificity of arbuscular mycorrhizal fungi in a boreonemoral forest. The New Phytologist 184(2): 424–437. https://doi.org/10.1111/j.1469-8137.2009.02920.x

Palmer JM, Jusino MA, Banik MT, Lindner DL (2018) Non-biological synthetic spike-in controls and the AMPtk software pipeline improve mycobiome data. PeerJ 6: e4925. https://doi.org/10.7717/peerj.4925

Parfitt D, Hunt J, Dockrell D, Rogers HJ, Boddy L (2010) Do all trees carry the seeds of their own destruction? PCR reveals numerous wood decay fungi latently present in sapwood of a wide range of angiosperm trees. Fungal Ecology 3(4): 338–346. https://doi.org/10.1016/j.funeco.2010.02.001

R Core Team (2020) R: A language and environment for statistical computing. https://www.R-project.org/

Rassi P, Hyvärinen E, Juslén A, Mannerkoski I (2010) The 2010 Red List of Finnish species. Ministry of the Environment & Finnish Environment Institute, 685 pp.

Rayner ADM, Boddy L (1988) Fungal communities in the decay of wood. Advances in Microbial Ecology 10: 115–166. https://doi.org/10.1007/978-1-4684-5409-3_4

Roberts DW (2019) Package 'labdsv'. Version 2.0-1. Ordination and multivariate analysis for ecology: 775. https://CRAN.R-project.org/package=labdsv

Rognes T, Flouri T, Nichols B, Quince C, Mahe F (2016) VSEARCH: A versatile open source tool for metagenomics. PeerJ 4: e2584. https://doi.org/10.7717/peerj.2584

Seibold S, Baessler C, Brandl R, Gossner MM, Thorn S, Ulyshen MD, Mueller J (2015) Experimental studies of dead-wood biodiversity – A review identifying global gaps in knowledge. Biological Conservation 191: 139–149. https://doi.org/10.1016/j.biocon.2015.06.006

Shumskaya M, Lorusso N, Patel U, Leigh M, Somervuo P, Schigel D (2022) Fungal communities in decaying poplar pins in Northeastern USA discovered by MycoPins method.

Siitonen J (2001) Forest management, coarse woody debris and saproxylic organisms: Fennoscandian boreal forests as an example. Ecological Bulletins 49: 11–41.

Simpson HJ, Schilling JS (2021) Using aggregated field collection data and the novel r package fungarium to investigate fungal fire association. Mycologia 113(4): 842–855. https://doi.org/10.1080/00275514.2021.1884816

Stokland J, Siitonen J, Jonsson B (2012) Biodiversity in dead wood. Cambridge University Press, 524 pp. https://doi.org/10.1017/CBO9781139025843

Tedersoo L, Gates G, Dunk CW, Lebel T, May TW, Koljalg U, Jairus T (2009) Establishment of ectomycorrhizal fungal community on isolated *Nothofagus cunninghamii* seedlings regenerating on dead wood in Australian wet temperate forests: Does fruit-body type matter? Mycorrhiza 19(6): 403–416. https://doi.org/10.1007/s00572-009-0244-3

White TJ, Bruns T, Lee S, Taylor J (1990) Amplification and direct sequencing of fungal ribosomal RNA genes for phylogenetics. PCR protocols: A guide to methods and applications. Academic Press, 315–322. https://doi.org/10.1016/B978-0-12-372180-8.50042-1

Zhang JJ, Kobert K, Flouri T, Stamatakis A (2014) PEAR: A fast and accurate Illumina Paired-End reAd mergeR. Bioinformatics (Oxford, England) 30(5): 614–620. https://doi.org/10.1093/bioinformatics/btt593

Supplementary material 1

Sequences of the primers used in the experiment and ITS2 fragment amplified from DNA extracted from saw dust of the pins

Authors: Maria Shumskaya, Nicholas Lorusso, Urvi Patel, Madison Leigh, Panu Somervuo, Dmitry Schigel

Data type: docx file

Link: https://doi.org/10.3897/mycokeys.96.101033.suppl1

MycoKeys 96: 97–112 (2023)
doi: 10.3897/mycokeys.96.98029
https://mycokeys.pensoft.net

RESEARCH ARTICLE

A peer-reviewed open-access journal
MycoKeys
Launched to accelerate biodiversity research

Pseudolepraria, a new leprose genus revealed in Ramalinaceae (Ascomycota, Lecanoromycetes, Lecanorales) to accommodate *Lepraria stephaniana*

Martin Kukwa[1], Magdalena Kosecka[1], Agnieszka Jabłońska[1], Adam Flakus[2], Pamela Rodriguez-Flakus[2], Beata Guzow-Krzemińska[1]

1 *Department of Plant Taxonomy and Nature Conservation, Faculty of Biology, University of Gdańsk, Wita Stwosza 59, PL-80-308 Gdańsk, Poland* **2** *W. Szafer Institute of Botany, Polish Academy of Sciences, Lubicz 46, PL-31-512 Kraków, Poland*

Corresponding authors: Martin Kukwa (martin.kukwa@ug.edu.pl);
Beata Guzow-Krzemińska (beata.guzow-krzeminska@ug.edu.pl)

Academic editor: Thorsten Lumbsch | Received 25 November 2022 | Accepted 25 February 2023 | Published 24 March 2023

Citation: Kukwa M, Kosecka M, Jabłońska A, Flakus A, Rodriguez-Flakus P, Guzow-Krzemińska B (2023) *Pseudolepraria*, a new leprose genus revealed in Ramalinaceae (Ascomycota, Lecanoromycetes, Lecanorales) to accommodate *Lepraria stephaniana*. MycoKeys 96: 97–112. https://doi.org/10.3897/mycokeys.96.98029

Abstract

The new genus *Pseudolepraria* Kukwa, Jabłońska, Kosecka & Guzow-Krzemińska is introduced to accommodate *Lepraria stephaniana* Elix, Flakus & Kukwa. Phylogenetic analyses of nucITS, nucLSU, mtSSU and RPB2 markers recovered the new genus in the family Ramalinaceae with strong support. The genus is characterised by its thick, unstratified thallus composed entirely of soredia-like granules, the presence of 4-*O*-methylleprolomin, salazinic acid, zeorin and unknown terpenoid, and its phylogenetic position. The new combination, *P. stephaniana* (Elix, Flakus & Kukwa) Kukwa, Jabłońska, Kosecka & Guzow-Krzemińska, is proposed.

Keywords

Lichenized fungi, morphology, Neotropics, secondary metabolites, sterile lichens, taxonomy

Introduction

During the evolution in some groups of lichenized fungi the ability to reproduce sexually has been apparently lost completely and some phylogenetic lineages are known to develop exclusively asexual lichenized propagules. This includes *Lepraria* Ach.

(Ascomycota, Lecanoromycetes, Lecanorales, Stereocaulaceae), a well-known genus which up to quite recently comprised only crustose lichens with morphologically simple thalli consisting of soredia-like granules laying directly on substrate or on a layer of hypothalline hyphae (e.g., Ekman and Tønsberg 2002; Kukwa 2002; Sipman 2004; Flakus and Kukwa 2009; Flakus et al. 2011a; Lendemer 2011a, b, 2013a; Lendemer and Hodkinson 2013; Guzow-Krzemińska et al. 2019a). However, Lendemer and Hodkinson (2013) found, based on molecular data, that some fruticose species previously referred to *Leprocaulon* Nyl. also represented *Lepraria* s.str. and they were subsequently transferred to the latter genus. In contrast to their simplified morphology, the species produce a vast variety of secondary lichen metabolites, which are an invaluable tool, together with morphological characters that may be sparse, in the recognition of species and their identification (e.g., Laundon 1989, 1992; Tønsberg 1992; Sipman 2004; Kantvilas and Kukwa 2006; Flakus and Kukwa 2007; Saag et al. 2009; Flakus et al. 2011a; Lendemer 2011a, 2013a; Lendemer and Hodkinson 2013; Guzow-Krzemińska et al. 2019a; Kukwa 2019). It is also noteworthy that some species until recently classified as *Lepraria* have been shown to belong to other genera (e.g., *Leprocaulon* and *Septotrapelia* Aptroot & Chaves; Bungartz et al. 2013; Lendemer and Hodkinson 2013) or even new genera were established for some peculiar species, e.g., *Andreiomyces* Hodkinson & Lendemer within Arthoniomycetes (Hodkinson and Lendemer 2013), *Botryolepraria* Canals et al., related to Verrucariaceae in Eurotiomycetes (Kukwa and Pérez-Ortega 2010) and *Lithocalla* Orange in Lecanorales (probably in Ramalinaceae) in Lecanoromycetes (Orange 2020).

Lepraria includes at present c. 75 species (Wijayawardene et al. 2017; Guzow-Krzemińska et al. 2019a; Barcenas-Peña et al. 2021), most of which were described based on chemical (secondary metabolites) and morphological features and some also by molecular markers (e.g., Laundon 1989, 1992; Tønsberg 1992; Lendemer 2011a, 2012, 2013a; Lendemer and Hodkinson 2013; Guzow-Krzemińska et al. 2019a; Barcenas-Peña et al. 2021). One of the species that was placed in *Lepraria* based solely on morphological similarity to other members of the genus was *L. stephaniana* Elix, Flakus & Kukwa (Flakus et al. 2011a). This species is characterised by the thick, unstratified and non-lobed thallus composed of coarse soredia-like granules with soft appearance, and the production of 4-*O*-methylleprolomin, salazinic acid and terpenoids. 4-*O*-methylleprolomin was known only in a single *Pannaria* species before its discovery in *L. stephaniana* (Flakus et al. 2011a). *Lepraria stephaniana* has been known until recently only from the type locality, however during field studies in 2017 in Bolivia we found two new localities of the species (one close to the type locality) (Guzow-Krzemińska et al. 2019b). Sequencing of molecular markers of those two recently collected specimens revealed that *L. stephaniana* is unrelated to other species of *Lepraria* s.str., but instead it appeared to be nested within Ramalinaceae as a previously unsequenced lineage close to *Cliostomum* Fr., *Ramalina* Ach. and allied genera. In this paper we introduce the new genus *Pseudolepraria* for this peculiar lineage within Ramalinaceae.

Materials and methods

Taxon sampling

The studied specimens are deposited in B, BG, KRAM, LPB, NY and UGDA herbaria. Morphology was examined by using Nikon SMZ 800N stereomicroscope. The secondary chemistry of all samples was studied by thin layer chromatography (TLC) following methods by Culberson and Kristinsson (1970) and Orange et al. (2001a).

DNA extraction, PCR amplification and DNA sequencing

DNA was extracted using a modified CTAB method (Guzow-Krzemińska and Węgrzyn 2000). We analysed four fungal markers: nucITS rDNA, mtSSU rDNA, nucLSU rDNA, and RPB2 gene. For this purpose we used the following primers: ITS1F (Gardes and Bruns 1993) and ITS4A (Kroken and Taylor 2001) for nucITS rDNA; mrSSU1 and mrSSU3R (Zoller et al. 1999) for mtSSU rDNA; ITS4A-5' (Kroken and Taylor 2001; Nelsen et al. 2011) and LR5 (Vilgalys and Hester 1990) for nucLSU rDNA; fRPB2-5F and fRPB2-7cR (Liu et al. 1999) for RPB2 gene. Additionally, nucITS rDNA region from green algal partner was amplified using Al1500bf (Helms et al. 2001) and ITS4M primers (Guzow-Krzemińska 2006). PCR was performed in a volume of 25 µl using StartWarm HS-PCR Mix (A&A Biotechnology) following the manufacturer's protocol. 1 µl of genomic DNA was used for amplification. The PCR cycling parameters are available in Suppl. material 1.

The efficiency of the PCR was checked by visualising the reaction products on a 1% agarose gels stained with SimplySafe (Eurx) dye in order to determine DNA fragment lengths. Afterwards, PCR products were purified using Clean-Up Concentrator (A&A Biotechnology). The sequencing was performed in Macrogen Europe (The Netherlands), using amplification primers. The newly obtained sequences were deposited in GenBank database and their accession numbers are listed in Table 1.

Sequence alignment and phylogenetic analysis

The newly generated sequences were compared to the sequences available in the GenBank database (http://www.ncbi.nlm.nih.gov/BLAST/) using BLASTn search (Altschul et al. 1990). For the phylogenetic analyses we used representatives of Ramalinaceae and *Boreoplaca ultrafrigida* Timdal and *Ropalospora lugubris* (Sommerf.) Poelt were used as outgroup taxa according to previous studies (Kistenich et al. 2018; Orange 2020; van den Boom and Magain 2020). The independent alignments for each marker were generated in MAFFT using auto option and default parameters (Katoh and Standley 2013). The datasets were then subjected to Guidance2 server (Landan and Graur 2008; Penn et al. 2010; Sela et al. 2015; http://guidance.tau.ac.il/) for further analysis. The MSA algorithm was set to MAFFT and 100 bootstrap replicates were used.

Table 1. Species used in this study with their GenBank accession numbers. New sequences are marked in bold.

Species	nucITS rDNA	nucLSU rDNA	mtSSU	RPB2	Algal nucITS rDNA
Aciculopsora salmonea	MG925948	–	MG925842	–	
Aciculopsora srilankensis	MK400258	–	MK400211	–	
Bacidia arceutina	AF282083	MG926041	MG925846	MG926230	
Bacidia rosella	AF282086	AY300829	AY300877	AM292755	
Bacidina arnoldiana	AF282093	MG926048	MG925854	MG926238	
Bacidina phacodes	AF282100	MG926049	AY567725	MG926240	
Badimia dimidiata	MG925956	MG926052	AY567774	–	
Bellicidia incompta	AF282092	MG926043	MG925849	MG926233	
Biatora globulosa	AF282073	MG926055	KF662414	KF662450	
Biatora vacciniicola	MG925960	MG926060	MG925861	MG926245	
Biatora vernalis	AF282070	DQ838752	DQ838753	–	
Bibbya albomarginata	MG926024	MG926115	MG925927	MG926286	
Bibbya vermifera	AF282109	MG926047	MG925852	MG926237	
Bilimbia sabuletorum	AM292670	AY756346	AY567721	AM292761	
Boreoplaca ultrafrigida	HM161512	DQ986797	DQ986813	DQ992421	
Catillaria scotinodes	AM292673	MG926064	AM292720	AM292763	
Catinaria atropurpurea	MG925965	MG926065	MG925865	MG926246	
Catolechia wahlenbergii	HQ650649	DQ986794	DQ986811	DQ992424	
Cenozosia inanis	–	MG926066	MG925866	–	
Cliomegalaria symmictoides	MW622003	MW621867	MW622006	–	
Cliostomum corrugatum	MG925966	MG926067	AY567722	KF662436	
Cliostomum haematommatis	MK446224	–	MK446223	–	
Eschatogonia prolifera	MG925969	MG926070	MG925870	MG926249	
Kiliasia athallina	MG926023	MG926114	–	MG926284	
Kiliasia sculpturata	MG926034	MG926122	MG925938	MG926295	
Krogia coralloides	MG925977	MG926072	MG925875	MG926251	
Lecania aipospila	MG925978	MG926073	MG925876	MG926252	
Lecania erysibe	AM292682	MG926074	AM292733	AM292769	
Lecania fuscella	AM292684	MG926075	MG925877	–	
Lecidea albohyalina	KF650950	MG926079	KF662398	KF662438	
Lithocalla ecorticata	KT962179	–	KT962184	–	
Lithocalla malouina	KT962178	–	MT857015	–	
Lueckingia polyspora	MG925984	MG926082	MG925882	–	
Megalaria grossa	AF282074	MG926083	MG925883	MG926257	
Megalaria versicolor	–	AY584651	AY584622	DQ912401	
Mycobilimbia pilularis	KF650954	–	KF662402	KF662442	
Mycobilimbia tetramera	–	KJ766600	KJ766439	KJ766957	
Niebla homalea	MG925987	–	MG925888	–	
Namibialina melanothrix	MG926038	MG926128	MG925945	MG926303	
Parallopsora brakoae	MG925989	–	MG925891	–	
Parallopsora leucophyllina	MG925994	–	MG925897	MG926265	
Phyllopsora breviuscula	MG925990	MG926087	MG925892	MG926262	
Phyllopsora gossypina	MG925967	MG926068	MG925867	MG926247	
Phyllopsora parvifoliella	MG925999	MG926092	MG925902	MG926267	
Physcidia wrightii	MN334233	–	MN334227	–	
***Pseudolepraria stephaniana* Kukwa 19740**	**OQ172237**	**OQ172242**	**OQ172251**	**–**	**OQ303855**
***Pseudolepraria stephaniana* Kukwa 19267**	**OQ172236**	**OQ172243**	**OQ172250**	**OQ160272**	**OQ303854**
Ramalina dilacerata	MG926013	MG926104	MG925917	–	
Ramalina fraxinea	MG926014	MG926105	MG925918	MG926277	
Ramalina mannii	MG926019	MG926111	–	MG926280	
Ramalina pollinaria	MG926017	MG926108	AM292752	MG926278	
Ramalina sinensis	MG926018	MG926110	MG925921	–	

Species	nucITS rDNA	nucLSU rDNA	mtSSU	RPB2	Algal nucITS rDNA
Rolfidium bumammum	MG926027	MG926117	MG925930	MG926288	
Ropalospora lugubris	MG926020	–	MG925922	–	
Scutula circumspecta	–	–	MG925848	–	
Sporacestra pertexta	MG926000	MG926093	MG925903	MG926268	
Stirtoniella kelica	MG926021	–	MG925923	–	
Thalloidima candidum	AF282117	MG926118	MG925932	MG926290	
Thalloidima toninianum	MG926036	MG926124	MG925942	MG926298	
Thamnolecania brialmontii	AF282066	MG926112	MG925925	MG926283	
Toninia cinereovirens	AF282104	AY756365	AY567724	AM292781	
Toninia populorum	MG925950	MG926039	MG925843	MG926228	
Toniniopsis aromatica	AF282126	MG926113	MG925926	MG926284	
Toniniopsis subincompta	AF282125	MG926046	MG925851	MG926236	
Tylocliostomum viridifarinosum	NR_174049	–	–	–	
Tylothallia biformigera	AF282077	MG926129	MG925946	MG926304	
Waynea californica	–	MG926130	MG925947	MG926305	
Vermilacinia breviloba	MN811352	MN811548	–	MN757330	

The Guidance confidence scores were calculated and columns with a score < 0.93 were excluded from the alignments. The terminal ends were trimmed. Single-locus matrices consisted of 61 sequences for nucITS, 62 sequences for mtSSU, 51 sequences for nucLSU, and 44 sequences for RPB2. The best ML tree was inferred for each locus using IQ-TREE with 1000 ultrafast bootstrap replicates as implemented in the IQ-TREE web server (Nguyen et al. 2015; Chernomor et al. 2016; Kalyaanamoorthy et al. 2017; Hoang et al. 2018). Congruence was examined by eye and no significant conflict between loci was observed.

For the final analysis, we concatenated four markers which resulted in a dataset of 66 terminals and 3766 positions. The concatenated dataset was subjected to IQ-TREE analysis to find best-fitting nucleotide substitution models (Nguyen et al. 2015; Chernomor et al. 2016; Kalyaanamoorthy et al. 2017; Hoang et al. 2018). The model selection was restricted to models implemented in MrBayes and the following nucleotide substitution models for the four predefined subsets were selected: GTR+F+I+G for mtSSU rDNA, K2P+I+G for nucITS, and SYM+I+G for both nucLSU rDNA and RPB2 markers. The search for maximum likelihood tree was performed in IQ-TREE and followed with 1000 standard bootstrap replicates (Nguyen et al. 2015; Chernomor et al. 2016; Kalyaanamoorthy et al. 2017; Hoang et al. 2018).

Bayesian analysis was carried out using a Markov Chain Monte Carlo (MCMC) method, in MrBayes v. 3.2.6 (Huelsenbeck and Ronquist 2001; Ronquist and Huelsenbeck 2003) on the CIPRES Web Portal (Miller et al. 2010) using previously selected models (see above). Two parallel MCMC runs were performed, each using four independent chains and ten million generations, sampling every 1000th tree. The resulting log files were analysed using Tracer 1.7.2 (Rambaut et al. 2018). Posterior probabilities (PP) were determined by calculating a majority-rule consensus tree after discarding the initial 25% trees of each chain as the burn-in. The convergence of the chains was confirmed by the convergent diagnostic of the Potential Scale Reduction Factor

(PSRF), which approached 1 and the 'average standard deviation of split frequencies' was < 0.01).

Phylogenetic trees were visualised using FigTree v. 1.4.3 (Rambaut 2009) and modified in Inkscape (https://inkscape.org/). Bootstrap support (BS values ≥ 70) and PP values (values ≥ 0.95) are given near the branches on the phylogenetic tree. The data were deposited at TreeBASE (Submission ID: 30149).

Results and discussion

For this work we successfully sequenced nucITS, mtSSUand nucLSU from two specimens and additionally RPB2 from one specimen of *Lepraria stephaniana* collected in Bolivia (Table 1). BLAST searches of the nucITS, nucLSU, mtSSU and RPB2 markers surprisingly showed the highest similarities to representatives of the family Ramalinaceae, i.e., the genera *Cenozosia* A. Massal., *Cliostomum* and *Ramalina*. Phylogenetic analysis of the concatenated dataset shows that *L. stephaniana* is nested inside Ramalinaceae. The newly sequenced specimens of the species were resolved in a distinct and highly supported clade sister to a clade consisting of *Cliostomum* s.str. represented by the type species *C. corrugatum* (Ach.) Fr., *Cenozosia inanis* (Mont.) A. Massal. and a subclade of several species of *Ramalina*, *Namibialina melanothrix* (Laurer) Spjut & Sérus., *Niebla* (Ach.) Rundel & Bowler and *Vermilacinia breviloba* Spjut & Sérus. (Fig. 1). A new monotypic genus, *Pseudolepraria*, is introduced for this lineage of *Lepraria stephaniana* and is characterised by a thick, unstratified thallus composed of soredia-like granules, and the presence of 4-*O*-methylleprolomin, salazinic acid, zeorin and unknown terpenoid.

Pseudolepraria is the first genus forming leprose and sterile thalli that can be placed with high support within Ramalinaceae. Orange (2020) described the genus *Lithocalla* and placed it with uncertainty in Ramalinaceae. In our phylogeny, *Lithocalla* forms the sister group to Ramalinaceae sensu Kistenich et al. (2018), but this may be an artifact of the taxon sampling. The particular placement of the genus was beyond the scope of this study. *Lithocalla* was introduced for two species, which were originally placed, due to morphological similarities, in *Lepraria*, i.e., *L. ecorticata* (J. R. Laundon) Kukwa and *L. malouina* Øvstedal (Kukwa 2006; Fryday and Øvstedal 2012). Both, *Lithocalla ecorticata* (J. R. Laundon) Orange known from Great Britain and Norway, and *L. malouina* (Øvstedal) Fryday & Orange found in the Falkland Islands (Fryday and Øvstedal 2012; Orange 2020), differ from *Pseudolepraria stephaniana*, in their distribution in colder climates, by the production of usnic and fatty acids, the absence of zeorin and the exclusively saxicolous habitat (Orange 2020).

Species resembling *Pseudolepraria* in the Ramalinaceae have up until recently been included in *Crocynia* (Ach.) A. Massal. This genus was established for lichens with a non-corticate, byssoid, felt-like thallus and historically included several species now placed mostly in *Lepraria* (e.g., Laundon 1989, 1992; Kistenich et al. 2018). According to Lücking et al. (2017) *Crocynia* comprised three species and two of them were included in the phylogeny of Ramalinaceae by Kistenich et al. (2018), where they

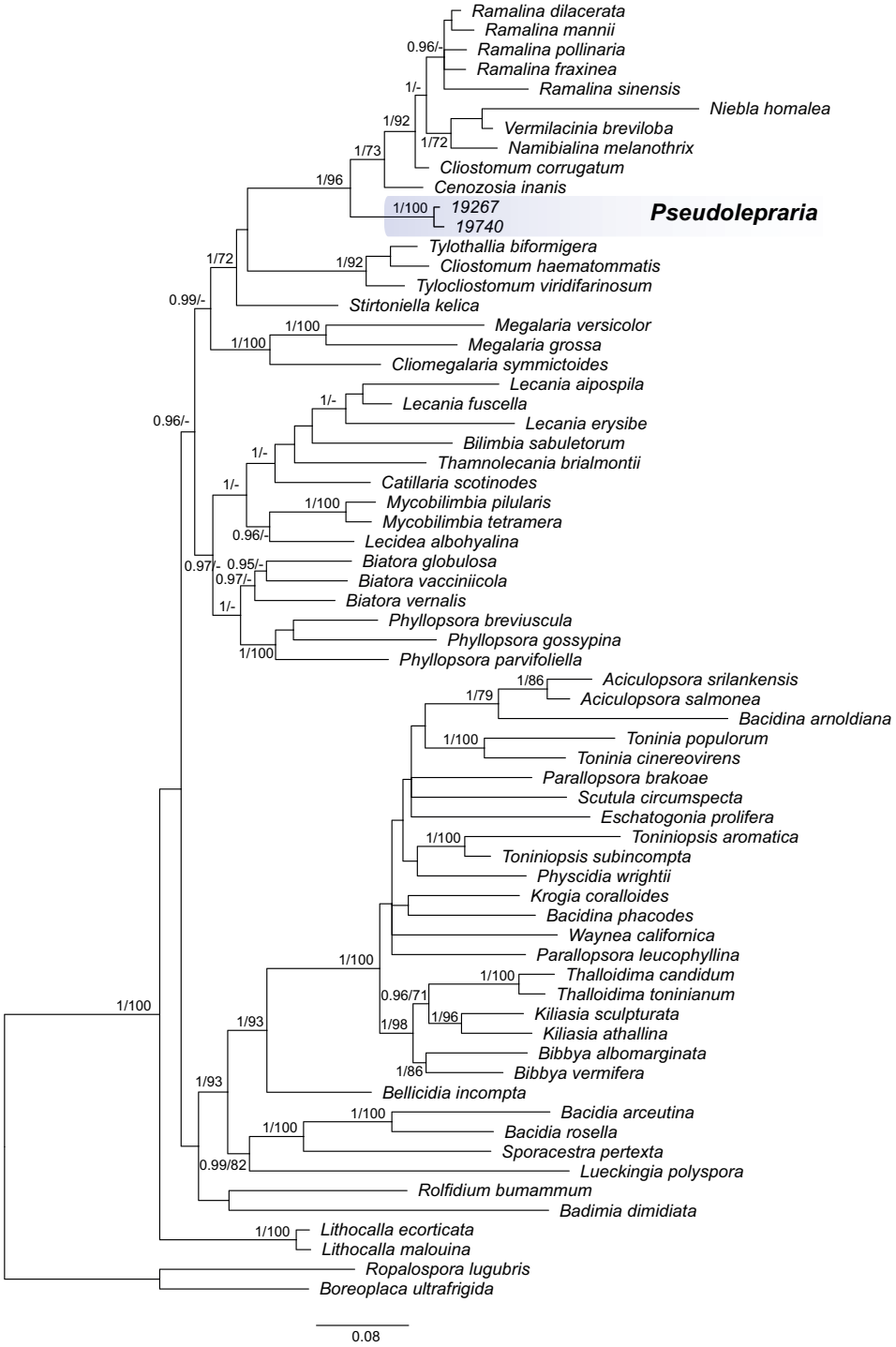

Figure 1. Majority-rule consensus tree resulting from MrBayes analysis of the concatenated mtSSU, nucITS, nucLSU and RPB2 markers with Bayesian PP (values ≥ 0.95) and IQ-TREE bootstrap support values (BS values ≥ 70) given near the branches. *Pseudolepraria* is marked in blue.

formed a clade nested inside *Phyllopsora* Müll. Arg. Consequently, *Crocynia* was synonymised with *Phyllopsora*, also because of morphological similarities (Kistenich et al. 2018). The status of the third species, *C. microphyllina* Aptroot (Lumbsch et al. 2011), and three species discussed by Sipman (2018) remains uncertain. The species historically placed in *Crocynia* differ from *Pseudolepraria* in the byssoid thalli not producing 4-*O*-methylleprolomin and in sometimes producing apothecia (Cáceres 2007; Lumbsch et al. 2011; Aptroot and Cáceres 2014; Sipman 2018).

Pseudolepraria is very similar to *Lepraria* s.str. in sharing the same thallus morphology and, to a certain extent, secondary chemistry (presence of salazinic acid and terpenoids) (e.g., Aptroot 2002; Sipman 2004; Saag et al. 2009; Flakus et al. 2011a; Lendemer 2011a, b). They differ, apart from the phylogenetic position, only in the presence of the very rarely reported 4-*O*-methylleprolomin, a diphenyl ether previously found only in one *Pannaria* species (Flakus et al. 2011a). *Pseudolepraria* differs also in the habitat preferences. It was found only in tropical forests at low elevations (300–470 m a.s.l.), whereas *Lepraria* in tropical South America, including Bolivian ecosystems, are found mostly above 1000 m above sea level (only one locality of *L. finkii* (B. de Lesd.) R.C. Harris found at the elevation of 890 m), in montane forests and open high Andean vegetation (Flakus and Kukwa 2007; Flakus et al. 2011a, b, 2012, 2015; Guzow-Krzemińska et al. 2019a). This is in agreement with the statement presented by Orange et al (2001b), who considered *Lepraria* to be restricted to montane habitats in the tropics.

Poelt (1987) considered the genus *Lepraria* as a 'box of analogous groups of lichens of completely different origin, held together by the same highly specialized thallus type'. Poelt (1987) also stated that the leprarioid thallus type and the loss of generative reproduction developed in evolution through the reduction of the thallus structures as an adaptation for growing in bark crevices and on over-hanging rocks in ecologically specialised group of lichenized fungi, which includes *Lepraria*, but also, as Poelt (1987) mentioned, *Leproplaca* (Nyl.) Nyl. and some species of the genus *Chrysothrix* Mont. (Poelt 1987). However, this is only partly true, as some lichen groups with this type of thallus (e.g., species of *Lepraria neglecta* group) can grow also in other habitats (e.g., Laundon 1992; Lendemer 2013b). Nevertheless, the statement of Poelt (1987) was true and innovative at this time and it was later shown that the leprarioid thallus indeed originated in several unrelated lichen lineages (e.g., Ekman and Tønsberg 2002; Kukwa and Pérez-Ortega 2010; Hodkinson and Lendemer 2013; Malíček et al. 2018; Guzow-Krzemińska et al. 2017; Orange 2020). Furthermore, some leprarioid genera are known exclusively in sterile state, like *Andreiomyces* (Arthoniales, Arthoniomycetes), *Botryolepraria* (Verrucariales, Eurotiomycetes), *Lepraria* and *Lithocalla* (both in Lecanorales, Lecanoromycetes) (Ekman and Tønsberg 2002; Kukwa and Pérez-Ortega 2010; Hodkinson and Lendemer 2013; Orange 2020). *Pseudolepraria* is another addition to this group, however, as only a few collections are available, it may eventually be found with ascomata.

Buschbom and Mueller (2006) suggested that the asexual way of reproduction is advantageous because the symbiosis with the optimal photobiont for a given environment allows the rapid dissemination of both partners. Therefore, it is more important for the mycobiont to keep the relationship with suitable algal species; however this does not mean that the symbiosis in asexually reproducing species cannot be broken.

Kosecka et al. (2021) showed for some *Lepraria* species that the mycobiont can form thalli with different, locally adapted algal strains. We partially sequenced the nucITS region of the photobiont of *Pseudolepraria stephaniana* (Table 1) and found that both thalli associate with the same green algal partner (100% of identity). BLAST hits were closest to *Symbiochloris*, *Dictyochloropsis*, *Massjukichlorella* and *Watanabea* spp., all of which were quite dissimilar to the photobiont sequences of *Pseudolepraria stephaniana*.

Taxonomy

Pseudolepraria **Kukwa, Jabłońska, Kosecka & Guzow-Krzemińska, gen. nov.**
MycoBank No: 847408

Diagnosis. Characterised by thick, unstratified thallus composed of soredia-like granules, the presence of 4-*O*-methylleprolomin, salazinic acid, zeorin, and unknown terpenoid, and the phylogenetic position within Ramalinaceae.

Generic type. *Pseudolepraria stephaniana* (Elix, Flakus & Kukwa) Kukwa, Jabłońska, Kosecka & Guzow-Krzemińska

Description. As this is a monotypic genus the description below constitutes the generic description.

Etymology. The new name refers to the similarity to the genus *Lepraria*, in which this particular species was originally placed.

Pseudolepraria stephaniana **(Elix, Flakus & Kukwa) Kukwa, Jabłońska, Kosecka & Guzow-Krzemińska, comb. nov.**
MycoBank No: 847409
Fig. 2

Lepraria stephaniana Elix, Flakus & Kukwa, in Flakus et al., Lichenologist 43: 64, 2011 (2010). Basionym.

Type. Bolivia. Dept. La Paz: Prov. Iturralde, between Ixiamas and Santa Rosa de Maravillas villages, elev. 305 m, 13°49'16"S, 68°07'18"W, preandean Amazon forest, on bark of tree, 28 July 2008, M. Kukwa 6828 (holotype: UGDA L!; isotypes: B!, BG!, KRAM!, LPB!, NY!).

Description (adopted from Flakus et al. 2011a). Thallus crustose, thick, usually not delimited nor lobed, green-grey to creamy-white, not stratified, but sometimes with a poorly differentiated, pseudo-medullary layer of decaying granules. Hypothallus indistinct. Granules coarse with soft appearance, irregularly rounded, up to 100(–200) μm in diam., composed of very lax hyphae mixed with algal cells, usually with projecting hyphae up to c. 30(–50) μm long. Photobiont green, cells globose, up to 12 μm in diam.

Chemistry. Substances detected: 4-*O*-methylleprolomin (major), salazinic acid (minor), zeorin (minor) and an unknown terpenoid (minor) with Rf class values A6,

Figure 2. Morphology of *Pseudolepraria stephaniana* (type). Scale bar: 0.5 mm.

B6, C6. Thallus reactions: K+ yellow turning brownish to red, P+ yellow, C–, KC– (see also Flakus et al. 2011a).

Distribution and habitat. The species is known only from three localities in Bolivia. It was found on bark of trees in transition Chaqueño-Amazon or preandean Amazon forests at elevation between c. 300 to 470 m a.s.l. (Flakus et al. 2011a; Guzow-Krzemińska et al. 2019b).

Specimens used for DNA extraction (Table 1). Bolivia. Dept. La Paz: Prov. Abel Iturralde, between Santa Rosa de Maravillas and Tumupasa, 13°58'43"S, 67°58'14"W, elev. 300 m, natural Preandean Amazon forest, corticolous, 25 May 2017, M. Kukwa 19740 (LPB, UGDA). Dept. Santa Cruz: Prov. Ichilo, Parque Nacional y Área Natural de Manejo Integrado Amboró, Sendero a la Cascada, near Villa Amboró, 17°44'02"S, 63°35'05"W, elev. 470 m, transition Chaqueño-Amazon forest, in the valley, corticolous, 11 May 2017, M. Kukwa 19267 (LPB, UGDA).

Acknowledgements

We are very grateful to James C. Lendemer (New York Botanical Garden), Tor Tønsberg (University of Bergen) and an anonymous reviewer for invaluable comments,

and the members of Herbario Nacional de Bolivia, Instituto de Ecología, Universidad Mayor de San Andrés, La Paz, for their generous cooperation. This research received funding from the National Science Centre (project no 2015/17/B/NZ8/02441).

References

Altschul SF, Gish W, Miller W, Myers EW, Lipman DJ (1990) Basic local alignment search tool. Journal of Molecular Biology 215(3): 403–410. https://doi.org/10.1016/S0022-2836(05)80360-2

Aptroot A (2002) New and interesting lichens and lichenicolous fungi in Brazil. Fungal Diversity 9: 15–45.

Aptroot A, Cáceres MES (2014) A key to the corticolous microfoliose, foliose and related crustose lichens from Rondônia, Brazil, with the description of four new species. Lichenologist 46(6): 783–799. https://doi.org/10.1017/S0024282914000358

Barcenas-Peña A, Diaz R, Grewe F, Widhelm T, Lumbsch HT (2021) Contributions to the phylogeny of *Lepraria* (Stereocaulaceae) species from the Southern Hemisphere, including three new species. The Bryologist 124(4): 494–505. https://doi.org/10.1639/0007-2745-124.4.494

Bungartz F, Hillmann G, Kalb K, Elix JA (2013) Leprose and leproid lichens of the Galapagos, with a particular focus on *Lepraria* (Stereocaulaceae) and *Septotrapelia* (Pilocarpaceae). Phytotaxa 150(1): 1–28. https://doi.org/10.11646/phytotaxa.150.1.1

Buschbom J, Mueller GM (2006) Testing "species pair" hypotheses: Evolutionary processes in the lichen-forming species complex *Porpidia flavocoerulescens* and *Porpidia melinodes*. Molecular Biology and Evolution 23(3): 574–586. https://doi.org/10.1093/molbev/msj063

Cáceres MES (2007) Corticolous crustose and microfoliose lichens of northeastern Brazil. Libri Botanici 22: 1–168.

Chernomor O, von Haeseler A, Minh BQ (2016) Terrace aware data structure for phylogenomic inference from supermatrices. Systematic Biology 65(6): 997–1008. https://doi.org/10.1093/sysbio/syw037

Culberson CF, Kristinsson H (1970) A standardized method for the identification of lichen products. Journal of Chromatography A 46: 85–93. https://doi.org/10.1016/S0021-9673(00)83967-9

Ekman S, Tønsberg T (2002) Most species of *Lepraria* and *Leproloma* form a monophyletic group closely related to *Stereocaulon*. Mycological Research 106(11): 1262–1276. https://doi.org/10.1017/S0953756202006718

Flakus A, Kukwa M (2007) New species and records of *Lepraria* (Stereocaulaceae, lichenized Ascomycota) from South America. Lichenologist 39(5): 463–474. https://doi.org/10.1017/S0024282907007116

Flakus A, Kukwa M (2009) *Lepraria glaucosorediata* sp. nov. (Stereocaulaceae, lichenized Ascomycota) and other interesting records of *Lepraria*. Mycotaxon 108(1): 353–364. https://doi.org/10.5248/108.353

Flakus A, Elix JA, Rodriguez P, Kukwa M (2011a) New species and records of *Lepraria* (Stereocaulaceae, lichenized Ascomycota) from South America. Lichenologist 43(1): 57–66. https://doi.org/10.1017/S0024282910000502

Flakus A, Oset M, Jabłońska A, Rodriguez Saavedra P, Kukwa M (2011b) Contribution to the knowledge of the lichen biota of Bolivia. 3. Polish Botanical Journal 56(2): 159–183.

Flakus A, Etayo J, Schiefelbein U, Ahti T, Jabłońska A, Oset M, Bach K, Rodriguez Saavedra P, Kukwa M (2012) Contribution to the knowledge of the lichen biota of Bolivia. 4. Polish Botanical Journal 7(2): 427–461.

Flakus A, Sipman HJM, Rodriguez Flakus P, Jabłońska A, Oset M, Meneses QRI, Kukwa M (2015) Contribution to the knowledge of the lichen biota of Bolivia. 7. Polish Botanical Journal 60(1): 81–98. https://doi.org/10.1515/pbj-2015-0001

Fryday AM, Øvstedal DO (2012) New species, combinations and records of lichenized fungi from the Falkland Islands (Islas Malvinas). Lichenologist 44(4): 483–500. https://doi.org/10.1017/S0024282912000163

Gardes M, Bruns TD (1993) ITS primers with enhanced specificity for basidiomycetes – application to the identification of mycorrhizae and rusts. Molecular Ecology 2(2): 113–118. https://doi.org/10.1111/j.1365-294X.1993.tb00005.x

Guzow-Krzemińska B (2006) Photobiont flexibility in the lichen *Protoparmeliopsis muralis* as revealed by ITS rDNA analyses. Lichenologist 38(5): 469–476. https://doi.org/10.1017/S0024282906005068

Guzow-Krzemińska B, Węgrzyn G (2000) Potential use of restriction analysis of PCR-amplified DNA fragments in taxonomy of lichens. Mycotaxon 76: 305–313.

Guzow-Krzemińska B, Malíček J, Tønsberg T, Oset M, Łubek A, Kukwa M (2017) *Lecanora stanislai*, a new, sterile, usnic acid containing lichen species from Eurasia and North America. Phytotaxa 329(3): 201–211. https://doi.org/10.11646/phytotaxa.329.3.1

Guzow-Krzemińska B, Jabłońska A, Flakus A, Rodriguez-Flakus P, Kosecka M, Kukwa M (2019a) Phylogenetic placement of *Lepraria cryptovouauxii* sp. nov. (Lecanorales, Lecanoromycetes, Ascomycota) with notes on other *Lepraria* species from South America. MycoKeys 53: 1–22. https://doi.org/10.3897/mycokeys.53.33508

Guzow-Krzemińska B, Flakus A, Kosecka M, Jabłońska A, Rodriguez-Flakus P, Kukwa M (2019b) New species and records of lichens from Bolivia. Phytotaxa 397(4): 257–279. https://doi.org/10.11646/phytotaxa.397.4.1

Helms G, Friedl T, Rambold G, Mayrhofer H (2001) Identification of photobionts from the lichen family Physciaceae using algal-specific ITS rDNA sequencing. Lichenologist 33(1): 73–86. https://doi.org/10.1006/lich.2000.0298

Hoang DT, Chernomor O, Von Haeseler A, Minh BQ, Vinh LS (2018) UFBoot2: Improving the ultrafast bootstrap approximation. Molecular Biology and Evolution 35(2): 518–522. https://doi.org/10.1093/molbev/msx281

Hodkinson BP, Lendemer JC (2013) Next-generation sequencing reveals sterile crustose lichen phylogeny. Mycosphere 4(6): 1028–1039. https://doi.org/10.5943/mycosphere/4/6/1

Huelsenbeck JP, Ronquist F (2001) MRBAYES: Bayesian inference of phylogeny. Bioinformatics 17(8): 754–755. https://doi.org/10.1093/bioinformatics/17.8.754

Kalyaanamoorthy S, Minh BQ, Wong TKF, von Haeseler A, Jermiin LS (2017) ModelFinder: Fast model selection for accurate phylogenetic estimates. Nature Methods 14(6): 587–589. https://doi.org/10.1038/nmeth.4285

Kantvilas G, Kukwa M (2006) A new species of *Lepraria* (lichenized Ascomycetes) from Tasmania's wet forests. Muelleria 23: 3–6. https://doi.org/10.5962/p.291578

Katoh K, Standley DM (2013) MAFFT: multiple sequence alignment software version 7: improvements in performance and usability. Molecular Biology and Evolution 30(4): 772–780. https://doi.org/10.1093/molbev/mst010

Kistenich S, Timdal E, Bendiksby M, Ekman S (2018) Molecular systematics and character evolution in the lichen family Ramalinaceae (Ascomycota: Lecanorales). Taxon 67(5): 871–904. https://doi.org/10.12705/675.1

Kosecka M, Guzow-Krzemińska B, Černajová I, Škaloud P, Jabłońska A, Kukwa M (2021) New lineages of photobionts in Bolivian lichens expand our knowledge on habitat preferences and distribution of *Asterochloris* algae. Scientific Reports 11(1): e8701. https://doi.org/10.1038/s41598-021-88110-0

Kroken S, Taylor JW (2001) A gene genealogical approach to recognize phylogenetic species boundaries in the lichenized fungus *Letharia*. Mycologia 93(1): 38–53. https://doi.org/10.1080/00275514.2001.12061278

Kukwa M (2002) Taxonomic notes on the lichen genera *Lepraria* and *Leproloma*. Annales Botanici Fennici 39: 225–226.

Kukwa M (2006) Notes on taxonomy and distribution of the lichen species *Lepraria ecorticata* comb. nov. Mycotaxon 97: 63–66.

Kukwa M (2019) *Lepraria juanfernandezii*, a new lichen species from the Southern Hemisphere. Plant and Fungal Systematics 64(2): 233–235. https://doi.org/10.2478/pfs-2019-0019

Kukwa M, Pérez-Ortega S (2010) A second species of *Botryolepraria* from the Neotropics and the phylogenetic placement of the genus within Ascomycota. Mycological Progress 9(3): 345–351. https://doi.org/10.1007/s11557-009-0642-0

Landan G, Graur D (2008) Local reliability measures from sets of co-optimal multiple sequence alignments. Pacific Symposium on Biocomputing 13: 15–24.

Laundon JR (1989) The species of *Leproloma*-the name for the *Lepraria membranacea* group. Lichenologist 21(1): 1–22. https://doi.org/10.1017/S0024282989000034

Laundon JR (1992) *Lepraria* in the British Isles. Lichenologist 24(4): 315–350. https://doi.org/10.1017/S002428299200046X

Lendemer JC (2011a) A taxonomic revision of the North American species of *Lepraria* s.l. that produce divaricatic acid, with notes on the type species of the genus *L. incana*. Mycologia 103(6): 1216–1229. https://doi.org/10.3852/11-032

Lendemer JC (2011b) A standardized morphological terminology and descriptive scheme for *Lepraria* (Stereocaulaceae). Lichenologist 43(5): 379–399. https://doi.org/10.1017/S0024282911000326

Lendemer JC (2012) Perspectives on chemotaxonomy: Molecular data confirm the existence of two morphologically distinct species within a chemically defined *Lepraria caesiella* (Stereocaulaceae). Castanea 77(1): 89–105. https://doi.org/10.2179/11-042

Lendemer JC (2013a) A monograph of the crustose members of the genus *Lepraria* Ach. s. str. (Stereocaulaceae, Lichenized Ascomycetes) in North America north of Mexico. Opuscula Philolichenum 12(1): 27–141.

Lendemer JC (2013b) Shifting paradigms in the taxonomy of lichenized fungi: Molecular phylogenetic evidence corroborates morphology but not chemistry in the *Lepraria neglecta* group. Memoirs of the New York Botanical Garden 108: 127–153.

Lendemer JC, Hodkinson BP (2013) A radical shift in the taxonomy of *Lepraria* s.l.: Molecular and morphological studies shed new light on the evolution of asexuality and lichen growth form diversification. Mycologia 105(4): 994–1018. https://doi.org/10.3852/12-338

Liu YJ, Whelen S, Hall BD (1999) Phylogenetic relationships among ascomycetes: Evidence from an RNA Polymerase II Subunit. Molecular Biology and Evolution 16(12): 1799–1808. https://doi.org/10.1093/oxfordjournals.molbev.a026092

Lücking R, Hodkinson BP, Leavitt SD (2017 [2016]) The 2016 classification of lichenized fungi in the Ascomycota and Basidiomycota – Approaching one thousand genera. The Bryologist 119(4): 361–416. https://doi.org/10.1639/0007-2745-119.4.361

Lumbsch HT, Ahti T, Altermann S, Amo De Paz G, Aptroot A, Arup U, Bárcenas Peña A, Bawingan PA, Benatti MN, Betancourt L, Björk CR, Boonpragob K, Brand M, Bungartz F, Cáceres MES, Candan M, Chaves JL, Clerc P, Common R, Coppins BJ, Crespo A, Dal-Forno M, Divakar PK, Duya MV, Elix JA, Elvebakk A, Fankhauser JD, Farkas E, Itatí Ferraro L, Fischer E, Galloway DJ, Gaya E, Giralt M, Goward T, Grube M, Hafellner J, Hernández M JE, Herrera Campos MA, Kalb K, Kärnefelt I, Kantvilas G, Killmann D, Kirika P, Knudsen K, Komposch H, Kondratyuk S, Lawrey JD, Mangold A, Marcelli MP, McCune B, Messuti MI, Michlig A, Miranda González R, Moncada B, Naikatini A, Nelsen MP, Øvstedal DO, Palice Z, Papong K, Parnmen S, Pérez-Ortega S, Printzen C, Rico VJ, Rivas Plata E, Robayo J, Rosabal D, Ruprecht U, Salazar Allen N, Sancho L, Santos De Jesus L, Santos Vieira T, Schultz M, Seaward MRD, Sérusiaux E, Schmitt I, Sipman HJM, Sohrabi M, Søchting U, Søgaard MZ, Sparrius LB, Spielmann A, Spribille T, Sutjaritturakan J, Thammathaworn A, Thell A, Thor G, Thüs H, Timdal E, Truong C, Türk R, Umaña Tenorio L, Upreti, DK van den Boom P, Vivas Rebuelta M, Wedin M, Will-Wolf S, Wirth V, Wirtz N, Yahr R, Yeshitela K, Ziemmeck F, Wheeler T, Lücking R (2011) One hundred new species of lichenized fungi: a signature of undiscovered global diversity. Phytotaxa 18: 1–127. https://doi.org/10.11646/phytotaxa.18.1.1

Malíček J, Palice Z, Vondrák J, Łubek A, Kukwa M (2018) *Bacidia albogranulosa* (Ramalinaceae, lichenized Ascomycota), a new sorediate lichen from European old-growth forests. MycoKeys 44: 51–62. https://doi.org/10.3897/mycokeys.44.30199

Miller MA, Pfeiffer W, Schwartz T (2010) Creating the CIPRES Science Gateway for inference of large phylogenetic trees. 2010 Gateway Computing Environments Workshop (GCE). 14 Nov. 2010. New Orleans Convention Center, New Orleans, 8 pp. https://doi.org/10.1109/GCE.2010.5676129

Nelsen MP, Lücking R, Mbatchou JS, Andrew CJ, Spielmann AA, Lumbsch TH (2011) New insights into relationships of lichen-forming Dothideomycetes. Fungal Diversity 51(1): 155–162. https://doi.org/10.1007/s13225-011-0144-7

Nguyen LT, Schmidt HA, Von Haeseler A, Minh BQ (2015) IQ-TREE: A fast and effective stochastic algorithm for estimating maximum-likelihood phylogenies. Molecular Biology and Evolution 32(1): 268–274. https://doi.org/10.1093/molbev/msu300

Orange A (2020) *Lithocalla* (Ascomycota, Lecanorales), a new genus of leprose lichens containing usnic acid. Lichenologist 52(6): 425–435. https://doi.org/10.1017/S0024282920000419

Orange A, James PW, White FJ (2001a) Microchemical Methods for the Identification of Lichens. British Lichen Society, London, 101 pp.

Orange A, Wolseley P, Karunaratne V, Bombuwala K (2001b) Two leprarioid lichens new to Sri Lanka. Bibliotheca Lichenologica 78: 327–333.

Penn O, Privman E, Ashkenazy H, Landan G, Graur D, Pupko T (2010) GUIDANCE: a web server for assessing alignment confidence scores. Nucleic Acids Research 38: W23–W28. https://doi.org/10.1093/nar/gkq443

Poelt J (1987) On the reduction of morphological structures in lichens. Bibliotheca Lichenologica 25: 35–45.

Rambaut A (2009) FigTree ver. 1.4.3. http://tree.bio.ed.ac.uk/software/figtree [Accessed 4 Oct. 2016]

Rambaut A, Drummond AJ, Xie D, Baele G, Suchard MA (2018) Posterior summarisation in Bayesian phylogenetics using Tracer 1.7. Systematic Biology 67(5): 901–904. https://doi.org/10.1093/sysbio/syy032

Ronquist F, Huelsenbeck JP (2003) MrBayes 3: Bayesian phylogenetic inference under mixed models. Bioinformatics 19(12): 1572–1574. https://doi.org/10.1093/bioinformatics/btg180

Saag L, Saag A, Randlane T (2009) World survey of the genus *Lepraria* (Stereocaulaceae, lichenized Ascomycota). Lichenologist 41(1): 25–60. https://doi.org/10.1017/S0024282909007993

Sela I, Ashkenazy H, Katoh K, Pupko T (2015) GUIDANCE2: accurate detection of unreliable alignment regions accounting for the uncertainty of multiple parameters. Nucleic Acids Research 43: W7–W14. https://doi.org/10.1093/nar/gkv318

Sipman HJM (2004) Survey of *Lepraria* species with lobed thallus margins in the tropics. Herzogia 17: 23–35.

Sipman HJM (2018) Three new lichen species and 48 new records from Vanuatu. Australasian Lichenology 82: 106–129.

Tønsberg T (1992) The sorediate and isidiate, corticolous, crustose lichens in Norway. Sommerfeltia 14(1): 1–331. https://doi.org/10.2478/som-1992-0002

van den Boom P, Magain N (2020) Three new lichen species from Macaronesia belonging in Ramalinaceae, with the description of a new genus. Plant and Fungal Systematics 65(1): 167–175. https://doi.org/10.35535/pfsyst-2020-0011

Vilgalys R, Hester M (1990) Rapid genetic identification and mapping of enzymatically amplified ribosomal DNA from several *Cryptococcus* species. Journal of Bacteriology 172(8): 4238–4246. https://doi.org/10.1128/jb.172.8.4238-4246.1990

Wijayawardene NN, Hyde KD, Rajeshkumar KC, Hawksworth DL, Madrid H, Kirk PM, Braun U, Singh RV, Crous PW, Kukwa M, Lücking R, Kurtzman CP, Yurkov A, Haelewaters D, Aptroot A, Lumbsch HT, Timdal E, Ertz D, Etayo J, Phillips AJL, Groenewald JZ, Papizadeh M, Selbmann L, Dayarathne MC, Weerakoon G, Jones EBG, Suetrong S, Tian Q, Castañeda-Ruiz RF, Bahkali AH, Pang K-L, Tanaka K, Qin DD, Sakayaroj J, Hujslová M, Lombard L, Shenoy BD, Suija A, Maharachchikumbura SSN, Thambugala KM, Wanasinghe DN, Sharma BO, Gaikwad S, Pandit G, Zucconi L, Onofri S, Egidi E, Raja HA, Kodsueb R, Cáceres MES, Pérez-Ortega S, Fiuza PO, Monteiro SJ, Vasilyeva LN, Shivas RG, Prieto M, Wedin M, Olariaga I, Lateef AA, Agrawal Y, Fazeli SAS, Amoozegar MA, Zhao GZ, Pfliegler WP, Sharma G, Oset M, Abdel-Wahab MA, Takamatsu S, Bensch K, de Silva NI, De Kesel A, Karunarathna A, Boonmee S, Pfister DH, Lu Y-Z, Luo Z-L, Boonyuen N, Daranagama DA, Senanayake IC, Jayasiri SC, Samarakoon MC, Zeng X-Y,

Doilom M, Quijada L, Rampadarath S, Heredia G, Dissanayake AJ, Jayawardana RS, Perera RH, Tang LZ, Phukhamsakda C, Hernández-Restrepo M, Ma X, Tibpromma S, Gusmao LFP, Weerahewa D, Karunarathna SC (2017) Notes for genera: Ascomycota. Fungal Diversity 86(1): 1–594. https://doi.org/10.1007/s13225-017-0386-0

Zoller S, Scheidegger C, Sperisen C (1999) PCR primers for the amplification of mitochondrial small subunit ribosomal DNA of lichen-forming ascomycetes. Lichenologist 31(5): 511–516. https://doi.org/10.1006/lich.1999.0220

Supplementary material 1

The PCR parameters

Authors: Beata Guzow-Krzemińska, Magdalena Kosecka

Data type: PCR parameters (word document)

Explanation note: The PCR parameters are presented for each marker.

Link: https://doi.org/10.3897/mycokeys.96.98029.suppl1

MycoKeys 96: 113–126 (2023)
doi: 10.3897/mycokeys.96.100621
https://mycokeys.pensoft.net

RESEARCH ARTICLE

A peer-reviewed open-access journal
MycoKeys
Launched to accelerate biodiversity research

Two new species of *Scolecobasidium* (Venturiales, Sympoventuriaceae) associated with true mangrove plants and *S. terrestre* comb. nov.

Shuang Song[1,2], Meng Li[1], Jun-En Huang[1,2], Fang Liu[1,2]

1 *State Key Laboratory of Mycology, Institute of Microbiology, Chinese Academy of Sciences, Beijing, 100101, China* **2** *University of Chinese Academy of Sciences, Beijing, 100049, China*

Corresponding author: Fang Liu (liufang@im.ac.cn)

Academic editor: Huzefa Raja | Received 15 January 2023 | Accepted 6 March 2023 | Published 29 March 2023

Citation: Song S, Li M, Huang J-E, Liu F (2023) Two new species of *Scolecobasidium* (Venturiales, Sympoventuriaceae) associated with true mangrove plants and *S. terrestre* comb. nov. MycoKeys 96: 113–126. https://doi.org/10.3897/mycokeys.96.100621

Abstract

Scolecobasidium is cosmopolitan and includes species that inhabit a wide range of ecosystems including soil, water, air, plant and cold-blooded vertebrates. During a fungal survey from mangrove, strains of *Scolecobasidium* occurring on leaf spots of true mangrove plants, *Aegiceras corniculatum* and *Acanthus ebracteatus*, were isolated from Futian Mangrove in Shenzhen and the Qi'ao-Dangan Island Mangrove in Zhuhai, China. Unlike most species in *Scolecobasidium* that produce dark conidia, our strains are characterized by hyaline to pale brown conidia and inconspicuous thread-like sterigmata. Further detailed morphological comparison and multi-locus (LSU, ITS, *tub2*, *tef1-α*) phylogenetic analyses revealed these collections as two new taxa, namely *S. acanthi* **sp. nov.** and *S. aegiceratis* **sp. nov.** We further emend the generic description of *Scolecobasidium*, propose one new combination, *S. terrestre* comb. nov., and clarify the taxonomic status of *S. constrictum*.

Keywords

Mangrove, phylogeny, plant pathogen, taxonomy

Introduction

Scolecobasidium was described based on two species, *S. terreum* and *S. constrictum*, with the former as the generic type (Abbott 1927). This genus is slow-growing, and characterized by brownish to black colonies, reduced, hyaline or pigmented conidiophores and septate, smooth- or rough-walled, brown, single, dry and rhexolytic conidia

(Abbott 1927; Barron and Busch 1962; Seifert and Gams 2011). A distinguishing feature of *Scolecobasidium* from other genera is the conidiophores, which are born on aerial hyphae as short non-septate structures producing conidia from the ends of thread-like sterigmata (Abbott 1927). Subsequently, more species with unbranched conidia were described in *Scolecobasidium* and the conidia of this genus are found to be variable in shape, especially its type species *S. terreum* producing Y-shaped or T-shaped conidia distinct from other species in the genus. Therefore, Hoog and von Arx (1973) introduced a separate genus *Ochroconis*, typified by *O. constricta* (syn. *S. constrictum*), and transferred many *Scolecobasidium* species into this genus (De Hoog 1973). At that time, *Ochroconis* was comprised of species with sympodial conidiogenesis and ellipsoidal, clavate or fusiform conidia, whereas the genus *Scolecobasidium* was restricted to species with T- or Y-shaped or bilobed, 1- or multiple septate conidia born on ampulliform conidiogenous cells possessing 1–3 conidial-containing denticles at the tip of the conidiophores (De Hoog 1973). Subsequently, Ellis (1976) classified *Ochroconis* as a synonym of *Scolecobasidium*, and Gams (2015) and Seifert and Gams (2011) agreed with this interpretation. In addition to the similar morphological characteristics of *Scolecobasidium* and *Ochroconis*, recent molecular analyses have clearly shown that the two genera constituted a polyphyletic complex and *Ochroconis* should not be treated as a separate genus (Hao et al. 2012; Samerpitak et al. 2014). Although the ex-type strains of both *S. terreum* (CBS 203.27) and *O. constricta* (CBS 202.27) are sterile after a long period of preservation, they were phylogenetically placed within the *Scolecobasidium* clade (Shen et al. 2020). Therefore, based on the principle of priority, the older generic name *Scolecobasidium* was chosen over *Ochroconis*, and 25 new combinations have been proposed (Shen et al. 2020; Crous et al. 2021; Wei et al. 2022).

Scolecobasidium is the largest genus within *Sympoventuriaceae*, *Venturiales*, *Dothideomycetes* (Shen et al. 2020) and about 98 epithets are currently listed in Index Fungorum (Index Fungorum accession date: 10.01.2023). *Scolecobasidium* is a cosmopolitan genus of saprotrophic soil hyphomycetes, some of which are also parasitic on plants (De Hoog 1985; Crous et al. 2016), human (Giraldo et al. 2014), fish (Ross and Yasutake 1973) or other animals (VanSteenhouse et al. 1988; Singh et al. 2006). In our study, during the fungal investigations of mangrove plants in China, several strains of *Scolecobasidium* were isolated from leaf spots on *Aegiceras corniculatum* and *Acanthus ebracteatus*, and they were revealed as two novel species through polyphasic analyses. In addition, on the basis of Shen et al. (2020) and Wei et al. (2022), we correct the taxonomic status of ambiguous species in this group.

Materials and methods

Sample collection and fungal isolation

During our fungal investigations on mangrove plants in China, 90 strains of 48 species have been isolated from true mangrove plants, *Acanthus ebracteatus* and *Aegiceras corniculatum* (Table 1). Among them, *Scolecobasidium*-like strains piqued our interest

Table 1. Pathogens and endophytes associated with true mangrove plant *Acanthus ebracteatus* and *Aegiceras corniculatum*.

Strains No.	Fungus species	Host plant	Remark
SS1	*Acrocalymma medicaginis*	*Ac. ebracteatus*	Pathogen
ds0003, SS2012, SS2094, SS2108, SS2009, SS2017, SS2096, SS2103	*Alternaria angustiovoidea*	*Ac. ebracteatus*	Endophyte
SS2047	*Arthrinium xenocordella*	*Ae. corniculatum*	Endophyte
ds0016	*Cercospora beticola*	*Ae. corniculatum*	Endophyte
SS2097, SS27	*Cladosporium austrohemisphaericum*	*Ae. corniculatum*	Endophyte
ds1001, ds1030, SS10	*Cladosporium cladosporioides*	*Ae. corniculatum*	Pathogen
SS2010	*Cladosporium colombiae*	*Ae. corniculatum*	Endophyte
ds0017, ds1043, ds1032, ds1042	*Cladosporium dominicanum*	*Ae. corniculatum*	Endophyte
SS8, SS42	*Cladosporium oryzae*	*Ac. ebracteatus*	Pathogen
SS2110	*Cladosporium rugulovarians*	*Ae. corniculatum*	Endophyte
ds1038-2	*Cladosporium sphaerospermum*	*Ae. corniculatum*	Pathogen
SS28	*Cladosporium tenuissimum*	*Ac. ebracteatus*	Pathogen
ds0011	*Colletotrichum gigasporum* complex	*Ac. ebracteatus*	Endophyte
SS2109, SS2046	*Cytospora* sp. nov.	*Ae. corniculatum*	Endophyte
SS2107	*Diaporthe hongkongensis*	*Ae. corniculatum*	Endophyte
SS2041	*Diaporthe perseae*	*Ae. corniculatum*	Endophyte
ds1038, SS2106	*Fusarium incarnatum*	*Ae. corniculatum*	Pathogen
ds1018	*Fusarium luffae*	*Ae. corniculatum*	Pathogen
SS14	*Fusarium solani*	*Ae. corniculatum*	Pathogen
ds1045	*Halorosellinia* sp. nov.	*Ae. corniculatum*	Pathogen
ds0021, ds0022	*Halorosellinia xylocarpi*	*Ac. ebracteatus*	Endophyte
ds1093, ds1094, ds1095	*Hortaea werneckii*	*Ae. corniculatum*	Pathogen
ds1044	*Hypocreales* sp. nov.	*Ae. corniculatum*	Pathogen
SS29	*Nemania* sp. nov.	*Ae. corniculatum*	Endophyte
ds1087	*Neodevriesia tabebuiae*	*Ae. corniculatum*	Pathogen
SS2015, SS2045, SS2100, ds1062, ds1075	*Neofusicoccum kwambonambiense*	*Ae. corniculatum*	Endophyte
ds1060	*Neopestalotiopsis eucalypticola*	*Ae. corniculatum*	Pathogen
ds1020	*Neopestalotiopsis phangngaensis*	*Ae. corniculatum*	Pathogen
ds1061	*Neopestalotiopsis* sp. nov.	*Ae. corniculatum*	Pathogen
SS2092	*Nigrospora oryzae*	*Ae. corniculatum*	Endophyte
ds1025	*Occultifur* sp. nov.	*Ac. ebracteatus*	Pathogen
SS2069, SS2038, SS2067, SS2068	*Penicillium brevicompactum*	*Ac. ebracteatus*	Endophyte
SS2051, SS2048, SS2052, SS2056, SS2058, SS2066, SS2077, SS2081, SS2083	*Penicillium chrysogenum*	*Ae. corniculatum*	Endophyte
SS2087	*Penicillium coffeae*	*Ae. corniculatum*	Endophyte
ds1019	*Pestalotiopsis kandelicola*	*Ae. corniculatum*	Pathogen
SS2011	*Phyllosticta capitalensis*	*Ac. ebracteatus*	Endophyte
ds1081	*Phyllosticta* sp. nov.	*Ae. corniculatum*	Pathogen
SS20	*Pseudopestalotiopsis chinensis*	*Ae. corniculatum*	Pathogen
ds1028	*Rhodotorula sphaerocarpa*	*Ac. ebracteatus*	Pathogen
ds1031	*Roussoella mediterranea*	*Ae. corniculatum*	Pathogen
LC19368	*Scolecobasidium acanthi* sp. nov.	*Ac. ebracteatus*	Pathogen
LC19369, LC19370	*Scolecobasidium aegiceratis* sp. nov.	*Ae. corniculatum*	Pathogen
SS2089	*Stemphylium solani*	*Ae. corniculatum*	Endophyte
ds1100	*Symmetrospora marina*	*Ae. corniculatum*	Pathogen
ds1084	*Thyridium pluriloculosum*	*Ae. corniculatum*	Pathogen
SS2044	*Tricharina ochroleuca*	*Ac. ebracteatus*	Endophyte
SS2040, SS2043	*Trichoderma harzianum*	*Ae. corniculatum*	Endophyte
ds1086, ds1026, ds1027, ds1079, ds1082, ds1026-2, ds1037	*Zasmidium anthuriicola*	*Ae. corniculatum*	Pathogen

because their unique characters differed from known species and were further studied herein. Type specimens made from ex-type strains of the novel species were preserved in the Fungarium (**HMAS**), Institute of Microbiology, CAS, and the living cultures

were preserved in the China General Microbiological Culture Collection Center (**CGMCC**) and LC culture collection (personal culture collection of Lei Cai housed in the Institute of Microbiology, Chinese Academy of Sciences).

Morphological observations

Colony features including color and growth rate were recorded for the strains grown on oatmeal agar (OA) and malt extract agar (MEA) after 14 days at 25 °C. To enhance sporulation, strains were incubated at 25 °C under near UV light with a 12 h photoperiod for 14 d or longer period. Morphological observations of reproductive structures were made in lactic acid and observed using a Nikon Eclipse 80i microscope using differential interference contrast (DIC) illumination. At least 30 measurements per structure were taken, and the mean value, standard deviation, and minimum–maximum values were given.

DNA extraction, PCR amplification and sequencing

Fresh fungal mycelia grown on potato dextrose agar (PDA) for 14 d at 25 °C were scraped from the colony margin and used for genomic DNA extraction using a modified CTAB protocol as described previously (Guo et al. 2000). Genomic DNA was diluted to 1 ng/μL using sterile water as the template for PCR. The amplification of internal transcribed spacer (ITS) region including the flanking 5.8S rRNA gene, was carried using the primer pairs ITS1 and ITS4 (White, Bruns, Lee, Taylor, 1990), the 28S nuclear large subunit (nuLSU) with LR0R/LR5 (White, Bruns, Lee, Taylor, 1990), with EF1-728F/EF-2 (Qiao et al. 2016) for the partial translation elongation factor 1-alpha gene (*tef1-α*) and Bt2a/Bt2b to amplify the partial beta-tubulin gene (*tub2*) (Glass and Donaldson 1995), respectively. The reaction volume of 25 μL consisted of 10× PCR buffer 2.5 μL, $MgCl_2$ 2 mM, dNTPs 50 μm/L, forward and reverse primers 0.1 μm/L, DNA polymerase 0.5 U, and DNA template 10 ng. PCR amplification reactions for LSU and ITS were performed as follows: pre-denaturation at 95 °C for 10 min, followed by 35 cycles of denaturation at 95 °C for 45 s, annealing at 52 °C for 45 s, extension at 72 °C for 1 min, and a final extension step at 72 °C for 10 min, but the annealing temperature was adjusted to 56 °C for *tef1-α* and *tub2*. PCR products were detected by 1% agarose gel electrophoresis and then sequenced by SinoGenoMax. MEGA v. 7 was used to obtain consensus sequences from DNA data generated from forward and reverse primers.

Phylogenetic analyses

Phylogenetic analysis was performed using sequences of LSU, ITS, *tub2*, and *tef1-α* from 64 type and reference strains of *Ochroconis*, *Scolecobasidium* and one outgroup *Verruconis calidifluminalis* CBS 125818 (Table 2). Single locus alignment was performed using an online version of MAFFT v. 7 (Katoh and Standley 2013) and then concatenated for Maximum Likelihood (ML) and Bayesian analysis (BA). ML and BA were implemented

Table 2. Strains used in the phylogenetic analysis of *Scolecobasidium* and GenBank accession numbers.

Species	Strain[a]	Genbank accession numbers[b]			
		ITS	LSU	*tub2*	*tef1*
S. acanthi	**CGMCC 3.24352 = LC19368^T**	**OQ448957**	**OQ448949**	**OQ442218**	**OQ442215**
S. aegiceratis	**CGMCC 3.24353 = LC19369^T**	**OQ448958**	**OQ448950**	**OQ442219**	**OQ442216**
S. aegiceratis	**CGMCC 3.24354 = LC1937**0	**OQ448959**	**OQ448951**	**OQ442220**	**OQ442217**
S. ailanthi	MFLU 18-2110	MK347731	–	MK412881	–
S. ailanthi	MFLUCC 17-0923^T	MK347730	MK347947	MK412883	–
S. anellii	CBS 284.64^T	FR832477	KF156138	KF156184	KF155995
S. anomalum	CBS 131816^T	HE575201	KF156137	KF156194	KF155986
S. aquaticum	CBS 140316^T	KX668258	KX668259	–	–
S. bacilliforme	CBS 100442^T	KP798632	KP798635	KT272059	KT272070
S. blechni	CBS 146055^T	MN562134	MN567641	MN556843	MN556826
S. camellicola	GUCC 18242^T	MZ503728	MZ503761	MZ546907	MZ546874
S. capsici	CBS 142096^T	KY173427	KY173518	–	–
S. constrictum	CBS 202.27^T	MH854929	MH866423	KF156161	KF156003
S. cordanae	CBS 412.51	HQ667540	KF156123	KF156200	KF155980
S. cordanae	CBS 475.80^T	KF156022	KF156122	KF156197	KF155981
S. crassihumicola	CBS 120700	KJ867429	KJ867430	KJ867433	KJ867428
S. dracaenae	CBS 141323^T	KX228283	KX228334	–	KX228377
S. echinulatum	GUCC 18247^T	MZ503733	MZ503766	MZ546912	MZ546879
S. echinulatum	GUCC 18248	MZ503734	MZ503767	MZ546913	MZ546880
S. ellipsoideum	CBS 131796^T	MN077367	–	–	–
S. ellipsoideum	GUCC 18264	MZ503750	MZ503783	MZ546929	MZ546896
S. ferulica	IRAN3232C^T	MF186874	MH400207	–	–
S. gamsii	CBS 239.78^T	KF156019	KF156150	KF156190	KF155982
S. globale	CBS 119644^T	KF961086	KF961097	KF961065	KF961075
S. globale	CBS 135924	KF961092	KF961104	KF961070	KF961079
S. guangxiensis	SS23^T	MK934570	MK956169	–	–
S. guangxiensis	X22	MK961215	MK961247	–	–
S. helicteris	NFCCI 4310^T	MK014833	–	MK321318	–
S. humicola	CBS 116655^T	HQ667521	KF156124	KF156195	KF155984
S. icarus	CBS 116645	HQ667525	–	LM644604	–
S. icarus	CBS 536.69^T	HQ667524	KF156132	KF156174	KF156009
S. lascauxense	CBS 131815^T	FR832474	KF156136	KF156183	KF155994
S. lascauxense	CBS 423.64	HQ667523	KF156131	KF156173	KF156008
S. leishanicola	GUCC 18259	MZ503745	MZ503778	MZ546924	MZ546891
S. leishanicola	HGUP1808^T	MK377301	MK377073	–	–
S. longiphorum	CBS 435.76^T	KF156038	KF156135	KF156182	KF155978
S. macrozamiae	CBS 137971^T	KJ869123	KJ869180	–	–
S. minimum	CBS 510.71^T	HQ667522	KF156134	KF156172	KF156007
S. mirabilis	CBS 413.51^T	HQ667536	KF156140	KF156164	KF156001
S. musae	CBS 729.95^T	KF156029	KF156144	KF156171	KF155999
S. musicola	CBS 144441^T	MH327824	MH327860	MH327898	MH327887
S. musicola	CPC 37308	MW063428	–	MW071116	MW071096
S. musicola	CPC 37309	MW063429	–	MW071117	MW071097
S. obovoideum	GUCC 18246^T	MZ503732	MZ503765	MZ546911	MZ546878
S. olivaceum	CBS 137170^T	LM644521	LM644564	LM644605	KT272067
S. pandanicola	CBS 140660^T	KT950850	KT950864	–	–
S. phaeophorum	CBS 206.96^T	KP798631	KP798634	KT272062	KT272098
S. podocarpi	CBS 143174^T	MG386032	MG386085	–	–
S. podocarpicola	CBS 146057^T	MN562138	MN567645	–	–
S. ramosum	CBS 137171	LM644522	LM644565	LM644606	KT272068
S. ramosum	CBS 137173^T	LM644524	LM644567	MZ546928	KT272069
S. robustum	CBS 112.97^T	KP798633	KP798636	KT272060	KT272071
S. sexuale	CBS 131965	KF156017	KF156119	KF156188	KF155977
S. sexuale	CBS 135765^T	KF156018	KF156118	KF156189	KF155976
S. spiralihyphum	GUCC 18245^T	MZ503731	MZ503764	MZ546910	MZ546877

Species	Strain[a]	Genbank accession numbers[b]			
		ITS	LSU	*tub2*	*tef1*
S. terrestre	CBS 211.53^{T}	NR_145365	NG_058014	KF156187	KF156005
S. terreum	CBS 203.27^{T}	HQ667544	–	HQ877665	–
S. tshawytschae	CBS 100438^{T}	HQ667562	KF156126	KF156180	KF155990
S. tshawytschae	CBS 228.66	KF156016	KF156128	KF156179	KF155992
S. variabile	NBRC 32268	DQ307334	EU107310	–	DQ307356
S. verrucaria	GUCC 18240^{T}	MZ503726	MZ503759	MZ546905	MZ546872
S. verrucosum	CBS 383.81^{T}	KF156015	KF156129	KF156185	KT272099
S. zunyiense	GUCC 18241^{T}	MZ503727	MZ503760	MZ546906	MZ546873
V. calidifluminalis	CBS 125818^{T}	AB385698	KF156108	KF156202	KF155959

Notes: [a]T refers to ex-type strains. [b]Bold indicates the sequences generated in this study. –, not applicable. **CBS**: Westerdijk Fungal Biodiversity Institute, Utrecht, the Netherlands; **CPC:** Culture collection of Pedro Crous, housed at Westerdijk Fungal Biodiversity Institute; **CGMCC**: Chinese General Microbiological Culture Collection Center, Beijing, China; **LC:** personal culture collection of Lei Cai housed in the Institute of Microbiology, Chinese Academy of Sciences; **GUCC**: Culture Collection of the Department of Plant Pathology, Agriculture College, Guizhou University, China; **HGUP**: Herbarium of the Department of Plant Pathology, Agricultural College, Guizhou University, China; **IRAN**: Fungal Culture Collections of the Iranian Research Institute of Plant Protection; **MFLU (CC)**: Mae Fah Luang University Culture Collection, Chiang Ria, Thailand; **NFCCI**: National Fungal Culture Collection of India, Pune, India; **NBRC**: Biological Resource Center.

using RAxML-HPC BlackBox v. 8.2.12 and MrBayes v. 3.2.7a, respectively, in the CIPRES Science Gateway portal (https://www.phylo.org/; Miller et al. 2010). For ML analysis, GTR+GAMMA substitution model with 1,000 bootstrap iterations was set. For BA, MrModeltest v. 2.4 (Guindon and Gascuel 2003; Matic et al. 2012) was firstly used to determine the best evolutionary model for each locus. Bayesian analysis was computed with four simultaneous Markov Chain Monte Carlo chains, 10,000,000 generations, and a sampling frequency of 1,000 generations, ending the run automatically when standard deviation of split frequencies fell below 0.01. The burn-in fraction was set to 0.25, after which the 50% majority rule consensus trees and posterior probability (PP) values were calculated. The resulting trees were plotted using FigTree v. 1.4.4 (http://tree.bio.ed.ac.uk/software/figtree) and the layout was edited in Adobe Illustrator 2020. Newly obtained sequences in this study are submitted to GenBank. New descriptions and nomenclature were deposited in MycoBank (www.MycoBank.org) (Crous et al. 2014).

Results

Phylogeny

The BLAST searches in the NCBI's GenBank nucleotide database using ITS sequences of LC19368, LC19369 and LC19370 showed their closest similarities to *Scolecobasidium* spp. In the following multi-locus phylogenetic analysis of *Scolecobasidium*, the dataset comprised 2,932 characters including alignment gaps (LSU: 855 bp, ITS: 818 bp, *tub2*: 542 bp, *tef1*-α: 717 bp). The ML search revealed a best tree with an InL of -34731.383727. For the Bayesian inference, a GTR+I+G model was selected for ITS, LSU, *tef1*-α and *tub2*. The BA was run for 1,535,000 generations, and a 50% consensus tree and posterior probabilities were calculated from 2,304 trees from two runs. The topologies of phylogenetic trees generated by ML and BA were congruent. Our strains were separated into two distinct clades from all known species of *Scolecobasidium* (Fig. 1).

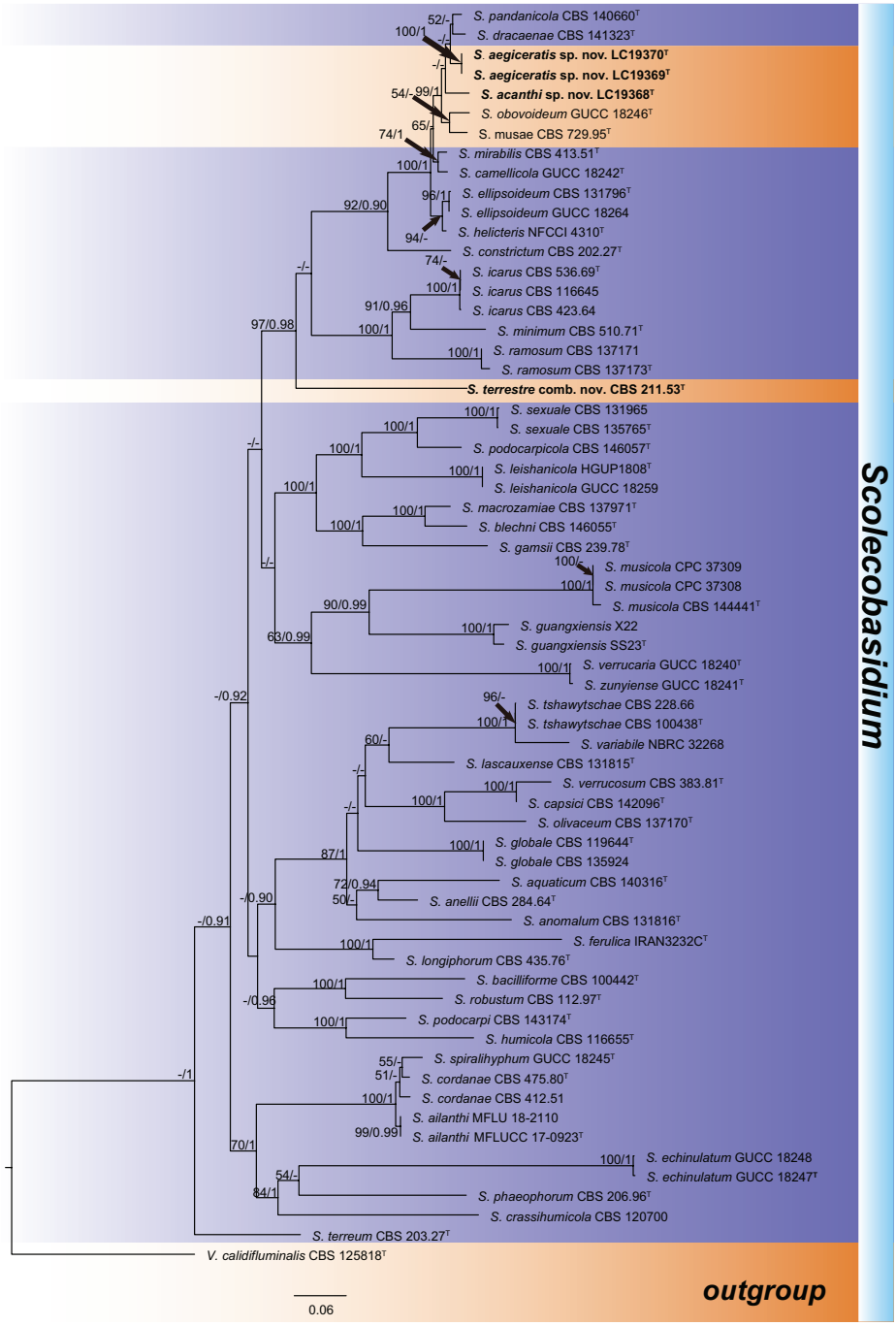

Figure 1. Phylogenetic tree of *Scolecobasidium* calculated with a maximum likelihood analysis of the combined ITS, LSU, *tef1-α*, and *tub2* sequences alignment. The tree was rooted with *Verruconis calidifluminalis* (CBS 125818). Bootstrap values (ML > 50%) and Bayesian posterior probabilities (PP > 0.90) are shown at the nodes in the order of ML/PP. T indicates ex-type strains. The novel taxa and new combination are showed in bold. The scale bar represents the expected changes per site.

Taxonomy

Scolecobasidium **E.V. Abbott, Mycologia 19: 30. 1927. emend. F. Liu**

Ochroconis de Hoog & Arx, Kavaka 1: 57. 1974 [1973]. Synonym.

Description. ***Colonies*** restricted, slow-growing, brown or olivaceous. ***Aerial hyphae*** smooth- or somewhat rough-walled, pigmented. ***Cleistothecia*** up to 40 μm in diam, dark brown; peridium wall composed of textura angularis. ***Ascomata*** bearing antler-shaped appendages, with serrate edges. ***Asci*** bitunicate, clavate, 8-spored; ascospores pale brown, verruculose, 1–3-septate. ***Conidiophores*** reduced, unbranched or sparingly branched, arising from the aerial hyphae or hyphal ropes, continuous or septate, hyaline or pigmented, ovoid, clavate, wedge-shaped, cylindrical, or irregular. ***Conidiogenous cells*** scattered, monoblastic or sympodial, elongate to cylindrical. ***Conidia*** produced in clusters or acropetal series from the ends of tubular extensions of the conidiophores; conidia 1–4-celled, pigmented or hyaline, smooth or verrucose, ellipsoidal, ovoid, cylindrical, or T- or Y-shaped. (emended from Abbott 1927; Barron and Busch 1962; Seifert and Gams 2011; Samerpitak et al. 2014).

Notes. Abbott (1927) summarized the asexual features of *Scolecobasidium* as its generic character based on only two species *S. terreum* and *S. constrictum*. Over time multiple species of *Scolecobasidium* have been described, and the boundaries between this genus and closely related genera have also been clarified (Barron and Busch 1962; Seifert and Gams 2011; Samerpitak et al. 2014; Shen et al. 2020; Wei et al. 2022). However, no one has updated the generic character of *Scolecobasidium*. In this study, we update the generic character of *Scolecobasidium* based on previous descriptions, especially the morphological features of the sexual stage of the fungus.

Type species. *Scolecobasidium terreum* E.V. Abbott.

Scolecobasidium acanthi **S. Song, L. Cai & F. Liu, sp. nov.**
MycoBank No: 847639
Fig. 2

Etymology. Named after the host plant *Acanthus* from which this fungus was isolated.

Type. China. Guangdong Province: Qi'ao-Dangan Island Provincial Nature Reserve, from leaf of *Acanthus ebracteatus*, Nov 2019, M. Li, Z.F. Zhang and J.E. Huang (Holotype HMAS 352373, culture ex-type CGMCC 3.24352 = LC19368).

Description. ***Sexual morph*****:** unknown. ***Asexual morph*****:** Mycelium consisting of branched, septate, hyaline to pale brown, smooth, and thick-walled hyphae. ***Conidiophores*** solitary, erect, brown, smooth, arising from superficial hyphae, subcylindrical, straight to geniculous, brown, thick-walled, 0(–2)-septate, 14.5–20.5 × 1.5–2 μm, often reduced to conidiogenous cells, bearing a few conidia near the apex.

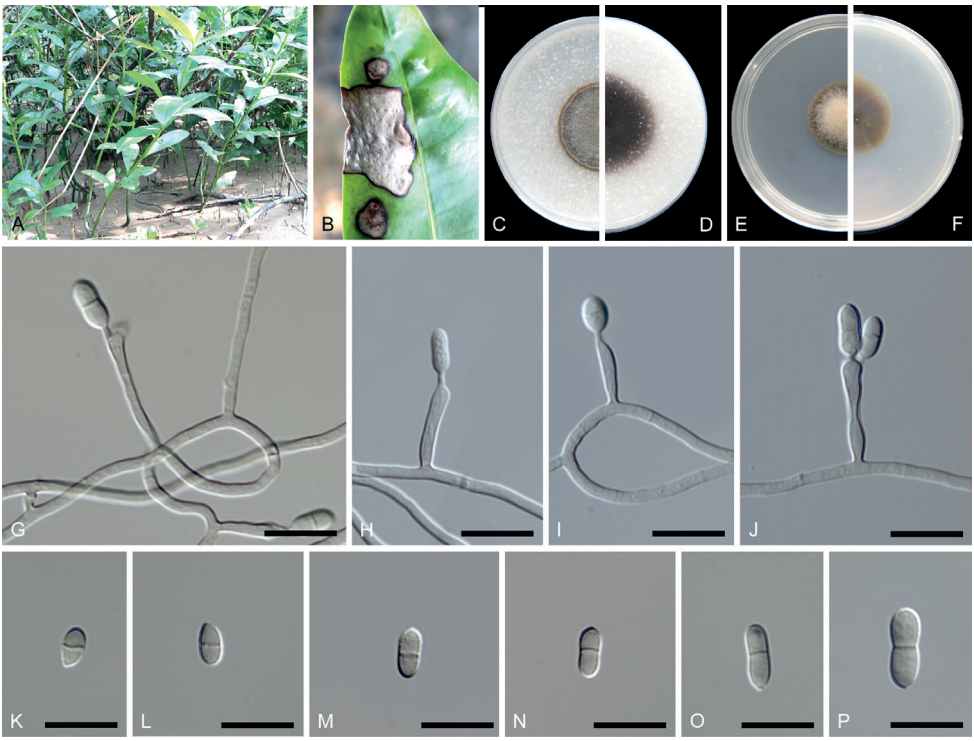

Figure 2. *Scolecobasidium acanthi* (ex-type CGMCC 3.24352) **A** the habitat of *Acanthus ebracteatus* **B** leaf spot on *Acanthus ebracteatus* **C, D** forward and reverse colony on OA after 14 days **E, F** forward and reverse colony on MEA after 14 days **G–J** conidiophores, conidiogenous cells and conidia **K–P** conidia. Scale bars: 10 μm (**G–P**).

Conidiogenous cells brown, smooth, 4.5–9.5 × 1.5–2 μm, terminal and lateral on conidiophores, containing several apical, cylindrical denticles. ***Conidia*** 1-septate, smooth-walled, subhyaline to pale brown, cylindrical, rarely pyriform, constricted at the septum, 5.5–8.5 × 2.5–4 μm (av. ± SD = 6.9 ± 0.7 × 3.05 ± 0.2 μm, n = 42).

Culture characteristics. Colonies reaching up to 16–20 mm diam after 14 days at 25 °C, producing dense aerial mycelium on MEA and OA. On MEA, surface wheat to greyish brown, reverse saddlebrown, felty, dry, margins smooth. On OA, surface burlywood to peru, reverse brown black, margins smooth.

Notes. Although represented by single strain, *S. acanthi* sp. nov. formed a distinct clade (Fig. 1) that was phylogenetically related to *S. aegiceratis* sp. nov. The two species differ from each other in 820/825 bp (99.39%) in LSU, 474/514 bp (92.22%) in ITS, 525/538 bp (97.58%) in *tef1-α*, and 433/464 bp (93.32%) in *tub2*. Morphologically, *S. acanthi* sp. nov. differs from *S. aegiceratis* sp. nov. in the septa number of conidiophores (0–2 vs. 0–1) and the size of conidiogenous cells (4.5–9.5 × 1.5–2 μm vs. 7.5–24 × 1.5–2.5 μm) and conidia (5.5–8.5 × 2.5–4 μm vs. 8–15(–26.5) × 2.5–3.5(–6.5) μm).

Scolecobasidium aegiceratis **S. Song, L. Cai & F. Liu, sp. nov.**
MycoBank No: 847640
Fig. 3

Etymology. Named after the host plant *Aegiceras* from which this fungus was isolated.

Type. China. Guangdong Province: Futian Mangrove National Nature Reserve, from leaf of *Aegiceras corniculatum*, July 2020, Z.F. Zhang (Holotype HMAS 352374, culture ex-type CGMCC 3.24353 = LC19369).

Other material examined. China. Guangdong Province: Futian Mangrove National Nature Reserve, from leaf of *Aegiceras corniculatum*, July 2020, Z.F. Zhang (Holotype HMAS 352375, culture ex-type CGMCC 3.24354 = LC19370).

Description. ***Sexual morph*****:** unknown. ***Asexual morph*****:** Mycelium consisting of branched, septate, hyaline to pale brown, smooth, and thick-walled hyphae. ***Conidiophores*** arising from the aerial hyphae or hyphal ropes, continuous or septate, usually reduced to conidiogenous cells, 0(–1)-septate. ***Conidiogenous cells*** solitary, hyaline to pale brown, smooth, subcylindrical, straight to geniculous-sinuous, thick-walled, 7.5–24 × 1.5–2.5 μm, bearing a few conidia near the apex. ***Conidia*** smooth-walled, subhyaline to pale brown, ellipsoidal or cylindrical, tapering torwards the base, mostly 1-septate, rarely 2–3-septate, sometimes constricted at the septum, 8–15(–26.5) × 2.5–3.5(–6.5) μm (av. ± SD = 9.3 ± 1.16 × 2.83 ± 0.26 μm, n = 40).

Culture characteristics. Colonies reaching up to 20–22 mm diam after 14 days at 25 °C, dense aerial mycelium on MEA and OA. On MEA, smooth to felty, dry, surface greyish brown to dark brown, reverse saddle brown. On OA, surface ivory to peru, reverse brown black.

Notes. *Scolecobasidium aegiceratis* is phylogenetically related to *S. dracaenae* (Fig. 1) and can be differentiated from the later by DNA sequences of LSU (99.52% similarity), ITS (93.55%) and *tef1-α* (96.60%) regions. Morphological characters of the two species are overlapping but their conidiophores and conidia show differences. *Scolecobasidium aegiceratis* can be distinguished from *S. dracaenae* as it produces hyaline to pale brown (vs. brown in *S. dracaenae*) conidiogenous cells. In addition, the dimensions of their conidia (8–15(–26.5) × 2.5–3.5(–6.5) μm vs. 6.5–10 × 3–4 μm) and conidiogenous cells (7.5–24 × 1.5–2.5 μm vs. 5–15 × 2.5–3 μm) are different (Crous et al. 2016).

Scolecobasidium constrictum **E.V. Abbott, Mycologia 19(1): 30. 1927.**

≡ *Ochroconis constricta* (E.V. Abbott) de Hoog & Arx, Kavaka 1: 57. 1974.
≡ *Dactylaria constricta* (E.V. Abbott) D.M. Dixon & Salkin, J. Clin. Microbiol. 24: 13. 1986.

Type. USA Louisiana, from soil, 1927, E.V. Abbott ex-type culture CBS 202.27 = MUCL 9471 (metabolically inactive).

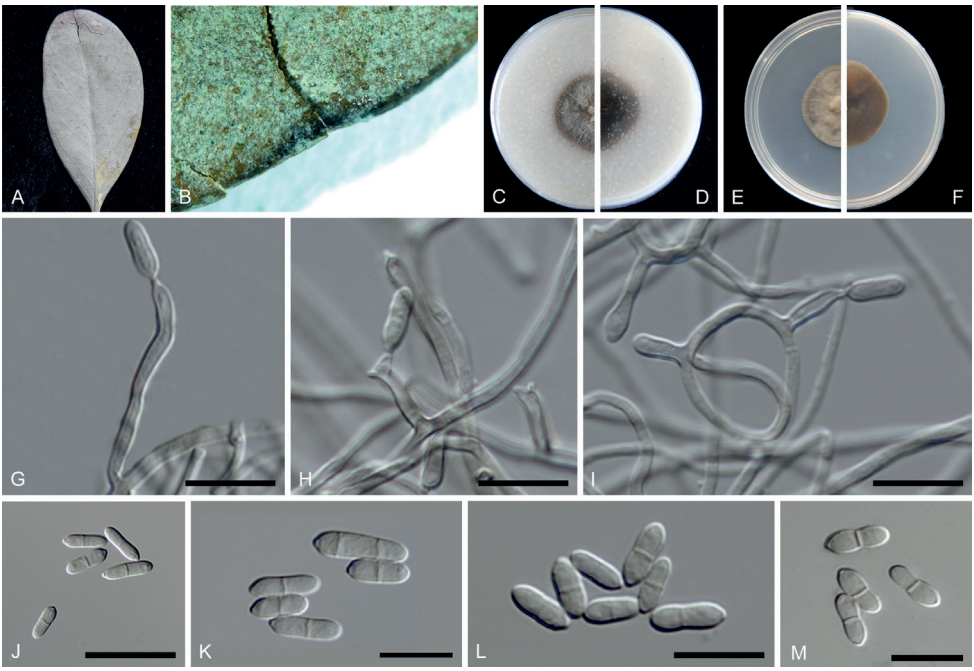

Figure 3. *Scolecobasidium aegiceratis* (ex-type CGMCC 3.24353) **A, B** leaf spots of *Aegiceras corniculatum* **C, D** forward and reverse colony on OA after 14 days **E, F** forward and reverse colony on MEA after 14 days **G–I** conidiophores, conidiogenous cells and conidia **J–M** conidia. Scale bars: 10 μm (**G–M**).

Notes. *Scolecobasidium constrictum* was introduced at the same time as the generic type of *Scolecobasidium*, *S. terreum*, by Abbott (1927). Later, *Heterosporium terrestre* was treated as a synonym of *S. constrictum* due to their similar morphological characteristics (Barron and Busch 1962). Their original descriptions differ, however, in that *H. terrestre* produces rough conidia and variable conidiophores both in shape and size, and has occasional phragmospores. Therefore, Barron (1962) thought that Abbott described only a facet of *S. constrictum* and emended the species description. Subsequently, *Ochroconis* was introduced to accommodate species with sympodial conidiogenesis and unbranched, subspherical to cylindrical or clavate, melanised conidia, and *S. constrictum* was transferred to this genus as *O. constricta* and designated as the generic type (De Hoog 1973).

With the help of molecular analyses, Shen et al. (2020) synonymized *Ochroconis* under *Scolecobasidium*, and *S. constrictum* should be resurrected as a result. We observed that the ex-type cultures of *H. terrestre* (CBS 211.53) and *S. constrictum* (CBS 202.27) were separated into two distinct clades with relatively long branches in the current study (Fig. 1) and sequences similarities between the two species were very low (LSU: 98.7%; ITS: 88%, *tef1*-α: 85%, *tub2*: 79%). Since *S. constrictum* (CBS 202.27) is now sterile (Shen et al. 2020), we could only make a detailed morphological comparison among multiple descriptions of ex-type cultures of *H. terrestre* (CBS 211.53)

and *S. constrictum* (CBS 202.27) (Abbott 1927; Atkinson 1952; Barron and Busch 1962; Samerpitak et al. 2014), and found that the two fungi were morphologically different in the shape (oval to ovate, short-cylindrical and long cylindrical to sole-shaped in *H. terrestre* vs. echinulate to verrucose in *S. constrictum*) and number of septa (0–3 vs. 0–1) in the conidia, as well as the size of conidiophores (2–31.5 × 1.5–2.5 μm vs. 5–8 × 2–2.5 μm). Based on morphology combined with the phylogeny, we consider that *H. terrestre* R.G. Atk. should not be treated as a synonym of *S. constrictum*, and a new combination *Scolecobasidium terrestre* comb. nov. is proposed in this study.

In addition, the type strain of *S. constrictum* should be CBS 202.27, rather than CBS 211.53, which was incorrectly listed in tables 2, 3 and figs 1, 2 in Wei et al. (2022).

Scolecobasidium terrestre **(R.G. Atk.) F. Liu, S. Song & L. Cai, comb. nov.**
MycoBank No: 847635

≡ *Heterosporium terrestre* R.G. Atk., Mycologia 44: 813. 1952.

Type. Canada. Ontario: Ancaster, obtained from soil obtained, isolated by R.G. Atkinson, 31 Oct. 1947, holotype DAOM 28282, ex-type culture CBS 211.53 (= ATCC 11419; DAOM 28282; IMI 051380; MUCL 9896).

Note. See the notes under *S. constrictum*.

Acknowledgements

Zhifeng Zhang is thanked for his help in sample collection. This work was supported by Science & Technology Fundamental Resources Investigation Program (Grant No. 2019FY100700), and the Youth Innovation Promotion Association of Chinese Academy of Sciences (2021085).

References

Abbott EV (1927) *Scolecobasidium*, a new genus of soil fungi. Mycologia 19(1): 29–31. https://doi.org/10.1080/00275514.1927.12020524

Atkinson RG (1952) A new species of *Heterosporium* from soil. Mycologia 44(6): 813–822. https://doi.org/10.1080/00275514.1952.12024239

Barron GL, Busch L (1962) Studies on the soil hyphomycete *Scolecobasidium*. Canadian Journal of Botany 40(1): 77–84. https://doi.org/10.1139/b62-009

Crous PW, Shivas RG, Quaedvlieg W, van der Bank M, Zhang Y, Summerell BA, Guarro J, Wingfield MJ, Wood AR, Alfenas AC, Braun U, Cano-Lira JF, García D, Marin-Felix Y, Alvarado P, Andrade JP, Armengol J, Assefa A, den Breeÿen A, Camele I, Cheewangkoon R, De Souza JT, Duong TA, Esteve-Raventós F, Fournier J, Frisullo S, García-Jiménez J,

Gardiennet A, Gené J, Hernández-Restrepo M, Hirooka Y, Hospenthal DR, King A, Lechat C, Lombard L, Mang SM, Marbach PAS, Marincowitz S, Marin-Felix Y, Montaño-Mata NJ, Moreno G, Perez CA, Pérez Sierra AM, Robertson JL, Roux J, Rubio E, Schumacher RK, Stchigel AM, Sutton DA, Tan YP, Thompson EH, Vanderlinde E, Walker AK, Walker DM, Wickes BL, Wong PTW, Groenewald JZ (2014) Fungal planet description sheets: 214–280. Persoonia 32(1): 184–306. https://doi.org/10.3767/003158514X682395

Crous PW, Wingfield MJ, Richardson DM, Leroux JJ, Strasberg D, Edwards J, Roets F, Hubka V, Taylor PWJ, Heykoop M, Martín MP, Moreno G, Sutton DA, Wiederhold NP, Barnes CW, Carlavilla JR, Gené J, Giraldo A, Guarnaccia V, Guarro J, Hernández-Restrepo M, Kolařík M, Manjón JL, Pascoe IG, Popov ES, Sandoval-Denis M, Woudenberg JHC, Acharya K, Alexandrova AV, Alvarado P, Barbosa RN, Baseia IG, Blanchette RA, Boekhout T, Burgess TI, Cano-Lira JF, Čmoková A, Dimitrov RA, Dyakov MY, Dueñas M, Dutta AK, Esteve-Raventós F, Fedosova AG, Fournier J, Gamboa P, Gouliamova DE, Grebenc T, Groenewald M, Hanse B, Hardy GESTJ, Held BW, Jurjević Ž, Kaewgrajang T, Latha KPD, Lombard L, Luangsa-ard JJ, Lysková P, Mallátová N, Manimohan P, Miller AN, Mirabolfathy M, Morozova OV, Obodai M, Oliveira NT, Ordóñez ME, Otto EC, Paloi S, Peterson SW, Phosri C, Roux J, Salazar WA, Sánchez A, Sarria GA, Shin H-D, Silva BDB, Silva GA, Smith MTH, Souza-Motta CM, Stchigel AM, Stoilova-Disheva MM, Sulzbacher MA, Telleria MT, Toapanta C, Traba JM, Valenzuela-Lopez N, Watling R, Groenewald JZ (2016) Fungal Planet description sheets: 400–468. Persoonia 36(1): 316–458. https://doi.org/10.3767/003158516X692185

Crous PW, Carlier J, Roussel V, Groenewald JZ (2021) *Pseudocercospora* and allied genera associated with leaf spots of banana (*Musa* spp.). Fungal systematics and evolution 7: 1–19. https://doi.org/10.3114/fuse.2021.07.01

De Hoog GS (1973) Revision of *Scolecobasidium* and *Pleurophragmium*. Kavaka 1: 55–60. https://xueshu.baidu.com/usercenter/paper/show?paperid=183y0ab0450p0eg0js300ps0gp481267

De Hoog GS (1985) Taxonomy of the *Dactylaria*-complex, IV. *Dactylaria*, Neta, *Subulispora* and *Scolecobasidium*. Studies in Mycology 26: 1–60. https://cir.nii.ac.jp/crid/1571980075064691712?lang=en

Ellis MB (1976) More dematiaceous hyphomycetes (1st edn.), 507 pp. https://doi.org/10.2307/3758674

Gams W (2015) An ex-type culture cannot always tell the ultimate truth. IMA Fungus 6(2): 1–69. https://doi.org/10.1007/BF03449357

Giraldo A, Sutton DA, Samerpitak K, de Hoog GS, Wiederhold NP, Guarro J, Gené J (2014) Occurrence of *Ochroconis* and *Verruconis* species in clinical specimens from the United States. Journal of Clinical Microbiology 52(12): 4189–4201. https://doi.org/10.1128/JCM.02027-14

Glass NL, Donaldson GC (1995) Development of primer sets designed for use with the PCR to amplify conserved genes from filamentous ascomycetes. Applied and Environmental Microbiology 61(4): 1323–1330. https://doi.org/10.1128/aem.61.4.1323-1330.1995

Guindon S, Gascuel O (2003) A simple, fast, and accurate method to estimate large phylogenies by maximum likelihood. Systematic Biology 52(5): 696–704. https://doi.org/10.1080/10635150390235520

Guo LD, Hyde KD, Liew EC (2000) Identification of endophytic fungi from *Livistona chinensis* based on morphology and rDNA sequences. The New Phytologist 147(3): 617–630. https://doi.org/10.1046/j.1469-8137.2000.00716.x

Hao L, Chen C, Zhang R, Zhu M, Sun G, Gleason ML (2012) A new species of *Scolecobasidium* associated with the sooty blotch and flyspeck complex on banana from China. Mycological Progress 12(3): 489–495. https://doi.org/10.1007/s11557-012-0855-5

Katoh K, Standley DM (2013) MAFFT multiple sequence alignment software version 7: improvements in performance and usability. Molecular Biology and Evolution 30(4): 772–780. https://doi.org/10.1093/molbev/mst010

Matic I, Ahel I, Hay R (2012) Reanalysis of phosphoproteomics data uncovers ADP-ribosylation sites. Nature Methods 9(8): 771–772. https://doi.org/10.1038/nmeth.2106

Miller MA, Pfeiffer W, Schwartz T (2010) Creating the CIPRES Science Gateway for inference of large phylogenetic trees. 2010 Gateway Computing Environments Workshop (GCE): 1–8. https://doi.org/10.1109/GCE.2010.5676129

Qiao TM, Zhang J, Li SJ, Han S, Zhu TH (2016) Development of nested PCR, multiplex PCR, and loop-mediated isothermal amplification assays for rapid detection of *Cylindrocladium scoparium* on Eucalyptus. The Plant Pathology Journal 32(5): 414–422. https://doi.org/10.5423/PPJ.OA.03.2016.0065

Ross AJ, Yasutake WT (1973) *Scolecobasidium humicola*, a fungal pathogen of fish. Journal of the Fisheries Research Board of Canada 30(7): 994–995. https://doi.org/10.1139/f73-161

Samerpitak K, Van der Linde E, Choi HJ, Gerrits van den Ende AHG, Machouart M, Gueidan C, de Hoog GS (2014) Taxonomy of *Ochroconis*, genus including opportunistic pathogens on humans and animals. Fungal Diversity 65(1): 89–126. https://doi.org/10.1007/s13225-013-0253-6

Seifert KA, Gams W (2011) The genera of Hyphomycetes–2011 update. Persoonia 27(1): 119–129. https://doi.org/10.3767/003158511X617435

Shen M, Zhang JQ, Zhao LL, Groenewald JZ, Crous PW, Zhang Y (2020) *Venturiales*. Studies in Mycology 96: 185–308. https://doi.org/10.1016/j.simyco.2020.03.001

Singh K, Flood J, Welsh RD, Wyckoff JH III, Snider TA, Sutton DA (2006) Fatal systemic phaeohyphomycosis caused by *Ochroconis gallopavum* in a dog (*Canis familaris*). Veterinary Pathology 43(6): 988–992. https://doi.org/10.1354/vp.43-6-988

VanSteenhouse JL, Padhye AA, Ajello L (1988) Subcutaneous phaeohyphomycosis caused by *Scolecobasidium humicola* in a cat. Mycopathologia 102(2): 123–127. https://doi.org/10.1007/BF00437449

Wei TP, Zhang H, Zeng XY, Crous PW, Jiang YL (2022) Re-evaluation of *Sympoventuriaceae*. Persoonia 48(1): 219–260. https://doi.org/10.3767/persoonia.2022.48.07

White TJ, Bruns T, Lee S, Taylor J (1990) Amplification and direct sequencing of fungal ribosomal RNA genes for phylogenetics. PCR protocols 18(1): 315–322. https://doi.org/10.1016/B978-0-12-372180-8.50042-1

MycoKeys 96: 127–142 (2023)
doi: 10.3897/mycokeys.96.98320
https://mycokeys.pensoft.net

RESEARCH ARTICLE

A peer-reviewed open-access journal
MycoKeys
Launched to accelerate biodiversity research

Elaphomyces castilloi (Elaphomycetaceae, Ascomycota) and *Entoloma secotioides* (Entolomataceae, Basidiomycota), two new sequestrate fungi from tropical montane cloud forest from south Mexico

Javier Isaac de la Fuente[1], Jesús García-Jiménez[2], Tania Raymundo[3], Marcos Sánchez-Flores[2], Ricardo Valenzuela[3], Gonzalo Guevara-Guerrero[2], Erika Cecilia Pérez-Ovando[4], César Ramiro Martínez-González[2]

1 *Colegio de Postgraduados, Km 36.5 Montecillo, Texcoco, 56230, Estado de México, Mexico* **2** *Tecnológico Nacional de México, Instituto Tecnológico de Ciudad Victoria, Blvd. Emilio Portes Gil #1301Pte, 87010, Ciudad Victoria, Tamaulipas, Mexico* **3** *Instituto Politécnico Nacional, Escuela Nacional de Ciencias Biológicas, Departamento de Botánica, Laboratorio de Micología, 11340, Ciudad de Mexico, Mexico* **4** *Instituto de ciencias biólogicas, Universidad de Ciencias y Artes de Chiapas, Libramiento Norte Poniente, 29039, Tuxtla Gutiérrez, Chiapas, Mexico*

Corresponding author: Jesús García-Jiménez (jgarjim@yahoo.com.mx)

Academic editor: Claudia Perin | Received 6 December 2022 | Accepted 15 March 2023 | Published 3 April 2023

Citation: de la Fuente JI, García-Jiménez J, Raymundo T, Sánchez-Flores M, Valenzuela R, Guevara-Guerrero G, Pérez-Ovando EC, Martínez-González CR (2023) *Elaphomyces castilloi* (Elaphomycetaceae, Ascomycota) and *Entoloma secotioides* (Entolomataceae, Basidiomycota), two new sequestrate fungi from tropical montane cloud forest from south Mexico. MycoKeys 96: 127–142. https://doi.org/10.3897/mycokeys.96.98320

Abstract

Two new species of sequestrate fungi are described from south Mexico based on morphological and molecular evidences. Here we describe *Elaphomyces castilloi* characterized by the yellowish mycelial mat, dull blue gleba and ascospores of 9.7–11.5 µm; *Entoloma secotioides* is characterized by the secotioid basidiomata, sulcate, pale cream pileus, and basidiospores of 7–13 × 5–9 µm. Both species grow in montane cloud forest under *Quercus* sp. in the state of Chiapas, Mexico. Descriptions, photographs, and multilocus phylogeny for both species are presented.

Keywords

Chiapas, hypogeous fungi, mycorrhizal fungi, phylogeny, truffle-like fungi

Introduction

Sequestrate fungi are characterized by producing hypogeous sporome, protected by a thick peridium to avoid desiccation, changes in temperature, and humidity (Thiers 1984). Due to this morphological modification, these species are not capable of dispersing their spores through the air, so they use other strategies such as producing aromas to attract animals that consume and disperse them through their feces (Castellano et al. 1986; Caiafa et al. 2021). Many species are ectomycorrhizal and are associated with the roots of angiosperms and gymnosperms, mainly trees and shrubs of the genera *Abies*, *Coccoloba*, *Dycimbe*, *Eucalyptus*, *Quercus*, and *Pinus* (Trappe et al. 2009). Some saprobic species are also known, mainly from tropical forests (de la Fuente et al. 2021). This diversity in the tropics is just beginning to be discovered and, according to Sulzbacher et al. (2016), there are more than 1,500 described species in the world with more being regularly added.

Hypogeous fungi have been studied in Mexico since the 1970's and the studies of García-Romero et al. (1970) and Trappe and Guzmán (1971), although the first record of a hypogeous fungus was *Melanogaster umbriniglebus* Trappe & Guzmán, recorded in Chihuahua by Lumbholz in the late 1800's (Cázares et al. 2008). Since the 2000's, species have been regularly described, mainly species from temperate forests. Approximately 100 species of hypogeous fungi are currently known, mainly from northeastern Mexico and the Neovolcanic axis, areas where more studies have been carried out (Trappe and Guzmán 1971; Cázares et al. 1992; Guevara-Guerrero et al. 2014; Gómez-Reyes et al. 2018);however, many Mexican states and different types of vegetation have been under-explored.

The state of Chiapas is located in southern Mexico and is an important reservoir of montane cloud forest (Williams-Linera 1991). This type of vegetation represents less than 1% of the national coverage and is declining alarmingly (SEMARNAT 2010). This kind of forest is located between 1500 to 2500 m above sea level. Annual precipitation exceeds 1500 mm. The most common trees in this forest type include *Pinus*, *Quercus*, *Lyquidambar* and *Magnolia* (González-Espinoza et al. 2012). Due to several species of fungi growth associated with the roots of trees, it is possible to carry out successful reforestation experiments with native species. Hence knowing the native fungi of the forest becomes a priority in their conservation (Martínez-Reyes et al. 2012). In this study, two new species of hypogeous fungi are described: *Elaphomyces castilloi*, characterized by the blackish ascoma covered with yellow mycelial mat and bluish gleba, and *Entoloma secotioides*, characterized by its pale-colored secotioid basidiome. Both species grow in montane cloud forest under *Quercus* species. Photographs, descriptions and multiloci phylogeny are presented for both species.

Materials and methods

Sampling data

Mycological explorations were carried out in the state of Chiapas, southern Mexico (Fig. 1). The dominant vegetation in the sampling site corresponds to a tropical

Figure 1. Montane cloud forest at La Trinitaria, Chiapas, Mexico.

montane cloud forest. For the collection of the specimens, the protocols proposed by Castellano et al. (1986) were followed. The specimens were registered and herborized. A color chart was used for color terminology (Kornerup and Wanscher 1978). Hand cuts were made on dried specimens and temporal preparation was mounted in order to observe microstructures. KOH 5% and Melzer's reagent were used to observe amyloid reactions. At least 30 spores and other microstructures were measured using an optical microscope (Motic ba310, San Antonio, USA) to obtain the average length (L), average width (W) and Q ratio (Q). The scanning electron microscope (Hitachi Su 1510, Hitachi, Japan) of IB-UNAM (Mexico City, Mexico) was utilized to observe spore ornamentation. The collected specimens were deposited in ITCV.

DNA extraction, amplification, and sequencing

The DNA was obtained from herbarium specimens (Tables 1, 2). The CTAB protocol of Martínez-González et al. (2017) was used to extract genomic DNA. The DNA was quantified with a Nanodrop 2000c (Thermo ScientificTM, Wilmington, USA). We prepared dilutions from each sample at 20 ng/μL to amplify the Internal Transcribed Spacer rDNA-ITS1 5.8S rDNA-ITS2 (ITS), the nuclear large subunit ribosomal DNA (LSU) and the second largest subunit of the RNA polymerase II gene (rpb2).

Table 1. GenBank accession numbers corresponding to the sequences used in the phylogenetic analyses for *Elaphomyces castilloi*. In bold the accessions of the new species.

Species name	Isolate/Voucher/strain	Locality	GenBank Accessions	
			ITS	nrLSU
Elaphomyces aculeatus	16952	Italy	JF907985	–
Elaphomyces adamizans	TH9660 (Type)	Guyana	KT694133	KT694144
Elaphomyces aff. *decipiens*	GO-2009-211	Mexico	KC152093	–
Elaphomyces castilloi	**García 18640 (Holotype)**	**Mexico**	**OP821418**	**OP824738**
	Guevara 1162 (Paratype)	**Mexico**	**OP821419**	**OP824739**
Elaphomyces citrinus	16955	Spain	JF907986	–
	LIP0001141	Spain	–	KX238822
Elaphomyces complexumurus	TH8880	Guyana	JN711441	–
	TH8880	Guyana	NR121522	–
Elaphomyces decipiens	Trappe 12436	USA	EU837229	–
	Trappe 28269	USA	EU846311	–
Elaphomyces digitatus	MCA1923	Guyana	–	JN713148
Elaphomyces favosus	TH10015	Cameroon	KT694134	KT694145
	TH9859 (type)	Cameroon	KT694138	KY694149
	TH9897	Cameroon	KT694136	KT694146
Elaphomyces granulatus	KM47712	UK	EU784197	–
Elaphomyces guangdongensis	KT-TW09-030	Taiwan	HM357249	–
	KT-TW09-031	Taiwan	HM357250	HM357248
Elaphomyces iupperticellus	TH9934	Cameroon	KT694141	KT694142
	THDJA 39 (type)	Cameroon	KT694139	KT694143
Elaphomyces labryinthinus	TH9918 (type)	Cameroon	KT694137	KT694148
Elaphomyces leveillei	16960	Italy	JF907987	–
Elaphomyces maculatus	16961	Italy	JF907988	–
Elaphomyces muricatus	Hy14	Finland	GU550112	–
	HA38	Latvia	KR019869	–
Elaphomyces sp.	HB1	Indonesia	–	LC010285
	YM144	Japan	–	AB848482
	AM3GA3A4	USA	–	JQ272414
	LM5570B	Hungary	–	KM576391
	73812	UK	–	FJ876187
	GM1332	USA	–	KF359559
Uncultured *Elaphomyces*	141A	Canada	KM403019	KM403019

The reaction mixture for PCRs was performed on a final volume of 15 µL containing 1× buffer, 0.8 mM dNTPs mix, 20 pmol of each primer, 2 units of GoTaq DNA (Promega, USA) and 100 ng of template DNA. The PCR products were verified by agarose gel electrophoresis. The gels were run for 1 h at 95 V cm^{-3} in 1.5% agarose and 1× TAE buffer (Tris Acetate-EDTA). The gel was stained with GelRed (Biotium, USA) and the bands were visualized in an Infinity 3000 transilluminator (Vilber Lourmat, Eberhardzell, Germany). The amplified products were purified with the ExoSAP Purification kit (Affymetrix, USA), following the manufacturer's instructions. They were quantified and prepared for the sequence reaction using a BigDye Terminator v.3.1 (Applied Biosystems, USA). These products were sequenced in both directions with an Applied Biosystem model 3730XL (Applied BioSystems, Foster City, USA), at the Instituto de Biología of the Universidad Nacional Autónoma de México (UNAM). The sequences obtained were compared with the original chromatograms to detect and correct possible reading errors. The sequences of both strands of each of the genes were analyzed,

Table 2. GenBank accession numbers corresponding to the sequences used in the phylogenetic analyses for *Entoloma secotioides*. The accessions of the new species are in bold.

Species name	Isolate/Voucher/strain	GenBank Accessions		
		ITS	nrLSU	*rpb2*
Entoloma aff. *prunuloides*	628	–	–	KC710159
Entoloma aff. *sinuatum*	TRTC156542	JN021020	–	–
Entoloma albidum	620	KC710102	KC710151	–
Entoloma albomagnum	427	KC710065	KC710137	–
Entoloma araneosum	14	GQ289153	GQ289255	GQ289293
Entoloma asterosporum	TENN064538	JF706309	–	JF706312
Entoloma baronii	L644	KC710093	–	–
Entoloma caccabus	17	KC710063	GQ289155	GQ289227
Entoloma caesiolamellatum	626	KC710126	KC710157	–
Entoloma callidermum	512	KC710115	KC710153	–
Entoloma secotioides	**García 18817 (Holotype)**	**OP821420**	**OP824740**	**KC265752**
	Guevara 1173 (Paratype)	**OP821421**	**OP824741**	**KC265753**
Entoloma cf. griseoluridum	LNM221111	KC710118	–	–
Entoloma chilense	MES 1012	KY462399	–	–
Entoloma clypeatum	41	KC710059	KC710136	–
Entoloma coeruleogracilis	216	KC710069	–	–
Entoloma conferendum	30	KC710055	KC710133	KC710191
Entoloma corneri	607	KC710058	KC710135	–
Entoloma cretaceum	2010039	KC710090	–	–
Entoloma flavifolium	621	KC710097	KC710150	–
Entoloma fumosobrunneum	MEN 2005113	KC710124	KC710155	–
Entoloma gracilior	2011043	KC710079	–	–
Entoloma hypogaeum	K382	NR119416	–	AB692019
Entoloma kermandii	222	–	GQ289173	GQ289244
Entoloma lividoalbum	233	KC710114	KC710152	–
Entoloma luridum	2005108	KC710091	KC710146	KC710192
Entoloma madidum	221	KC710127	KC710158	–
	67195	KC710130	–	–
Entoloma manganaense	215	KC710085	KC710143	–
Entoloma myrmecophilum	231	KC710120	–	–
Entoloma ochreoprunuloides	15721	KC710111	–	–
	632	KC710092	KC710147	–
Entoloma ochreoprunuloides f. *hyacinthinum*	6	KC710105	–	–
Entoloma perbloxamii	2010037	KC710095	–	–
Entoloma prismaticum	K381	AB691998	–	AB692016
Entoloma prunuloides	40	KC710073	GQ289184	GQ289255
Entoloma pseudoprunuloides	627	KC710078	KC710140	–
Entoloma sequestratum	MFLU 12-2045	MH323431	MT344186	MT349886
Entoloma sinuatum	182	KC710116	KC710154	–
Entoloma sordidulum	1	KC710062	GQ289194	GQ289265
Entoloma sphagneti	209	KC710061	GQ289195	–
Entoloma subsinuatum	YL2269	KC710096	KC710149	–
Entoloma trachyosporum	405	KC710088	GQ289198	–
Entoloma turbidum	27	KC710060	GQ289201	GQ289269
Entoloma whiteae	629	KC710084	KC710142	–
Entoloma alcedicolor	210	KC710123	GQ289152	GQ289224
Entocybe nitidum	24	KC710122	GQ289175	GQ289246

edited and assembled using the BioEdit v. 7.0.5 (Hall 1999) to generate a consensus sequence which compared with those deposited in GenBank using the tool BLASTN v. 2.2.9 (Zhang et al. 2000).

Phylogenetic analyses

To explore the phylogenetic relationships of the new species of *Elaphomyces*, an alignment was made based on the taxonomic sampling employed by Paz et al. (2017). Outgroup was selected according to Paz et al. (2017). Each gene region was independently aligned using the online version of MAFFT v. 7 (Katoh et al. 2002, 2017; Katoh and Standley 2013). Alignment was reviewed in PhyDE v.10.0 (Müller et al. 2005), followed by minor manual adjustments to ensure character homology between taxa. The matrix was formed for ITS by 24 taxa (697 characters), while LSU by 19 taxa (845 characters). The aligned matrices were concatenated into a single matrix (32 taxa, 1542 characters). Two partitioning schemes were established: one for the ITS and one for the LSU, which were established using the option to minimize the stop codon with Mesquite v3.70 (Maddison and Maddison 2017).

To explore the phylogenetic relationships of the new species of *Entoloma*, an alignment was made based on the taxonomic sampling employed by Elliott et al. (2020). The outgroup was selected according to Elliott et al. (2020). Each gene region was independently aligned using the online version of MAFFT v. 7 (Katoh et al. 2002, 2017; Katoh and Standley 2013). Alignment was reviewed in PhyDE v.10.0 (Müller et al. 2005), followed by minor manual adjustments to ensure character homology between taxa. The matrix was formed for ITS by 45 taxa (700 characters), for LSU by 31 taxa (831 characters), while rpb2 consisted of 17 taxa (670 characters). The aligned matrices were concatenated into a single matrix (47 taxa, 2201 characters). Five partitioning schemes were established: one for the ITS, one for the LSU and three for rpb2 gene region, which were established using the option to minimize the stop codon with Mesquite v3.70 (Maddison and Maddison 2017).

Phylogenetic inferences were estimated with maximum likelihood (ML) in RAxML v. 8.2.10 (Stamatakis 2014) with a GTR + G model of nucleotide substitution. To assess branch support, 10,000 nonparametric rapid bootstrap pseudoreplicates were run with the GTRCAT model. For Bayesian posterior probability (PP), the best evolutionary model for alignment was sought using Partition Finder (Frandsen et al. 2015; Lanfear et al. 2014, 2017). Phylogeny analyses was performed using MrBayes v. 3.2.6 ×64 (Huelsenbeck and Ronquist 2001). The information block for the matrix includes two simultaneous runs, four Montecarlo chains, temperature set to 0.2 and sampling 10 million generations (standard deviation ≤ 0.1) with trees sampled every 1000 generations. The first 25% of samples were discarded as burn-in, and stationarity was checked in Tracer v. 1.6 (Rambaut et al. 2014). Trees were visualized and optimized in FigTree v. 1.4.4 (Rambaut 2014), and then edited in Adobe Illustrator vCS4 (Adobe Systems, Inc., San Jose, CA).

Results

Phylogenetic analyses

The ITS and LSU sequences obtained from *Elaphomyces castilloi* and ITS, LSU and rpb2 from *Entoloma secotioides* were deposited in GenBank. The two simultaneous Bayesian runs continued until the convergence parameters were met, and the standard deviation fell below 0.001 after 10 million generations for *Elaphomyces castilloi* and 0.002 for *Entoloma secotioides*. No significant changes in tree topology trace or cumulative split frequencies of selected nodes were observed after about 0.33 million generations for *E. castilloi* and 0.45 million generations for *E. secotioides*, so the first 2,500,000 sampled trees (25%) were discarded as burn-in. Both the Bayesian analyses and Maximum Likelihood (Figs 2, 3) recovered *Elaphomyces castilloi* supporting the

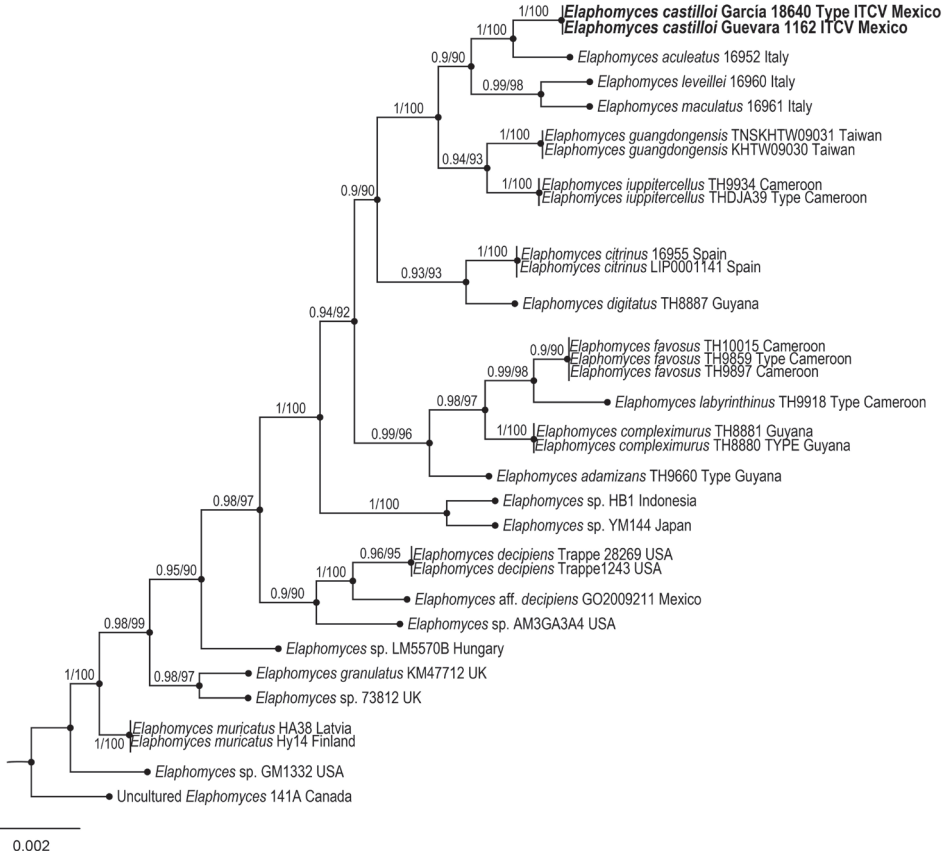

Figure 2. Bayesian inference phylogram of ITS-LSU sequences data for *Elaphomyces castilloi*. Posterior probability (left of slash) from Bayesian analysis and Bootstrap support (right of slash).

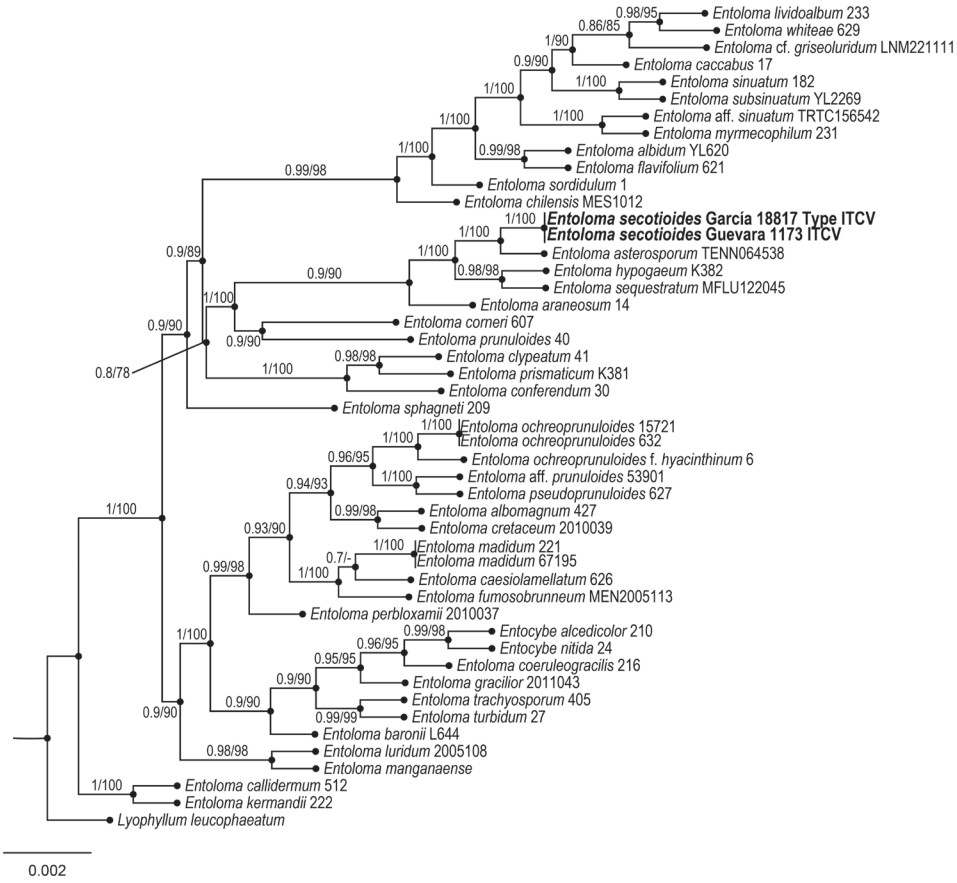

Figure 3. Bayesian inference phylogram of ITS-LSU-RPB2 sequences for *Entoloma secotioides*. Posterior probability (left of slash) from Bayesian analysis and Bootstrap support (right of slash).

existence of one new taxon distinctive from related species of *Elaphomyces* (1 Bayesian Posterior Probability and 100% bootstrap proportion for Maximum Likelihood) and *Entoloma secotioides*, supporting the existence of one new taxon distinctive from related species of *Entoloma* (1 Bayesian Posterior Probability and 100% bootstrap proportion for Maximum Likelihood).

Taxonomy

***Elaphomyces castilloi* J. García, Guevara & de la Fuente, sp. nov.**
MycoBank No: MB842037
GenBank: LSU: OP824738, ITS: OP821418.
Fig. 4A–G

Type material. ***Holotype.*** Mexico. Chiapas: la Trinitaria Municipality, Lagunas de Monte bello, alt. 1004 m, 16°53'N, 93°27'W, 16 August 2019, J. García 18640 (Holotype-ITCV).

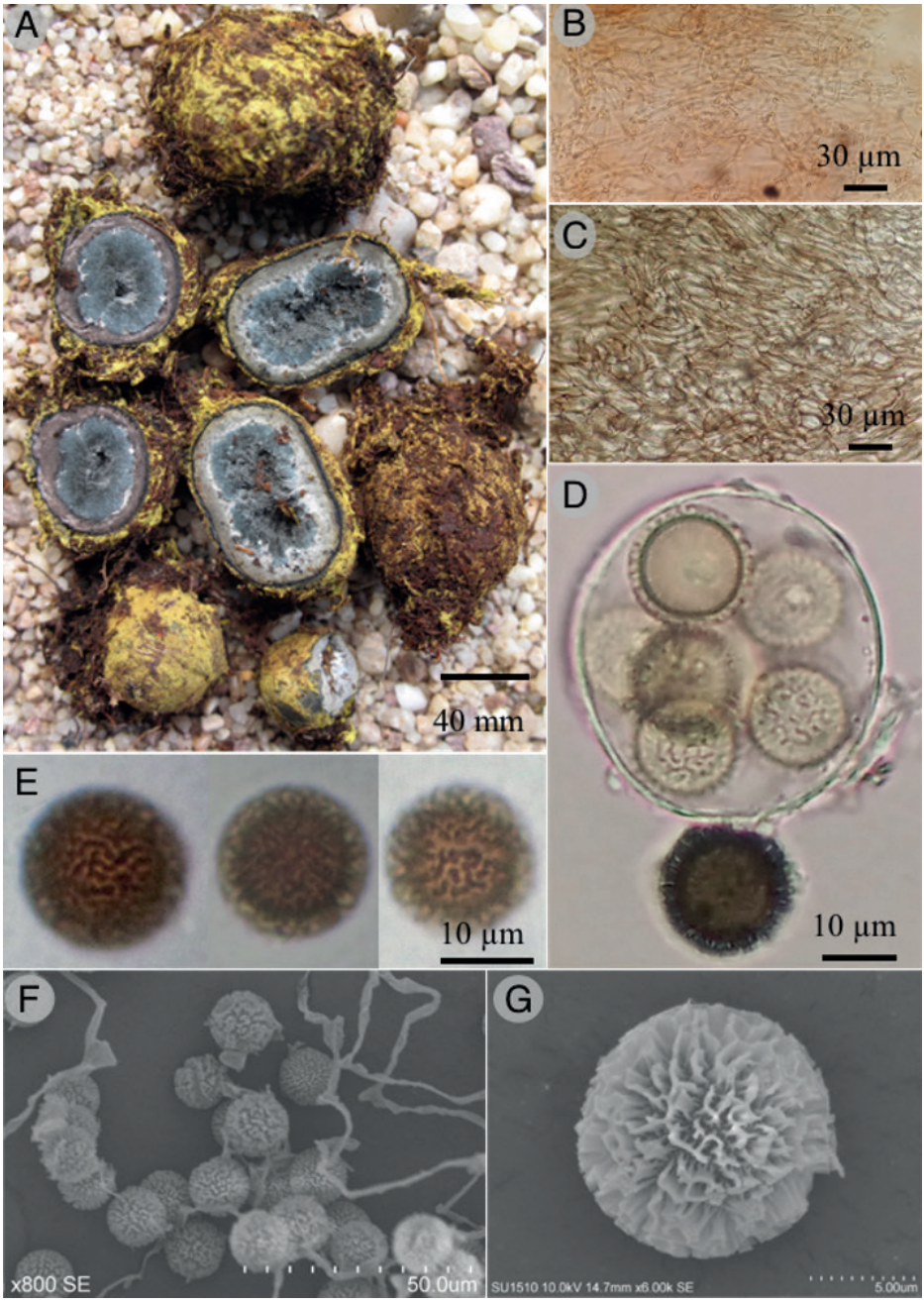

Figure 4. *Elaphomyces castilloi* (Holotype) **A** ascomata **B** mycelial mat hyphae **C** subcutis **D** asci **E, F** ascospores in KOH **G** detail of ascospore ornamentation in SEM.

Diagnosis. *Elaphomyces castilloi* differs from other species of the genus by the following combination of characteristics: ascomata embedded in a yellow mycelial mat, dull blue powdery gleba, and globose reticulate ascospores (9.7–11.5 µm).

Etymology. The species was named *castilloi* in honor of José Castillo Tovar (*ad memoriam*), a Mexican pioneer mycologist dedicated to studying the fungi from northeast Mexico.

Description. ***Ascomata*** globose to ellipsoid, 14–32 mm, embedded in a thick, yellowish orange (4A7) to deep yellow (4A8), with a membranous mycelial mat, occasionally incorporating soil particles, and debris, loose but compacted near the peridium, easily detachable. ***Peridium*** surface black, slightly rough, carbonaceous, inner peridium grayish brown (8D3), sometimes with white mycelial strand, near the gleba forming a discontinuous layer. ***Gleba*** powdery, dull blue (23D5), compacted when young, becoming loose when mature, with scattered grey hyphae (25C1); odor and taste fungoid.

Mycelial mat hyphae cylindrical, 2–6 µm diameter, septate, hyaline, thin-walled, loosely arranged. ***Epicutis*****:** 125–200 µm diameter, composed of compacted hyphae, 3–8 µm diameter, strongly interwoven, subglobose to irregular, black in 5% KOH, thick-walled. ***Subcutis*** 500–650 µm diameter, composed by prostrated and compacted hyphae, 8–15 µm in diameter, hyaline to dull grey in 5% KOH (25D4), becoming irregular near the gleba, thin-walled. ***Asci*** subglobose, 32–38 × 25.8–30.1 µm, 5 to 8-spored, hyaline, thin-walled. ***Ascospores*** 9.7–11.5 µm (n = 30), globose, rarely subglobose, reticulated, projecting up to 1.9–2.7 µm, forming small bridges (less than 2 µm), with obtuse tips, golden brown color (5D7), thick-walled.

Additional material examined. Mexico. Chiapas: la Trinitaria Municipality, Lagunas de Monte bello, alt. 1004 m, 16°53'N, 93°27'W, 16 August 2011, Guevara 1102 (Paratype-ITCV). ITS: OP821419, LSU: OP824739.

Distribution. Known only from the Mexican state of Chiapas, growing scattered, and hypogeous under *Quercus* sp. in montane cloud forest.

Notes. *Elaphomyces castilloi* is phylogenetically close to *Elaphomyces aculeatus* Vittad. from Italy, the last one with similar ascospore color and ornamentation. It was previously reported from Mexico by Gómez-Reyes et al. (2012). *Elaphomyces aculeatus* has a reddish peridium and dark-brown gleba; meanwhile, *E. castilloi* has dark peridium and bluish gleba. The yellow mycelial mat and the small ascospores resemble those of *Elaphomyces citrinus* Vittad. (Section *Malacodermei*). However, it differs by the smaller ascocarp (less than 10 mm), the brownish peridium in young specimens, and by its geographic distribution (Europe) (Pegler et al. 1993). Although the morphological features of the new species are typical in the *Malacodermei*, these are also seldom observed in the *Ceratogaster* (Paz et al. 2017).

Entoloma secotioides **J. García, Guevara & de la Fuente, sp. nov.**
MycoBank No: MB842038
GenBank: ITS: OP821420; LSU: OP824740; RPB2: KC265752.
Fig. 5A–F

Type material. ***Holotype*****.** Mexico. Chiapas: la Trinitaria Municipality, Lagunas de Monte bello, alt. 1004 m, 16°53'N, 93°27'W, 16 August 2019, J. García 18817 (Holotype-ITCV).

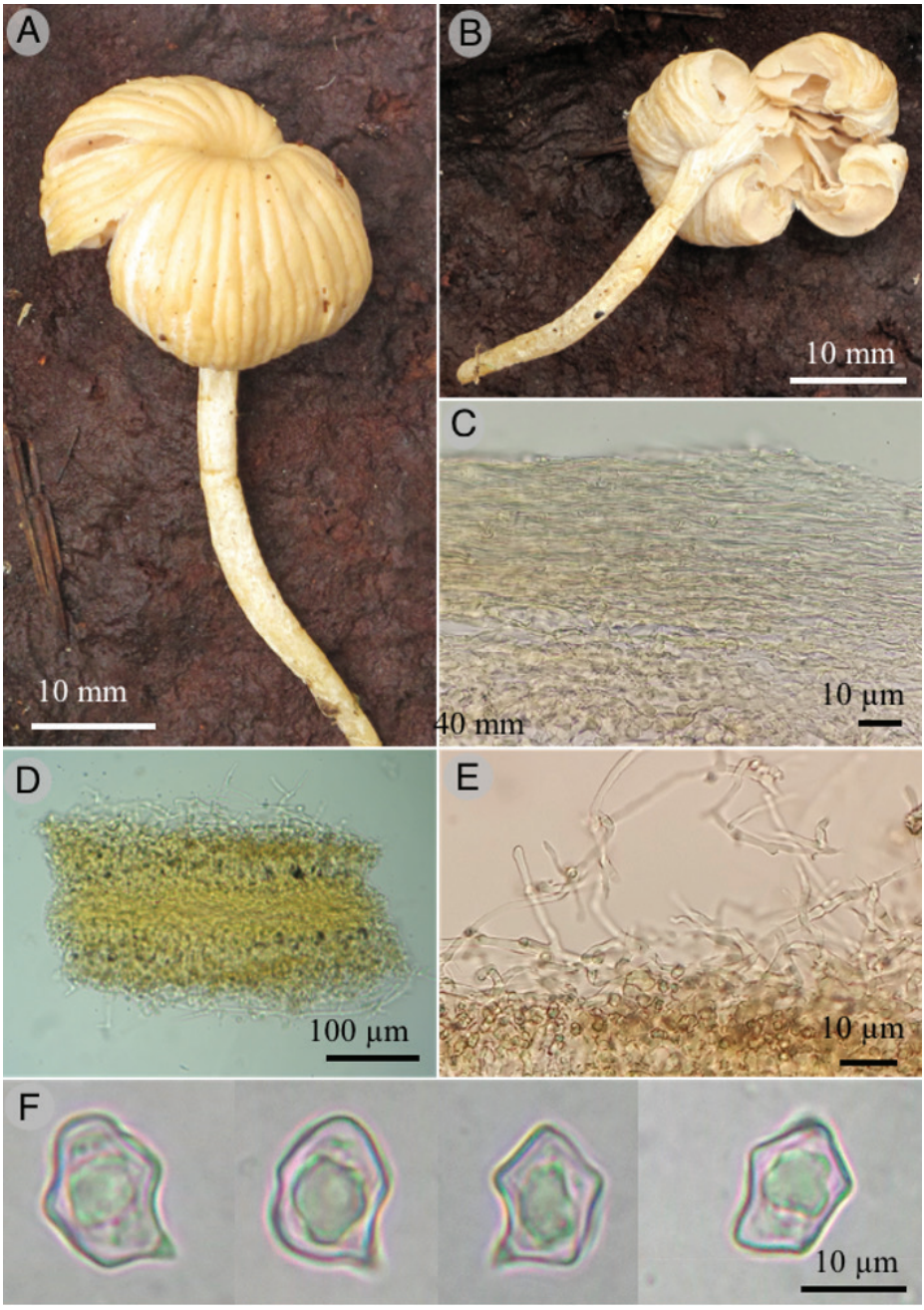

Figure 5. *Entoloma secotioides* (Holotype) **A, B** basidiomata showing the pileus, hymenia, and stipe **C** peridium **D, E** details of the hymenium **F** basidiospores in KOH.

Diagnosis. *Entoloma secotioides* is characterized by cream colored, sulcate, secotioid basidiomata, not anastomosed gills, and angular basidiospores (7–13 × 5–9 µm).

Etymology. Named *secotioides* due to the secotioid basidiomata.

Description. Pileus 12–15 mm, subglobose, flattened when young, becoming depressed when mature, sulcate, pale yellow (4A3) to light yellow (4A5), slightly velvety, margin incurved enclosing the hymenium, dry in appearance, sometimes with brownish fibrils. Hymenophore lamellate, slightly irregular, pale orange to orange white (5A2) to light yellow (4A5), not exposed even in mature specimens. Stipe 4–9 × 3–4 mm, cylindrical or absent, light yellow (4A5), smooth or finely fibrillose. Taste and odor fungoid, mild.

Peridium 70–300 μm composed of loosely interwoven or horizontally arranged hyphae, 4–7 μm in diameter, septate, bifurcate, hyaline to pastel green in 5% KOH (27A4), not reacting with Melzer, with clavate terminal cells, thin-walled. ***Hymenophoral trama*** 45–110 μm in diameter, composed of interwoven compacted hyphae, 4–9 μm in diameter, light orange in 5% KOH (5A4), thin-walled. ***Basidia*** 27–35 × 5–10 μm forming palisades, clavate, hyaline, thin-walled, embedded by a layer of loosely interwoven hyphae which arise from the trama, 6–11 μm diameter, sometimes branched, inflate at the septum, sometimes with terminal cells cystidioid or cylindrical, thin-walled. ***Basidiospores*** 7–13 × 5–9 μm, (L = 10.2, W = 7.1, Q = 1–2.2, n = 30), angular, rare nodulose, with 6–8 sides, some with conspicuous hilar appendix up to 3 μm, hyaline to pastel green (27A4), not reacting with Melzer reagent, smooth, thin-walled.

Distribution. Known only from the state of Chiapas, growing sub hypogeous under *Quercus* sp. and *Pinus* sp. in montane cloud forest.

Additional material studied. Mexico. Chiapas: la Trinitaria Municipality, Lagunas de Monte bello, alt. 1004 m, 16°53'N, 93°27'W, 16 August 2019, Guevara 1173 (Paratype-ITCV). ITS: OP821421; LSU: OP824741; RPB2: KC265753.

Notes. *Entoloma secotioides* is characterized by pale-cream basidiomata, enclosed, not anastomosed gills, and angular basidiospores 7–13 × 5–9 μm. *Entoloma calongei* (E. Horak & G. Moreno) Noordel. & Co-David has gray-brown pileus, loculate gleba, and basidiospores 6–10 μm (Horak and Moreno 1998); *Entoloma chilensis* (E. Horak) Noordel. & Co-David also has grayish pileus, loculate gleba, and basidiospores 9–11 × 6.5–7.5 μm (Horak 1963). Both species differ from *E. secotioides* mainly in the basidiomata color (pale-cream *vs.* grayish-brown) and hymenophore shape (slightly irregular *vs.* locules). The new species is phylogenetically close to *E. asterosporum* (Coker & Couch) T.J. Baroni & Matheny, differing from *E. secotioides* by having the globose sporome, pungent odor and smell, and larger spores (up to 16 μm) (Baroni and Matheny 2011).

Discussion

Hypogeous fungi in Mexico have been scarcely studied compared to epigeous fungi; however, from the 2000s, new species have been regularly described, mainly from temperate forests (Guevara-Guerrero et al. 2014; Gómez-Reyes et al. 2018). In the case of *Elaphomyces*, it is one of the best represented genera in the country because it is associated with a large number of hosts, mainly *Pinus* and *Quercus* (Trappe and Guzmán 1971; Cázares et al. 1992; Castellano et al. 2012; Gómez-Reyes et al. 2012). Some species of *Elaphomyces* have even been described as culturally important. *Elaphomyces muricatus* has been reported for ritual or medicinal use (Trappe et al. 1979). For

Entoloma secotioides, this is the first record of a sequestrate *Entoloma* in Mexico, these being mostly of the previously recorded species pileate-stipitate. Although the species has been described growing under *Quercus* species, there are no data on its ecological habits and these are presented here as putatively associated with *Quercus*.

Chiapas is one of the states with the greatest biological richness in Mexico, only surpassed by Oaxaca (López-Guzmán et al. 2017). The diversity of fungi in this state spans approximately 850 species. Recent research suggests a fungal diversity between 20,000 and 49,000 species (Chanona-Gómez et al. 2007; Ruan-Soto et al. 2013; Kong et al. 2018). Efforts are currently being made to document this diversity, which is threatened by land use change. *Elaphomyces castilloi* represents the first record of the genus *Elaphomyces* in Chiapas and represents the southernmost distribution of the genus in Mexico. Another species reported in southern Mexico is *E. maculatus*, which has been reported in north Oaxaca in oak forests (Trappe et al. 1979).

The sequestrate fungi have been studied mostly in the temperate regions of the north and center of the country; *Elaphomyces castilloi* and *Entoloma secotioides* are new contributions that represent the first findings of sequestrate fungi from the montane cloud forest in Chiapas, more than 50%; of which have unfortunately disappeared; montane cloud forest constitutes less than 1% of the Mexican territory. However, it is vital to carry out samplings that include taxa from this ecosystem considering that its losses are so high. Some localities are deemed critical for conservation of this ecosystem which is considered "endangered" under the definition of the Official Mexican Law (SEMARNAT 2010). The degradation of the montane cloud forests in Chiapas is high, therefore the level of threat to the habitat of the new two species is also high. So far, they are only known from the type locality and it is necessary to increase the sampling to assess the current status of the species. Keeping the taxonomical studies about the fungi from the montane cloud forest could help to encourage its conservation and management.

Acknowledgements

Sánchez-Flores, Martínez-González, Guevara-Guerrero, García-Jiménez and de la Fuente thank CONACYT, PRODEP, Tecnológico Nacional de México, Instituto Tecnológico de Ciudad Victoria for financial support; María Berenit Mendoza-Garfias, Head of the Laboratory of Scanning Electron Microscopy facility at IB-UNAM; Raymundo and Valenzuela thank the Instituto Politécnico Nacional with the project (SIP): 20230017 and 20230624. Also, we thank to reviewers and editors for their kind observations on the document.

References

Baroni TJ, Matheny PB (2011) A re-evaluation of gasteroid and cyphelloid species of Entolomataceae from eastern North America. Harvard Papers in Botany 16(2): 293–310. https://doi.org/10.3100/0.25.016.0205

Caiafa MV, Jusino MA, Wilkie AC, Díaz IA, Sieving KE, Smith ME (2021) Discovering the role of Patagonian birds in the dispersal of truffles and other mycorrhizal fungi. Current biology 31: P5558–5570.E3. https://doi.org/10.1016/j.cub.2021.10.024

Castellano MA, Trappe JM, Maser Z, Maser S (1986) Key to Spores of the Genera of Hypogeous Fungi of North America, with Reference to Animal Mycophagy. Mad River Press, Eureka, 185 pp.

Castellano MA, Guevara-Guerrero G, García-Jiménez J, Trappe JM (2012) *Elaphomyces appalachiensis* and *E. verruculosus* sp. nov. (Ascomycota Eurotiales, Elaphomycetaceae) from eastern North America. Revista Mexicana de Micología 35: 17–22.

Cázarez E, Guevara G, García J, Trappe JM (2008) *Melanogaster minisporus* sp. nov., a new sequestrate member of the Boletales from Mexico. Revista Mexicana de Micología 28: 67–69.

Cázares E, García J, Castillo J, Trappe JM (1992) Hypogeous fungi from northern Mexico. Mycologia 84(3): 341–359. https://doi.org/10.1080/00275514.1992.12026147

Chanona-Gómez F, Andrade-Gallegos RH, Castellanos-Albores J, Sánchez JE (2007) Macromicetos del Parque Educativo Laguna Bélgica, municipio de Ocozocoautla de Espinosa, Chiapas, México. Revista Mexicana de Biodiversidad 78(2): 369–381.

de la Fuente JI, Pinzón JP, Guzmán-Dávalos L, Uitzil-Colli MO, Gohar D, Lebel T, Bahram M, García-Jiménez J (2021) Revision of the genus *Restingomyces*, including two new species from Mexico. Mycologia 113: 1316–1326. https://doi.org/10.1080/00275514.2021.1958544

Elliott TF, Nelsen DJ, Karunarathna SC, Stephenson SL (2020) *Entoloma sequestratum*, a new species from northern Thailand, and a worldwide key to sequestrate taxa of *Entoloma* (Entolomataceae). Fungal Systematics and Evolution 6(1): 253–263. https://doi.org/10.3114/fuse.2020.06.12

Frandsen PB, Calcott B, Mayer C, Lanfear R (2015) Automatic selection of partitioning schemes for phylogenetic analyses using iterative k-means clustering of site rates. BMC Evolutionary Biology 15(1): 1–13. https://doi.org/10.1186/s12862-015-0283-7

García-Romero L, Guzmán G, Herrera T (1970) Especies de macromicetos citados de México I. Ascomycetes, Tremellales y Aphylloporales. Boletín de la Sociedad Mexicana de Micología 4: 54–76.

Gómez-Reyes VM, Hernández-Salmerón IR, Terrón-Alfonso A, Guevara-Guerrero G (2012) Estudio taxonómico de *Elaphomyces* spp. (Ascomycota, Eurotiales, Elaphomycetaceae) de Michoacán, México. Revista Mexicana de Micología 36: 57–82.

Gómez-Reyes VM, Vázquez-Marrufo G, Ortega-Gómez AM, Guevara-Guerrero G (2018) Ascomicetos hipogeos de la región occidental del Sistema Volcánico Transversal, México. Acta Botánica Mexicana 125(125): 13–48. https://doi.org/10.21829/abm125.2018.1327

González-Espinoza M, Meave JA, Ramírez-Marcial N, Toledo-Aceves T, Lorea-Hernández FG, Ibarra-Manríquez G (2012) Los Bosques de Niebla de México: Conservación y restauración de su componente arbóreo. Ecosistemas 21: 36–52.

Guevara-Guerrero G, Cázares-González E, Bonito G, Healy RA, Stielow B, García J, Garza-ocañas F, Castellano M, Trappe J (2014) Hongos hipógeos de Tamaulipas, México. In: Correa SA, Horta JV, Garcia J, Barrientos L (Eds) Biodiversidad Tamaulipeca (Vol. 2). Tecnológico Nacional de México-Instituto Tecnológico de Ciudad Victoria. Mexico city, 87–102.

Hall TA (1999) BioEdit: A user-friendly biological sequence alignment editor and analysis program for Windows 95/98/NT. Nucleic Acids Symposium Series 41: 95–98.

Horak E (1963) Fungi Austroamericani. 3. *Rhodogaster* gen. nov. A new link from Chile towards the Rhodophyllaceae. Sydowia 17: 190–192.

Horak E, Moreno G (1998) *Rhodogaster calongei* sp. nov. (Basidiomycota), first European record of the secotiaceous entolomatoid genus from northern Spain. Sydowia 50: 187–191.

Huelsenbeck JP, Ronquist F (2001) MrBayes: Bayesian inference of phylogeny. Bioinformatics 17(8): 754–755. https://doi.org/10.1093/bioinformatics/17.8.754

Katoh K, Standley DM (2013) MAFFT multiple sequence alignment software version 7: Improvements in performance and usability. Molecular Biology and Evolution 30(4): 772–780. https://doi.org/10.1093/molbev/mst010

Katoh K, Misawa K, Kuma K, Miyata T (2002) MAFFT: A novel method for rapid multiple sequence alignment based on fast Fourier transform. Nucleic Acids Research 30(14): 3059–3066. https://doi.org/10.1093/nar/gkf436

Katoh K, Rozewicki J, Yamada KD (2017) MAFFT online service: Multiple sequence alignment, interactive sequence choice and visualization. Briefings in Bioinformatics 20(4): 1160–1166. https://doi.org/10.1093/bib/bbx108

Kong A, Montoya A, García-de Jesús S, Ramírez-Terrazo A, Andrade R, Ruan-Soto F, Rodríguez-Palma MM, Estrada-Torres A (2018) Hongos ectomicorrizógenos del Parque Nacional Lagunas de Montebello, Chiapas. Revista Mexicana de Biodiversidad 89: 741–756. https://doi.org/10.22201/ib.20078706e.2018.3.2527

Kornerup A, Wanscher JH (1978) Methuen Handbook of Colour (3th edn.). Eyre Methuen, London.

Lanfear R, Calcott B, Kainer D, Mayer C, Stamatakis A (2014) Selecting optimal partitioning schemes for phylogenomic datasets. BMC Evolutionary Biology 14(1): 1–82. https://doi.org/10.1186/1471-2148-14-82

Lanfear R, Frandsen PB, Wright AM, Senfeld T, Calcott B (2017) Partition Finder 2: New methods for selecting partitioned models of evolution for molecular and morphological phylogenetic analyses. Molecular Biology and Evolution 34(3): 772–773. https://doi.org/10.1093/molbev/msw260

López-Guzmán LM, Chacón S, Bautista-Gálvez A (2017) Adiciones al conocimiento sobre la diversidad de los hongos (macromicetes) de Chiapas, México. Revista Mexicana de Micología 45: 27–35. https://doi.org/10.33885/sf.2017.0.1165

Maddison WP, Maddison DR (2017) Mesquite: a modular system for evolutionary analysis. Version 3.31. http://mesquiteproject.org

Martínez-González CR, Ramírez-Mendoza R, Jiménez-Ramírez J, Gallegos-Vázquez C, Luna-Vega I (2017) Improved method for genomic DNA extraction for *Opuntia* Mill. (Cactaceae). Plant Methods 13(1): 1–10. https://doi.org/10.1186/s13007-017-0234-y

Martínez-Reyes M, Pérez-Moreno J, Villareal-Ruiz L, Ferrara-Cerrato R, Xoconostle-Cázares B, Vargas-Hernández JJ, Honrubia-García M (2012) Crecimiento y contenido nutrimental de *Pinus greggii* Engelm. inoculado con el hongo comestible ectomicorrícico Hebeloma mesophaeum (Pers.) Quél. Revista Chapingo Serie Ciencias Forestales y del Ambiente 18(2): 183–192. https://doi.org/10.5154/r.rchscfa.2010.11.112

Müller K, Quandt D, Müller J, Neinhuis C (2005) PhyDE-Phylogenetic data editor. Program distributed by the authors, versión 10.0. https://www.phyde.de

Paz A, Bellanger JM, Lavoise C, Molia A, Ławrynowicz M, Larsson E, Ibarguren IO, Jeppson M, Læssøe T, Sauve M, Richard F, Moreau PA (2017) The genus *Elaphomyces* (Ascomycota, Eurotiales): A ribosomal DNA-based phylogeny and revised systematics of European 'deer truffles'. Persoonia 38(1): 197–239. https://doi.org/10.3767/003158517X697309

Pegler DN, Spooner BM, Young TWK (1993) British Truffles: Revision of British Hypogeous Fungi. Royal Botanical Gardens Kew, London.

Rambaut A, Suchard MA, Xie D, Drummond AJ (2014) Tracer v1.6. http://beast.bio.ed.ac.uk/Tracer

Rambaut A (2014). FigTree ver. 1.4.2. http://tree.bio.ed.ac.uk/software/figtree/

Ruan-Soto F, Hernández-Maza M, Pérez-Ovando E (2013) Estado actual del conocimiento de la diversidad fúngica en Chiapas. In: Conabio (Ed.) La biodiversidad en Chiapas: Estudio de Estado. Conabio/ Gobierno del Estado de Chiapas, Mexico city, 75–83.

SEMARNAT (2010) Norma Oficial Mexicana NOM-059-SEMARNAT-2010. Protección ambiental-Especies nativas de México de flora y fauna silvestres-Categorías de riesgo y especificaciones para su inclusión, exclusión o cambio-Lista de especies en riesgo. Diario Oficial de la Federación. Segunda Sección, México, Distrito Federal. http://www.profepa.gob.mx/innovaportal/file/435/1/NOM_059_SEMARNAT_2010.pdf [Accessed June 12, 2022]

Stamatakis A (2014) RAxML version 8: a tool for phylogenetic analysis and post-analysis of large phylogenies. Bioinformatics 30: 1312–1313. https://doi.org/10.1093/bioinformatics/btu033

Sulzbacher MA, Grebenc T, Giachini AJ, Baseia IG, Nohura R (2016) Hypogeous sequestrate fungi in South America – How well do we know them? Symbiosis 71(1): 9–17. https://doi.org/10.1007/s13199-016-0461-4

Thiers HD (1984) The secotioid syndrome. Mycologia 76(1): 1–8. https://doi.org/10.1080/00275514.1984.12023803

Trappe JM, Guzmán G (1971) Notes on some hypogeous fungi from Mexico. Mycologia 63(2): 317–332. https://doi.org/10.1080/00275514.1971.12019112

Trappe JM, Guzmán G, Vázquez-Salinas C (1979) Observaciones sobre la identificación, distribución y uso de los hongos del género *Elaphomyces* en México. Boletín de la Sociedad Mexicana de Micología 13: 145–150.

Trappe JM, Molina R, Luoma DL, Cázares D, Pilz E, Smith JE, Castellano MA, Miller SL, Trappe MJ (2009) Diversity, ecology, and conservation of truffle fungi in forests of the Pacific Northwest. General Technical Reports PNW-GTR-772-Department of Agriculture, Forest Service, Pacific Northwest Research Station. Portland. https://doi.org/10.2737/PNW-GTR-772

Williams-Linera G (1991) Nota sobre la estructura del estrato arbóreo del bosque mesófilo de montaña en los alrededores del campamento El Triunfo, Chiapas. Acta Botánica 13(13): 1–7. https://doi.org/10.21829/abm13.1991.604

Zhang Z, Schwartz S, Wagner L, Miller W (2000) A greedy algorithm for aligning DNA sequences. Journal of Computational Biology 7(1–2): 203–214. https://doi.org/10.1089/10665270050081478

MycoKeys 96: 143–157 (2023)
doi: 10.3897/mycokeys.96.102669
https://mycokeys.pensoft.net

FORUM PAPER

A peer-reviewed open-access journal
MycoKeys
Launched to accelerate biodiversity research

How, not if, is the question mycologists should be asking about DNA-based typification

R. Henrik Nilsson[1], Martin Ryberg[2], Christian Wurzbacher[3], Leho Tedersoo[4,5], Sten Anslan[4], Sergei Põlme[6], Viacheslav Spirin[1,7], Vladimir Mikryukov[6], Sten Svantesson[1,2], Martin Hartmann[8], Charlotte Lennartsdotter[1], Pauline Belford[9], Maryia Khomich[10], Alice Retter[11], Natàlia Corcoll[1], Daniela Gómez Martinez[1], Tobias Jansson[1], Masoomeh Ghobad-Nejhad[12], Duong Vu[13], Marisol Sanchez-Garcia[14], Erik Kristiansson[15], Kessy Abarenkov[16]

1 *Gothenburg Global Biodiversity Centre, Department of Biological and Environmental Sciences, University of Gothenburg, Box 461, 405 30 Göteborg, Sweden* **2** *Department of Organismal Biology, Uppsala University, Norbyvägen 18D, 752 36 Uppsala, Sweden* **3** *Chair of Urban Water Systems Engineering, Technical University of Munich, Am Coulombwall 3, 85748 Garching, Germany* **4** *Mycology and Microbiology Center, University of Tartu, Liivi 2, 50409 Tartu, Estonia* **5** *College of Science, King Saud University, 1145 Riyadh, Saudi Arabia* **6** *Institute of Ecology and Earth Sciences, University of Tartu, Liivi 2, 50409 Tartu, Estonia* **7** *Botany Unit (Mycology), Finnish Museum of Natural History, University of Helsinki, P.O. Box 7, FI-00014, Helsinki, Finland* **8** *Department of Environmental Systems Science, ETH Zürich, Universitätstrasse 2, 8092 Zürich, Switzerland* **9** *Interaction Design and Software Engineering, Chalmers University of Technology, Lindholmsplatsen 1, 417 56 Göteborg, Sweden* **10** *Department of Clinical Science, University of Bergen, Box 7804, 5020 Bergen, Norway* **11** *Department of Functional and Evolutionary Ecology, University of Vienna, Djerassiplatz 1, A-1030 Vienna, Austria* **12** *Department of Biotechnology, Iranian Research Organization for Science and Technology, PO Box 3353-5111, Tehran 3353136846, Iran* **13** *Westerdijk Fungal Biodiversity Institute, Uppsalalaan 8, 3584 CT Utrecht, Netherlands* **14** *Department of Forest Mycology and Plant Pathology, Swedish University of Agricultural Sciences, Box 7026, 750 07 Uppsala, Sweden* **15** *Department of Mathematical Sciences, Chalmers University of Technology, Göteborg, Sweden* **16** *Natural History Museum, University of Tartu, Vanemuise 46, Tartu 51014, Estonia*

Corresponding author: R. Henrik Nilsson (henrik.nilsson@bioenv.gu.se)

Academic editor: T. Lumbsch | Received 25 February 2023 | Accepted 28 March 2023 | Published 10 April 2023

Citation: Nilsson RH, Ryberg M, Wurzbacher C, Tedersoo L, Anslan S, Põlme S, Spirin V, Mikryukov V, Svantesson S, Hartmann M, Lennartsdotter C, Belford P, Khomich M, Retter A, Corcoll N, Gómez Martinez D, Jansson T, Ghobad-Nejhad M, Vu D, Sanchez-Garcia M, Kristiansson E, Abarenkov K (2023) How, not if, is the question mycologists should be asking about DNA-based typification. MycoKeys 96: 143–157. https://doi.org/10.3897/mycokeys.96.102669

Abstract

Fungal metabarcoding of substrates such as soil, wood, and water is uncovering an unprecedented number of fungal species that do not seem to produce tangible morphological structures and that defy our best attempts at cultivation, thus falling outside the scope of the International Code of Nomenclature for algae, fungi, and plants. The present study uses the new, ninth release of the species hypotheses of the UNITE database to show that species discovery through environmental sequencing vastly outpaces traditional, Sanger sequencing-based efforts in a strongly increasing trend over the last five years. Our findings challenge the present stance of some in the mycological community – that the current situation is satisfactory and that no change is needed to "the code" – and suggest that we should be discussing not whether to allow DNA-based descriptions (typifications) of species and by extension higher ranks of fungi, but what the precise requirements for such DNA-based typifications should be. We submit a tentative list of such criteria for further discussion. The present authors hope for a revitalized and deepened discussion on DNA-based typification, because to us it seems harmful and counter-productive to intentionally deny the overwhelming majority of extant fungi a formal standing under the International Code of Nomenclature for algae, fungi, and plants.

Keywords

Dark taxa, ICN, nomenclature, species description, taxonomy, type principle

Introduction

Dark matter is an astronomical concept that denotes mass of a hitherto unknown nature. That mass is detectable indirectly through the gravity it exerts – such as the bending of passing light – but its exact nature has so far defied scientific explanation. Mycology offers an analogy in the form of dark taxa, a concept that we define as taxa that do not seem to produce tangible morphological structures and that we cannot seem to cultivate in the lab (cf. Page 2016). As with dark matter, dark taxa are chiefly detected by means other than direct observation, notably through DNA sequencing (Grossart et al. 2016; Lücking et al. 2021). The field of mycology has become intimately entwined with the concept of dark taxa in the wake of environmental metabarcoding, where seemingly dark taxa often make up more than half of the taxa recovered (e.g., Retter et al. 2019). Dark taxa seem to permeate the fungal tree of life and are known from all major fungal lineages. Indeed, more than 20 class-level lineages of fungi seem to be constituted solely by dark taxa (Tedersoo et al. 2014, 2017, 2020a). Studying the fungal kingdom without its dark components is to study a paraphyletic group, something that contemporary phylogenetic thinking advises strongly against.

Most of the present authors have spent considerable time in the company of dark fungal taxa (DFT) as recovered through environmental metabarcoding and as manifested in the UNITE database for molecular identification of fungi (Nilsson et al. 2019; Abarenkov et al. 2022). The sheer magnitude of extant sequence data from DFT signals a need to take these taxa seriously. Yet it seems to the present authors that

contemporary mycology often treats DFT as if they had a lesser – in fact, no – biological objectivity. The International Code of Nomenclature for algae, fungi, and plants (ICN; Turland et al. 2018) does not permit species descriptions typified from DNA sequences alone, and a recent effort to bring about change in this regard was overthrown by overwhelming majority (May et al. 2018). Similarly, DFT are routinely ignored in the context of, e.g., phylogenetic inference, ecology, and nature conservation (Ryberg and Nilsson 2018). Indeed, it is as if the DFT have no standing at all, scientific or otherwise. This goes very much against the experience of the present authors, who have used DFT to tease out branching orders, dominant but entirely overlooked taxa, and major ecological patterns that otherwise would have been lost on science (Nilsson et al. 2011, 2016; Khan et al. 2020; Tedersoo et al. 2022). Similarly, in an attempt to accord some taxonomic standing to the DFT, UNITE has assigned DOI-based digital identifiers to all DFT known from nuclear ribosomal internal transcribed spacer region (ITS) data to facilitate and promote unambiguous scientific communication across datasets and studies (Kõljalg et al. 2013). Although these DOI-based digital identifiers have been adopted by GenBank and the European Nucleotide Archive as LinkOuts to UNITE SH DOI pages – and were included in the Global Biodiversity Information Facility backbone classification already in 2018 (https://www.gbif.org/news/2LrgV5t3ZuGeU2WIymSEuk/adding-sequence-based-identifiers-to-backbone-taxonomy-reveals-dark-taxa-fungi) – these efforts have largely fallen short of sparking the debate they were hoping to.

In the present forum paper, we wish to visualize the relative contribution of DFT to molecular mycological species discovery over time. We do this through two molecular datasets, both of which reflect current knowledge but also biases in various ways. These datasets are: 1) all full-length fungal ITS sequences in the international nucleotide sequence database collaboration (INSDC; Arita et al. 2021) as of October 11, 2022 and 2) the five large metabarcoding datasets – chiefly of soil fungi (Ilves 2019; Tedersoo et al. 2020b, 2021; Lindahl et al. 2021; Runnel et al. 2022) – so far incorporated into the UNITE database. We find that the DFT overwhelmingly dominate the species discovery process, and it seems patently clear that extant fungal diversity presents us with patterns that cannot be accurately represented only by species defined by morphology or cultivation alone. It strikes us as unfortunate that what seems to be the absolute majority of fungi fall outside the scope of the ICN, and we hope that the present results will serve to add depth and dimension to the debate on how and when we should allow formal species descriptions based on DNA sequence data alone.

Material and method

The full flow of operation behind the UNITE database is described elsewhere (Kõljalg et al. 2013, 2020; Nilsson et al. 2019). In brief, UNITE clusters the fungal ITS sequences of INSDC jointly with the UNITE-contributed DFT ITS sequences into spe-

cies hypotheses (SHs) at distance thresholds 0.5% through to 3.0% in steps of 0.5%. These operational taxonomic units can be thought of as entities roughly at the species level. The sequences and the SHs are available for web-based interaction as well as for download in various formats (https://unite.ut.ee/repository.php).

We downloaded all sequences included in the October 2022 version 9 release of the UNITE species hypothesis system. To allow us to contrast the species discovery from taxonomic and metabarcoding studies, we made the admittedly coarse assumption that all SHs that contained at least one sequence from the INSDC could be considered as taxonomy-derived SHs, that is, SHs with some sort of footing in traditional taxonomy. In contrast, all SHs containing only metabarcoding sequences were considered to be DFT. Based on the date of initial submission of each sequence (submission to INSDC and to UNITE, respectively, for INSDC and DFT sequences), we examined the accumulation of SHs over time. We plotted the accumulation of taxonomy-derived and DFT-only SHs against date of initial discovery in R v. 4.2.2 (R Core Team 2020). We similarly plotted the number of new fungal species descriptions per year (2002–2022) based on MycoBank (Robert et al. 2013), excluding recombinations, orthographic variants, invalid names, and illegitimate names.

While there is little hope of piecing together the ecological context of these sequences in an automated way, at least there is an opportunity to visualize the country of collection for many of the sequences in INSDC and UNITE. We thus sought to illustrate the geographical component of the SH accumulation curves by summarizing the country of collection of the taxonomy-derived and DFT sequences. In total, 63% of the taxonomy-derived, and 99.9% of the DFT, sequences were tagged with an explicit country of origin. The 20 most common countries of origin in each dataset were compiled using R.

Results

We retrieved a total of 1.26 M taxonomy- (Sanger sequencing-) derived sequences from INSDC and 7.1 M metabarcoding-derived DFT sequences from UNITE (https://unite.ut.ee/repository.php). The taxonomy-derived sequences were found to stem from a total of 88,665 distinct published and unpublished studies as defined by the combination of the INSDC fields AUTHORS, TITLE, and JOURNAL. The DFT sequences were found to stem from 5 studies. The SH accumulation curves at the dynamic 1.5% similarity threshold level are shown in Fig. 1, as is the number of new species of fungi described formally during the period. Table 1 shows the top 20 countries of origin for the taxonomy-derived and DFT sequences for which this data was available. Fig. 2 shows the collection localities for all Sanger and metabarcoding sequences with geo-coordinates.

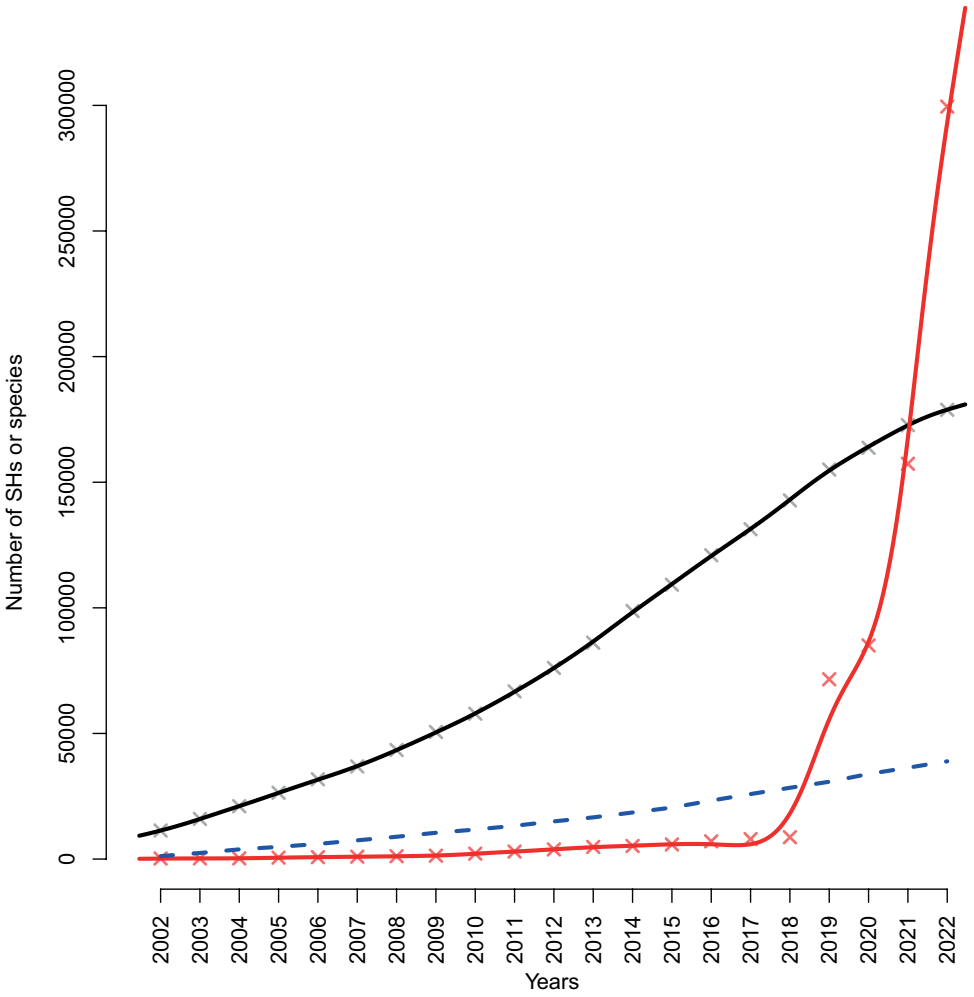

Figure 1. The accumulation of SHs at the 1.5% distance threshold over time in the Sanger (black; 88,665 studies of various sizes) and the DFT (red; 5 large studies) datasets. The Y axis depicts the number of SHs, and the X axis depicts year of sequence deposition. Solid trend lines were calculated using cubic smoothing splines. Also plotted (blue) is the cumulative number of newly described species for the period 2002–2022 (excluding recombinations, orthographic variants, invalid names, and illegitimate names). The numbers of species described in ca 2020–2022 may be slight underestimates due to widespread violation of the ICN recommendation F.5A to "inform the recognised repository of the complete bibliographic details upon publication of the name". In reality, also the Sanger (INSDC) dataset is likely to hold some proportion of DFT. DFT sequences are notoriously difficult to tell apart in an automated way from sequences that are unidentified for other reasons (Abarenkov et al. 2022). The present study errs on the side of caution by treating all Sanger sequences as taxonomy-derived, meaning that Fig. 1 presumably under-estimates the proportion of DFT in the underlying data.

Table 1. The 20 most common countries of collection for the Sanger and the DFT sequences. The DFT dataset is dominated by sequences from Estonia, from which most of the five metabarcoding studies were run. Estonia is not known as any particularly rich hotspot of biodiversity, perhaps suggesting that additional worldwide sampling would have produced even more dramatic increases in the number of DFT SHs.

INSDC country	INSDC seq.	DFT country	DFT seq.
Unknown	463524	Estonia	1788894
United States	133496	United States	350869
China	117292	Italy	287842
India	31788	Brazil	285473
Japan	29754	Czechia	260611
Brazil	27765	Russian Federation	228979
Canada	26038	Mexico	210643
Spain	22362	Norway	208422
Australia	22205	Colombia	204172
Germany	19971	Australia	177777
Italy	18078	Sweden	177318
Mexico	16326	Latvia	169168
France	14896	Lithuania	166553
Korea, Republic of	12434	Georgia	146440
Russian Federation	11668	Finland	127258
Iran, Islamic Republic of	11285	India	123706
Poland	10969	Argentina	116852
New Zealand	10956	China	100143
Thailand	10708	Papua New Guinea	96253
South Africa	10642	Tanzania, United Republic of	95203

Discussion

The present study approximated fungal species accumulation over time as deduced from taxonomic and metabarcoding efforts. We found that the DFT account for the clear majority of the new species discovered in the last five years (although some limited proportion of both the Sanger-derived and the DFT sequences may possibly correspond to described, but so far unsequenced, species). We reached this conclusion based on a very limited number of metabarcoding studies – in fact, just five – of soil fungal communities and in almost complete absence of metabarcoding data from, e.g., water, air, wood, and plant material. One can only imagine that Fig. 1 would have shown an even more dramatic trend had a wider selection of metabarcoding datasets been available in UNITE. Fig. 2 paints a similar picture with respect to the geographical coverage. It shows that whereas the sampling effort of the five metabarcoding studies was wide, it pales in comparison to that of the combined Sanger-derived studies. It is reasonable to think that at least some of the unsampled geographical regions are rich in DFT and would have contributed to an even steeper trend in Fig. 1, had they been sampled.

When data are sparse, opinions may be maintained and cherished for longer than necessary. Our results show that data are no longer sparse; DFT, in view of their di-

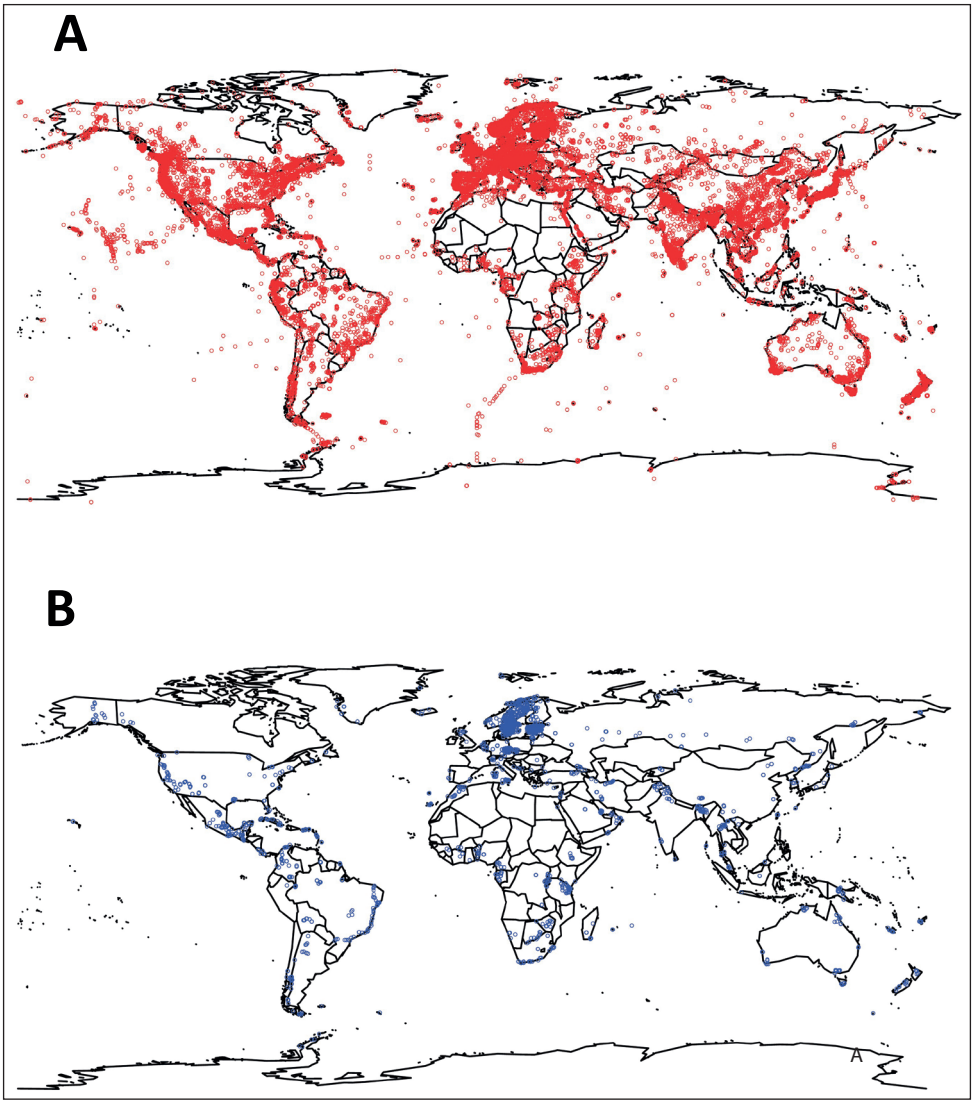

Figure 2. Maps showing the collection localities for the (**A**) Sanger sequences and (**B**) metabarcoding sequences that came with geo-coordinates (36,559 Sanger collection localities and 3,688 metabarcoding collection localities).

versity and abundance, form a major, inextricable component of the fungal kingdom. They simply cannot be ignored. It is not scientifically defensible to exclude them from mycological efforts in phylogeny, ecology, or biogeography. We therefore argue that it does not make sense to deny them a formal standing under the ICN. We feel that it is time – in fact, long overdue – to resume and deepen the discussion initiated by, e.g., Hibbett et al. (2009, 2016), Hawksworth et al. (2016), and De Beer et al. (2016) and focus the debate on what the requirements should be for DFT to be formally consid-

ered under the ICN. Clearly, morphological structures or cultivability cannot be part of those requirements. We would like to reiterate the observation of Lücking et al. (2021) that a limited number of thought-through requirements would probably suffice. These should reflect the need for scientific reproducibility and should be stringent enough that only particularly well-vetted and documented DFT can be considered for DNA-based typification and formal description. At the same time, they should be realistic and reasonable enough that formal taxonomic description does become possible for such particularly well-vetted and documented DFT. We submit the following as tentative criteria:

- All DFT should be deduced and described based on the three nuclear ribosomal markers small-subunit (SSU/18S), the intercalary ITS region, and the large-subunit (LSU/28S). Of these, the ITS region is the most likely to reflect species-level distinctness in most groups of fungi. Parts of both the LSU and perhaps to a lesser extent SSU are likely to be at least somewhat informative of the species level in many groups of fungi, and unlike the ITS region they can typically be robustly aligned beyond the genus level in the pursuit of large-scale taxonomic affiliation. An initial recovery of an interesting ITS sequence can be extended to include SSU and LSU also from environmental samples using the design of specific primers as explored by Tedersoo et al. (2017) and Wurzbacher et al. (2019). In contrast, teasing out non-contiguous and/or non-ribosomal genes and genetic markers from complex, multi-species substrates such as soil or water in a way that ensures that the ribosomal, and the non-contiguous/non-ribosomal, markers come from the same individual is likely to remain problematic for the foreseeable future. We believe that allowing description of DFT based on any genetic marker would lead to irreconcilable species definitions and datasets. Having all DFT rooted in the ribosomal markers would provide a common ground from which mycology can proceed to solve taxonomic and nomenclatural issues and complications in a non-redundant way. The ribosomal markers will presumably not differentiate all DFT at the actual species level, and we imagine that additional genetic markers may have to be targeted (once technology allows) to reflect the species level properly. However, we don't view that as a sustainable argument to allow DNA-based typification based on any genetic marker.
- A minimum length/coverage for the underlying sequence data, namely all of SSU, ITS, and LSU in their full lengths and in a contiguous stretch.
- Sufficiently high read quality.
- Stringent sequence quality control for, e.g., chimeras.
- At least two independent recoveries (each with some minimum read count in the case of metabarcoding) of the taxon across separate datasets from separate research teams from separate molecular laboratories.
- A thorough analysis of the public sequence databases for relevant additional sequences to maximize the penetration of available data and to minimize redundant descriptions.
- An underlying phylogenetic analysis based on a multiple sequence (SSU plus LSU) alignment. The new, contiguous SSU-ITS-LSU sequence(s) can then be in-

corporated into, e.g., a kingdom-wide SSU+LSU multiple sequence alignment obtained from merging the SSU+LSU alignments of James et al. (2006) and Tedersoo et al. (2018). This would allow reasonably robust phylogenetic positioning of the new sequence(s). A more fine-grained phylogenetic tree can be produced from ITS sequences only, or ITS+LSU, as alignability allows.

- Bundling of open, richly annotated raw sequence data/FASTQ/chromatograms and metadata on, e.g., the ecological and geographical specifics of the sampling sites.
- Publication in a peer-reviewed scientific journal with a formal impact factor or perhaps in any of a list of peer-reviewed journals revised annually by the Nomenclature Committee for Fungi or the International Commission on the Taxonomy of Fungi. The purpose would be to curtail mass description of DFT species through, e.g., self-publication or outlets not regularly considered by the mycological community.
- It furthermore seems reasonable to us to allow DNA sequences as types only in fungal groups that are predominantly or exclusively dark at, say, the order or supra-order level. We would be against DNA-based typifications in groups where morphological structures and/or cultivation may be within reach (e.g., *Agaricales* and *Hypocreales*). The order *Archaeorhizomycetales* may serve as an example of what a "predominantly" dark lineage could be. Soil sequencing has revealed an enormous species-level diversity within this order, yet cultures (and thus names) have been successfully worked out for only two species (Khan et al. 2020). The present authors are for DNA-based typifications in this order. While both *Agaricales* and *Hypocreales* can be expected to feature DFT, we are against DNA-based typification in these orders.
- At least one mycological taxonomist should be involved in the description of DFT (indeed, all fungi). There is no shortage of potential complications that, if overlooked, could lead to needless and haphazard introduction of new species and genera in DFT and beyond. For instance, it is well known that some extant genera offer examples of very divergent ITS (or other ribosomal) regions (e.g., *Basidiodendron*, *Oliveonia*, and *Cantharellus*; Feibelman et al. 1994; Alm Rosenblad et al. 2016, 2022). When considered in isolation and out of context – in, say, a molecular ecology dataset – such sequences could be incorrectly interpreted to warrant new species and genus descriptions. Needless to say, the present authors are against premature description of species and other taxonomic groups. While the concept of "a mycological taxonomist" may be amorphous, we submit the definition "someone who has [co-]authored at least one fungal species name as indexed in Index Fungorum/MycoBank/Fungal Names" for further discussion.

There is clearly room for refinement of the requirements mentioned here, and we are furthermore certain that the mycological community can come up with additional prerequisites to further increase stringency and reduce the risk for haphazard, more or less irreproducible or irresponsible use of DNA sequences as types (cf. Hibbett et al. 2016; Lücking et al. 2018; Zamora et al. 2018; Renner 2021). The present authors warmly welcome – indeed, invite – such a discussion. We understand that a special purpose committee for DNA-based typification under the auspices of the Nomenclature Committee for Fungi (http://www.ima-mycology.org/nomenclature/

nomenclature-committee-fungi) will be put together and will hold an introductory meeting in April 2023. To that committee we would like to stress the urgency and the high stakes of the situation at hand.

It could be argued that a separate nomenclature code should be erected for the DFT, akin perhaps to the *Candidatus* concept in bacteria (Murray and Stackebrandt 1995; Pallen 2021) or to the extant DOI-based species identifiers of UNITE. We remain sceptical, however, and we argue for full-fledged integration of the DFT into the ICN. It seems likely to us that DFT as governed by a separate and more or less unofficial code or naming convention would simply remain relegated to some state of secondary – in practice, no – importance in the eyes of large parts of the mycological community and beyond. That is not the message delivered by Fig. 1, however, and not a state fit to reflect the crucial roles fungi are increasingly understood to play in the ecosystems of the world – by the scientific community and the general public alike. On the contrary, DFT seem to dominate the fungal kingdom. This puts the ICN in a position where it governs an ever-dwindling proportion of the extant fungi – maybe just some few percent. Such a position would seem untenable and, ultimately, vulnerable to usurpation. After all, the new and rebellious prokaryotic SeqCode (Hedlund et al. 2022) grew out of frustration at the inability of the International Code of Nomenclature of Prokaryotes (ICNP) to adapt enough to be able to reflect extant prokaryotic diversity properly. Naturally enough, the SeqCode makes no specific provisions for eukaryotes (or viruses, for that matter; Simmonds et al. 2017) at this stage, although we suppose that there is nothing – at least in principle – that would rule out such an expansion of target groups and inclusiveness over time. While the ultimate fate of SeqCode remains to be seen (Marinov et al. 2022), it does set an example of what the future may hold in store for ICN should DFT continue to be ignored. The present authors feel that it would be much better to modify the ICN than to consider more drastic actions. Specifically, we argue that formal scientific names for DFT are necessary for them to be taken seriously. Similarly, formal names will in practice be needed in biological conservation and in efforts exploring DFT for, e.g., medical and industrial use. These fungi deserve and need formal names, and it is our firm belief and opinion that this is achievable.

Acknowledgements

The GenBank staff is gratefully acknowledged for assistance with establishing the date of submission for the INSDC entries. We thank Nathan Smith for useful feedback on scientific publishing and mycological journals. David Hibbett and Conrad Schoch are acknowledged for valuable feedback on an earlier draft of the manuscript. Konstanze Bensch and MycoBank are acknowledged for assistance with species description statistics. The work of KA was supported by the Estonian Research Council (grant PRG1170).

References

Abarenkov K, Kristiansson E, Ryberg M, Nogal-Prata S, Gómez-Martínez D, Stüer-Patowsky K, Jansson T, Põlme S, Ghobad-Nejhad M, Corcoll N, Scharn R, Sánchez-García M, Khomich M, Wurzbacher C, Nilsson RH (2022) The curse of the uncultured fungus. MycoKeys 86: 177–194. https://doi.org/10.3897/mycokeys.86.76053

Alm Rosenblad M, Martín MP, Tedersoo L, Ryberg M, Larsson E, Wurzbacher C, Abarenkov K, Nilsson RH (2016) Detection of signal recognition particle (SRP) RNAs in the nuclear ribosomal internal transcribed spacer 1 (ITS1) of three lineages of ectomycorrhizal fungi (Agaricomycetes, Basidiomycota). MycoKeys 13: 21–33. https://doi.org/10.3897/mycokeys.13.8579

Alm Rosenblad M, Larsson E, Walker A, Thongklang N, Wurzbacher C, Nilsson RH (2022) Evidence for further non-coding RNA genes in the fungal rDNA region. MycoKeys 90: 203–213. https://doi.org/10.3897/mycokeys.90.84866

Arita M, Karsch-Mizrachi I, Cochrane G (2021) The international nucleotide sequence database collaboration. Nucleic Acids Research 49(D1): D121–D124. https://doi.org/10.1093/nar/gkaa967

De Beer ZW, Marincowitz S, Duong TA, Kim JJ, Rodrigues A, Wingfield MJ (2016) *Hawksworthiomyces* gen. nov. (*Ophiostomatales*), illustrates the urgency for a decision on how to name novel taxa known only from environmental nucleic acid sequences (ENAS). Fungal Biology 120(11): 1323–1340. https://doi.org/10.1016/j.funbio.2016.07.004

Feibelman T, Bayman P, Cibula WG (1994) Length variation in the internal transcribed spacer of ribosomal DNA in chanterelles. Mycological Research 98(6): 614–618. https://doi.org/10.1016/S0953-7562(09)80407-3

Grossart H-P, Wurzbacher C, James T, Kagami M (2016) Discovery of dark matter fungi in aquatic ecosystems demands a reappraisal of the phylogeny and ecology of zoosporic fungi. Fungal Ecology 19: 28–38. https://doi.org/10.1016/j.funeco.2015.06.004

Hawksworth DL, Hibbett DS, Kirk PM, Lücking R (2016) [308–310] Proposals to permit DNA sequence data to serve as types of names of fungi. Taxon 65(4): 899–900. https://doi.org/10.12705/654.31

Hedlund BP, Chuvochina M, Hugenholtz P, Konstantinidis KT, Murray AE, Palmer M, Parks DH, Probst AJ, Reysenbach A-L, Rodriguez LM, Rossello-Mora R, Sutcliffe IC, Venter SN, Whitman WB (2022) SeqCode: A nomenclatural code for prokaryotes described from sequence data. Nature Microbiology 7(10): 1702–1708. https://doi.org/10.1038/s41564-022-01214-9

Hibbett DS, Ohman A, Kirk PM (2009) Fungal ecology cathes fire. The New Phytologist 184(2): 279–282. https://doi.org/10.1111/j.1469-8137.2009.03042.x

Hibbett D, Abarenkov K, Kõljalg U, Öpik M, Chai B, Cole J, Wang Q, Crous P, Robert V, Helgason T, Herr JR, Kirk P, Lueschow S, O'Donnell K, Nilsson RH, Oono R, Schoch C, Smyth C, Walker DM, Porras-Alfaro A, Taylor JW, Geiser GM (2016) Sequence-based classification and identification of Fungi. Mycologia 108(6): 1049–1068. https://doi.org/10.3852/16-130

Ilves K (2019) Tartu Botanical Garden Root and Leaf Endophytes. PlutoF. Occurrence dataset. https://doi.org/10.15468/mbgysk [accessed via GBIF.org on 2023-03-23]

James TY, Kauff F, Schoch CL, Matheny PB, Hofstetter V, Cox CJ, Celio G, Gueidan C, Fraker E, Miadlikowska J, Lumbsch HT, Rauhut A, Reeb V, Arnold AE, Amtoft A, Stajich JE, Hosaka K, Sung G-H, Johnson D, O'Rourke B, Crockett M, Binder M, Curtis JM, Slot JC, Wang Z, Wilson AW, Schüßler A, Longcore JE, O'Donnell K, Mozley-Standridge S, Porter D, Letcher PM, Powell MJ, Taylor JW, White MW, Griffith GW, Davies DR, Humber RA, Morton JB, Sugiyama J, Rossman AY, Rogers JD, Pfister DH, Hewitt D, Hansen K, Hambleton S, Shoemaker RA, Kohlmeyer J, Volkmann-Kohlmeyer B, Spotts RA, Serdani M, Crous PW, Hughes KW, Matsuura K, Langer E, Langer G, Untereiner WA, Lücking R, Büdel B, Geiser DM, Aptroot A, Diederich P, Schmitt I, Schultz M, Yahr R, Hibbett DS, Lutzoni F, McLaughlin DJ, Spatafora JW, Vilgalys R (2006) Reconstructing the early evolution of Fungi using a six-gene phylogeny. Nature 443(7113): 818–822. https://doi.org/10.1038/nature05110

Khan F, Kluting K, Tångrot J, Urbina H, Ammunet T, Sahraei SE, Rydén M, Ryberg M, Rosling A (2020) Naming the untouchable–environmental sequences and niche partitioning as taxonomical evidence in fungi. IMA Fungus 11(1): 1–12. https://doi.org/10.1186/s43008-020-00045-9

Kõljalg U, Nilsson RH, Abarenkov K, Tedersoo L, Taylor AFS, Bahram M, Bates ST, Bruns TD, Bengtsson-Palme J, Callaghan TM, Douglas B, Drenkhan T, Eberhardt U, Dueñas M, Grebenc T, Griffith GW, Hartmann M, Kirk PM, Kohout P, Larsson E, Lindahl BD, Lücking R, Martín MP, Matheny PB, Nguyen NH, Niskanen T, Oja J, Peay KG, Peintner U, Peterson M, Põldmaa K, Saag L, Saar I, Schüßler A, Scott JA, Senés C, Smith ME, Suija A, Taylor DL, Telleria MT, Weiss M, Larsson K-H (2013) Towards a unified paradigm for sequence-based identification of fungi. Molecular Ecology 22(21): 5271–5277. https://doi.org/10.1111/mec.12481

Kõljalg U, Nilsson HR, Schigel D, Tedersoo L, Larsson K-H, May TW, Taylor AFS, Stjernegaard Jeppesen T, Guldberg Frøslev T, Lindahl BD, Põldmaa K, Saar I, Suija A, Savchenko A, Yatsiuk I, Adojaan K, Ivanov F, Piirmann T, Pöhönen R, Zirk A, Abarenkov K (2020) The taxon hypothesis paradigm – On the unambiguous detection and communication of taxa. Microorganisms 8(12): e1910. https://doi.org/10.3390/microorganisms8121910

Lindahl BD, Kyaschenko J, Varenius K, Clemmensen KE, Dahlberg A, Karltun E, Stendahl J (2021) A group of ectomycorrhizal fungi restricts organic matter accumulation in boreal forest. Ecology Letters 24(7): 1341–1351. https://doi.org/10.1111/ele.13746

Lücking R, Kirk PM, Hawksworth DL (2018) Sequence-based nomenclature: A reply to Thines et al. and Zamora et al. and provisions for an amended proposal "from the floor" to allow DNA sequences as types of names. IMA Fungus 9(1): 185–198. https://doi.org/10.5598/imafungus.2018.09.01.12

Lücking R, Aime MC, Robbertse B, Miller AN, Aoki T, Ariyawansa HA, Cardinali G, Crous PW, Druzhinina IS, Geiser DM, Hawksworth DL, Hyde KD, Irinyi L, Jeewon R, Johnston PR, Kirk PM, Malosso E, May TW, Meyer W, Nilsson RH, Öpik M, Robert V, Stadler S, Thines M, Vu D, Yurkov AM, Zhang N, Schoch CL (2021) Fungal taxonomy and sequence-based nomenclature. Nature Microbiology 6(5): 540–548. https://doi.org/10.1038/s41564-021-00888-x

Marinov M, Fitzhugh K, Reis RE, Engel MS (2022) Putting the cart before the horse: SeqCode's attempt to solve systematics issues with changes to nomenclature. Bionomina 31(1): 97–107. https://doi.org/10.11646/bionomina.31.1.6

May TW, Redhead SA, Lombard L, Rossman AY (2018) XI International Mycological Congress: Report of Congress action on nomenclature proposals relating to fungi. IMA Fungus 9(2): xxii–xxvii. https://doi.org/10.1007/BF03449448

Murray RGE, Stackebrandt E (1995) Taxonomic note: Implementation of the provisional status Candidatus for incompletely described prokaryotes. International Journal of Systematic Bacteriology 45(1): 195–196. https://doi.org/10.1099/00207713-45-1-186

Nilsson RH, Ryberg M, Sjökvist E, Abarenkov K (2011) Rethinking taxon sampling in the light of environmental sequencing. Cladistics 27(2): 197–203. https://doi.org/10.1111/j.1096-0031.2010.00336.x

Nilsson RH, Wurzbacher C, Bahram M, Coimbra VRM, Larsson E, Tedersoo L, Eriksson J, Duarte C, Svantesson S, Sánchez-García M, Ryberg MK, Kristiansson E, Abarenkov K (2016) Top 50 most wanted fungi. MycoKeys 12: 29–40. https://doi.org/10.3897/mycokeys.12.7553

Nilsson RH, Larsson KH, Taylor AFS, Bengtsson-Palme J, Jeppesen TS, Schigel D, Kennedy P, Picard K, Glöckner FO, Tedersoo L, Saar I, Kõljalg U, Abarenkov K (2019) The UNITE database for molecular identification of fungi: Handling dark taxa and parallel taxonomic classifications. Nucleic Acids Research 47(D1): D259–D264. https://doi.org/10.1093/nar/gky1022

Page DM (2016) DNA barcoding and taxonomy: Dark taxa and dark texts. Philosophical Transactions of the Royal Society of London. Series B, Biological Sciences 371(1702): e20150334. https://doi.org/10.1098/rstb.2015.0334

Pallen MJ (2021) The status *Candidatus* for uncultured taxa of Bacteria and Archaea: SWOT analysis. International Journal of Systematic and Evolutionary Microbiology 71(9): 1–9. https://doi.org/10.1099/ijsem.0.005000

R Core Team (2020) R: A language and environment for statistical computing. R Foundation for Statistical Computing, Vienna. https://www.R-project.org/

Renner SS (2021) (093–096) Proposals to permit nuclear DNA sequences as nomenclatural types when preservation of specimens is not feasible. Taxon 70(6): 1380–1381. https://doi.org/10.1002/tax.12607

Retter A, Nilsson RH, Bourlat SJ (2019) Exploring the taxonomic composition of two fungal communities on the Swedish west coast through metabarcoding. Biodiversity Data Journal 7: e35332. https://doi.org/10.3897/BDJ.7.e35332

Robert V, Vu D, Amor ABH, van de Wiele N, Brouwer C, Jabas B, Szoke S, Dridi A, Triki M, Daoud SB, Chouchen O, Vaas L, de Cock A, Stalpers JA, Stalpers D, Verkley GJM, Groenewald M, Dos Santos FB, Stegehuis G, Li W, Wu L, Zhang R, Ma J, Zhou M, Gorjón SP, Eurwilaichitr L, Ingsriswang S, Hansen K, Schoch C, Robbertse B, Irinyi L, Meyer W, Cardinali G, Hawksworth DL, Taylor JW, Crous PW (2013) MycoBank gearing up for new horizons. IMA Fungus 4(2): 371–379. https://doi.org/10.5598/imafungus.2013.04.02.16

Runnel K, Abarenkov K, Copoț O, Mikryukov V, Kõljalg U, Saar I, Tedersoo L (2022) DNA barcoding of fungal specimens using PacBio long-read high-throughput sequencing. Molecular Ecology Resources 22(8): 2871–2879. https://doi.org/10.1111/1755-0998.13663

Ryberg M, Nilsson RH (2018) New light on names and naming of dark taxa. MycoKeys 30: 31–39. https://doi.org/10.3897/mycokeys.30.24376

Simmonds P, Adams MJ, Benkő M, Breitbart M, Brister JR, Carstens EB, Davison AJ, Delwart E, Gorbalenya AE, Harrach B, Hull R, King AMQ, Koonin EV, Krupovic M, Kuhn JH, Lefkowitz EJ, Nibert ML, Orton R, Roossinck MJ, Sabanadzovic S, Sullivan MB, Suttle CA, Tesh RB, van der Vlugt RA, Varsani A, Zerbini FM (2017) Virus taxonomy in the age of metagenomics. Nature Reviews. Microbiology 15(3): 161–168. https://doi.org/10.1038/nrmicro.2016.177

Tedersoo L, Bahram M, Põlme S, Kõljalg U, Yorou NS, Wijesundera R, Abell S, Villarreal Ruiz L, Thu PQ, Suija A, Smith ME, Sharp C, Saluveer E, Saitta A, Rosas M, Riit T, Ratkowsky D, Pritsch K, Põldmaa K, Piepenbring M, Phosri C, Peterson M, Parts K, Pärtel K, Vasco-Palacios AM, Otsing E, Nouhra E, Njouonkou AL, Nilsson RH, Mayor J, May TW, Majuakim L, Lee SS, Larsson K-H, Kohout P, Hosaka K, Hiiesalu I, Henkel TW, Harend H, Guo L-D, Greslebin A, Grelet G, Geml J, Morgado LN, Gates G, Dunstan W, Dunk C, Drenkhan R, Dearnaley J, De Kesel A, Dang T, Chen X, Buegger F, Brearley FQ, Bonito G, Anslan S, Abarenkov K (2014) Global diversity and geography of soil fungi. Science 346(6213): e1256688. https://doi.org/10.1126/science.1256688

Tedersoo L, Bahram M, Puusepp R, Nilsson RH, James TY (2017) Novel soil-inhabiting clades fill gaps in the fungal tree of life. Microbiome 5(1): 1–10. https://doi.org/10.1186/s40168-017-0259-5

Tedersoo L, Sánchez-Ramírez S, Kõljalg U, Bahram M, Döring M, Schigel D, May T, Ryberg M, Abarenkov K (2018) High-level classification of the Fungi and a tool for evolutionary ecological analyses. Fungal Diversity 90(1): 135–159. https://doi.org/10.1007/s13225-018-0401-0

Tedersoo L, Anslan S, Bahram M, Kõljalg U, Abarenkov K (2020a) Identifying the 'unidentified' fungi: A global-scale long-read third-generation sequencing approach. Fungal Diversity 103(1): 273–293. https://doi.org/10.1007/s13225-020-00456-4

Tedersoo L, Anslan S, Bahram M, Drenkhan R, Pritsch K, Buegger F, Padari A, Hagh-Doust N, Mikryukov V, Gohar D, Amiri R, Hiiesalu I, Lutter R, Rosenvald R, Rähn E, Adamson K, Drenkhan T, Tullus H, Jürimaa K, Sibul I, Otsing E, Põlme S, Metslaid M, Loit K, Agan A, Puusepp R, Varik I, Kõljalg U, Abarenkov K (2020b) Regional-scale in-depth analysis of soil fungal diversity reveals strong pH and plant species effects in northern Europe. Frontiers in Microbiology 11: e1953. https://doi.org/10.3389/fmicb.2020.01953

Tedersoo L, Mikryukov V, Anslan S, Bahram M, Khalid AN, Corrales A, Agan A, Vasco-Palacios A-M, Saitta A, Antonelli A, Rinaldi AC, Verbeken A, Sulistyo BP, Tamgnoue B, Furneaux B, Ritter CD, Nyamukondiwa C, Sharp C, Marín C, Dai DQ, Gohar D, Sharmah D, Biersma EM, Cameron EK, De Crop E, Otsing E, Davydov EA, Albornoz FE, Brearley FQ, Buegger F, Gates G, Zahn G, Bonito G, Hiiesalu I, Hiiesalu I, Zettur I, Barrio IC, Pärn J, Heilmann-Clausen J, Ankuda J, Kupagme JY, Sarapuu J, Maciá-Vicente JG, Fovo JD, Geml J, Alatalo JM, Alvarez-Manjarrez J, Monkai J, Põldmaa K, Runnel K, Adamson K, Bråthen KA, Pritsch K, Tchan KI, Armolaitis K, Hyde KD, Newsham KK,

Panksep K, Adebola LA, Lamit LJ, Saba M, da Silva Cáceres ME, Tuomi M, Gryzenhout M, Bauters M, Bálint M, Wijayawardene N, Hagh-Doust N, Yorou NS, Kurina O, Mortimer PE, Meidl P, Nilsson RH, Puusepp R, Casique-Valdés R, Drenkhan R, Garibay-Orijel R, Godoy R, Alfarraj S, Rahimlou S, Põlme S, Dudov SV, Mundra S, Ahmed T, Netherway T, Henkel TW, Roslin T, Fedosov VE, Onipchenko VG, Yasanthika WAE, Lim YW, Piepenbring M, Klavina D, Kõljalg U, Abarenkov K (2021) The Global Soil Mycobiome consortium dataset for boosting fungal diversity research. Fungal Diversity 111(1): 573–588. https://doi.org/10.1007/s13225-021-00493-7

Tedersoo L, Mikryukov V, Zizka A, Bahram M, Hagh-Doust N, Anslan S, Prylutskyi O, Delgado-Baquerizo M, Maestre FT, Pärn J, Öpik M, Moora M, Zobel M, Espenberg M, Mander U, Khalid AN, Corrales A, Agan A, Vasco-Palacios A-V, Saitta A, Rinaldi AC, Verbeken A, Sulistyo BP, Tamgnoue B, Furneaux B, Ritter CD, Nyamukondiwa C, Sharp C, Marín C, Gohar D, Klavina D, Sharmah D, Dai DQ, Nouhra E, Biersma EM, Rähn E, Cameron EK, De Crop E, Otsing E, Davydov EA, Albornoz FE, Brearley FQ, Buegger F, Zahn G, Bonito G, Hiiesalu I, Barrio IC, Heilmann-Clausen J, Ankuda J, Kupagme JY, Maciá-Vicente JG, Fovo JD, Geml J, Alatalo JM, Alvarez-Manjarrez J, Põldmaa K, Runnel K, Adamson K, Bråthen KA, Pritsch K, Tchan KI, Armolaitis K, Hyde KD, Newsham KK, Panksep K, Lateef AA, Tiirmann L, Hansson L, Lamit LJ, Saba M, Tuomi M, Gryzenhout M, Bauters M, Piepenbring M, Wijayawardene N, Yorou NS, Kurina O, Mortimer PE, Meidl P, Kohout P, Nilsson RH, Puusepp R, Drenkhan R, Garibay-Orijel R, Godoy R, Alkahtani S, Rahimlou S, Dudov SV, Põlme S, Ghosh S, Mundra S, Ahmed T, Netherway T, Henkel TW, Roslin T, Nteziryayo V, Fedosov VE, Onipchenko VG, Yasanthika WAE, Lim YW, Soudzilovskaia NA, Antonelli A, Kõljalg U, Abarenkov K (2022) Global patterns in endemicity and vulnerability of soil fungi. Global Change Biology 28(22): 6696–6710. https://doi.org/10.1111/gcb.16398

Turland NJ, Wiersema JH, Barrie FR, Greuter W, Hawksworth DL, Herendeen PS, Knapp S, Kusber W-H, Li D-Z, Marhold K, May TW, McNeill J, Monro AM, Prado J, Price MJ, Smith GF (2018) International Code of Nomenclature for algae, fungi, and plants (Shenzhen Code) adopted by the Nineteenth International Botanical Congress Shenzhen, China, July 2017. Regnum Vegetabile 159. Koeltz Botanical Books, Glashütten. https://doi.org/10.12705/Code.2018

Wurzbacher C, Larsson E, Bengtsson-Palme J, Van den Wyngaert S, Svantesson S, Kristiansson E, Kagami M, Nilsson RH (2019) Introducing ribosomal tandem repeat barcoding for fungi. Molecular Ecology Resources 19(1): 118–127. https://doi.org/10.1111/1755-0998.12944

Zamora JC, Svensson M, Kirschner R, Olariaga I, Ryman S, Parra LA, Geml J, Rosling A, Adamčík S, Ahti T, Aime MC, Ainsworth AM, Albert L, Albertó E, García AA, Ageev D, Agerer R, Aguirre-Hudson B, Ammirati J, Andersson H, Angelini C, Antonín V, Aoki T, Aptroot A, Argaud D, Sosa BIA, Aronsen A, Arup U, Asgari B, Assyov B et al. (2018) Considerations and consequences of allowing DNA sequence data as types of fungal taxa. IMA Fungus 9(1): 167–175. https://doi.org/10.5598/imafungus.2018.09.01.10

MycoKeys 96: 159–171 (2023)
doi: 10.3897/mycokeys.96.101745
https://mycokeys.pensoft.net

RESEARCH ARTICLE

A peer-reviewed open-access journal
MycoKeys
Launched to accelerate biodiversity research

Two new species of genus *Leucoagaricus* (Agaricaceae, Agaricales) from Pakistan

Shazia Ashraf[1], Arooj Naseer[1], Muhammad Usman[1], Abdul Nasir Khalid[1]

1 *Fungal Biology and Systematics Research Laboratory, Institute of Botany, University of the Punjab, Quaid-e-Azam Campus 54590, Lahore, Pakistan*

Corresponding author: Arooj Naseer (arooj.hons@pu.edu.pk)

Academic editor: María P. Martín | Received 10 February 2023 | Accepted 26 March 2023 | Published 10 April 2023

Citation: Ashraf S, Naseer A, Usman M, Khalid AN (2023) Two new species of genus *Leucoagaricus* (Agaricaceae, Agaricales) from Pakistan. MycoKeys 96: 159–171. https://doi.org/10.3897/mycokeys.96.101745

Abstract

The genus of basidiomycetous fungi, *Leucoagaricus*, occurs worldwide, from subtropical to boreal latitudes. Several collections of *Leucoagaricus* were made during mycological field trips conducted in different forests of Margalla, Pakistan. An integrative framework combining morphological and phylogenetic data was employed for their study. As a result, the two species *La. margallensis* and *La. glareicolor* are here described as new to science. Detailed macro- and micro-morphological descriptions, and a molecular phylogenetic reconstruction based on nrITS and LSU sequence data are provided and used to discriminate the new species from morphologically and phylogenetically close taxa. Whereas, our phylogenetic tree inference gave unequivocal support for the inclusion of these two species within the section *Leucoagaricus*.

Keywords

Bayesian analysis, Islamabad, Margalla, systematics

Introduction

The genus *Leucoagaricus* Locq. ex Singer, is a relatively well known mushroom-forming genus of basidiomycetous fungi, characterized by the small to medium-sized, thin or fleshy basidiomata; pileus surfaces ranges from radially fibrillose, floccose, squamulose to fibrillose-scaly or rarely granulose; entire or very short striated margins; and central, equal to bulbous stipe that have membranous, sometimes movable annuli; thin-walled and smooth basidiospores generally lack well-defined germ pores; and the pileipellis is

either a trichoderm or a cutis of repent and radially arranged hyphae lacking sphaerocysts (Singer 1986; Vellinga 2001).

Taxonomic studies on *Leucoagaricus* throughout the whole of Pakistan are, in fact, scant. Only 12 species of *Leucoagaricus* have been reported from Pakistan so far (Ahmad et al. 1997; Ge et al. 2015; Qasim et al. 2015; Hussain et al. 2018; Usman and Khalid 2018; Ullah et al. 2019; Asif et al. 2021). All in all, further research on the diversity of this genus in the whole region is required. The aim of the present work is to provide new insights about the diversity of *Leucoagaricus* species from Pakistan.

Materials and methods

Morphological and anatomical studies

Basidiomata were collected following Lodge et al. (2014) and photographed in their natural habitats using a Nikon D70S camera. Morphological features were recorded from fresh specimens. Colors were designated with reference to mColorMeter application (Yanmei He, Mac App Store). Collections of the newly described species were deposited in the Herbarium of the Department of Botany, University of the Punjab, Lahore, Pakistan (acronym LAH). Microscopic characters are based on freehand sections from fresh and dried specimens mounted in 5% (w/v) aqueous Potassium Hydroxide (KOH) solution and examined using a Meiji Techno MX4300H compound microscope. A total of 30 basidiospores, basidia, cystidia and hyphae from pilei were measured from each collection. For basidiospores, the abbreviation "*n/m/p*" indicates *n* basidiospores measured from *m* fruit bodies of *p* collections. Dimensions for basidiospores are given using length × width (L × W), and extreme values are given in parentheses. The range contains a minimum of 90% of the values. Measurements include the arithmetic mean of spore length and width.

Laboratory procedures, sequence alignment and phylogenetic analyses

Genomic DNA was extracted from portions of lamellae following a modified CTAB extraction method (Bruns 1995). ITS and LSU regions of nuclear rDNA were amplified using the pairs of primers ITS1F-ITS4B and LR0R-LR5 (Vilgalys and Hester 1990; White et al. 1990; Gardes and Bruns 1993). Polymerase chain reactions (PCR) were performed in a total volume of 25 µL and consisted of an initial 4 minutes denaturation step at 94 °C, 40 cycles of 1 minute at 94 °C, 1 min at 55 °C, 1 min at 72 °C, and a final extension step of 10 minutes at 72 °C. Visualization of PCR products on a 1.5% agarose electrophoretic gel was done staining with SYBR Green. Successful amplicons were purified by enzymatic purification using Exonuclease I and Shrimp Alkaline Phosphatase enzymes (Werle et al. 1994). Bidirectional sequencing of purified products was done by Macrogen (Republic of Korea). Chromatograms were checked and assembled using SeqmanII v.5.07 (Dnastar Inc.). Once sequences were assembled and edited they were deposited in GenBank (http://www.ncbi.nlm.nih.gov).

The online tool BLAST and the databases GenBank (http://www.ncbi.nlm.nih.gov/) was used to check for possible PCR-product contamination and to identify and retrieve available, highly similar *Leucoagaricus* nrITS and LSU sequences to the newly produced sequences. A comprehensive representation of currently available sequences, in NCBI database with similarity up to 92% identity and 95% query cover for ITS Phylogenetic tree and 95% identity and 98% query cover for LSU Phylogenetic tree, were used for the phylogenetic analyses and all the sequence of section *Leucoagaricus* from recent publications were also included. The final dataset consists of 54 sequences as ingroup and one sequence of *Cystolepiota seminuda* (Lasch) Bon (AY176350 for ITS and AY176351 for LSU) from the Netherlands was used as outgroup. The dataset for the phylogenetic tree was made by MUSCLE alignment in SEA VIEW software version 5.0.5 (Gouy et al. 2010). The final Maximum Likelihood phylogram was made in RAxML-HPC2 using XSEDE tool (8.2.10) with 1000 bootstrap values. We used jModelTest 2.1.6 (Darriba et al. 2012) to verify the best nucleotide substitution model, using the Akaike information criterion. The Maximum Likelihood analyses were performed using RAxML v.8 (Stamatakis 2014), with the GTRGAMMA model and 1000 replicates. Phylogenetic analyses were based on maximum likelihood (ML) and Bayesian (B/MCMC) approaches, performed on the Cipres Science Gateway webserver (https://www.phylo.org/). The ML analysis was performed using RAxML v.8 (Stamatakis 2014), with the GTRGAMMA model and 1000 bootstrap replicates. Branches with bootstrap values ≥ 80% for ML were considered to be supported.

For the tree reconstruction based on Bayesian inference, the program MrBayes 3.2.7 (Ronquist et al. 2012) was used with two parallel Markov chain Monte Carlo (MCMC) chains with 10 million generations, saving every 1000th tree. The first 25% of the sampled trees was discarded as burn-in and 50% percent majority rule tree was generated along with posterior probabilities (PPs) of ≥0.80 by FigTree v. 1.4.2 (Rambaut 2012). Newly generated sequences were deposited in GenBank.

Results

Phylogenetic analyses (Figs 1, 2)

Sequences of the nr DNA ITS region basidiomata MH63 (LAH37453), MH111 (LAH37454), MH65 (LAH37575) and MH169 (LAH37456) were obtained with both primers and the final sequences consisted of 780, 770, 753, and 656 base pairs, respectively and 1090, 936, 977 and 953 base pairs, respectively for LSU. These four samples belong to two different taxa described here under the name of *Leucoagaricus margallensis* and *Leucoagaricus glareicolor*. For ITS, the aligned final dataset comprised 719 characters including gaps; out of these, 422 characters were conserved, 286 were variable, 199 were parsimony informative and 87 were singletons. For LSU, the aligned final dataset comprised 947 characters including gaps; out of these, 763 characters were conserved, 178 were variable, 131 were parsimony informative and 47 were singletons. Our taxa are separating from their closest species with strong bootstrap value of 100 for ML and 1 PP for BI and there was no conflict in both analyses in the position of our taxa.

Figure 1. Molecular phylogenetic analyses by maximum likelihood (ML) and Bayesian Inference (BI) method based on ITS sequences. Bootstrap and Posterior probability values are shown at the branches as ML/BI and novel sequences generated during this study are in bold.

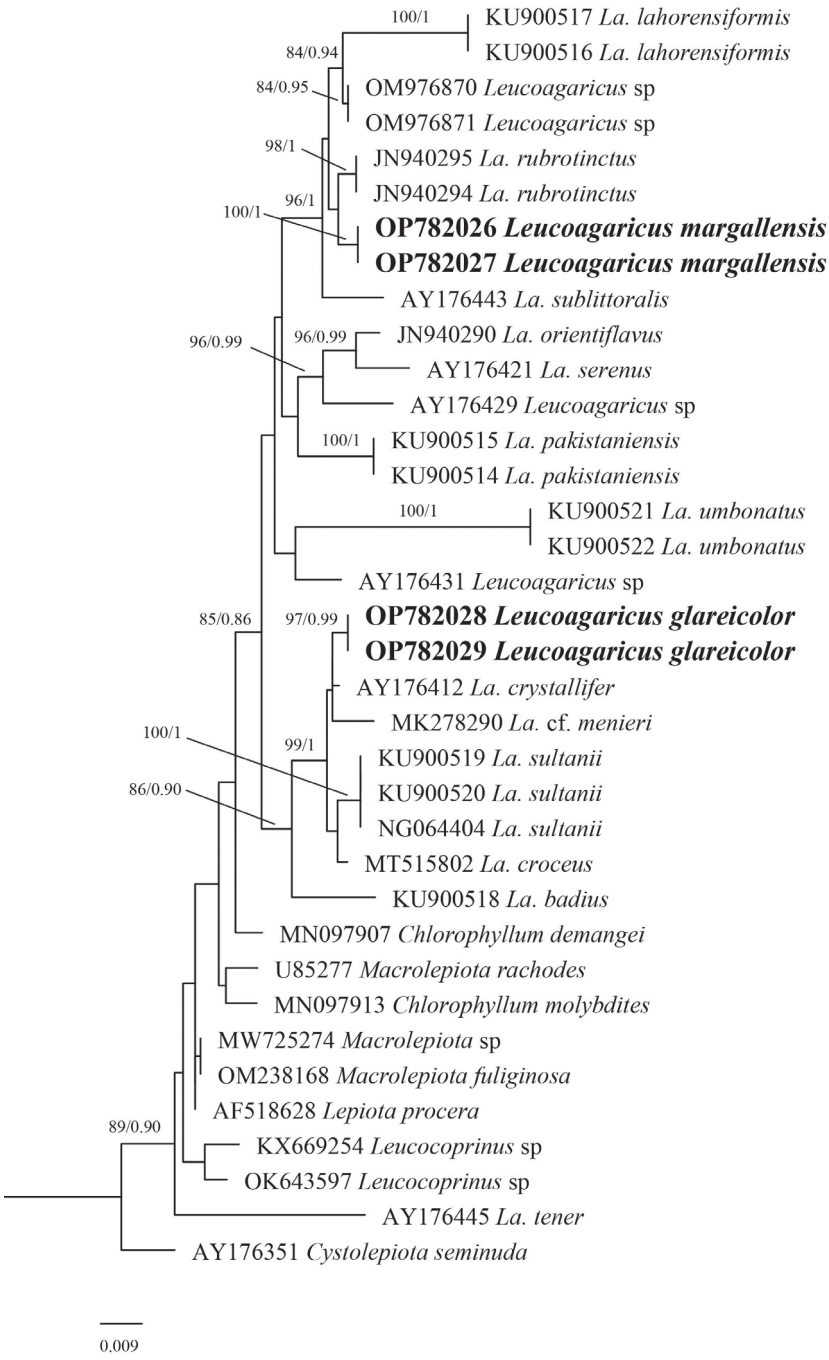

Figure 2. Molecular phylogenetic analyses by maximum likelihood (ML) and Bayesian Inference (BI) method based on LSU sequences. Bootstrap and Posterior probability values are shown at the branches as ML/BI and novel sequences generated during this study are in bold.

Taxonomy

Leucoagaricus margallensis **Ashraf, S., Naseer, A. & Khalid, A.N., sp. nov.**
MycoBank No: 846300
Figs 3, 4

Etymology. The specific epithet *margallensis* (Latin) refers to type locality Margalla.

Diagnosis. *Leucoagaricus margallensis* can be distinguished by small, umbonate pileus with minute, fragile annulus, bulbous stipe, smaller basidiospores (6.27 × 4.67 μm) and cheilocystidia without crystals on its apex.

Holotype. Pakistan, Islamabad, Margalla Hills National park, trail 5, 33°45'01.1"N, 73°05'14.5"E, 1303 m.a.s.l., July 27, 2018, Shazia Ashraf & Arooj Naseer, MH-63, Holotype (LAH 37543), GenBank: OP605606 (ITS), OP782026 (LSU).

Description. ***Basidiomata*** medium-sized, shiny, smooth, moderately fleshy, solitary. ***Pileus*** 1.5–2.5 cm in diameter, hemispherical to parabolic when young, expanding convex to plano convex, plane at maturity, umbonate, radially fibrillose to rugulose, whole pileus orange (0.5YR 3.2/8.7) when immature, then yellowish orange (9.4YR 6.1/7.2) on maturity, margin incurved in mature and striated, context white, smooth, thick at center. ***Lamellae*** free to thin, milky white (2.2GY 6.8/0.9), spacing fine and close, 1–1.5 mm wide, edges entire, lamellae regular, 3-4 tiers. ***Lamellulae*** irregular, alternating with lamella, in 2-3 tiers. ***Stipe*** 4.5–7 × 0.5–1 cm, cylindrical, central, thin, white (2.2GY 6.8/0.9), smooth, shiny, even, clavate. Annulus simple, white, located in upper half of stipe, membranous upturned. Flavor and odor not distinctive.

Basidiospores [90/5/3] (6–) 6.2 – 8.0 (–8.2) × (3.43–) 4.11 – 4.7(–4.9) μm, 6.1–8.1 × 3.7–4.8 μm, av. Q = 1.58–1.42, Qav = 1.49, hyaline to light yellowish in 5% KOH, oval to ellipsoid at face view, lacrymoid to amygdaliform in side-view, guttulate, smooth, dextrinoid, thin-walled and apiculate. ***Basidia*** (12.06–) 13.08 – 23.5 (–24.03) × (6.86–) 7.7 – 8.72 (–9.72) μm, 12.9–18.5 × 5.8–7.7 μm, av. L =19.29 μm, av. W = 7.54 μm, narrowly clavate, hyaline in 5% KOH, smooth, with 2–4 prominent sterigmata, oil droplets present,no clamp at base. ***Cheilocystidia*** (15.12–) 16.12 – 24.9 (–25.98) × (6.88–) 7.8 – 8.4 (–9.43) μm, 15–26 × 6.8–9.4 μm, hyaline in 5% KOH, thick-walled, broadly clavate and smooth, without internal content and clamp. Pleurocystidia absent. Pileipellis an intricate trichoderm, made up of 5.6–7.7 μm, av w=5.99 μm, wide, septate, interwoven, thin-walled hyphae, hyaline in 5% KOH, clamp connections absent.

Stipitipellis as compactly arranged cutis, made up of septate, cylindrical hyphae, 3.4–4.9 μm in diam., thin-walled, light yellowish in 2% KOH, clamp connections absent.

Additional specimen. Pakistan, Islamabad, Margalla Hills National park, trail 5, 33°45'01.1"N, 73°05'14.5"E, 1303 m a.s.l., July 22, 2021, Shazia Ashraf, MH-111(LAH 37454), GenBank for ITS (OP605607) LSU (OP782027).

Comments. *Leucoagaricus margallensis* has a combination of striking features like small, umbonate pileus with minute, fragile annulus and broader bulbous stipe. Anatomically, it has smaller basidiospores (6.27 × 4.67 μm), smaller cheliocystidia and absence of crystals at apex of cheliocystidia.

Figure 3. Morphological description of *Leucoagaricus* spp. from Pakistan **A, C** *Leucoagaricus margallensis* **B, D** *Leucoagaricus glareicolor*.

Leucoagaricus margallensis resembles *La. rubrotinctus* including similar pileus size and shape, fibrillose surface, stipe color and shape. But *Leucoagaricus margallensis* differs from *La. rubrotinctus* by minute fragile annulus while *La. rubrotinctus* has prominent white annulus. Anatomically, *Leucoagaricus margallensis* has ellipsoid, smaller (6.27 × 4.67 μm) basidispores as compared to *La. rubrotinctus* larger and amygdaliform basidiospores. Furthermore, *Leucoagaricus margallensis* has smaller cheliocystidia (15–26 × 6.8–9.4 μm) as compared to *La. rubrotinctus* (30–50 × 5–10 μm), narrow pilleipellis hyphae (5–10 μm) in *La. rubrotinctus*. The other closely related taxa in phylogenetic tree is *L. rubroconfusus* Migl. & Coccia, characterized by centrally depressed, larger (up to 7.5 cm) pileus with orange fibrillose squamules as compared to umbonate, smaller (2.5 cm) yellowish orange fibrils on white pileus of Pakistani taxon. Anatomically, both taxa lack crystals at apex of cheilocystidia. Our taxon *Leucoagaricus margallensis* is

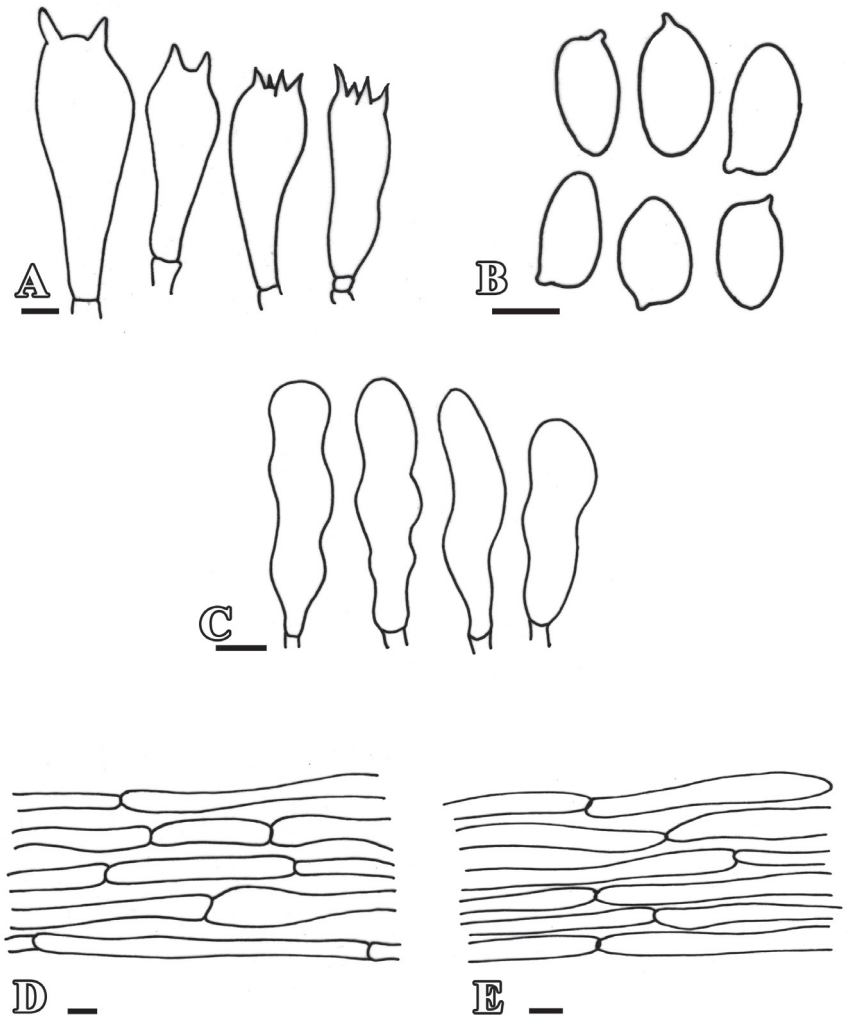

Figure 4. Anatomical features of *Leucoagaricus margallensis* **A** basidia **B** basidiospores **C** cheilocystidia **D** pileipellis **E** stipitipellis. Scale bars: 10 μm (**A**); 5 μm (**B–E**).

differentiated from *L. rubroconfusus* due to smaller (6.27 × 4.67 μm) basidiospores as compared to basidiospores of *L. rubroconfusus* (5.5–8(9.5)) μm.

Leucoagaricus subpurpureolilacinus Z.W. Ge & Zhu L. Yang, from southwestern China differs in its broad, brown to dark ruby umbo, larger basidiospores and clavate cheilocystidia with gelatinized covering intermixed with crystals (Ge et al. 2015). Our taxon can also be differentiated from *La. purpureolilacinus*. *Leucoagaricus purpureolilacinus* has a pinkish brown pileus with a dark purple brown disk, a stipe attenuating toward the base, amygdaliform spores and clavate cheilocystidia often with constrictions in the middle (Vellinga 2001).

Leucoagaricus glareicolor **Ashraf, S., Naseer, A. & Khalid, A.N., sp. nov.**
MycoBank No: 846302
Figs 3–5

Etymology. The specific epithet *glareicolor* (Latin) refer to the brownish black color of umbo and fibrils on pileus.

Diagnosis. Is distinguished due to brown to blackish brown, broadly umbonate, white pileus with blackish brown fibrillose to rugulose, smooth sub-bulbous stipe with annulus in upper 1/3 of stipe, smaller (5.65–7.70 × 3.44–5.63 µm) basidiospores and cheilocystidia without crystals at apex.

Holotype. Pakistan, Islamabad, Margalla Hills National Park, Trail 5, 33°45'01.1"N, 73°05'14.5"E, 1303 m a.s.l., August 28, 2018, Shazia Ashraf & Arooj Naseer MH-169 (LAH37456) GenBank: OP605605 (ITS) and OP782028 (LSU)

Description. ***Basidiomata*** medium to large-sized, soft shiny, fragile solitary. ***Pileus*** 4-4.2 cm, plano-convex to plane at maturity, radially fibrillose to rugulose towards margins, broadly umbonate, umbo brown when young, becoming blackish brown with age, disc creamy white (1.7GY 6.4/1.6) with dark brown (3.8Y 3.5/3.2) to blackish brown (4.8Y 5.5/8.2) rugulose towards margins, shiny and sericeous, on maturity broadly striated and overextended blackish brown fibrils darker in center and lighter towards margin, margin incurved and appendiculate. ***Lamellae*** free to approximate, adnexed, distant, fragile, edges entire, yellowish creamy (1.7GY 6.4/1.6) to grayish brown (4.8Y 5.5/8.2). ***Lamellulae*** irregular, alternating with lamella, in 2-3 tiers. ***Stipe*** 6.2–6.7 cm in length, tapering upwards, 0.5 cm at apex, 1.7 cm at base, sub bulbous, yellowish creamy (1.7GY 6.4/1.6) central, cylindrical, smooth, shiny. ***Annulus*** present, superior, thin, made up of cottony scales, non-persistent in nature. Flavor and odor not distinctive. ***Basidiospores*** [60/3/2] (5.65–) 5.66 – 7.73 (–7.76) × (3.43–) 4.11 – 4.6 (–5.63) µm, 5.65–7.70 × 3.44–5.63 µm, Q = 1.23–1.70, Qav = 1.48, hyaline in 5% KOH, oval at face view, lacrymoid to amygdaliform in side-view, guttulate, smooth, dextrinoid, thin-walled and apiculate. ***Basidia*** (12.06–) 13.08 – 23.5 (–24.03) × (6.86–) 7.7 – 8.72 (–9.72) µm, 12.9–18.5 × 5.8–7.7 µm, narrowly clavate, hyaline in 5% KOH, smooth, with 2–4 prominent sterigmata, oil droplets present, no clamp at base. ***Cheilocystidia*** (15.12–) 16.12 – 24.9 (–25.98) × (6.88–) 7.8 – 8.4 (–9.43) µm, 15–26 × 6.8–9.4 µm, hyaline in 5% KOH, thin-walled, clavate to narrowly clavate, smooth, without internal content and clamp. ***Pleurocystidia*** absent. Many layers of isodiametric irregular epithelial cells av = 7.87 µm in diameter, at the base of basidia and cystidia. ***Pileipellis*** trichoderm, made up of septate, cylindrical hyphae 5.6–7.7µm in diam., thin-walled, light brown to reddish pigment in the center, light orange to yellowish pigment towards margin in 2% KOH, clamp connections absent. ***Stipitipellis*** cutis compactly arranged, made up of septate, cylindrical hyphae 3.4–7.1µm in diam., av. w = 5.86 µm thin-walled, hyaline in 2% KOH, clamp connections absent.

Additional material examined. Pakistan, Islamabad, Margalla Hills National park, Trail 5, 33°45'01.1"N, 73°05'14.5"E, 1303 m.a.s.l., July 27, 2018 Shazia Ashraf & Arooj Naseer, MH-65 (LAH37555), GenBank for ITS OP605604 & OP782029 for LSU).

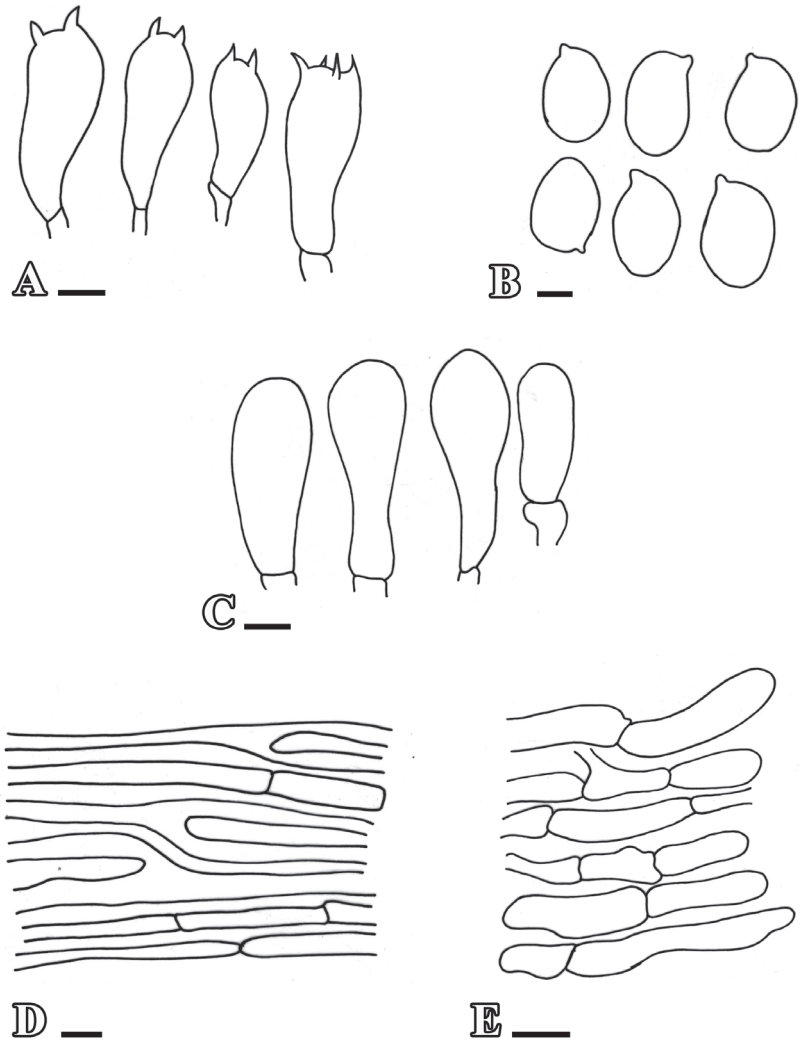

Figure 5. Anatomical features of *L. glareicolor* **A** basidia **B** basidiospores **C** cheilocystidia **D** pileipellis **E** stipitipellis. Scale bars: 5 μm (**A–C**); 10 μm (**D, E**).

Comments. *Leucoagaricus glareicolor* is characterized by broad umbo that is brown to blackish brown, fibrillose to rugulose white pileus. The stipe is smooth, sub-bulbous with annulus that is present in upper 1/3 of stipe. Anatomically, *Leucoagaricus glareicolor* has smaller (5.65–7.70 × 3.44–5.63 μm) basidiospores and cheilocystidia without crystals at apex.

Leucoagaricus glareicolor shows close relationship with *L. subvolvatus* and *L. menieri*. *Leucoagaricus subvolvatus* and *L. glareicolor* share many similarities like same pileus color, size and shape. However, *L. subvolvatus* has broad yellow umbo with yellow, fine fibrils while *L. glareicolor* has very prominent, blackish brown umbo with blackish

brown fibrils. *Leucoagaricus subvolvatus* is characterized by stipe base with a marginal bulb. *Leucoagaricus glareicolor* has slightly bulbous stipe. Furthermore, *Leucoagaricus subvolvatus* has annulus at lower part of stipe while *Leucoagaricus glareicolor* has prominent annulus in upper 1/3 half of stipe. Furthermore, *Leucoagaricus subvolvatus* has cheilocystidia with crystals at apex whereas *Leucoagaricus glareicolor* cheilocystidia lacks crystals at apex (Candusso and Lanzoni 1990).

Compared to *Leucoagaricus menieri*, characterized by light yellow, slightly umbonate pileus which is milky white while *Leucoagaricus glareicolor* has brownish black umbo, creamy white pileus with blackish brown fibrils. The stipe in the former is more bulbous (4–5 mm) as compared to subbulbous (0.5–1.7 cm) stipe in *Leucoagaricus glareicolor*. Anatomically *Leucoagaricus menieri* is differentiated from *Leucoagaricus glareicolor* by longer basidiospores {(6.9–)7.4(–8.7)} and the presence of crystals at apex of cheilocystidia. Another closely related taxon is *Leucoagaricus sardous* that is differentiated by our taxa by broader {5–6.8 (7.3)} basidiospores and larger (upto 75 µm) cheilocystidia. The next closely related taxon is *L. volvatus* that is characterized by the gelatinized, white pileus with olivaceous tinges and presence of crystals on cheilocystidia.

Molecular phylogenetic analyses based on ITS and LSU sequences also support *La. glareicolor* as a distinct species with strong bootstrap support.

Discussion

In this paper, two new species of *Leucoagaricus* were studied morphologically and sequences of two DNA regions were analyzed for each species. With the new data provided in the present study, the number of *Leucoagaricus* species for all of Pakistan increases to fourteen. All in all, these data suggest that our knowledge of the diversity of *Leucoagaricus* in high mountain areas in Asia and the Margala forests of Pakistan is still in its infancy. These two new species provide evidence that further research is needed to collect and identify the fungal diversity of Asia.

Acknowledgements

We are thankful to reviewers for their valuable suggestions to improve the quality of manuscript. The corresponding author is thankful to University of the Punjab, Lahore for providing financial support (Research Grant 2022-2023) to Arooj Naseer for this Research work.

References

Ahmad S, Iqbal SH, Khalid AN (1997) Fungi of Pakistan. Sultan Ahmad Mycological Society, Lahore, Pakistan.

Asif M, Niazi AR, Izhar A, Khalid AN, Bashir H (2021) *Leucoagaricus fragilis* sp. nov. (Agaricaceae) from Punjab, Pakistan. Phytotaxa 501(1): 140–150. https://doi.org/10.11646/phytotaxa.501.1.5

Bruns TD (1995) Thoughts on the processes that maintain local species diversity of ectomycorrhizal fungi. Plant and Soil 170(1): 63–73. https://doi.org/10.1007/BF02183055

Candusso M, Lanzoni G (1990) Fungi Europaei 4. Lepiota s.l. Giovanna Biella, Saronno, Italy, 743 pp.

Darriba D, Taboada GL, Doallo R, Posada D (2012) JModelTest 2: More models, new heuristics and parallel computing. Nature Methods 9(8): 772–772. https://doi.org/10.1038/nmeth.2109

Gardes M, Bruns TD (1993) ITS primers with enhanced specificity for basidiomycetes – application to the identification of mycorrhizae and rusts. Molecular Ecology 2(2): 113–118. https://doi.org/10.1111/j.1365-294X.1993.tb00005.x

Ge ZW, Yang ZL, Qasim T, Nawaz R, Khalid AN, Vellinga EC (2015) Four new species in *Leucoagaricus* (Agaricaceae, Basidiomycota) from Asia. Mycologia 107(5): 1033–1044. https://doi.org/10.3852/14-351

Gouy M, Guindon S, Gascuel O (2010) SeaView version 4: A multiplatform graphical user interface for sequence alignment and phylogenetic tree building. Molecular Biology and Evolution 27(2): 221–224. https://doi.org/10.1093/molbev/msp259

Hussain S, Jabeen S, Khalid AN, Afshan NS, Ahmad H, Sher H, Pfister DH (2018) Underexplored regions of Pakistan yield five new species of *Leucoagaricus*. Mycologia 110(2): 387–400. https://doi.org/10.1080/00275514.2018.1439651

Lodge DJ, Padamsee M, Matheny PB, Aime MC, Cantrell SA, Boertmann D, Kovalenko A, Vizzini A, Dentinger B, Kirk P, Ainsworth M, Moncalvo JM, Vilgalys R, Larsson E, Lücking R, Griffith G, Smith M, Norvell LL, Desjardin DE, Redhead SA, Ovrebo CL, Lickey E, Ercole E, Hughes KW, Courtecuisse R, Young A, Binder M, Minnis A, Lindner DL, Ortiz-Sanatan B, Haight J, Læssøe T, Baroni TJ, Geml J, Hattori T (2014) Molecular phylogeny, morphology, pigment chemistry and ecology in Hygrophoraceae (Agaricales). Fungal Diversity 64(1): 1–99. https://doi.org/10.1007/s13225-013-0259-0

Qasim T, Amir T, Nawaz R, Niazi AR, Khalid AN (2015) *Leucoagaricus lahorensis*, a new species of *L.* sect. *Rubrotincti*. Mycotaxon 130(2): 533–541. https://doi.org/10.5248/130.533

Rambaut A (2012) FigTree v1. 4.0. University of Oxford, Oxford, UK.

Ronquist F, Teslenko M, Van der Mark P, Ayres DL, Darling A, Höhna S, Larget B, Liu L, Suchard MA, Huelsenbeck JP (2012) MrBayes 3.2: Efficient Bayesian phylogenetic inference and model choice across a large model space. Systematic Biology 61(3): 539–542. https://doi.org/10.1093/sysbio/sys029

Singer R 1986. The *Agaricales* in modern taxonomy, 4th edn. Koeltz Scientific Books, Koenigstein, 981 pp.

Stamatakis A (2014) RAxML version 8: A tool for phylogenetic analysis and post-analysis of large phylogenies. Bioinformatics 30(9): 1312–1313. https://doi.org/10.1093/bioinformatics/btu033

Ullah Z, Jabeen S, Faisal M, Ahmad H, Khalid AN (2019) *Leucoagaricus brunneus* sp. nov. from Khyber Pakhtunkhwa, Pakistan. Mycotaxon 134(4): 601–611. https://doi.org/10.5248/134.601

Usman M, Khalid AN (2018) *Leucoagaricus pabbiensis* sp. nov. from Punjab, Pakistan. Mycotaxon 133(2): 355–364. https://doi.org/10.5248/133.355

Vellinga EC (2001) *Lepiota* (Pers.: Fr.) S.F. Gray. In: Noordeloos ME et al. (Eds) Flora Agaricina Neerlandica, Vol. 5. A.A. Balkema, Rotterdam, 109–151.

Vilgalys R, Hester M (1990) Rapid genetic identification and mapping of enzymatically amplified ribosomal DNA from several *Cryptococcus* species. Journal of Bacteriology 172(8): 4238–4246. https://doi.org/10.1128/jb.172.8.4238-4246.1990

Werle E, Schneider C, Renner M, Völker M, Fiehn W (1994) Convenient single-step, one tube purification of PCR products for direct sequencing. Nucleic Acids Research 22(20): 4354–4355. https://doi.org/10.1093/nar/22.20.4354

White TJ, Bruns T, Lee SJWT, Taylor JW (1990) Amplification and direct sequencing of fungal ribosomal RNA genes for phylogenetics. PCR protocols: a guide to methods and applications 18(1): 315–322. https://doi.org/10.1016/B978-0-12-372180-8.50042-1

MycoKeys 96: 173–191 (2023)
doi: 10.3897/mycokeys.96.100743
https://mycokeys.pensoft.net

RESEARCH ARTICLE

A peer-reviewed open-access journal
MycoKeys
Launched to accelerate biodiversity research

Taxonomy and phylogeny of *Sidera* (Hymenochaetales, *Rickenella* clade) from China and North America revealing two new species

Zhan-Bo Liu[1], Hong-Min Zhou[1], Hong-Gao Liu[2], Yuan Yuan[1]

1 *School of Ecology and Nature Conservation, Beijing Forestry University, Beijing 100083, China* **2** *School of Agronomy and Life Sciences, Zhaotong University, Zhaotong 657000, China*

Corresponding author: Yuan Yuan (yuanyuan1018@bjfu.edu.cn)

Academic editor: Maria-Alice Neves | Received 18 January 2023 | Accepted 3 April 2023 | Published 20 April 2023

Citation: Liu Z-B, Zhou H-M, Liu H-G, Yuan Y (2023) Taxonomy and phylogeny of *Sidera* (Hymenochaetales, *Rickenella* clade) from China and North America revealing two new species. MycoKeys 96: 173–191. https://doi.org/10.3897/mycokeys.96.100743

Abstract

Sidera, belonging to the *Rickenella* clade of Hymenochaetales, is a worldwide genus with mostly poroid hymenophore of wood-inhabiting fungi. Two new species in the genus, *Sidera americana* and *S. borealis*, are described and illustrated from China and North America based on morphological and molecular evidence. They were mainly found growing on rotten wood of *Abies*, *Picea* and *Pinus*. *S. americana* is characterized by annual, resupinate basidiomata with silk sheen when dry, round pores (9–11 per mm), a dimitic hyphal system, and allantoid basidiospores measuring 3.5–4.2 × 1 µm. *S. borealis* is characterized by annual, resupinate basidiomata with cream to pinkish buff dry pore surface, angular pores (6–7 per mm), a dimitic hyphal system, and allantoid basidiospores measuring 3.9–4.1 × 1–1.1 µm. Phylogenetic analysis based on a combined 2-locus dataset [ITS1-5.8S-ITS2 (ITS) + nuclear large subunit RNA (nLSU)] shows that the two species are members of *Sidera*, and they are compared with morphologically similar and phylogenetically related species, respectively. An identification key to 18 accepted species of *Sidera* in worldwide is provided.

Keywords

Phylogenetic analysis, polypore, wood-rotting fungi

Introduction

Larsson et al. (2006) used the name '*Rickenella* clade' for species in *Rickenella* Raithelh. and 18 additional genera for the first time. *Athelopsis lunata* (Romell ex Bourdot & Galzin) Parmasto [= *Sidera lunata* (Romell ex Bourdot & Galzin) K.H. Larss.] is a member of *Rickenella* clade in their phylogenetic analysis of Hymenochaetales. Miettinen and Larsson (2011) established the new genus *Sidera* Miettinen & K.H. Larss. to accommodate *Athelopsis lunata*, *Ceriporiopsis lowei* Rajchenb. [= *Sidera lowei* (Rajchenb.) Miettinen], *Skeletocutis lenis* (P. Karst.) Niemelä [= *Sidera lenis* (P. Karst.) Miettinen] and *Skeletocutis vulgaris* (Fr.) Niemelä & Y.C. Dai [= *Sidera vulgaris* (Fr.) Miettinen], because these four species formed a monophyletic group and didn't group together with any other species or genera within *Rickenella* clade in their phylogenetic analysis of 5.8S + nLSU. Yu et al. (2021) studied the taxonomic positions of the genera *Resinicium* Parmasto and *Skvortzovia* Bononi & Hjortstam, which belong to *Rickenella* clade. With the much richer sampling available to us, the phylogenetic analyses also prompted us to study the taxonomic position of *Sidera* within the *Rickenella* clade.

Sidera, a genus with mostly poroid hymenophore of wood-inhabiting fungi distributed in most continents except Africa (Miettinen and Larsson 2011; Liu et al. 2022; Wu et al. 2022a), is treated as a member of *Rickenella* clade within Hymenochaetales, with *Sidera lenis* as the generic type. To date, 16 species are accepted in *Sidera* (Miettinen and Larsson 2011; Du et al. 2019, 2020; Liu et al. 2021, 2022). Seven species of *Sidera* have previously been recorded from China: *S. inflata* Z.B. Liu & Y.C. Dai, *S. minutissima* Y.C. Dai et al., *S. parallela* Dai et al., *S. punctata* Z.B. Liu & Y.C. Dai, *S. roseo-bubalina* Z.B. Liu & Y.C. Dai, *S. salmonea* Z.B. Liu et al., and *S. tibetica* Z.B. Liu et al. (Du et al. 2020; Liu et al. 2021, 2022).

Morphologically, *Sidera* is characterized by resupinate, white to cream or buff, mostly waxy fresh basidiomata, mostly poroid (one hydnoid species) hymenophore, a dimitic or monomitic hyphal system with generative hyphae with clamp connections, the presence of rosette-like crystals, and allantoid to lunate, hyaline, thin-walled basidiospores (Miettinen and Larsson 2011; Liu et al. 2021). Species in the genus cause a white rot.

In this study, we focus on *Sidera* represented by eight resupinate specimens from China, and North America. Phylogenetic analysis based on the ITS and nLSU rDNA sequences is carried out and two new species are described. The current study aims to further explore the species diversity of *Sidera* in the Asia-Pacific region, and more importantly, to confirm the taxonomic position of *Sidera* within the *Rickenella* clade of Hymenochaetales, based on the ITS+nLSU phylogenetic analysis. Morphological characters of all 18 currently accepted species of *Sidera* are summarized in Table 1. Furthermore, an identification key to accepted species is provided in the paper.

Table 1. The main characteristics of *Sidera* species. Pore and basidiospore sizes mainly from Liu et al. (2022). New species are shown in bold.

Species	Growing habit	Hymenophore	Hyphal system	Cystidioles	Skeletal hyphae in KOH	Spores shape	Spore dimension (µm)
S. americana	**Annual**	**Poroid, 9–11/mm**	**Dimitic**	**Present**	**Almost unchanged**	**Allantoid**	**3.5–4.2 × 1**
S. borealis	**Annual**	**Poroid, 6–7/mm**	**Dimitic**	**Present**	**Almost unchanged**	**Allantoid**	**3.9–4.1 × 1–1.1**
S. inflata	Annual	Poroid, 9–10/mm	Dimitic	Present	Swollen	Allantoid	3–3.3 × 0.9–1.1
S. lenis	Perennial	Poroid, 4–6/mm	Dimitic	Present	Swollen	Allantoid to lunate	3.9–4.9 × 1.5–2
S. lowei	Annual	Poroid, 6–8/mm	Monomitic	Present, some branched	–	Allantoid	3.5–5 × 1–1.2
S. lunata	Annual	Hydnoid, 8–9/mm	Monomitic	Present	–	Allantoid	2.5–3.8 × 1.6–1.9
S. malaysiana	Annual	Poroid, 9–11/mm	Dimitic	Present	Swollen	Lunate	2.9–3.2 × 1–1.2
S. minutipora	Annual	Poroid, 5–7/mm	Dimitic	Present	Swollen	Allantoid	3.7–4.3 × 1–1.3
S. minutissima	Annual	Poroid, 7–9/mm	Dimitic	Present	Almost unchanged	Allantoid	3.8–4.4 × 0.9–1.3
S. parallela	Annual	Poroid, 6–8/mm	Dimitic	Present	Almost unchanged	Lunate	2.8–3.3 × 0.9–1.2
S. punctata	Annual	Poroid, 8–9/mm	Monomitic	Absent	–	Allantoid to lunate	3.8–4.8 × 1–1.3
S. roseo-bubalina	Annual	Poroid, 6–7/mm	Monomitic	Present	–	Lunate	3.9–4.5 × 0.8–1
S. salmonea	Annual	Poroid, 7–9/mm	Dimitic	Present	Almost unchanged	Lunate	3–3.5 × 0.9–1.1
S. srilankensis	Annual	Poroid, 6–8/mm	Dimitic	Present	Almost unchanged	Lunate	3.5–4 × 1–1.3
S. tenuis	Annual	Poroid, 8–10/mm	Dimitic	Present	Almost unchanged	Allantoid	4.2–5 × 0.8–1
S. tibetica	Annual	Poroid, 7–8/mm	Dimitic	Present	Almost unchanged	Lunate	2.9–3.1 × 1–1.1
S. vesiculosa	Annual	Poroid, 7–9/mm	Monomitic	Present	–	Allantoid to lunate	2.9–3.7 × 0.6–1
S. vulgaris	Perennial	Poroid, 6–8/mm	Dimitic	Present, some branched	Almost unchanged	Allantoid to lunate	2.9–3.6 × 0.9–1.4

Materials and methods

Morphological studies

Macro-morphological descriptions were based on field notes and dry herbarium specimens. Microscopic measurements and drawings were made from slide preparations of dried tissues stained with Cotton Blue and Melzer's reagent as described by Dai (2010). Pores were measured by subjectively choosing as straight a line of pores as possible and measuring how many per mm. The following abbreviations are used in the description: CB = Cotton Blue; CB– = acyanophilous in Cotton Blue; IKI = Melzer's reagent; IKI– = neither amyloid nor dextrinoid in Melzer's reagent; KOH = 5% potassium hydroxide; n (a/b) = number of spores (a) measured from given number of specimens (b); L = mean spore length (arithmetic average of all the spores); W = mean spore width (arithmetic average of all the spores); and Q = variation in the L/W ratios between the specimens studied. When the variation in spore size is shown, 5% of the measurements were excluded from each end of the range, and these values are shown in parentheses. Special color terms follow Petersen (1996) and then herbarium abbreviations follow Thiers (2018). Voucher specimens from the study were deposited in the herbarium of the Institute of Microbiology, Beijing Forestry University (**BJFC**).

DNA extraction, PCR and sequencing

Total genomic DNA was extracted from dried specimens by a CTAB rapid plant genome extraction kit (Aidlab Biotechnologies Company, Limited, Beijing, China) according to the manufacturer's instructions with some modifications (Li et al. 2014). The ITS regions were amplified with primers ITS4 and ITS5 (White et al. 1990). The nLSU regions were amplified with primers LR0R and LR7 (Vilgalys and Hester 1990).

The polymerase chain reaction (PCR) procedure for ITS was as follows: initial denaturation at 95 °C for 3 min, followed by 35 cycles at 94 °C for 40 sec, 58 °C for 45 sec, and 72 °C for 1 min, and a final extension of 72 °C for 10 min. The PCR procedure for nLSU was as follows: initial denaturation at 94 °C for 1 min, followed by 35 cycles at 94 °C for 30 sec, 48 °C for 1 min, and 72 °C for 1.5 min, and a final extension of 72 °C for 10 min (Zhao et al. 2015). Aliquots of PCR products were examined on 2% agarose gels stained with GelStar Nucleic Acid Gel Stain (Lonza Rockland, Inc., Rockland, YN, USA) and examined under UV light. The sequencing of the PCR products was conducted by the Beijing Genomics Institute, Beijing, China, with the same primers used in the PCR reactions. Species were identified by sequence comparison with accessions in the NCBI databases using the BLAST program.

Phylogenetic analyses

Phylogenetic trees were constructed using ITS + nLSU rDNA sequences, and phylogenetic analyses were performed with the Maximum Likelihood (ML), Maximum Parsimony (MP) and Bayesian Inference (BI) methods. Sequences of the species and strains were primarily adopted from ITS-based and 28S-based tree topology as described by Miettinen and Larsson (2011) and Liu et al. (2022). New sequences generated in this study, along with reference sequences retrieved from GenBank (Table 2), were aligned by MAFFT 7 (Katoh et al. 2019; http://mafft.cbrc.jp/alignment/server/) using the "G-INS-i" strategy and manually adjusted in BioEdit v.7.2.5 (Hall 1999). Unreliably aligned sections were removed before the analyses, and efforts were made to manually inspect and improve the alignment. The data matrix was edited in Mesquite v3.70 (Maddison and Maddison 2021; https://www.mesquiteproject.org/). The sequence alignment was deposited at TreeBase. Sequences of *Exidia candida* Lloyd and *Exidiopsis calcea* (Pers.) K. Wells outside Hymenochaetales obtained from GenBank were used as outgroups to root the tree in the ITS + nLSU analysis.

Maximum Parsimony analysis was applied to the ITS + nLSU dataset sequences. The approaches to phylogenetic analysis utilized those conducted by Liu et al. (2022), and the tree was constructed using PAUP* version 4.0 beta 10 (Swofford 2002). All the characters were equally weighted, and gaps were treated as missing data. Trees

Table 2. Information for the sequences used in this study. * Newly generated sequences for this study. New species are shown in bold.

Species	Specimen no.	Locality	GenBank accession no.	
			ITS	nLSU
Atheloderma mirabile	TAA 169235	Estonia	DQ873592	DQ873592
Contumyces rosella	Redhead 7501	–	U66452	U66452
Cyphellostereum laeve	JJ 020909	Sweden	EU118621	EU118621
Exidia candida	VS 8588	Russia	KY801871	KY801896
Exidiopsis calcea	MW 331	Canada	AF291280	AF291326
Globulicium hiemale	KHL 961221	Sweden	EU118626	EU118626
G. hiemale	Hjm 19007	Sweden	DQ873595	DQ873595
Hyphoderma capitatum	KHL 8464	Sweden	DQ677491	DQ677491
H. orphanellum	NH 12208	Russia	DQ677500	DQ677500
Odonticium romellii	KHL 1514b	Norway	DQ873639	DQ873639
Peniophorella praetermissa	KHL 13164	Estonia	DQ873597	DQ873597
P. tsugae	NH 7473	Sweden	–	DQ677505
Repetobasidium conicum	KHL 12338	USA	DQ873647	DQ873647
Resinicium austroasianum	LWZ 20180417-5	Malaysia	MW414504	MW414450
R. bicolor	Miettinen 14049	Finland	MF319079	MF318936
R. chiricahuaense	JLL-14605	Canada	–	DQ863692
R. confertum	FP-102863	USA	DQ826538	–
R. friabile	CBS 126043	New Zealand	MH864058	MH875513
R. grandisporum	GGGUY13-008	French Guiana	KY995325	–
R. lateastrocystidium	LWZ 20180414-15	Malaysia	MW414509	MW414455
R. monticola	FP-150360	Jamaica	DQ826552	DQ863697
R. mutabile	FP-102989	Puerto Rico	DQ826556	DQ863699
R. rimulosum	FP-150328	Jamaica	DQ826546	–
R. saccharicola	FP-102754	Puerto Rico	DQ826547	DQ863691
R. tenue	FP-150354	Jamaica	DQ826539	–
R. sp.	LWZ 20171015-31	Vietnam	MW414511	MW414457
Rickenella fibula	P. Salo 1882		MF319088	–
R. mellea	Lamoure 74	–	U66438	U66438
Sidera americana	**Dai 19173**	**Canada**	**MW198477***	**MW192005***
	Dai 12730	**USA**	**MW198478***	**–**
S. borealis	**Dai 22822**	**China**	**OM974254***	**OM974246***
	Dai 24120	**China**	**OQ134533***	–
	Cui 11216	**China**	**MW198485***	–
	Dai 23962	**China**	**OQ134534***	–
	Dai 23803	**China**	**OQ134535***	–
	Dai 24187	**China**	**OQ134536***	**OQ134528***
	Dai 23960	**China**	**OQ134537***	–
S. inflata	Cui 13610	China	MW198480	–
S. lenis	Miettinen 11036	Finland	FN907914	FN907914
	Dai 22834	China	OQ134538*	OQ134529*
	Dai 22854	China	OQ134539*	OQ134530*
S. lowei	Miettinen X419	Venezuela	FN907917	FN907917
	Miettinen X426	New Zealand	FN907919	FN907919
S. lunata	JS 15063	Norway	DQ873593	DQ873593
S. malaysiana	Dai 18570	Malaysia	MW198481	MW192007
S. minutipora	Gates FF257	Australia	FN907922	FN907922
	Cui 16720	Australia	MN621349	MN621348

Species	Specimen no.	Locality	GenBank accession no.	
			ITS	nLSU
S. minutissima	Dai 19529	Sri Lanka	MN621352	MN621350
	Dai 22495	China	OM974248	OM974240
	Dai 18471A	China	MW198482	MW192008
S. parallela	Dai 22038	China	MW477793	MW474964
S. parallela	Cui 10346	China	MK346145	–
	Cui 10361	China	MK346144	–
	Dai 22635	China	OQ134540*	OQ134531*
S. punctata	Dai 22119	China	MW418438	MW418437
S. roseo-bubalina	Dai 11277	China	MW198483	–
S. salmonea	Dai 23343	China	OM974249	OM974241
	Dai 23354	China	OM974250	OM974242
	Dai 23428	China	OM974251	OM974243
	Dai 23612	China	–	OM974247
S. sp.	Dollinger 922	USA	KY264044	–
S. srilankensis	Dai 19581	Sri Lanka	MN621345	MN621347
	Dai 19654	Sri Lanka	MN621344	MN621346
S. tibetica	Dai 23407	China	OM974252	OM974244
	Dai 23648	China	OM974253	OM974245
	Dai 21057	Belarus	MW198484*	MW192009*
	Dai 22151	China	MW477794*	MW474965*
S. tenuis	Dai 18697	Australia	MK331865	MK331867
	Dai 18698	Australia	MK331866	MK331868
S. vesiculosa	Dai 17835	Singapore	MH636565	MH636567
	Dai 17845	Singapore	MH636564	MH636566
S. vulgaris	Ryvarden 37198	New Zealand	FN907918	FN907918
Skvortzovia dabieshanensis	LWZ 20201012-22	China	MW414512	MW414458
S. furfuracea	KHL 11738	Finland	DQ873648	DQ873648
S. furfurella	KHL 10180	Puerto Rico	DQ873649	DQ873649
S. georgica	KHL 12019	Norway	DQ873645	DQ873645
S. meridionalis	FP-150236	–	–	AY293197
S. pinicola	KHL 12224	USA	DQ873637	DQ873637
S. qilianensis	LWZ 20180904-16	China	MW414518	MW414464
Skvortzoviella lenis	LWZ 20180921-7	China	MW414521	MW414467
	LWZ 20180921-17	China	MW414522	MW414468

were inferred using the heuristic search option with tree bisection and reconnection (TBR) branch swapping, and 1000 random sequence addition maxtrees were set to 5000. Branches of zero length were collapsed, and all the parsimonious trees were saved. Clade robustness was assessed using a bootstrap (BT) analysis with 1000 replicates (Felsenstein 1985). Descriptive tree statistics, including the Consistency Index (CI), Homoplasy Index (HI), Rescaled Consistency index (RC), Retention Index (RI), and tree length (TL), were calculated for each Maximum Parsimonious Tree (MPT) generated.

The research using ML was conducted using RAxML-HPC v.8.2.3 (Stamatakis 2014) and RAxML-HPC through the CIPRES Science Gateway V. 3.3 (Miller et al.

2010; http://www.phylo.org). Statistical support values (BS) were obtained using non-parametric bootstrapping with 1000 replicates. The BI analysis was performed with MrBayes 3.2.7a (Ronquist et al. 2012). Four Markov chains were run for two runs from random starting trees for 5 million generations until the split deviation frequency value < 0.01, and the trees were sampled at every 1000 generation. The first 25% of the sampled trees were discarded as burn-in, and the remaining ones were used to reconstruct a majority rule consensus tree and calculate the Bayesian Posterior Probabilities (BPP) of the clades.

A total of 24 models of evolution was scored using PAUP* version 4.0 beta 10 (Swofford 2002). Optimal substitution models for the combined dataset were then determined using the Akaike Information Criterion (AIC) implemented in MrModeltest 2.3 (Posada and Crandall 1998; Nylander 2004). The model GTR + I + G was selected for use in the Maximum Likelihood (ML) and Bayesian Inference (BI) analyses.

Branches that received bootstrap support for Maximum Likelihood (BS), Maximum Parsimony (BP), and Bayesian Posterior Probabilities (BPP) > 70% (BS), 50% (BP), and 0.95 (BPP) were considered to be significantly supported. In addition, the ML analysis resulted in the best tree, and only the ML tree is shown along with the support values from the MP and BI analyses. FigTree v1.4.4 (Rambaut 2018) was used to visualize the resulting tree.

Results

The concatenated ITS+nLSU dataset contained sequences from 81 fungal specimens representing 18 *Sidera* taxa (Table 2). The dataset had an aligned length of 2313 characters, of which 1218 were constant, 269 were variable but parsimony-uninformative, and 826 were parsimony-informative. MP analysis yielded three equally parsimonious trees (TL = 5471, CI = 0.369, RI = 0.694, RC = 0.256, HI = 0.631). And the average standard deviation of split frequencies was 0.009886 (BI).

The phylogeny (Fig. 1) inferred from the ITS + nLSU sequences confirmed the taxonomic position of *Sidera* (Fig. 1B), *Resinicium* (Fig. 1C), and *Skvortzovia* (Fig. 1D) within the *Rickenella* clade (Fig. 1A) of Hymenochaetales. Species in *Sidera* clustered together with strong support (98% BS, 96% BP, 1.00 BPP) and new species *Sidera americana* and *S. borealis* clustered in the *Sidera* clade. *S. americana* grouped with *S. parallela* with strong support (98% BS, 100% BP, 1.00 BPP). *S. borealis* grouped with *S. vulgaris* with strong support (100% BS, 100% BP, 1.00 BPP).

Besides, we collected two *Sidera lenis* on rotten wood of *Picea* in Yunnan Province, China: Dai 22834 (BJFC 037407) and Dai 22854 (BJFC 037427). This is the first time the species has been reported in China. We have uploaded ITS and nLSU sequences of the two specimens to GenBank (https://www.ncbi.nlm.nih.gov/genbank/) and added them to our phylogenetic analysis (Fig. 1).

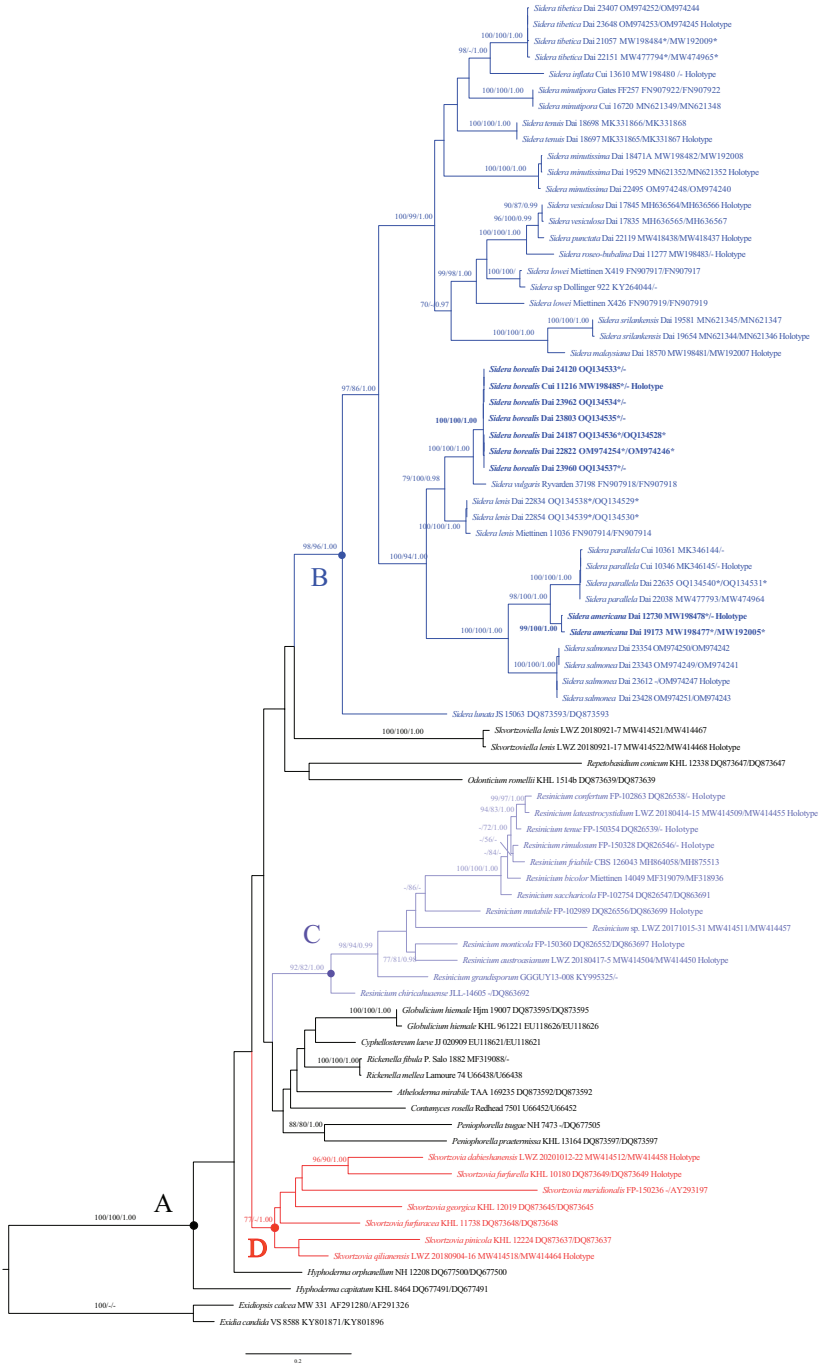

Figure 1. Phylogeny of *Sidera* and other genera in the *Rickenella* clade generated by ML analyses based on combined ITS+nLSU sequences **A** the *Rickenella* clade **B** the genus *Sidera* in modena **C** the genus *Resinicium* in purple **D** the genus *Skvortzovia* in red. Branches are labelled with Maximum Likelihood bootstrap > 70%, parsimony bootstrap proportions > 50%, and Bayesian Posterior Probabilities > 0.95, respectively. New species are indicated in bold. * Newly generated sequences for this study.

Taxonomy

***Sidera americana* Z.B. Liu & Yuan Yuan, sp. nov.**
MycoBank No: 838379
Figs 2, 3

Diagnosis. *Sidera americana* is characterized by annual, resupinate basidiomata with silk sheen when dry, round pores (9–11 per mm), a dimitic hyphal system, and allantoid basidiospores measuring 3.5–4.2 × 1 µm.

Holotype. USA. Connecticut, New Haven, West Rock Park, on rotten stump of *Pinus*, 15.VII.2012, Dai 12730 (BJFC 013037, isotype in CFMR).

Etymology. *Americana* (Lat.): referring to the species occurring in North America.

Basidiomata. Annual, resupinate, soft and without odor or taste when fresh, soft corky when dry, up to 14 cm long, 6 cm wide, and approximately 2 mm thick at center; pore surface white when fresh, becoming cream to buff with silk sheen when dry; sterile margin indistinct; pores round, 9–11 per mm; dissepiments thin, lacerate; subiculum very thin to almost absent; tubes concolorous with poroid surface, up to 2 mm long.

Hyphal structure. Hyphal system dimitic; generative hyphae with clamp connections; skeletal hyphae dominant; all hyphae IKI–, CB–; tissue unchanged in KOH.

Subiculum. Generative hyphae hyaline, thin-walled, unbranched, 1–2.5 µm in diam; skeletal hyphae dominant, thick-walled with a wide lumen, frequently branched, flexuous, interwoven, 2–3 µm diam.

Tubes. Generative hyphae hyaline, thin-walled, unbranched, 1–2 µm in diam, dominating at dissepiment edges; skeletal hyphae dominant in tube trama except dissepiment edges, thick-walled with a wide lumen, unbranched, flexuous, interwoven, 2–3 µm diam; rosette-like crystals abundant, 3–12.5 µm in diam; cystidia absent;

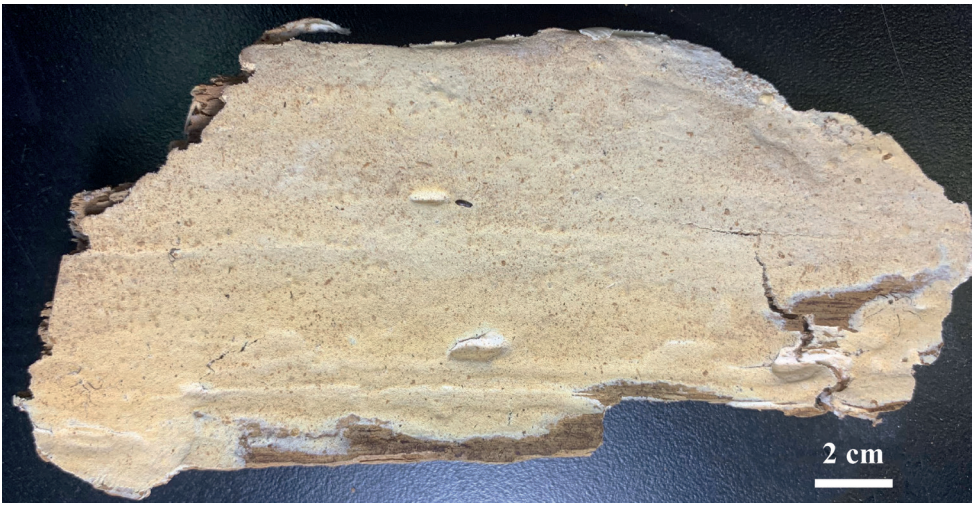

Figure 2. Basidiomata of *Sidera americana* (Holotype, Dai 12730). Photo by: Zhan-Bo Liu.

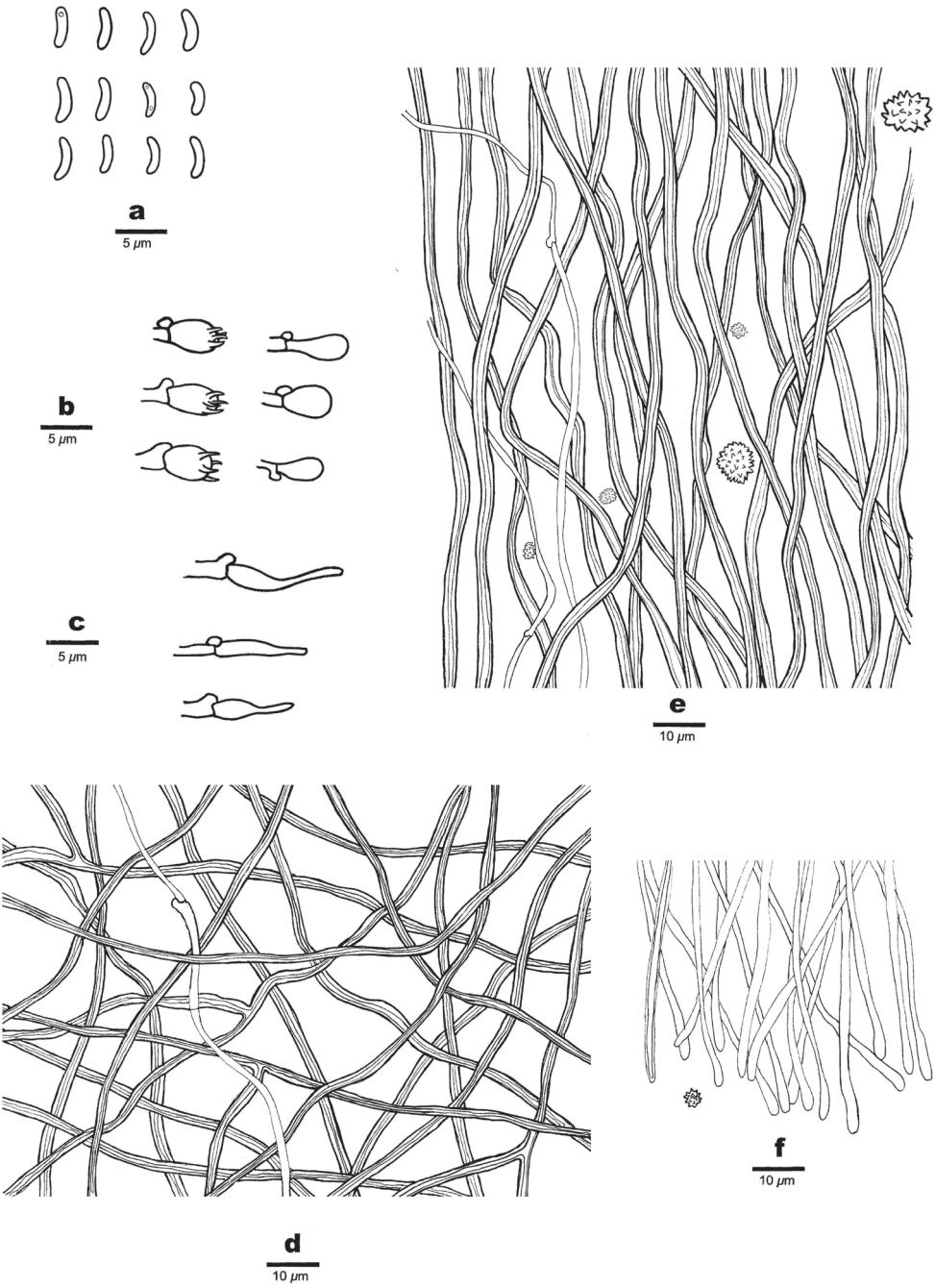

Figure 3. Microscopic structures of *Sidera americana* (Holotype, Dai 12730) **a** basidiospores **b** basidia and basidioles **c** cystidioles **d** hyphae from subiculum **e** hyphae from trama **f** hyphae at dissepiment edge. Drawings by: Hong-Min Zhou.

cystidioles present, fusoid, hyaline, thin-walled, basally swollen, with a sharp or often hyphoid neck, 13.4–15 × 3.2–4 μm; basidia barrel-shaped, hyaline, bearing four sterigmata and with a basal clamp connection, 6–7 × 3–4.2 μm; basidioles in shape similar to basidia, but slightly shorter.

Spores. Basidiospores allantoid, hyaline, thin-walled, smooth, occasionally with one or two guttules, IKI–, CB–, (3.2–)3.5–4.2(–5) × 1(–1.3) μm, L = 4 μm, W = 1.04 μm, Q = 3.74–3.96 (n = 60/2).

Additional specimen examined. Canada, Ontario, Hamilton, McMaster University, Botanical Garden, on rotten angiosperm wood, 18–20.VII.2017, Dai 19173 (BJFC 027641).

***Sidera borealis* Z.B. Liu & Yuan Yuan, sp. nov.**
MycoBank No: 838385
Figs 4, 5

Diagnosis. *Sidera borealis* is characterized by annual, resupinate basidiomata with cream to pinkish buff dry pore surface, angular pores (6–7 per mm), a dimitic hyphal system, and allantoid basidiospores measuring 3.9–4.1 × 1–1.1 μm.

Holotype. China, Shannxi Province, Zhashui County, Niubeiliang Forest Park, on fallen angiosperm trunk, 16.IX.2013, Cui 11216 (BJFC 015331).

Etymology. *Borealis* (Lat.): referring to the species occurring in boreal areas of China.

Basidiomata. Annual, resupinate, soft corky and without odor or taste when fresh, corky when dry, up to 5 cm long, 2 cm wide, and less than 1 mm thick at center; pore surface white to cream or pale buff when fresh, becoming cream to pinkish buff when dry; sterile margin indistinct, white, cottony, thinning out; pores angular, 6–7 per mm; dissepiments thin, entire; subiculum very thin to almost absent; tubes concolorous with poroid surface, less than 1 mm long.

Hyphal structure. Hyphal system dimitic; generative hyphae with clamp connections; skeletal hyphae dominant; all hyphae IKI–, CB–; tissue unchanged in KOH.

Subiculum. Generative hyphae hyaline infrequent, thin-walled, occasionally branched, 1–2 μm in diam; skeletal hyphae dominant, thick-walled with a narrow to medium lumen, occasionally branched, flexuous, interwoven, 1–3 μm diam.

Tubes. Generative hyphae hyaline occasionally present, thin-walled, rarely branched, 1–2 μm in diam, dominating at dissepiment edges; skeletal hyphae thick-walled with a narrow to wide lumen, occasionally branched, flexuous, interwoven, 1–3 μm diam; rosette-like crystals present, 3–6 μm in diam; cystidia absent; cystidioles present, fusoid, hyaline, thin-walled, basally swollen, with a sharp or often hyphoid neck, 17–19 × 2.5–3 μm; basidia barrel-shaped, hyaline, bearing four sterigmata and with a basal clamp connection, 7–8 × 3.5–4 μm; basidioles in shape similar to basidia, but slightly shorter.

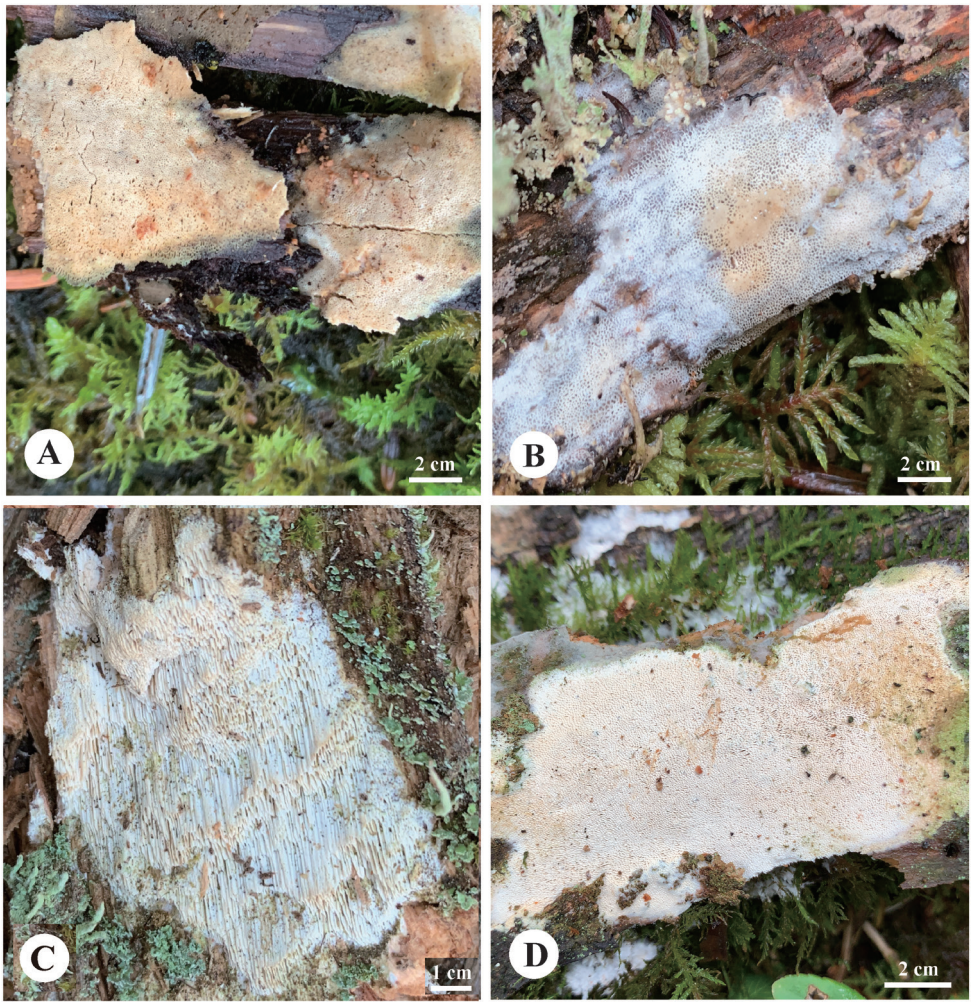

Figure 4. Basidiomata of *Sidera borealis* (Paratypes) **A** Dai 24120 **B** Dai 22822 **C** Dai 23960 **D** Dai 24187. Photo by: Yu-Cheng Dai.

Spores. Basidiospores allantoid, hyaline, thin-walled, smooth, occasionally with one or two guttules, IKI–, CB–, (3.5–)3.9–4.1(–4.2) × (0.8–)1–1.1(–1.4) µm, L = 4.01 µm, W = 1.06 µm, Q = 3.78 (n = 60/1).

Additional specimens examined. China, Gansu Province, Zhuoni County, Yaohe Nature Reserve, on rotten wood of *Abies*, 19.VIII.2022, Dai 24187 (BJFC 039430); on rotten wood of *Picea*, 18.VIII.2022, Dai 24120 (BJFC 039364); Jilin Province, Antu County, Dongfanghong Forest Farm, on rotten wood of *Pinus*, 25.VII.2022, Dai 23803 (BJFC 039047); Qinghai Province, Nangqian County, Baizha Forest Farm,

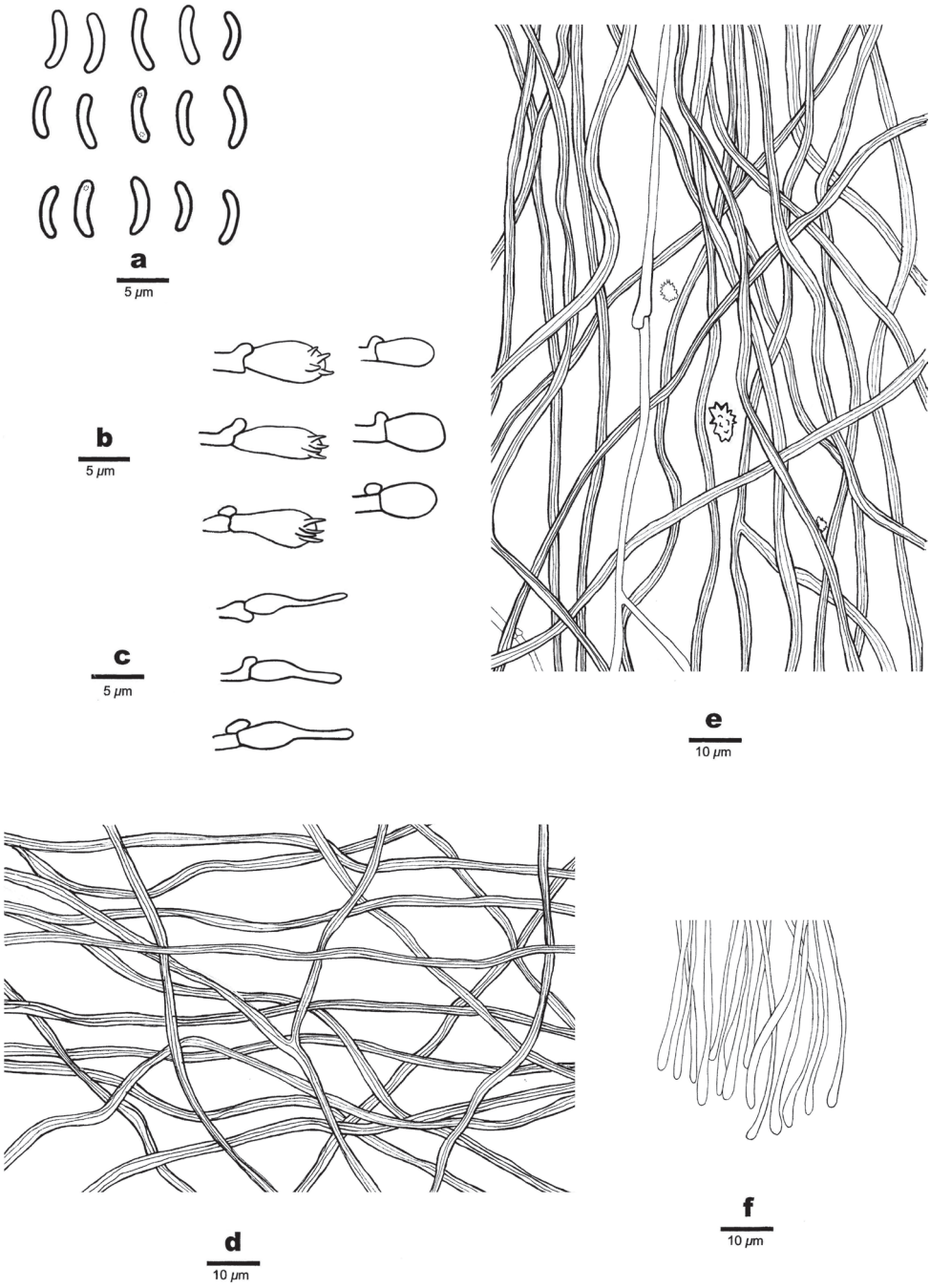

Figure 5. Microscopic structures of *Sidera borealis* (Holotype, Cui 11216) **a** basidiospores **b** basidia and basidioles **c** cystidioles **d** hyphae from subiculum **e** hyphae from trama **f** hyphae at dissepiment edge. Drawings by: Hong-Min Zhou.

on rotten wood of *Picea*, 7.VIII.2022, Dai 23960 (BJFC 039204); Dai 23962 (BJFC 039206); Yunnan Province, Deqin County, Baimaxueshan Nature Reserve, on rotten wood of *Picea*, 5.IX.2021, Dai 22822 (BJFC 037395).

***Sidera tibetica* Z.B. Liu, Jian Yu & F. Wu, Journal of Fungi 8: 7 (2022)**
Fig. 6

Description. See Liu et al. (2022). Liu et al. (2022) described *Sidera tibetica* as a new species based on Tibetan specimens and a photo of holotype. Subsequently, more specimens of the species from Belarus and China (Guangxi, Yunnan and

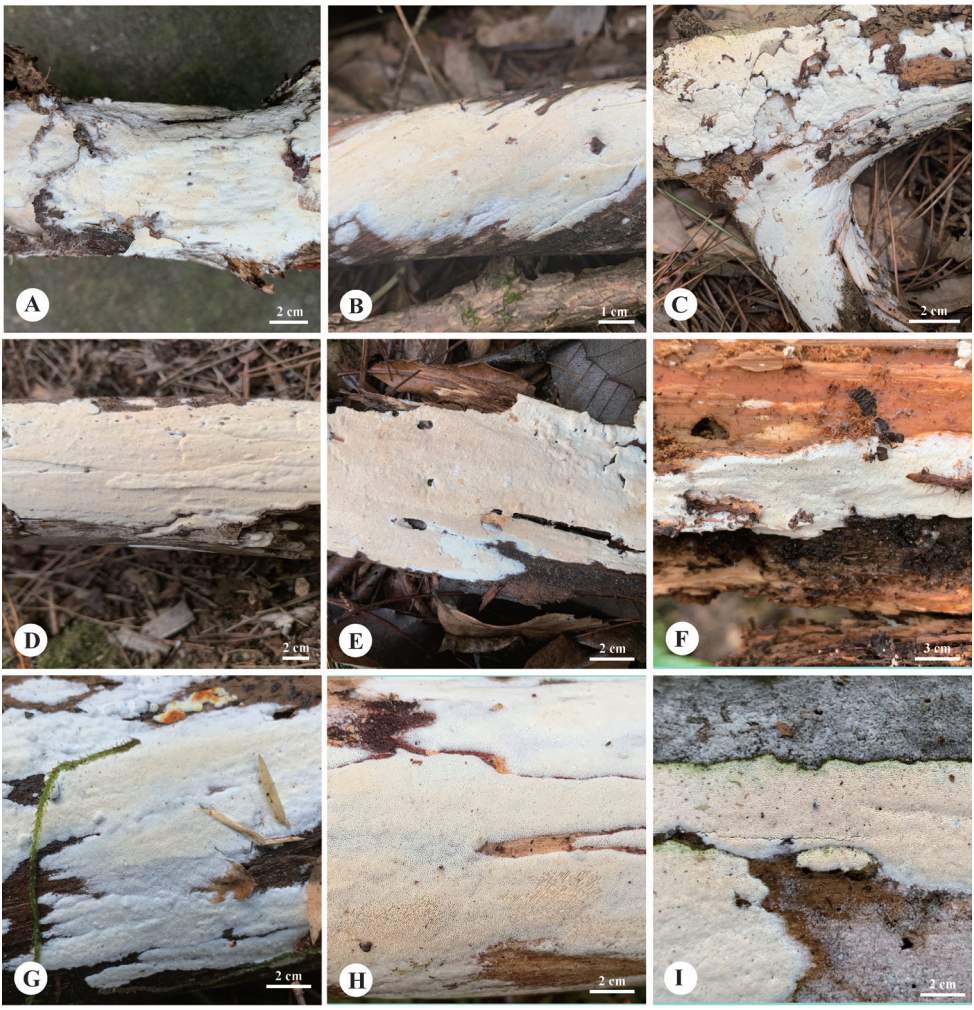

Figure 6. Basidiomata of *Sidera tibetica* **A** Dai 22321 **B** Dai 22639 **C** Dai 22663 **D** Dai 22151 **E** Dai 20342 **F** Dai 23407 **G** Dai 23486 **H** Dai 23648 (Holotype) **I** Dai 21057. Photo by: Yu-Cheng Dai.

Zhejiang) were collected and we took many photos of the fungus at different stages of growth on different hosts to make it easier for taxonomists to recognize the fungus in the field.

Materials studied. Belarus, Brestskaya Voblasts, Belavezhskaya Pushcha National Park, on rotten wood of *Picea*, 19.X.2019, Dai 21057 (BJFC 032716, paratype). China, Guangxi, Guiping County, Xishan Forest Park, on rotten wood of *Pinus*, 25.XII.2020, Dai 22151 (BJFC 036043, paratype); Xizang, Bomi County, Gangcun Spruce Park, on a rotten branch of *Pinus armandii*, 27.X.2021, Dai 23648 (BJFC 038220, holotype); Yigong, on a rotten branch of *Pinus armandii*, 24.X.2021, Dai 23407 (BJFC 037979, paratype); on rotten wood of *Pinus yunnanensis*, 24.X.2021, Dai 23486 (BJFC 038058, paratype); Yunnan Province, Jianchuan County, Yinhe Mountain, on fallen trunk of *Pinus*, 27.IX.2021, Dai 23097 (BJFC 037668, paratype), 28.IX.2021, Dai 23121 (BJFC037692, paratype); on fallen branch of *Pinus*, 27.IX.2021, Dai 23106 (BJFC037677, paratype). Mouding County, Huafoshan Nature Reserve, on rotten wood of *Pinus yunnanensis*, 31.VIII.2021, Dai 22639 (BJFC 037213, paratype); Dai 22663 (BJFC 037237, paratype); on rotten wood of *Pinus*, 31.VIII.2021, Dai 22667 (BJFC 037241, paratype). Wuding County, Shizishan Nature Reserve, on fallen angiosperm trunk, 15.VIII.2019, Dai 20326 (BJFC 031994, paratype); on rotten wood of *Pinus*, 15.VIII.2019, Dai 20342 (BJFC 032010, paratype); Zhejiang Province, Pingyang County, Nanyandangshan Forest Park, on rotten wood of *Pinus*, 3.VI.2021, Dai 22321 (BJFC 036909, paratype).

A key to accepted species of *Sidera* in worldwide

1	Hymenium grandinioid to odontioid	***S. lunata***
–	Hymenium poroid	**2**
2	Hyphal system monomitic	**3**
–	Hyphal system dimitic	**6**
3	Basidiospores mostly < 1 μm in width	**4**
–	Basidiospores mostly > 1 μm in width	**5**
4	Pores 7–9 per mm; basidiospores 2.9–3.7 μm long	***S. vesiculosa***
–	Pores 6–7 per mm; basidiospores 3.9–4.5 μm long	***S. roseo-bubalina***
5	Pores 6–8 per mm; cystidioles present, some branched	***S. lowei***
–	Pores 8–9 per mm; cystidioles absent	***S. punctata***
6	Basidiospores > 1.5 μm in width	***S. lenis***
–	Basidiospores < 1.5 μm in width	**7**
7	Skeletal hyphae becoming swollen in KOH	**8**
–	Skeletal hyphae almost unchanged in KOH	**10**
8	Pores 5–7 per mm; basidiospores 3.7–4.3 μm long	***S. minutipora***
–	Pores 9–11 per mm; basidiospores 2.9–3.3 μm long	**9**
9	Basidiospores allantoid, skeletal hyphae distinctly swollen in KOH	***S. inflata***
–	Basidiospores lunate, skeletal hyphae slightly swollen in KOH	***S. malaysiana***
10	Tramal hyphae parallel along the tubes	***S. parallela***
–	Tramal hyphae interwoven	**11**

11	Generative hyphae at dissepiments even	**12**
–	Generative hyphae at dissepiments with swollen tips	**16**
12	Basidiospores > 3.5 μm long	**13**
–	Basidiospores < 3.5 μm long	**15**
13	Pores < 9 per mm	***S. americana***
–	Pores > 9 per mm	**14**
14	Skeletal hyphae occasionally branched in subiculum and tube trama	***S. borealis***
–	Skeletal hyphae unbranched in subiculum and tube trama	***S. srilankensis***
15	Sterile margin distinct, white; basidiospore length/width > 3	***S. salmonea***
–	Sterile margin indistinct to almost absent; basidiospore length/width < 3	***S. tibetica***
16	Basidiospores < 3.6 μm long	***S. vulgaris***
–	Basidiospores > 3.8 μm long	**17**
17	Sterile margin distinct, fimbriate; basidiospore length/width < 4	***S. minutissima***
–	Sterile margin indistinct to almost absent; basidiospore length/width > 4	***S. tenuis***

Discussion

Sidera americana is discovered in USA and Canada, and the species is characterized by annual, resupinate basidiomata with silk sheen when dry, round pores (9–11 per mm), a dimitic hyphal system, and allantoid basidiospores measuring 3.5–4.2 × 1 μm. In our phylogeny, two specimens of *S. americana* form a lineage with strong support (99% BS, 100% BP, 1.00 BPP, Fig. 1). *S. americana* is closely related to *S. parallela* (98% BS, 100% BP, 1.00 BPP, Fig. 1), but basidiospores are longer in *S. americana* than in *S. parallela* (3.5–4.2 μm vs. 2.8–3.3 μm, Du et al. 2020). In addition, *S. parallela* has parallel tramal hyphae, while they are interwoven in *S. americana*.

Sidera borealis is discovered in boreal areas of China, including Gansu, Jilin, Qinghai, Shannxi, and Yunnan. The species is characterized by annual, resupinate basidiomata with cream to pinkish buff dry pore surface, angular pores (6–7 per mm), a dimitic hyphal system, and allantoid basidiospores measuring 3.9–4.1 × 1–1.1 μm. Phylogenetically, *S. borealis* clustered together with *S. vulgaris* with strong support (100% BS, 100% BP, 1.00 BPP, Fig. 1). Morphologically, *S. vulgaris* is different from *S. borealis* by the presence of capitate hyphal ends and "halocystidia" in tube mouths. Besides, basidiospores are longer in *S. borealis* than in *S. vulgaris* (3.9–4.1 μm vs. 2.9–3.6 μm, Niemelä and Dai 1997). *S. borealis* resembles *S. minutipora* by cream to buff fresh pores and similar pores (6–7 per mm vs. 5–7 per mm, Du et al. 2020). However, skeletal hyphae of *S. minutipora* become swollen in KOH, while they are unchanged in KOH in *S. borealis*. Besides, both species are distantly related (Fig. 1).

Sidera americana and *S. borealis* are described from North China and North America; like most other species of *Sidera*, the two new species grow mostly on gymnosperm

wood in temperate or boreal forests, but they are distinguished from existing species in the genus by morphology, geographic distribution and DNA sequences.

Boreal areas of China have the most important virgin forests in the country, and such forests provide favorable environments for some special wood-decaying fungi, e.g. *Heterobasidion* Bref., *Skeletocutis* Kotl. & Pouzar and *Sidera*, because fewer morphological characteristics existed among different species of each genus, and many species in the traditional definition are, in fact, the species complex. In recent years, the introduction of molecular systematics has greatly improved our understanding of the diversity of wood-rotting fungi in the boreal forests. Numerous new species have been found there (Dai et al. 2007, 2021; Yuan and Dai 2008; Tian et al. 2013; Li et al. 2014; Chen et al. 2015, 2016; Cui et al. 2019; Wang et al. 2021; Wu et al. 2021, 2022b), and we believe that more boreal new species will be found in the future.

Acknowledgements

The research is supported by the National Natural Science Foundation of China (Project No. 32161143013) and the Second Tibetan Plateau Scientific Expedition and Research Program (STEP, Grant No. 2019QZKK0503). Special thanks are due to Prof. Yu-Cheng Dai (Beijing Forestry University, China) for forwarding his specimens and photos for our study.

References

Chen JJ, Cui BK, Zhou LW, Korhonen K, Dai YC (2015) Phylogeny, divergence time estimation, and biogeography of the genus *Heterobasidion* (Basidiomycota, Russulales). Fungal Diversity 71(1): 185–200. https://doi.org/10.1007/s13225-014-0317-2

Chen H, Zhou JL, Cui BK (2016) Two new species of *Fomitiporia* (Hymenochaetales, Basidiomycota) from Tibet, southwest China. Mycologia 108(5): 1010–1017. https://doi.org/10.3852/16-011

Cui BK, Li HJ, Ji X, Zhou JL, Song J, Si J, Dai YC (2019) Species diversity, taxonomy and phylogeny of Polyporaceae (Basidiomycota) in China. Fungal Diversity 97(1): 137–302. https://doi.org/10.1007/s13225-019-00427-4

Dai YC (2010) Hymenochaetaceae (Basidiomycota) in China. Fungal Diversity 45(1): 131–343. https://doi.org/10.1007/s13225-010-0066-9

Dai YC, Yu CJ, Wang HC (2007) Polypores from eastern Xizang (Tibet), western China. Annales Botanici Fennici 44: 135–145.

Dai YC, Yang ZL, Cui BK, Wu G, Yuan HS, Zhou LW, He SH, Ge ZW, Wu F, Wei YL, Yuan Y, Si J (2021) Diversity and systematics of the important macrofungi in Chinese forests. Mycosystema 40: 770–805. https://doi.org/10.13346/j.mycosystema.210036

Du R, Wang L, Zhou M, Chen JJ (2019) A new species of *Sidera* (Hymenochaetales, Basidiomycota) from tropical Asia. Phytotaxa 387(2): 165–171. https://doi.org/10.11646/phytotaxa.387.2.9

Du R, Wu F, Gate GM, Dai YC, Tian XM (2020) Taxonomy and phylogeny of *Sidera* (Hymenochaetales, Basidiomycota): Four new species and keys to species of the genus. MycoKeys 68: 115–135. https://doi.org/10.3897/mycokeys.68.53561

Felsenstein J (1985) Confidence intervals on phylogenetics: An approach using bootstrap. Evolution; International Journal of Organic Evolution 39(4): 783–791. https://doi.org/10.2307/2408678

Hall TA (1999) Bioedit: A user-friendly biological sequence alignment editor and analysis program for Windows 95/98/NT. Nucleic Acids Symposium Series 41: 95–98.

Katoh K, Rozewicki J, Yamada KD (2019) MAFFT online service: Multiple sequence alignment, interactive sequence choice and visualization. Briefings in Bioinformatics 20(4): 1160–1166. https://doi.org/10.1093/bib/bbx108

Larsson KH, Parmasto E, Fischer M, Langer E, Nakasone KK, Redhead SA (2006) Hymenochaetales: A molecular phylogeny for the hymenochaetoid clade. Mycologia 98(6): 926–936. https://doi.org/10.1080/15572536.2006.11832622

Li HJ, Cui BK, Dai YC (2014) Taxonomy and multi-gene phylogeny of *Datronia* (Polyporales, Basidiomycota). Persoonia 32(1): 170–182. https://doi.org/10.3767/003158514X681828

Liu ZB, Zhou M, Yuan Y, Dai YC (2021) Global diversity and taxonomy of *Sidera* (Hymenochaetales, Basidiomycota): Four new species and keys to species of the genus. Journal of Fungi 7(4): e251. https://doi.org/10.3390/jof7040251

Liu ZB, Zhou M, Wu F, Yu J (2022) Two new species of *Sidera* (Hymenochaetales, Basidiomycota) from Southwest China. Journal of Fungi 8(4): e385. https://doi.org/10.3390/jof8040385

Maddison WP, Maddison DR (2021) Mesquite: A modular system for evolutionary analysis, version 3.70. http://www.mesquiteproject.org

Miettinen O, Larsson KH (2011) *Sidera*, a new genus in Hymenochaetales with poroid and hydnoid species. Mycological Progress 10(2): 131–141. https://doi.org/10.1007/s11557-010-0682-5

Miller MA, Pfeiffer W, Schwartz T (2010) Creating the CIPRES Science Gateway for inference of large phylogenetic trees. Proceedings of the Gateway Computing Environments Workshop (GCE), 14 Nov. 2010, New Orleans, 8 pp. https://doi.org/10.1109/GCE.2010.5676129

Niemelä T, Dai YC (1997) Polypore *Skeletocutis lenis* and its sib *S. vulgaris*. Annales Botanici Fennici 34: 133–140.

Nylander JAA (2004) MrModeltest v2. Program distributed by the author. Evolutionary Biology Centre, Uppsala University.

Petersen JH (1996) The Danish Mycological Society's colour-chart. Foreningen til Svampekundskabens Fremme, Greve.

Posada D, Crandall KA (1998) Modeltest: Testing the model of DNA substitution. Bioinformatics 14(9): 817–818. https://doi.org/10.1093/bioinformatics/14.9.817

Rambaut A (2018) Molecular Evolution, Phylogenetics and Epidemiology. FigTree ver. 1.4.4 Software. http://tree.bio.ed.ac.uk/software/figtree/

Ronquist F, Teslenko M, Mark P, Ayres DL, Darling A, Höhna S, Larget B, Liu L, Suchard MA, Huelsenbeck JP (2012) MrBayes 3.2: Efficient Bayesian phylogenetic inference and

model choice, across a large model space. Systematic Biology 61(3): 539–542. https://doi.org/10.1093/sysbio/sys029

Stamatakis A (2014) RAxML Version 8: A tool for phylogenetic analyses and post analyses of large phylogenies. Bioinformatics 30(9): 1312–1313. https://doi.org/10.1093/bioinformatics/btu033

Swofford DL (2002) PAUP*: phylogenetic analysis using parsimony (*and other methods), version 4.0b10. Sinauer Associates, Sunderland. https://doi.org/10.1002/0471650129.dob0522

Thiers B (2018) Index Herbariorum: A global directory of public herbaria and associated staff. New York Botanical Garden's Virtual Herbarium, New York. http://sweetgum.nybg.org/science/ih/

Tian XM, Yu HY, Zhou LW, Decock C, Vlasák J, Dai YC (2013) Phylogeny and taxonomy of the *Inonotus linteus* complex. Fungal Diversity 58(1): 159–169. https://doi.org/10.1007/s13225-012-0202-9

Vilgalys R, Hester M (1990) Rapid genetic identification and mapping of enzymatically amplified ribosomal DNA from several *Cryptococcus* species. Journal of Bacteriology 172: 4238–4246. https://doi.org/10.1128/jb.172.8.4238-4246.1990

Wang K, Chen SL, Dai YC, Jia ZF, Li TH, Liu TZ, Phurbu D, Mamut R, Sun GY, Bau T, Wei SL, Yang ZL, Yuan HL, Zhang XG, Cai L (2021) Overview of China's nomenclature novelties of fungi in the new century (2000–2020). Mycosystema 40: 822–833. https://doi.org/10.13346/j.mycosystema.210064

White TJ, Bruns T, Lee S, Taylor J (1990) Amplification and direct sequencing of fungal ribosomal RNA genes for phylogenetics. In: Innis MA, Gefand DH, Sninsky JJ, White JT (Eds) PCR Protocols: A Guide to Methods and Applications. Academic Press, San Diego, 315–322. https://doi.org/10.1016/B978-0-12-372180-8.50042-1

Wu F, Tohtirjap A, Fan LF, Zhou LW, Alvarenga RLM, Gibertoni TB, Dai YC (2021) Global diversity and updated phylogeny of Auricularia (Auriculariales, Basidiomycota). Journal of Fungi 7(11): e933. https://doi.org/10.3390/jof7110933

Wu F, Man XW, Tohtirjap A, Dai YC (2022a) A comparison of polypore funga and species composition in forest ecosystems of China, North America, and Europe. Forest Ecosystems 9: e100051. https://doi.org/10.1016/j.fecs.2022.100051

Wu F, Zhou LW, Vlasák J, Dai YC (2022b) Global diversity and systematics of Hymenochaetaceae with poroid hymenophore. Fungal Diversity 113(1): 1–192. https://doi.org/10.1007/s13225-021-00496-4

Yu J, Wang XW, Liu SL, Shen S, Zhou LY (2021) Taxonomy and phylogeny of *Resinicium* sensu lato from Asia-Pacific revealing a new genus and five new species (Hymenochaetales, Basidiomycota). IMA Fungus 12(1): 1–19. https://doi.org/10.1186/s43008-021-00071-1

Yuan HS, Dai YC (2008) Polypores from northern and central Yunnan Province, Southwestern China. Sydowia 60: 147–159.

Zhao CL, Cui BK, Song J, Dai YC (2015) Fragiliporiaceae, a new family of Polyporales (Basidiomycota). Fungal Diversity 70(1): 115–126. https://doi.org/10.1007/s13225-014-0299-0